Effect of curcumin and black tea polyphenols on carcinogen-induced cell proliferation and apoptosis in experimental models

By

Gaurav Kumar

[LIFE09200704008]

Tata Memorial Centre

Mumbai

A thesis submitted to the

Board of Studies in Life Sciences

In partial fulfillment of requirements

For the Degree of

DOCTOR OF PHILOSOPHY

Of

HOMI BHABHA NATIONAL INSTITUTE

AUGUST, 2013

HOMI BHABHA NATIONAL INSTITUTE

Recommendations of the Viva Voce Board

As members of the Viva Voce Board, we certify that we have read the dissertation prepared by Gaurav Kumar entitled "Effect of curcumin and black tea polyphenols on carcinogen-induced cell proliferation and apoptosis in experimental models" and recommend that it may be accepted as fulfilling the dissertation requirements for the Degree of Doctor of Philosophy.

---Date: 13.8.2013

Chairperson: -- Dr. Malini Krishna

---Date: 13.08.2013

Convener: -- Dr. Girish B. Maru

---Date: 13.08.2013

Member 1: -- Dr. Milind M. Vaidya

---Date: 13/8/2013

Member 2: -- Dr. Sanjay Gupta

---Date:

External Examiner: -- Dr. Kalpagam Polasa 13/8/13

Final approval and acceptance of this dissertation is contingent upon the candidate's submission of the final copies of the dissertation to HBNI.

I hereby certify that I have read this dissertation prepared under my direction and recommend that it may be accepted as fulfilling the dissertation requirement.

Date: 13.08.2013

Place: Navi-Mumbai

Dr. G. B. Maru

STATEMENT BY AUTHOR

This dissertation has been submitted in partial fulfillment of requirements for an advanced degree at Homi Bhabha National Institute (HBNI) and is deposited in the Library to be made available to borrowers under rules of the HBNI.

Brief quotations from this dissertation are allowable without special permission, provided that accurate acknowledgement of source is made. Requests for permission for extended quotation from or reproduction of this manuscript in whole or in part may be granted by the Competent Authority of HBNI when in his or her judgment the proposed use of the material is in the interests of scholarship. In all other instances, however, permission must be obtained from the author.

Navi Mumbai, Gaurav Kumar

Date:

DECLARATION

I, hereby declare that the investigation presented in the thesis has been carried out by me. This work is original and has not been submitted earlier as a whole or in part for a degree / diploma at this or any other Institution / University.

Navi Mumbai,
August 2013.

Gaurav Kumar

CERTIFICATE

I certify that the thesis titled ‘Effect of curcumin and black tea polyphenols on carcinogen-induced cell proliferation and apoptosis in experimental models’ submitted for the degree of Doctor of Philosophy by Gaurav Kumar is a record of the research carried out by him during the period August 2007 to March 2013 under my supervision. This work has not formed the basis for the award of any degree, diploma, associateship or fellowship at this or any other institute or university.

Navi Mumbai,
August 2013.

Girish B. Maru

ACKNOWLEDGEMENTS

This PhD work would have been impossible without the help and support of many people and I feel immensely honored to get this opportunity to convey my gratitude to everyone who has supported and guided me during my PhD work. Firstly, I express my deepest sense of gratitude to my Guide, Dr. Girish B. Maru for being a patient and motivating mentor. Sir, thank you for introducing me to the fields of carcinogenesis and chemoprevention and granting me complete freedom to explore my potential and help me out in all types of circumstances. You have always been the greatest source of appreciation and criticism for my work. Your enthusiasm to teach has helped me learn to think logically about experiments and deal with difficult problems. You have been inspirational during my tenure as a PhD student and will try and adhere to some of the ideas imparted by you for which I am very thankful to you. I am thankful to Dr. Rajiv Sarin (Director, ACTREC) and Dr. Surekha Zingde (Deputy Director, ACTREC) for providing me an opportunity to work in this institute and for making the institute well equipped with readily available infrastructure and constant attention to the progress of the students. I would like to thank my Doctoral Committee Members- Dr. Malini Krishna, Dr. Milind M. Vaidya and Dr. Sanjay Gupta for their expert comments, critical analysis of my data and helpful suggestions towards the progress of my work. I am indebted to ACTREC for awarding me a Junior Research Fellowship from 2007-2008 and also to the Council for Scientific and Industrial Research (CSIR) for awarding me a Junior/Senior Research Fellowship from 2008-2012. I thank ACTREC, National Tea Research Foundation (NTRF) for partial financial support to this project. It was a great pleasure being a part of Maru Lab and thank all the scientific and technical staff members for providing me with adequate support. I would also extend my special thanks to scientific officers Dr. Manoj Mahimkar, Dr. Asha G. Ramchandani, Dr. S. Pakhle, Dr. Milind M. Vaidya and Dr. Arvind Ingle, all of whom have helped me in different ways at some points or the other during my tenure as a Ph.D. student. Words fall short to express my gratitude for Dr. A. G. Ramchandani for helping in innumerable ways. I fall short of words to express my gratitude to Dr. Arvind Ingle, Dr. Rahul Thorat and entire staff of animal house without their help animal experiments would not have succeeded. I am very much thankful to the staff of Common Instrument, Microscopy, Photography,

Administration, Accounts, Library, BTIS, Workshop, Engineering, IT Department, Stores and Purchase for their cooperation and help. My special thanks to Vaishali Dange, Uday Dandekar, Seema, Sujata, Vaishali, Jairaj, Tanuja, Aruna, Gitanjli, Roshni and Chandni for their support and help. I would also like to thank Dr. Chiplunkar, Dr Robin, Dr. Kalraiya, Dr. Mulherkar for their help and support. I would also like to thank all my senior labmates Rachana Garg, Rachana Patel, Suvarna Erande and Rajesh Krishnan for their support and help. I am very much thankful to my Lab members Dhananjay, Phase, Jagtap Ji, Raghu, Tanuja, Pawar, Shubhangi, Pooja, Khushi, Priyanka, Manoj, Rasika for keeping the lab environment lively and pleasant. I am very thankful for all the technical assistance provided by Mr. Prasad Phase and Jagtap Ji without which I would not have been able to execute animal experiments as well as other laboratory work. I am also immensely thankful to all trainees who have worked with me and helped me in my work without complaining and also making the lab atmosphere lively and cheerful. I am especially grateful to Pooja, for all the help with the experiments in the last 2 years of my PhD and during manuscript and thesis writing.

It was nice to have batchmates like Sumeer, Ratika, Ajit, Dimpu, Akhil, Bihari, Vinayak, Dilip, Hamant and Harsh. Everybody of you have made the initial days (coursework duration) in ACTREC very lively and pleasant. I would like to thank the entire ACTREC student's community and my seniors, including Satyajeet, Srikant B, Shailendra, Shrikanth A, Rohan, Amitabho, Bhairav, Cheryl, Atul, Ajit Chande, Lalit, Deepika, Asha, Poulmi, Tabish, Amit Singh and Amit Gautam for all their support, cooperation throughout the tenure, and in troubleshooting the difficulties and failures in the experiments. I will also cherish my stay during my PhD spent with my wonderful roommates Sumeer, Amitabho, Nishikant. After being tired of the hectic schedule in the lab, returning back to room/hostel had always given me relaxation; sometimes cooking and dining with these friends. I'm going to miss all those birthday celebrations, Friday movie night, late night gossiping, hanging around in Kharghar and Belapur, especially with Sumeer and Ratika and/or batchmates.

I am blessed with a large friend circle outside ACTREC. I would like to thank all of them for all their moral support and encouragement throughout this journey. Some of them deserved to be mentioned here are Sumit and his wife Manju, Abhishek, Ankit and his wife Meenu, Smita, Shivendra, Manish, Ashish, Anuj and Visva were the one who had actually motivated me for pursuing PhD and were a constant source of encouragement. I

also thank all others not mentioned here and who have been equally helpful towards me in various ways.

I am also thankful to my family for being on my side at all times. I know that I have reached so far only because you believed in me. Both of you had been my strength throughout. It would have been impossible to reach here without the support, love and affection of my sister, jijaji, my nephew (Krishna) and their family.

I thank almighty God who has helped and blessed me through the entire voyage and have made this day possible.

Last but not the least; I would like to thank all those who made Google, scientific and statistical software's, computers and machines which I have used during my PhD tenure.

- Gaurav Kumar

CONTENTS

PAGE NO.

Synopsis		I
List of abbreviations		XVI
List of tables		XIX
List of figures		XX
CHAPTER-1	***Introduction***	1-36
1.1	Cancer	1
1.2	Types of cancer	1
1.3	Causes of cancer	3
1.4	Treatment of cancer	5
1.5	Disadvantages of current cancer treatmants	6
1.6	Cancer chemoprevention	7
1.7	Carcinogenesis	7
1.8	Food derived chemopreventive agents	9
1.9	Stages in the development of a chemopreventive agent for clinical use	10
1.10	Tea and tea polyphenols	15
1.11	Turmeric	24
1.12	Targets of chemopreventive agents - PBPS and/or curcumin	27
1.12.1	Mechanism(s) of anti-initiating action	27
1.12.2	Mechanism(s) of anti-promoting action	29
CHAPTER 2	***Aims and objectives***	37
CHAPTER 3	***Materials and methods***	38 - 63
3.1	Materials	38
3.2	Diet preparation	43
3.3	Animals	43
3.4	Preparation of various cellular fractions	44
3.5	Determination of protein content	48
3.6	Protein immunoblotting	48
3.7	Immunoprecipitation	53

3.8	Protein kinase C activity and protein level measurements	54
3.9	Immunohistochemical staining	55
3.10	Terminal deoxynucleotidyl transferase biotin-dUTP nick end labeling (TUNEL) assay for measuring apoptotic index	56
3.11	Histopathological analysis	57
3.12	Confocal microscopy	57
3.13	Cell culture experiments	58
3.14	Immunostaining of cells	59
3.15	PI3K activity	59
3.16	Isothermal titration calorimetry (ITC)	60
3.17	UV absorption spectra and mass spectrometry	61
3.18	Measurement of GSH/GSSG ratio in epithelial cell extracts	61
3.19	Measurement of DNA in epithelial cell extracts	62
3.20	Statistical analysis	63

CHAPTER 4	***Polymeric black tea polyphenols modulate the localization and activity of 12-O-tetradecanoyl phorbol-13-acetate-mediated kinase(s) in mouse skin: mechanisms of their anti-tumor-promoting action***	64-101
4.1	**INTRODUCTION**	64
4.2	**METHODS**	65
4.2.1	Isolation of PBP fractions using Soxhlet continuous extractor	65
4.2.2	Determination of contamination by other black tea components	67
4.2.3	Animal treatment	67
4.2.4	PKC enzyme assays and levels	67
4.2.5	Protein immunoblotting	68
4.2.6	Immunoprecipitation	68
4.2.7	Confocal microscopy	69
4.2.8	Cell culture experiments	70
4.2.9	Immunostaining of cells	70
4.2.10	PI3K activity	71
4.2.11	Determination of *in vitro* interaction between TPA and PBP-3 or PBP-5	71
4.2.12	Statistical analysis	72

4.3	**RESULTS**	72
4.3.1	Isolation of PBP fractions using Soxhlet continuous extractor	72
4.3.2	Determination of contamination by other black tea components	73
4.3.3	PBP pre-treatment inhibits TPA-induced PKC translocation	73
4.3.4	Inhibition of TPA-induced phosphorylation of PKC by kinase inhibitors and PBP-3 or PBP-5	87
4.3.5	Modulation of TPA-induced cell proliferation and apoptosis markers by PBP-3 or PBP-5	93
4.3.6	Lack of interaction between TPA and PBP-3 or PBP-5	94
4.3.7	Prevention of TPA-mediated decrease in GSH/GSSG ratio by PBP-3	96
4.4	**DISCUSSION**	97
CHAPTER 5	***Dietary turmeric post-treatment decreases DMBA-induced hamster buccal pouch tumor growth by altering cell proliferation and apoptosis- related markers***	102-130
5.1	**INTRODUCTION**	102
5.2	**METHODS**	103
5.2.1	Animal treatment	103
5.2.2	Protein immunoblotting	105
5.2.3	Immunohistochemical staining	106
5.2.4	Terminal deoxynucleotidyl transferase biotin-dUTP nick end labeling (TUNEL) assay	106
5.2.5	Prostaglandin E-2 (PGE-2) measurement	106
5.2.6	Statistical analysis	108
5.3	**RESULTS**	108
5.3.1	Dietary turmeric post-treatment inhibits DMBA-induced tumor growth in hamsters	108
5.3.2	Dietary turmeric post-treatment increases the DMBA-mediated apoptosis	113
5.3.3	Dietary turmeric post-treatment decreases DMBA-mediated cell proliferation	119
5.3.4	Dietary turmeric post-treatment decreases the DMBA-induced activation of nuclear transcription factors and MAPK	121
5.3.5	Dietary turmeric post-treatment decreases the DMBA-induced inflammation	124
5.4	**DISCUSSION**	124

CHAPTER 6 ***Dietary curcumin post-treatment enhances the disappearance of B(a)P-derived DNA adducts in mouse liver and lungs*** 131-165

6.1 INTRODUCTION 131

6.2 METHODS 132

6.2.1 Animal treatment 132

6.2.2 Protein immunoblotting 133

6.2.3 Measurement of BPDE-DNA adducts 134

6.2.4 Digital image analysis 135

6.2.5 Terminal deoxynucleotidyl transferase biotin-dUTP nick end labeling (TUNEL) assay 136

6.2.6 Statistical analysis 137

6.3 RESULTS 137

6.3.1 Effect of dietary curcumin post-treatment on disappearance of BPDE-DNA adducts in mouse tissues 140

6.3.2 Effect of dietary curcumin post-treatment on levels of apoptosis in mouse tissues 146

6.3.3 Effect of dietary curcumin post-treatment on levels of cell proliferation markers in mouse tissues 160

6.4 DISCUSSION 162

CHAPTER 7 ***Dietary curcumin inhibits the B(a)P-induced lung tumors by modulating apoptosis and cell proliferation markers in A/J mice*** 166-187

7.1 INTRODUCTION 166

7.2 METHODS 167

7.2.1 Animal treatment 167

7.2.2 Histopathological analysis 168

7.2.3 Protein immunoblotting 169

7.2.4 Immunohistochemical staining and analysis 169

7.2.5 Terminal deoxynucleotidyl transferase biotin-dUTP nick end labeling (TUNEL) assay 170

7.2.6 Statistical analysis 171

7.3 RESULTS 171

7.3.1 Effect of dietary curcumin on B(a)P-induced pulmonary tumors 171

7.3.2 Effect of curcumin treatment on B(a)P-mediated apoptosis in lung tumor tissue of mouse 176

7.3.3	Effect of curcumin treatment on B(a)P-induced cell proliferation and survival-related proteins in lungs/lung tumor tissue of mouse	179
7.3.4	Effect of curcumin treatment on B(a)P-induced inflammation marker in lung tumor tissue of mouse	183
7.4	**DISCUSSION**	183
CHAPTER 8	***Summary and future directions***	188-196
8.1	**SUMMARY OF THE WORK**	188
8.1.1	Chapter 4	188
8.1.2	Chapter 5	189
8.1.3	Chapter 6	190
8.1.4	Chapter 7	119
8.2	**CONCLUSIONS**	191
8.3	**CONTRIBUTION OF THE PRESENT STUDY TO THE EXISTING LITERATURE**	193
8.4	**SHORTCOMINGS OF THE STUDY AND FUTURE PERSPECTIVE**	194
	BIBLIOGRAPHY	197
	LIST OF PUBLICATIONS	

SYNOPSIS

Homi Bhabha National Institute

Ph. D. PROGRAMME

1. Name of the Student: Mr. Gaurav Kumar

2. Name of the Constituent Institution: Tata Memorial Centre**,** Advanced Centre for Treatment Research and Education in Cancer

3. Enrolment No. : LIFE09200704008 (21/08/2007)

4. Title of the Thesis: Effect of curcumin and black tea polyphenols on carcinogen-induced cell proliferation and apoptosis in experimental models

5. Board of Studies: Life Sciences

INTRODUCTION

Cancer is a growing health problem around the world. Majority of human cancers are caused or mediated by the complex interactions between exogenous (environmental) and endogenous (genetic, hormonal and immunological) factors. Despite the improvements of medical technologies and therapeutic approaches, the mortality rates for cancer have not declined in the past 50 years. Efforts to eliminate known human carcinogens like tobacco from the environment and current cancer treatment approaches have met with limited success. Based on the experience with some infectious and cardiovascular diseases, prevention of disease appears to be one of the achievable, cost effective and attractive approaches. Chemoprevention is thus, gaining considerable attention as a promising alternative strategy for the control of cancer [1].

Carcinogenesis is a long evolving, multi-factorial and multi-step process (characterized by three steps: initiation, promotion and progression). Hence, chemopreventive interventions are possible at each of these steps. Cancer chemoprevention can be defined as the use of natural or synthetic compounds to prevent, suppress/delay, or reverse the development of invasive carcinoma. Amongst various chemopreventives, use of plant-derived anti-oxidants is highly desirable because of their low toxicity and high tolerability [2, 3].

Number of plant derived extracts and pure compounds have shown chemo-protective activities *in vitro* as well as *in vivo*. Earlier studies from our and other lab have shown turmeric/curcumin and tea-derived compounds to posses chemopreventive activities in experimental systems [2, 4]. Studies on the mechanism(s) of chemopreventive actions of turmeric and tea-derived compounds are on-going [5, 6]. As a part of this on-going programme, complementary and additional studies to understand the

mechanisms of chemopreventive actions and commonality and/or differences in the observed mechanisms were planned and undertaken.

AIMS AND OBJECTIVE

1) To investigate the mechanism(s) of anti-promoting activity of PBPs on 12-*O*-tetradecanoylphorbol-13-acetate (TPA)-induced biochemical alterations in mouse skin.

2) To evaluate the effects of dietary turmeric post-treatment on tumor growth, markers of cell proliferation and apoptosis in DMBA-induced hamster buccal pouch (HBP) model.

3) To evaluate the effect(s) of dietary curcumin post-treatment on the disappearance/persistence of B(a)P-derived DNA adducts and apoptosis of cells in liver and lung of mice.

MATERIALS AND METHODS

1) To investigate the mechanism(s) of anti-promoting activity of PBPs on 12-*O*-tetradecanoylphorbol-13-acetate (TPA)-induced biochemical alterations in mouse skin.

Five PBP fractions were isolated from a popular brand of black tea powder (Brooke Bond Red Label, India) in our laboratory, employing a Soxhlet extractor [7]. Briefly, black tea powder was serially extracted in a Soxhlet extractor with chloroform, ethyl acetate and n-butanol. The ethyl acetate extract yielded PBP-1, whereas the n-butanol extract contained PBP-2 and PBP-3. The tea powder residue was then brewed with distilled water, the resultant solution acidified with sulfuric acid and extracted with n-butanol to obtain PBP-4 and PBP-5. The PBP fractions were confirmed to be free from other biologically active black tea derived contaminants such as caffeine, catechin(s), and theaflavins.

To study the mechanism of anti-promoting effects of PBP fractions isolated from black tea, female S/RV/Cri-ba mice-hairless mutants that are highly susceptible to skin tumorigenesis [8] were employed. Six to eight-week old female Swiss bare mice were randomized into eighteen different treatment groups (each group with at least five animals), viz., vehicle control (acetone), TPA (5 nmol), individual PBP 1-5 each/EGCG (200 µg), curcumin (10 µmol) and Ro-31-8220 (PKC inhibitor, 1 nmol) treated group, test groups [topically pre-treated with individual PBP 1-5/EGCG/curcumin/Ro-31-8220 followed by TPA after 20 min]. For all groups, mice were sacrificed 4 h after TPA application. The experimental conditions such as doses, route of administration, treatment regime and sacrifice time were selected based on previous studies from our lab or from initial optimization. Epidermis was gently separated from the skin using Watson skin grafting knife and levels, activity, localization and phosphorylation status of PKC isozymes were analyzed. To study the effect of PBPs on PKC translocation, the protein levels and activity of PKC isozymes (α, β, η, γ, ε) were assayed in cytosolic and particulate fraction prepared from mouse skin [9] by immunoblotting using isozyme-specific antibodies. To complement the results from western blot analyses and PKC activity, confocal microscopic evaluations were undertaken in epidermal layers of mouse skin and *in vitro* in HaCat cells. Initially, HaCat cells were treated with varying doses of TPA to evaluate the optimal dose, which was further used for all subsequent experiments. HaCat cells were pretreated with PBP-3 or PBP-5 (200 µg/ml of medium) for 20 min followed by TPA treatment (200 µg/ml of medium) for 1 h. Translocation of PKC is dependent on phosphorylation, which in turn is regulated by upstream kinase(s) such as PDK, AKT and PI3K. Animals were pre-treated with PBP-3, PBP-5, inhibitors (2 µmol) for specific kinase(s) (BAG 956 - PDK and PI3K inhibitor; OSU-03012 - PDK1 inhibitor; PDK1/AKT/Fit dual inhibitor - PDK1 and AKT inhibitor; wortmannin - PI3K inhibitor

and cocktail of all above four inhibitors- each 500 nmol) for 20 min followed by TPA (5 nmol) treatment for 4 h. Effects of PBPs and specific inhibitors of upstream kinase(s) were studied on phosphorylation of PKC and upstream kinase(s). To studies the effects of PBPs on TPA-responsive molecular markers involved in signaling cascades leading to cell proliferation (cyclin D1, PCNA), cell death (Bax, Bcl-2), stress or inflammation (cox-2) were analyzed by immunoblotting in epidermal total cell lysates [10]employing specific antibodies. Further, effects of PBPs on TPA-modulated protein levels of NF-κB family proteins such as IKK, IκB-α, pIκB-α and NF-κB, pNF-κB were assayed in cytosolic and nuclear fractions, respectively by immunoblotting. β-actin and histone H1 were used as the loading control for proteins assayed in total cell, cytosolic and nuclear lysates, respectively. Data i.e., the mean ± SE of three to five independent samples in each group, were compared and analyzed. Densitometry of various analyte proteins was performed using Image J 1.43 (NIH) software.

2) To evaluate the effects of dietary turmeric post-treatment on tumor growth, markers of cell proliferation and apoptosis in DMBA-induced hamster buccal pouch (HBP) model.

Turmeric rhizomes were purchased from the local market of Mumbai, washed with deionised water, sun dried and powdered in a grinding mill. The resultant turmeric powder was stored in an air-tight container at room temperature throughout the experiments. The standard laboratory diet prepared in ACTREC animal house was collected in the powdered form. Quantities of turmeric/curcumin (Sigma) powder required for preparation of 1% turmeric and 0.05% curcumin diet were weighed and added to the pre-weighed standard laboratory diet. Turmeric/curcumin powder was thoroughly mixed in the diet while adding aldehyde-free distilled ethanol (upto 2% concentration) to ensure its uniform distribution. Aldehyde-free distilled ethanol was also

added to the standard laboratory diet (control diet). Ethanol from control as well as experimental diets (with turmeric/curcumin) was allowed to evaporate completely and then, the diets were used. Control and experimental diet(s) were prepared twice a month.

HBP is a well-established animal model for studying oral carcinogenesis [11] and efficacy of preventive and therapeutic agents. Initially to induce tumors, 0.5% DMBA (thrice a week for 12 consecutive weeks) in corn oil or vehicle corn oil (carcinogen untreated control, group C) [12] was topically painted on the right buccal pouch of inbred male Syrian golden hamsters (6–8 wks old) (Animal house, ACTREC, India). After tumor development at 12 weeks, animals were either shifted to a powdered control diet (standard laboratory diet, groups 12DC2 and 12DC3) or an experimental diet containing 1% turmeric in standard laboratory diet (groups 12DT2 and 12DT3) for 2 weeks in experiment 1 and for 3 weeks in experiment 2.

In subsequent experiments (3 and 4), animals with DMBA-induced HBP tumors at 12 weeks with or without pre-defined tumor volumes ranges as well as appropriate controls, were randomized into five groups. Of these, half of the animals continued on the powdered control diet (group 12DC4) and the other half were shifted to a powdered experimental diet (group 12DT4) for 4 weeks, respectively. The dosage of turmeric was equivalent to the level of curcumin (0.05%) showing biological activity in experimental systems [13]. To rule out DMBA discontinuation as a cause of decrease in tumor burden, DMBA treatment was continued until the end of the experiment in another set of animals that were shifted to a powdered control diet (group 16DC4) and a powdered experimental diet (group 16DT4). Hamsters were euthanized (by CO_2 chamber) 16 weeks after the first dose of the carcinogen. Hamsters were scored for multiplicity (average number of tumors per animal) and tumor burden (mean tumor volume × mean number of tumors). Their buccal pouches were excised, and a portion of the tissue (tumor and non-tumor) was fixed

in 10% buffered formalin for histopathological evaluation and immunohistochemical staining, while the rest of the tissue was snap frozen in liquid nitrogen and stored at −80°C until preparation of different extracts. Tumor bearing buccal pouch parts were taken and analysed for markers associated with cell proliferation, apoptosis, and inflammation by immunoblotting and further complemented by immunohistochemical analysis in tumor parts of HBP. The molecular markers such as Bax, Bcl-2, survivin, caspase-3, caspase-9, p-ERK, p-p38, cox-2, PCNA and cyclin D1 were analyzed in total cell lysate prepared from buccal pouch of hamsters belonging to the different treatment groups. Protein levels of, c-jun, c-fos, NF-κB were studied in nuclear extracts while that of IKK, IκB-α, pIκB-α were measured in cytosolic lysates. β-actin and histone H1 were used as the loading control in respective cellular compartments. The ratio of Bax:Bcl-2 was calculated as a measure of apoptosis. Apoptosis in tumor parts of buccal pouch was further confirmed with in-situ TUNEL assay (wherein cells undergoing apoptosis were detected as brown stained nuclei). Additionally, level of PGE-2 was quantitated in the buccal pouch by enzyme-immuno assay, as a measure of inflammation.

3) To evaluate the effect(s) of dietary curcumin post-treatment on the disappearance/persistence of B(a)P-derived DNA adducts and apoptosis of cells in liver and lung of mice.

Six to eight weeks of male Swiss albino mice (6-8 wks old) were taken and two different set of experiments were carried out. In experiment no. 1, animals were randomized into control (C) and treated (T) group. Control (C) animals received corn oil whereas treated (T) animals received 1 mg B(a)P in corn oil though gavage in order to develop a equivalent level of B(a)P-DNA adducts in all experimental mice. After 24 h of B(a)P administration, both the C and T group mice were randomized into 7 subgroups. One of the subgroups from both the groups (C and T) was sacrificed immediately after

randomization (i.e. C0 and T0 group, at 0 time point). Out of remaining 6 subgroups, half of the subgroups were continued on control diet and half of the subgroups were shifted to 0.05% curcumin diet and sacrificed at 24, 72 and 120 h. Similar to experiment 1, in another set of experiment, mice were randomized as described above and sacrificed after 1, 2 and 4 wks. At the time of sacrifice, liver and lungs of mice were perfused, excised and a small part of the tissue was fixed in 10% buffered formalin while, the remaining tissue was snap frozen and stored at -80°C. B(a)P-derived DNA adducts were analyzed by immunohistochemical staining in formalin fixed tissue sections using specific antibody. Extent of cell turnover was determined by calculating cells undergoing apoptosis employing in-situ TUNEL assay; carried out in the consecutive formalin fixed tissue sections. The % of nuclei with BPDE-DNA adducts and apoptotic index was calculated as number of positively stained brown cells x 100/ total number of cells. Semi quantitative analysis was done by Image J 1.43 (NIH) software by counting the number of positively stained cells in photographs of atleast 10 randomly selected fields per animals. In addition, markers of apoptosis (p53, Bax, caspase-3) and cell proliferation (cyclin D1 and PCNA) were analyzed in total cell lysates by immunoblotting, with β-actin included as loading control.

RESULTS AND DISCUSSION

1) The yields of PBP-1, PBP-2, PBP-3, PBP-4 and PBP-5 were 2.68%, 3.79%, 1.34%, 2.20% and 0.32%, respectively. The percentage yield in descending order, was, PBP-2 > PBP-4 > PBP-1 > PBP-3> PBP-5. Amongst all PBPs, the yield for PBP-2 was highest and that for PBP-5 was lowest. PBP fractions did not show any presence of other known biologically active, mobile components, such as free catechins, theaflavins or caffeine, known to be present in black tea, and PBPs were retained at the origin in thin layer chromatography (TLC) analysis, showing strong solid matrix reactivity.

Anti-promoting effects and mechanisms of actions of PBP fractions were studied in mouse skin model after confirming their purity. Compared to controls, a single topical application of TPA to mouse skin increased the translocation of PKC from cytosol to membrane. Pretreatment with PBPs 1-3 decreased TPA-induced translocation of PKC isozyme(s) (α, β, η, γ, ε) from cytosol to membrane, while PBPs 4-5 were less effective. The levels of PKC δ and ζ in cytosol/membrane were similar in all the treatment groups. Complementary confocal microscopic evaluation showed decrease in TPA-induced PKCα fluorescence in PBP-3 pretreated membranes, whereas pretreatment with PBP-5 did not show a similar decrease. Based on the experiments with specific enzyme inhibitors and phospho-specific antibodies, both PBP-3 and PBP-5 were observed to decrease TPA-induced level and/or activity of PI3K and AKT1 (pS473). An additional ability of PBP-3 to inhibit site-specific phosphorylation of PKCα at all the three positions, responsible for its activation [PKCα (pT497), PKC PAN (βII pS660), PKC α/βII (pT638/641)] and AKT1 at Thr 308 position, along with decrease in TPA-induced PDK1 protein level correlated with the inhibition of translocation of PKC that may impart relatively stronger chemoprotective activity to PBP-3 than PBP-5. Altogether, PBP-mediated decrease in TPA-induced PKC phosphorylation correlated well with decreased TPA-induced NF-κB phosphorylation and downstream target proteins associated with proliferation, apoptosis and inflammation in mouse skin. Results suggest that anti-promoting effects of PBPs are due to modulation of TPA-induced PI3K-mediated signal transduction.

2) Based on the net bodyweight gain, survival, and histopathological evaluation of tissues, no toxicity or mortality was observed in animals belonging to the various treatment groups during the experimental period. Application of 0.5% DMBA thrice a wk for 12 wks led to 100% tumor incidence in buccal pouches of hamsters. All the animals developed squamous cell carcinomas (SCCs) with dysplastic changes in their buccal

pouches, and the average number of tumors per animal was 1.7, 4.7, 3.5 and 7 in experiment 1-4, respectively. Post-treatment of 1% dietary turmeric inhibited the tumor growth i.e. tumor burden and multiplicity in animals shifted on the turmeric diet (groups 12DT2 and 12DT3) for 2 and 3 wks, compared to the animals on control diet (groups 12DC2 and 12DC3), respectively. The observed inhibition in tumor growth may have been due to dietary turmeric exposure and/or to discontinuation of carcinogen (DMBA) exposure. To rule out the role of DMBA discontinuation; in experiment 3, following tumor development (12 wks), animals were randomized into four groups wherein the duration of treatment with dietary turmeric was increased to 4 wks to reveal more pronounced effects. When the relative changes in the tumor burden (16 wk/12 wk) were analyzed at the end of experiment, there was a significant decrease in the tumor burden in group 12DT4 receiving turmeric compared to control group 12DC4, although there was no statistically significant decrease in tumor burden in group 16DT4, which received turmeric, compared to control group 16DC4, despite a 56% decrease in tumor burden (16 wks - 12 wks) between group 16DT4 (treated) vs. group 16DC4 (control). The lack of statistical significance in tumor burden appears to be due to large variations/uncommon distribution of tumor volumes in group 16DC4 and 16DT4. To get better insights into effects of dietary turmeric (if any), an experiment 4 was undertaken wherein tumors were induced by applying DMBA with a Camlin no. 4 paintbrush and animals having narrow range of DMBA-induced HBP tumors (1-5 mm diameters) were randomized into four groups and effect of dietary turmeric was determined. Tumor burden calculated using the difference in the mean tumor volumes in animals at week 16 and 12 of DMBA treatment showed that the animals receiving 1% dietary turmeric without or with continuation of carcinogen treatments after week 12 showed a tumor burden that significantly decreased by 63% and 55%, respectively. Furthermore, 1% dietary turmeric resulted in a significant

decrease in the DMBA-induced tumor multiplicity in groups 12DT4 and 16DT4 (43% and 42%, respectively), when compared to respective controls (groups 12DC4 and 16DC4). Buccal pouch of hamsters bearing tumors receiving turmeric diet showed: (a) decreased cell proliferation (diminished PCNA, cyclin D1 and Bcl-2) and PCNA labeling index, (b) enhanced apoptosis (increased Bax, caspase-3, caspase-9, cytochrome-c and decreased survivin) and apoptotic index, (c) decreased inflammation (decreased cox-2) and (d) decreased MAPK activation (p-ERK and p-p38), when compared to hamsters bearing tumors continued on control diet. Data suggest decrease in the tumor growth was due to the modulation of cellular pathways associated with cell proliferation and apoptosis.

3) Based on initial and final body weights and histopathological evaluation of tissues, no toxicity and mortality was observed in animals belonging to the different treatment groups during the experimental period. Since, dietary curcumin pretreatment has earlier been shown to decrease the BPDE-DNA adduct formation in mouse tissues, the effect of curcumin on disappearance of BPDE-DNA adducts was studied in lung and liver of mice wherein, exposure to curcumin occurred after B(a)P treatment, so as to allow the formation of equivalent levels of BPDE-DNA adducts in tissues of mice belonging to the different treatment groups. It was observed that compared to T0 group (mice sacrificed at 0 time point), mice continued on control diet for 24, 72 and 120 h showed significant decrease in BPDE-DNA adducts observed in terms of decrease in % of stained (brown) nuclei at all time points. Interestingly, mice that were shifted to 0.05% curcumin diet and sacrificed at 24, 72 and 120 h showed a relatively higher decrease in BPDE-DNA adducts when compared to T0, as well as respective time-matched controls i.e. TC24, TC72 and TC120. It may be noted that BPDE-DNA adduct containing brown stained nuclei was not detected in tissues of vehicle/or curcumin treated group. The observed decrease of DNA

adducts can be attributed to increased cell turn-over and/or enhanced repair and/or dilution of DNA adducts. To investigate the effect of dietary curcumin post-treatment on B(a)P induced cell turn over in mouse tissue, TUNEL assay was employed. It was observed that compared to T0, the apoptotic index increased in liver and lungs tissues of mice at all-time points 24, 72, 120 h. Interestingly, mice that were shifted to 0.05% curcumin diet and sacrificed at 24, 72 and120 h showed a relatively higher apoptotic index when compared to T0 as well as respective time-matched controls i.e. TC72 and TC120 except at 24 h. This was further complemented with the immunoblot analysis of markers associated with apoptosis such as p53, Bax, Bcl-2 and caspase-3. Relatively higher Bax:Bcl-2 ratio was observed in mice shifted on curcumin diet compared to respective controls. Results, thus hint that curcumin-mediated increase in cell turn over, to be one of the plausible reasons for the observed decrease in B(a)P-derived DNA adducts (increased apoptosis of adduct containing cells) following curcumin post-treatment, however, the possibility of enhanced DNA repair cannot be ruled out.

In experiment 2, compared to T0 group, mice continued on control diet for 1, 2, and 4 wk showed significant decrease in BPDE-DNA adducts observed in terms of decrease in % of stained (brown) nuclei at all-time points in liver and lung of mouse. Interestingly, mice that were shifted to 0.05% curcumin diet and sacrificed at 1, 2, and 4 wk showed a relatively higher decrease in brown stained nuclei in mouse liver when compared to respective time-matched controls i.e. TC 1wk, TC 2wk and TC 4wk. The observed decrease of DNA adducts can be attributed to increased cell turn-over and/or enhanced repair. To investigate effect of dietary curcumin post-treatment on B(a)P induced cell turn over in mouse liver, TUNEL assay was employed. However, no significant difference was observed in apoptotic index any of the treatment groups in

liver. This observation indirectly suggests the role of enhanced DNA repair in removal of adduct containing cell in liver.

CONCLUSIONS

1) The present findings suggest strong chemo-protective activities of PBP-3 compared to PBP-5, which may be due to differences in inhibition of TPA-induced PKC translocation/activity and specific phosphorylation. Our study demonstrates that PBPs modulate TPA-induced molecular and biochemical alterations in mouse skin through a PKC-dependent mechanism via the PI3K/AKT/PDK1 pathway.

2) Our findings suggest that dietary turmeric inhibits DMBA-induced cell inflammation markers (cox-2 and PGE-2) by blocking the MAPK and NF-κB signaling cascade, which may provide a molecular basis for suppression of tumor promotion (through apoptosis and cell proliferation) in DMBA-induced HBP tumors.

3) Our findings suggest that dietary curcumin post-treatment augments apoptosis of adducted containing cells resulting in enhanced decrease in DNA adducts in liver and lung of mice sacrificed at 24, 72, 120 h. However, in experiment where animal were sacrificed after 1, 2 and 4 wks there was no enhancement in apoptosis both liver and lung due to curcumin treatment. Hence, observed decrease in DNA adducts in liver suggests the role of enhanced DNA repair.

Altogether, our results suggests that mechanisms implicated in the inhibition of carcinogenesis by PBPs/turmeric/curcumin involve modulation of signalling kinase(s) or xenobiotic-induced activation/translocation of kinases or modulation of tumor-induced responses ultimately leading to effects on genes and cell signalling pathways at multiple levels.

BIBLIOGRAPHY

[1] Tsao, A. S.; Kim, E. S.; Hong, W. K. Chemoprevention of cancer. *CA: a cancer journal for clinicians* **54:**150-180; 2004.

[2] Kumar, G.; Pillare, S. P.; Maru, G. B. Black tea polyphenols-mediated in vivo cellular responses during carcinogenesis. *Mini reviews in medicinal chemistry* **10:**492-505; 2010.

[3] Patel, R.; Garg, R.; Erande, S.; G, B. M. Chemopreventive herbal anti-oxidants: current status and future perspectives. *Journal of clinical biochemistry and nutrition* **40:**82-91; 2007.

[4] Maru, G. B.; Ramchandani, A. G.; Kumar, G.; Garg, R. Curcumin-Mediated Cellular Responses in Chemical Carcinogenesis. In: Watson, R. R.; Preedy, V. R., eds. *Bioactive Foods and Extracts*: CRC Press; 2010: 181–203.

[5] Aggarwal, B. B.; Kumar, A.; Bharti, A. C. Anticancer potential of curcumin: preclinical and clinical studies. *Anticancer research* **23:**363-398; 2003.

[6] Chung, F. L.; Schwartz, J.; Herzog, C. R.; Yang, Y. M. Tea and cancer prevention: studies in animals and humans. *J Nutr* **133:**3268S-3274S; 2003.

[7] Krishnan, R.; Maru, G. B. Isolation and analyses of polymeric polyphenol fractions from black tea. *Food Chemistry* **94:**331-340; 2006.

[8] Bhisey, R. A.; Veturkar, P. L.; Borges, A. Comparison of sensitivity of Swiss albino and hairless Swiss bare mice to two stage skin tumorigenesis. *Indian J Exp Biol* **25:**90-96; 1987.

[9] Szaefer, H.; Kaczmarek, J.; Rybczynska, M.; Baer-Dubowska, W. The effect of plant phenols on the expression and activity of phorbol ester-induced PKC in mouse epidermis. *Toxicology* **230:**1-10; 2007.

[10] Afaq, F.; Saleem, M.; Aziz, M. H.; Mukhtar, H. Inhibition of 12-O-tetradecanoylphorbol-13-acetate-induced tumor promotion markers in CD-1 mouse skin by oleandrin. *Toxicology and applied pharmacology* **195:**361-369; 2004.

[11] Salley, J. J. Experimental carcinogenesis in the cheek pouch of the Syrian hamster. *Journal of dental research* **33:**253-262; 1954.

[12] Lin, L. M.; Chen, Y. K.; Huang, Y. L.; Mostofi, R.; Toto, P. Cytokeratins in hamster cheek pouch epithelium during DMBA-induced carcinogenesis. *J Oral Pathol Med* **18:**287-290; 1989.

[13] Thapliyal, R.; Maru, G. B. Inhibition of cytochrome P450 isozymes by curcumins in vitro and in vivo. *Food Chem Toxicol* **39:**541-547; 2001.

a. PUBLISHED:

PUBLICATION FROM THE THESIS

1) **Gaurav Kumar**, Prerana Dange, Vaishali Kailaje, Milind M. Vaidya, Asha G. Ramchandani, Girish B. Maru. Polymeric black tea polyphenols modulate the localization and activity of 12-*O*-tetradecanoylphorbol- 13-acetate-mediated kinases in mouse skin: mechanisms of their anti-promoting action. Free Radical Biology & Medicine, 2012, 53: 1358-1370.

2) **Gaurav Kumar**, Pooja Tajpara, Girish B. Maru. Dietary turmeric post-treatment decreases DMBA-induced hamster buccal pouch tumor growth by altering cell proliferation and apoptosis related markers. Journal of Environmental Pathology, Toxicology, and Oncology, 2012, 31(4): 295-312.

3)**Gaurav Kumar,** Shubhangi P. Pillare and Girish B. Maru.Black tea polyphenols-mediated *in vivo* cellular responses during carcinogenesis. Mini-Reviews in Medicinal Chemistry, 2010, 10: 492-505.

4) Girish B. Maru, Asha G. Ramchandani, **Gaurav Kumar**, Rachana Garg. Curcumin-mediated cellular responses in chemical carcinogenesis: In vivo Studies. Chapter Xth, 181-204, 2010.Bioactive foods and Extracts Cancer treatment and Prevention.Edited By Ronald Ross Watson and Victor R. Preedy.

Signature of Student:

Date:

LIST OF ABBREVIATIONS

ABC	Avidin-biotin conjugate
ADP	Adenosine diphosphate
AhR	Aryl hydrocarbon receptor
AhRE	Aryl hydrocarbon receptor regulatory element
AHH	Aryl hydrocarbon hydroxylase
AMP	Adenosine monophosphate
APN	Aminopeptidase N
ANOVA	Analysis of variance
AP-1	Activated protein-1
APS	Ammonium persulfate
ARNT	Aryl hydrocarbon nuclear translocator
ARE	Antioxidant response element
ATP	Adenosine tri-phosphate
bHLH	Basic helix-loop-helix
B(a)P	Benzo(a)pyrene
Blk	Blank
BME	β-Mercaptoethanol
BPB	Bromophenol blue
BPDE	Benzo(a)pyrene diol epoxide
BSA	Bovine serum albumin
C	Catechin
Cox-2	Cyclooxygenase-2
CPM	Counts per minute
CYP 450	Cytochrome P-450
DAB	Diaminobenzidine
DAG	Diacylglycerol
DAPI	4', 6-diamidino-2-phenylindole
DEN/ NDEA	Diethylnitrosoamine/ N-Nitrosodiethylamine
D/W	Distilled water
DMBA	7,12-Dimethylbenz(a)anthracene
DMSO	Dimethyl sulphoxide
DNA	Deoxyribonucleic acid
DPA	Diphenylamine
DMEM	Dulbecco's modified Eagle's medium
DTT	Dithiothreitol
EC	Epicatechin
ECG	Epicatechin gallate
ECL	Enhanced chemiluminescence
ECOD	Ethoxycoumarin *O*-dealkylase
EDTA	Ethylene diaminetetraacetic acid
EGTA	Ethylene glycol tetra acetic acid
EGC	Epigallocatechin
EGCG	Epigallocatechin gallate
EIA	Enzyme immuno assay
ERK	Extracellular-signal-regulated protein kinase
FBS	fetal bovine serum
FT-IR	Fourier-transformed infra red
GC	Gallocatechin

GCG	Gallocatechin gallate
GSH	Glutathione reduced
GST	Glutathione S-transferase
GSSG	Glutathione oxidized
HBP	Hamster buccal pouch
H & E	Haematoxylin and eosin
HEPES	(N-[2-Hydroxyethyl] piperazine-N'-[2-ethanesulfonic acid]) sodium salt
HPO_3	Meta phosphoric acid
HRP	Horseradish peroxidase
Hsp	Heat-shock protein
IAP	Inhibitor of apoptosis protein
IHC	Immunohistochemical staining
I3C	Indole-3-carbinol
ILs	Interleukins
ITC	Isothermal titration calorimetry
i.p.	Intraperitoneal
IKK	Inhibitory kappa B kinase
IκB-α	Inhibitor of NF-κB
KCl	Potassium chloride
LSC	Liquid scintillation counter
MAPK	Mitogen activated protein kinase
MgCl2	Magnesium chloride
ml	Millilitre
mmol	Millimoles
M	Molar
mM	Millimolar
MS	Mass spectrometry
MRP	Multidrug resistance proteins
μg	Microgram
μl	Microlitre
NaCl	Sodium chloride
NADPH	Nicotinamide adenine dinucleotide phosphate, reduced
Na3VO4	Sodium orthovanadate
NNK	4-(N-methylnitrosamino)-1-(3-pyridyl)-1-butanone
NF-κB	Nuclear factor-kappa B
nmol	Nanomoles
NaF	Sodium fluoride
NEM	N-ethylmaleimide
NMR	Nuclear magnetic resonance
NQO1	NAD(P)H quinone oxidoreductase1
Nrf2	NF-E2-related factor-2
Nrf1	NF-E2-related factor-1
NSAIDs	Non-steroidal anti-inflammatory drugs
NSB	Nonspecific binding
ODC	Ornithine decarboxylase
OPT	*O*-Phthalaldehyde
p38	p38 protein kinase
pmol	Picomoles
PAGE	Polyacrylamide gel electrophoresis

PAHs	Polycyclic aromatic hydrocarbons
PBP	Polymeric black tea polyphenol
PBPE	Polymeric black tea polyphenol extract
PBS	Phosphate buffer saline
PCNA	Proliferating cell nuclear antigen
PI(3,4,5)P3	Phosphatidylinositol 3,4,5-triphosphate
PI(3,4,)P2	Phosphatidylinositol 3,4,5-triphosphate
PI(4,5)P2	Phosphatidyl-inositol 4,5-bisphosphate
PI3K	Phosphatidylinositol 3-kinase
PDK	Phosphatidylinositol-dependent kinase
PH	Pleckstrin-homology
p-ERK	Phosphorylated extracellular signal-regulated kinase
p-JNK	Phosphorylated c-Jun N-terminal kinase
PGE-2	Prostaglandin E-2
PI3K	Phosphoinositide 3-kinase
PKC	Protein kinase C
POPOP	1,4-bis[5-phenyl-2-oxazolyl] benzene;2,2'-p-phenylene-bis[5-phenyloxazole]
PPO	Polyphenol oxidase
PMSF	Phenyl methane sulphonyl fluoride
PVDF	Polyvinylidene difluoride
RT	room temperature
RNA	Ribonucleic Acid
RNase	Ribonuclease
ROS	Reactive oxygen species
RT	Room temperature
SCC	Squamous cell carcinoma
SDS	Sodium dodecyl sulfate
TA	Total activity
TBS	Tris-buffered saline
TEMED	N, N, N', N' - Tetramethylene diamine
TFs	Theaflavins
TPA	12-O-tetradecanoylphorbol-13-acetate
THC	Tetrahydrocurcumin
TFu	Theafulvins
TGF-α / -β	Transforming growth factor -α / -β
TLC	Thin layer chromatography
TNF-α	Tumor necrosis factor -α
TPA	12-O-Tetradecanoyl phorbol-13-acetate
TRs	Thearubigins
TBS	Tris buffer saline
T-TBSL	Tween-20-tris-buffered saline
TUNEL	Terminal deoxynucleotidyl transferase biotin-dUTP nick end labeling
UV	Ultraviolet
VEGF	Vascular endothelial growth factor
XRE	Xenobiotic response element

LIST OF TABLES

Table No.	Table Title	Page No.
Table 1.1	Polyphenol content of green and black tea	18
Table 1.2	*In vivo* chemopreventive effects of black tea extract/polyphenols/constituents in different rodent models	20
Table 1.3	*In vivo* chemopreventive effects of turmeric/curcumin in different rodent models	33
Table 3.1	Lysis buffer (for total cell lysate) composition	44
Table 3.2	Composition of buffer A (for cytosolic fraction)	46
Table 3.3	Composition of buffer B (for nuclear fraction)	46
Table 3.4	Composition of buffer	47
Table 3.5	Effective range of separation of SDS-polyacrylamide gels	49
Table 3.6	Composition of resolving gel	49
Table 3.7	Composition of stacking gel	50
Table 3.8	Buffer compositions for SDS-PAGE	51
Table 5.1	Incidence, multiplicity and volumes of tumors in various treatment groups	109
Table 5.2	Tumor volumes in HBP in animals belonging to different treatment groups, experiment 3	110
Table 5.3	Tumor volumes in HBP in animals belonging to different treatment groups, experiment 4	112
Table 7.1	Effects of dietary curcumin on B(a)P-induced lung tumors incidence and multiplicity in A/J mice	172
Table 7.2	Relative differences (%) in incidence, multiplicity and area of lung tumors/microscopic lesions in B(a)P and curcumin + B(a)P treated A/J mice	173
Table 7.3	Effect of dietary curcumin on B(a)P-induced microscopic pulmonary lesions numbers in A/J mice	175
Table 7.4	Effect of dietary curcumin on area of B(a)P-induced microscopic pulmonary lesions in A/J mice	175

LIST OF FIGURES

Figure No.	Figure Title	Page No.
Fig 1.1	(A) Mechanisms of normal and cancer cell division (B) Benign vs. Malignant Tumors	1
Fig 1.2	Different types of cancer	2
Fig 1.3	Hallmarks of cancer	3
Fig 1.4	Different stages of carcinogenesis	8
Fig 1.5	Schematic diagram showing multistep process of carcinogenesis and steps at which chemopreventive agents exhibit their biological effects and observed defense mechanisms in experimental systems *in vivo*	9
Fig 1.6	Representative chemopreventive phytochemicals and their dietary sources	13
Fig 1.7	Path for optimum evaluation of dietary constituents as chemopreventive agents	15
Fig 1.8	Methods of manufacturing process of different types of tea	17
Fig 1.9	Structure of major polyphenols in green and black tea	19
Fig 1.10	Percentile composition of the different classes of phenolics in the green and black tea	19
Fig 1.11	Chemical structures of curcumin(s)	24
Fig 4.1	Solid (tea powder) – liquid extraction of polymeric black tea polyphenols (PBPs), employing the Soxhlet continuous extractor	66
Fig 4.2	Polymeric black tea polyphenol (PBPs) fractions	73
Fig 4.3	Thin layer chromatogram of different green and black tea polyphenols for confirming the purity of PBPs fractions	73
Fig 4.4	Effect of PBPs 1-3 and curcumin on the levels of TPA-induced PKC isoforms in cytosolic and particulate cell lysate from mouse skin epidermis - Representative blots and relative P/C+P O.D.	75
Fig 4.5	Effect of PBPs 1-3 and curcumin on the levels of TPA-induced PKC isoforms in cytosolic and particulate cell lysate from mouse skin epidermis - Relative cytosolic and particulate fraction O.D.	76
Fig 4.6	Effect of PBPs 4 and 5, EGCG and Ro-31-8220 on the levels of TPA-induced PKC isoforms in cytosolic and particulate cell lysate from mouse skin epidermis - Representative blots and relative P/C+P O.D.	77
Fig 4.7	Effect of PBPs 4 and 5, EGCG and Ro-31-8220 on the levels of TPA-induced PKC isoforms in cytosolic and particulate cell lysate from mouse skin epidermis- Relative cytosolic and particulate fraction O.D.	78
Fig 4.8	Effect of PBPs 1-5, curcumin, EGCG and Ro-31-8220 on PKC activity in cytosolic and particulate cell lysate from mouse skin epidermis	79
Fig 4.9	Effect of PBP-3 or PBP-5 on TPA-induced localization of PKC isoforms (α and δ) in epidermal layer of mouse skin by confocal microscopy	81
Fig 4.10	Effect of EGCG on TPA-induced localization of PKC isoforms (α	83

	and δ) in epidermal layer of mouse skin evaluated by confocal microscopy	
Fig 4.11	Effect of Ro-31-8220 on TPA-induced localization of PKC isoforms (α and δ) in epidermal layer of mouse skin evaluated by confocal microscopy	84
Fig 4.12	Effect of PBP-3 or PBP-5 on the levels of TPA-induced PKCα in cytosolic and particulate cell lysate from HaCat cells	85
Fig 4.13	Effect of PBP-3 or PBP-5 on TPA-induced localization of PKC isoforms (α and δ) in HaCat cells by confocal microscopy	86
Fig 4.14	Effect of PBP-3 or PBP-5 on TPA-induced levels of PKC and AKT in particulate cell lysate from mouse skin epidermis	87
Fig 4.15	Effect of PBP-3 or PBP-5 on TPA-induced levels and activity of PKC in particulate cell lysate from mouse skin epidermis	89
Fig 4.16	Effect of PBP-3 or PBP-5 on TPA-induced levels and activity of PDK1 and AKT1 in particulate cell lysate from mouse skin epidermis	91
Fig 4.17	Effect of PBP-3 or PBP-5 on TPA-induced levels and activity of PI3K in particulate cell lysate from mouse skin epidermis	92
Fig 4.18	Effect of PBP-3 or PBP-5 on TPA-responsive markers in cell lysate from mouse skin epidermis	94
Fig 4.19	Effect of PBP-3 or PBP-5 on TPA-induced activation of nuclear transcription factor related proteins in mouse skin epidermis and HaCat cells	95
Fig 4.20	UV-Vis spectra of PBP-3 or PBP-5 or TPA and their mixtures	96
Fig 4.21	Titration microcalorimetry of TPA by PBP-3 or PBP-5	97
Fig 5.1	Experimental design for evaluating the effects of dietary turmeric post-treatment on DMBA-induced HBP tumors	104
Fig 5.2	Effect of dietary-turmeric (1%) post-treatment on DMBA-induced tumor volume and tumor multiplicity in HBP tumors	111
Fig 5.3	Effect of dietary-turmeric (1%) post-treatment on DMBA-induced HBP tumors	114
Fig 5.4	Effect of dietary turmeric (1%) post-treatment on DMBA-induced apoptosis-related markers in HBP tumor tissue - Representative blots, levels and immunohistochemical analysis of Bax and Bcl-2	115
Fig 5.5	Effect of dietary turmeric (1%) post-treatment on DMBA-induced apoptosis-related markers in HBP tumor tissue - Apoptotic index and representative blots and levels of caspase-3, caspase-9 and cytochrome c	117
Fig 5.6	Effect of dietary turmeric (1%) post-treatment on DMBA-induced apoptosis-related markers in HBP tumor tissue - Representative blots and levels of p53 and p21 and p53 Labeling index	118
Fig 5.7	Effect of dietary turmeric (1%) post-treatment on DMBA-induced survivin in HBP tumor tissue	119
Fig 5.8	Effect of dietary turmeric (1%) post-treatment on DMBA-induced cell proliferation markers in HBP tumors tissue	120
Fig 5.9	Effect of dietary turmeric (1%) post-treatment on DMBA-mediated alterations in transcription factors related proteins	121
Fig 5.10	Effect of dietary turmeric (1%) post-treatment on DMBA-mediated alterations in cytosolic NF-κB family proteins	123

Fig 5.11	Effect of dietary turmeric (1%) post-treatment on DMBA-mediated alterations in MAPK proteins	123
Fig 5.12	Effect of dietary turmeric (1%) post-treatment on DMBA-induced inflammatory response in HBP tumor tissue	125
Fig 6.1	Experimental design for studying the effect of curcumin post-treatment on disappearance of BPDE-DNA adducts in mouse tissues	133
Fig 6.2	Representation of digital image analysis algorithm to calculate the levels of BPDE-DNA adducts and apoptotic nuclei in photomicrographs of mouse tissue sections	137
Fig 6.3	Effect of curcumin post-treatment on B(a)P-induced alterations in tissue of mice (Experiment 1)	138
Fig 6.4	Effect of curcumin post-treatment on B(a)P-induced alterations in tissue of mice (Experiment 2)	139
Fig 6.5	Effect of curcumin post-treatment on levels of BPDE-DNA adducts in mouse liver (Experiment 1)	141
Fig 6.6	Effect of curcumin post-treatment on levels of BPDE-DNA adducts in mouse lungs (Experiment 1)	142
Fig 6.7	Effect of curcumin post-treatment on levels of BPDE-DNA adducts in mouse liver (Experiment 2)	144
Fig 6.8	Effect of curcumin post-treatment on levels of BPDE-DNA adducts in mouse lungs (Experiment 2)	145
Fig 6.9	Levels of BPDE-DNA adducts in mouse liver and lungs (Experiments 1 and 2)	146
Fig 6.10	Effect of curcumin post-treatment on apoptosis in B(a)P-treated mouse liver (Experiment 1)	148
Fig 6.11	Effect of curcumin post-treatment on apoptosis in B(a)P-treated mouse lungs (Experiment 1)	149
Fig 6.12	Effect of curcumin post-treatment on apoptosis in B(a)P-treated mouse liver (Experiment 2)	151
Fig 6.13	Effect of curcumin post-treatment on apoptosis in B(a)P-treated mouse lungs (Experiment 2)	152
Fig 6.14	Levels of apoptosis in mouse liver and lungs (Experiments 1 and 2)	153
Fig 6.15	Effect of curcumin post-treatment on apoptosis-related biochemical markers in B(a)P-treated mouse liver (Experiment 1).	155
Fig 6.16	Effect of curcumin post-treatment on apoptosis-related biochemical markers in B(a)P-treated mouse lungs (Experiment 1).	156
Fig 6.17	Effect of curcumin post-treatment on apoptosis-related biochemical markers in B(a)P-treated mouse liver (Experiment 2)	158
Fig 6.18	Effect of curcumin post-treatment on apoptosis-related biochemical markers in B(a)P-treated mouse lungs (Experiment 2)	159
Fig 6.19	Effect of curcumin post-treatment on cell proliferation markers in B(a)P-treated mouse tissues (Experiments 1 and 2)	161
Fig 6.20	Levels of PCNA in mouse liver and lungs	162
Fig 7.1	Experimental design for studying the effect of curcumin treatment on B(a)P-induced lungs tumors A/J mouse model	168
Fig 7.2	Haematoxylin & Eosin (H & E) stained images of representative cross-sections of normal lungs tissues from animals belonging to vehicle control group	173
Fig 7.3	Different microscopic proliferative lesions in the B(a)P-induced lung tumors of A/J mouse (Based on recommendations published by the	173

	Mouse Models of Human Cancer Consortium)	
Fig 7.4	Haematoxylin & Eosin (H & E) and tile scan images of representative cross-sections of left lung lobe from animals belonging to different treatment groups	174
Fig 7.5	Effect of curcumin treatment on apoptosis-related markers in B(a)P-treated mouse lungs/lung tumors	177
Fig 7.6	Effect of curcumin treatment on apoptosis-related markers in B(a)P-treated mouse lungs measured by immunohistochemical staining	178
Fig 7.7	Effect of curcumin treatment on apoptotic index in B(a)P-treated mouse lungs measured by TUNEL assay	179
Fig 7.8	Effect of curcumin treatment on cell proliferation markers in B(a)P-treated mouse lungs/lung tumors	180
Fig 7.9	Effect of curcumin treatment on cell proliferation markers in B(a)P-treated mouse lungs measured by immunohistochemical staining	181
Fig 7.10	Effect of curcumin treatment on AKT phosphorylation in B(a)P-treated mouse lungs measured by immunohistochemical staining	182
Fig 7.11	Effect of curcumin treatment on cell inflammation markers in B(a)P-treated mouse lungs/lung tumors	183
Fig 8.1	Summary of in vivo chemopreventive effects of turmeric/curcumin and/or black tea extract/polyphenols and underlying mechanisms	192

1.1 CANCER

Cancer is a complex group of diseases characterized by the loss of control of cellular growth leading to uncontrolled and abnormal proliferation of cells with potential to spread to other organs. Agents inducing cancer are known as carcinogens. In cancer, cells divide and grow uncontrollably, forming tumors. Tumors can be either benign or malignant (Fig. 1.1A).

Benign tumors are not cancerous, mean these are tumors with self-limited growth which do not invade or metastasize, although some benign tumors may become malignant. These types of tumor grow slowly and can usually be removed and do not come back in most cases, whereas **malignant tumors** can invade and damage the nearby tissues and spread to other parts of the body usually through bloodstream or lymphatic system to form secondary tumors in other parts of the body via a process known as metastasis (Fig. 1.1B).

(A) (B)

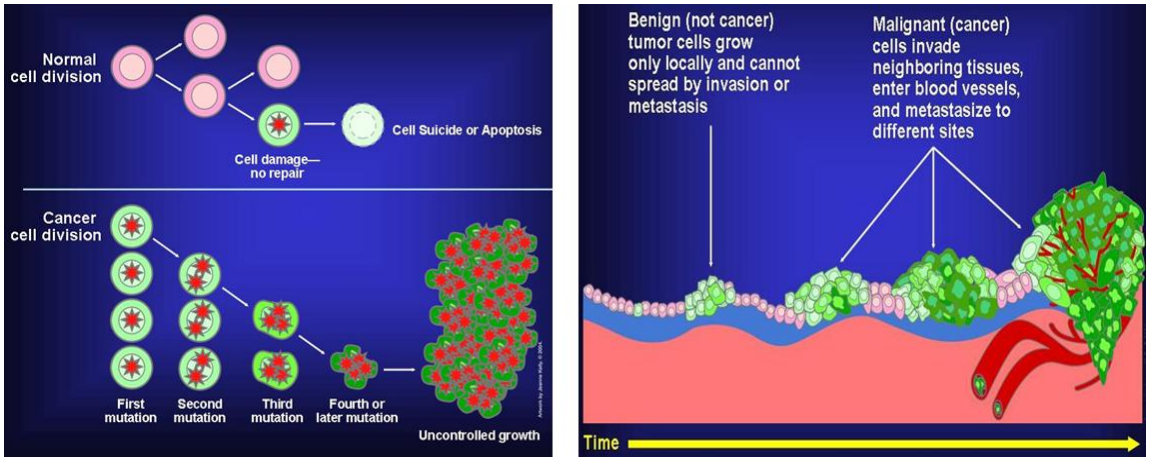

FIGURE 1.1: (A) Mechanisms of normal and cancer cell division (B) Benign vs. Malignant Tumors (Adapted from http://www.cancer.gov/cancertopics/understanding cancer/cancer).

1.2 TYPES OF CANCER

Each cancer is unique in the way it grows and develops, its chances of spreading, the way it affects one's body and the symptoms one may experience. Several factors, including location and how the cancerous cells appear under the microscope, determine how cancer is diagnosed. Cancers are classified by the type of cell that the tumor cells resemble and are therefore presumed to be the origin of the tumor. These are the histology and the location, respectively (Fig. 1.2). These types include:-

1.2.1 Carcinoma: Malignant tumors derived from epithelial cells. It is a tumor that arises in the tissues that line the body`s organs like the colon, the penis, breast, prostrate, urinary bladder, and the ureter. About 80% of all cancer cases are carcinomas. This group includes many of the most common cancers and includes nearly all those developing in the breast, prostate, lung, pancreas and colon.

1.2.2 Sarcoma: Malignant tumors derived from the connective tissues or mesenchymal cells. These are tumors that originate in bone, muscle, cartilage, fibrous tissue or fat. Ewing sarcoma (Family of tumors) and Kaposi`s sarcoma are the common types of sarcomas.

1.2.3 Leukemia and Lymphoma: Malignancies derived from hematopoietic (blood-forming) cells. These are cancers of the blood or blood-forming organs. When leukemia develops, the body produces a large number of abnormal blood cells. In most types of leukemia, the abnormal cells are white blood cells. Leukemia can either be acute or chronic, whereas lymphomas affect the lymphatic system, a network of vessels and nodes that acts as the body's filter. There are over 20 types of lymphoma. Hodgkin`s disease is one type of lymphoma.

- ✓ **Germ cell tumor**: Tumors derived from totipotent cells, most often present in the testicles or the ovary (seminoma and dysgerminoma, respectively).
- ✓ **Blastoma**: Tumors derived from immature "precursor" cells or embryonic tissue. Many of these tumors are more common in children than in older adults.

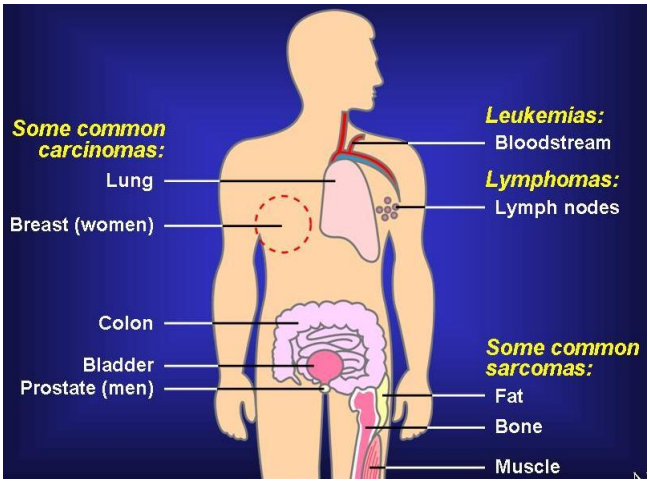

FIGURE 1.2: Different types of cancer (Adapted from http://www.cancer.gov/cancertopics/understandingcancer/cancer).

Hanahan and Weinberg, 2011, suggested that the complexity of vast catalogue of cancer cell genotypes is a manifestation of 10 essential alterations in cell physiology that collectively dictate malignant growth (Fig. 1.3) [1]. These are:-

- Self-sufficiency in growth signals
- Insensitivity to anti-growth signals
- Evading apoptosis
- Limitless reproductive potential
- Sustained angiogenesis
- Tissue invasion and metastasis
- Abnormal metabolic pathways
- Evading the immune system
- Chromosome abnormalities and unstable DNA
- Inflammation

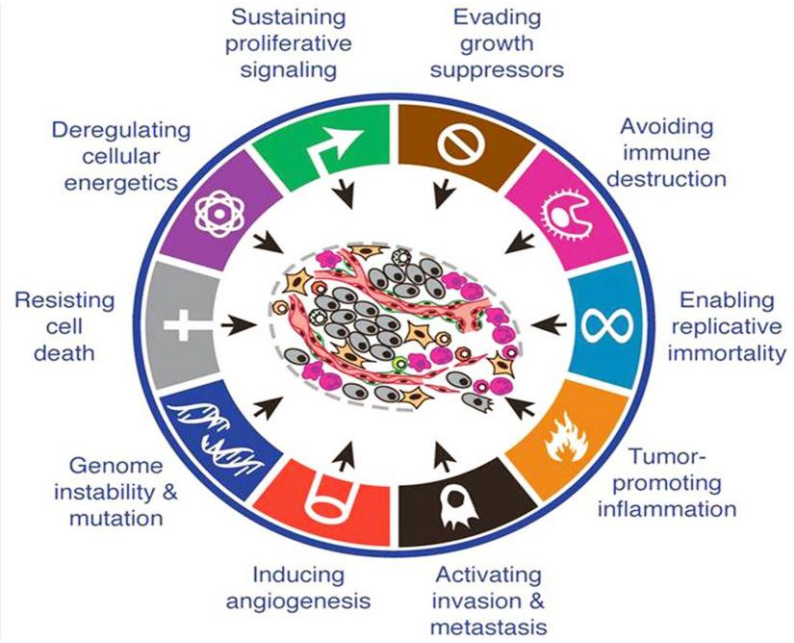

FIGURE 1.3: Hallmarks of cancer (Adapted from Hanahan and Weinberg, 2011, Cell, 144(5), 646-74) [1].

1.3 CAUSES OF CANCER

Commonly occurring human cancers have multifactorial etiology that involves complex interaction between environmental exposures and genetic/acquired host (susceptibility or protective) factors. 'Environmental exposures' make a substantial contribution to human cancers. Common environmental factors leading to cancer death include: tobacco 25-30%, diet 30-35%, infections 15-20%, obesity 10-20%, alcohols 4-

6% and other environmental agents/factors 10-15%. These environmental factors cause abnormalities in the genetic material of cells. Cancer continues to be one of the major causes of death worldwide and only modest progress has been made in reducing the morbidity and mortality of this dreadful disease. The causative agents of cancer can be classified in brief as biological agents like infections caused by certain viruses, physical agents like radiations and chemical agents.

1.3.1 Environmental agents: Radiations in the environment like X-rays and UV rays damage DNA and increase the risk of cancer like leukemia, melanoma and skin cancer.

1.3.2 Biological agents: This includes viruses which cause genetic changes in the cell leading to cancer. Examples of cancer causing viruses are Human Papilloma virus (cervical carcinoma), Human polyomavirus (brain tumor), Epstein Barr virus (B-cell lymphoproliferative disease and nasopharyngeal carcinoma), Hepatitis B and C virus (hepatocellular carcinoma), Human T-cell leukemia virus-1 (T-cell leukemia) etc.

Experimental and epidemiological data imply a causative role for viruses and they appear to be the second most important risk factor for cancer development in humans, exceeded only by tobacco usage.

1.3.3 Physical agents: Radiation can be classified as physical agents that can cause cancer. High levels of radiation like those from radiation therapies and x-rays (repeated exposure) can damage normal cells and increase the risk of developing leukemia, as well as cancers of the breast, thyroid, lungs, stomach and other organs. UV radiations from the sun are directly linked to the melanoma and other forms of skin cancer. These harmful rays of the sun cause premature aging and damage the skin. Artificial sources of UV radiation, such as sun lamps and tanning booths, also increase the risk of skin cancer.

1.3.4 Chemical agents: A chemical agent which causes cancer is known as the chemical carcinogen. Long term exposure to chemicals such as pesticides, uranium, nickel, asbestos, radon, benzene etc. can increase the chances of cancer in the exposed cell. Such carcinogens may act alone or in combination with another carcinogen, such as cigarette smoke, to increase the risk of cancer and other lungs diseases. Cigarette smoking and regular exposure to tobacco smoke greatly increase lungs cancer. Cigarette smokers are more likely to develop several other types of cancer like those of the mouth, larynx, esophagus, pancreas, bladder, kidney and cervix. Smoking may also increase the

likelihood of developing cancers of the stomach, liver, prostate, colon and rectum. The uses of other tobacco products, such as chewing tobacco, are linked to cancers of the mouth, tongue and throat. Heavy drinkers face an increased risk of cancers of the mouth, throat, esophagus, larynx and liver. Some studies suggest that even moderate drinking may slightly increase the risk of breast cancer.

1.3.5 Risk factors: Factors like diet, lifestyle, age, physical activity, immunity and inheritance play an important role in development of cancer in an individual.

1.4 TREATMENT OF CANCER

The primary way to reduce the incidence of cancer would be elimination of all the potential cancer causing agents from the environment. The treatment of cancer includes surgery, chemotherapy or radiation therapy. In addition, immunotherapy and biological therapy are also used to treat cancer. Treatment of cancer is decided on the basis of the location and stage of cancer and spread of tumor. Also factors like age and immunity are considered while suggesting the treatment.

1.4.1 Surgery: It is the removal of tumor or cancerous cells from the body. It is one of the ways to prevent the spread of cancer to other body parts and diagnose the stage of cancer. It is often performed in conjunction with chemotherapy or radiation therapy. For those whose cancer is not treatable, palliative surgery may be an option to relieve pain that may be caused by the cancer. Palliative surgery is not intended to treat or cure the cancer, or even to prolong life, but more to lessen discomfort. Surgery can be regarded as temporary cure. Even if few cancerous cells are left behind there are always chances of reoccurrence of cancer.

1.4.2 Chemotherapy: Chemotherapy (also called chemo) is the type of treatment that uses drugs to treat cancer. The drug is given either as pills or intravenously. The drugs generally target the multiplying cancer cells and work by stopping or slowing the growth of cancer cells, which grow and divide quickly. But it has the disadvantage of being non specific in its action and so it also affects those tissues which are not cancerous i.e. it also affects the normal growing cells in the body like hair follicles and has many side effects like nausea, vomiting, bleeding, diarrhea, mouth ulcers, skin rashes, fall in blood pressure, weakness, numbness, fever, liver and kidney damage, lungs scarring, sterility, bone marrow damage, and many more side effects. The cytotoxic drugs used in the

chemotherapy affects many other tissues of body and may lead to complications rather than cure. Single drug is given or drugs are given in combinations and are also given along with surgery and radiation.

1.4.3 Radiation: Radiation therapy is also an extensively used therapy. Cancer cells or tumors are targeted with high energy radiations like gamma rays which damage the DNA of the cancer cells making them unable to multiply leading to shrinkage of tumor. But like chemotherapy, radiation also damage and kills the surrounding normal and healthy cells. This treatment can also be given with chemotherapy and surgery.

1.4.4 Biological therapy: Biological therapy is a type of treatment that works with your immune system. Some types of targeted therapies work by blocking the biological processes of tumors that allow tumors to thrive and grow. Other types of therapies cut off the blood supply to the tumor, causing it to basically starve and die because of a lack of blood. Targeted therapy is used in selected types of cancer and is not available for everyone. It is given in conjunction with other cancer treatments.

1.5 DISADVANTAGES OF CURRENT CANCER TREATMANTS

They are non-specific, costly and not full-proof. These treatments are useful only to some extent and not successful in reducing the mortality rate of cancers in past 50 years. Although chemotherapy and/or radiotherapy have long been practiced to combat cancer, it may only contribute to patient's survival with compromised quality of life. All these methods, which are currently used, have many side effects and are not very effective in reducing the death rates due to cancers. Moreover, an increasing trend of chemo/radio-resistance and the recurrence of secondary tumors result in limitations in the fight against cancer. In this context, the approach of cancer prevention by major changes in lifestyle such as decline in tobacco use and obesity and the use plant foods- i.e. non-toxic chemical/dietary entities termed 'chemoprevention', is considered to be an alternative, probably more realistic, cost effective and fundamental strategy for the control of this dreaded disease. In fact, alternative agents obtained from various plants to prevent or slow down/delay cancer initiation/promotion/progression have garnered great interest in understanding the efficacy and/or limitations in experimental studies and clinical trials.

1.6 CANCER CHEMOPREVENTION

This term was initially coined by Michael Sporn in 1970. Cancer chemoprevention can be defined as the use of natural or synthetic compounds to prevent, suppress or delay the development of clinically detectable cancer or invasive carcinoma [2-4]. This is a "prescription" approach and may form an adjunct to other cancer control and prevention strategies. The primary goal of chemoprevention research is to identify effective agents and/or develop efficient strategies for clinical trials and ultimately, application to human populations. Chemoprevention offers a promising approach to primary cancer prevention for a variety of organ systems. Based on empirical experiments and clinical evaluations many compounds belonging to diverse chemical classes have been identified as potential chemopreventive agents [5]. These include vitamins, minerals, naturally occurring phytochemicals and synthetic compounds. The scientific rationale for the use of cancer chemoprevention is based on the multi-step nature of carcinogenesis [6].

1.7 CARCINOGENESIS

Carcinogenesis is a complex, multi-step and multi-factorial process characterized by at least three stages viz. initiation, promotion and progression (Figs. 1.4 and 1.5).

Initiation, an irreversible event, begins when the cells in normal tissues are exposed to carcinogen and their genomic DNA undergoes damage and subsequent fixation of the damage. In case of chemically-induced carcinogenesis, initiation involves uptake of a given carcinogenic agent with subsequent distribution and transport to organs and tissues where metabolism occurs, the interaction of a reactive metabolite with cellular DNA with subsequent structural alterations in the DNA molecule, and final fixation of the genotoxic damage to cause mutation (Figs. 1.4 and 1.5).

Promotion refers to clonal expansion of initiated cells to form an actively proliferating multi-cellular pre-malignant tumor cell population. In early stages, it is reversible process. In this the initiated/ mutated cell is susceptible to the effect of promoters which promote the clonal expansion of the initiated cells giving rise to the large number of daughter cells containing the mutation created by the initiator. Eventually

a benign tumor becomes evident. This step is reversible at the early stage but irreversible at the later stage. Promoters bind to receptors on the cell surface in order to affect intra-cellular pathways that lead to increased cell proliferation. In human cancers, hormones, cigarette smoke, or bile acids are substances that are involved in promotion (Figs. 1.4 and 1.5).

Progression, an irreversible process which produces a new clone of tumor cells with increased proliferative capacity, invasiveness and metastatic potential. The term progression, coined by Leslie Foulds, refers to the stepwise transformation of a benign tumor to a neoplasm and to malignancywhich is irreversible process.Progression is associated with a karyotypic changes coupled with an increased growth rate, invasiveness, metastasis and an alteration in biochemistry and morphology (Figs. 1.4 and 1.5).

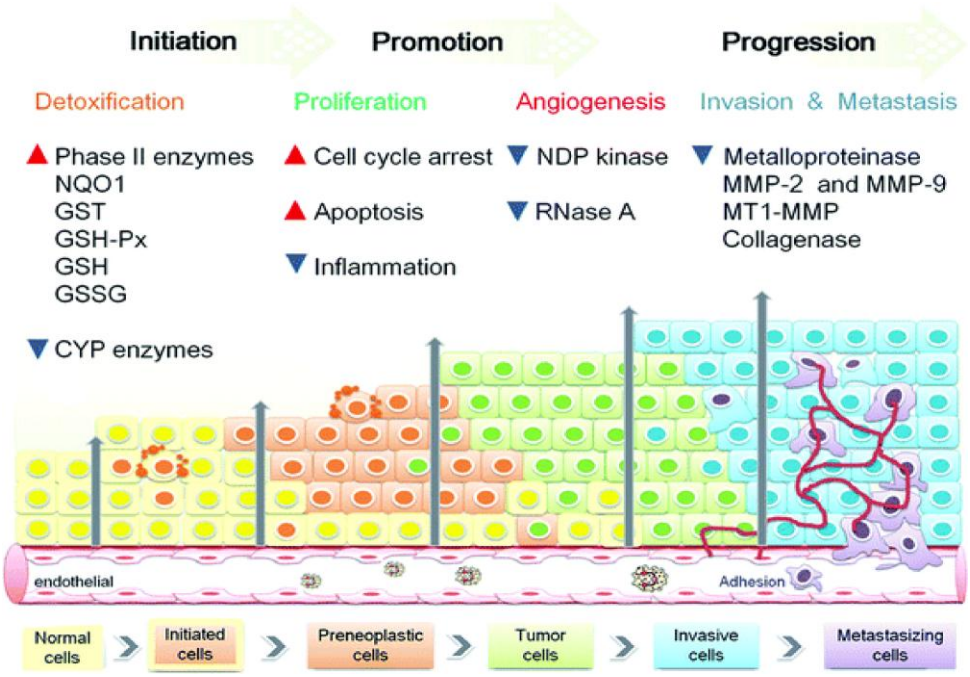

FIGURE 1.4: Different stages of carcinogenesis (Adapted from Pan et al., 2011, Food & Function, 2(2), 101-10) [7].

Compounds that inhibit any stage of carcinogenesis and delay or prevent cancer are called as chemopreventive agents. Based on their mode of action, chemopreventive agents can be classified into two groups [8](Fig. 1.5).

a) Blocking agents, which impede the initiation stage either by inhibiting the formation of carcinogens or preventing the carcinogens from reaching the target sites, from

undergoing metabolic activation or, from subsequently interacting with crucial cellular macromolecules (for example, DNA, RNA and proteins) [6].

b) Suppressing agents, which arrest or reverse the promotion and progression of cancer, mainly by affecting or perturbing crucial factors that control cell proliferation, differentiation, senescence or apoptosis (Fig. 1.5).

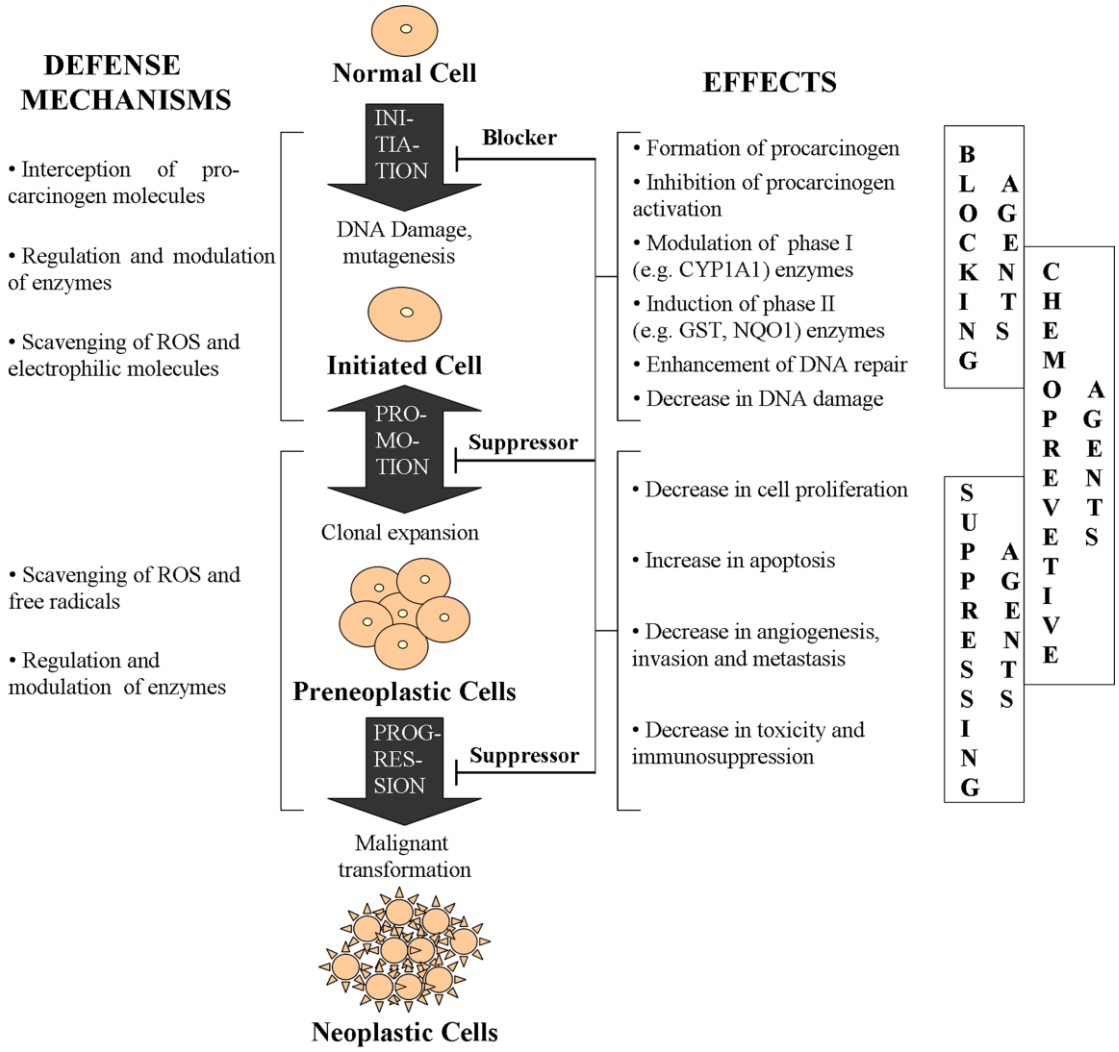

FIGURE 1.5: Schematic diagram showing multistep process of carcinogenesis and steps at which chemopreventive agents exhibit their biological effects and observed defense mechanisms in experimental systems *in vivo* (Modified from Maru et al., 2013; Book-Polyphenols in Health and Disease, Elsevier, in press) [9].

1.8 FOOD DERIVED CHEMOPREVENTIVE AGENTS

Because of their safety and the fact that they are not perceivedas "medicine," food-derived products are highly interestingfor development as chemopreventive agents that may find widespread, long-termuse in populations at normal risks. Examples include

green and black tea polyphenols, soyisoflavones, Bowman-Birk soy protease inhibitor, curcumin, phenethylisothiocyanate, sulforaphane, lycopene, indole-3-carbinol, perillylalcohol, vitamin D, vitamin E, selenium and calcium.

1.9 STAGES IN THE DEVELOPMENT OF A CHEMOPREVENTIVE AGENT FOR CLINICAL USE:

Research in the area of cancer chemoprevention can be broadly divided into following four activities: screening and identification, pre-clinical and efficacy studies, pre-clinical safety studies, and clinical development.

1.9.1 Screening for chemopreventive efficacy

Potential chemopreventive agents are subjected to rigorous *in vitro* and *in vivo* screening assays to determine their efficacies against different stages of carcinogenesis, in defined model systems and investigate the mechanism(s) of chemo-modulation [10,11]. *In vitro* assays (e.g. bacteria, mammalian cells, tissues, organ cultures, cancer cell lines, cell free extracts or biochemical reactions etc.) are employed as rapid screens for determining the chemopreventive efficacy based on modulation of different events presumed to be mechanistically linked to carcinogenesis. Chemopreventive agents are screened for their abilities to inhibit carcinogen/mutagen-induced effects (mutations, chromosomal aberrations, clastogenic effects, DNA adduct and free radical formation, DNA strand breaks, levels and activity of metabolic and repair enzymes etc.) or to inhibit cell proliferation (colony growth in soft agar, transformed cell foci or alterations in response to a known stimuli) or to enhance cell differentiation and apoptosis [12,13]. These tests have generated voluminous and useful information about the chemo-preventive properties, concentrations that might need to be achieved *in vivo,* organ specificity, toxicity of potential agents and mechanism of action of large number of environmental agents (under defined conditions). However, these properties are not always reproducible in *in vivo* systems, and the probable reasons for these are: (a) doses of chemopreventive agent(s) employed in *in vitro* studies are not achievable *in vivo,* (b) metabolic incompetence and lower inducibility of metabolic enzymes in cell lines as compared to tissues, (c) differences in absorption, distribution, metabolism and contribution of other cell types and several other organs and repair processes between the two system(s) and (d) lack of proper controls (e.g. normal cell counterpart in assays

employing cancer cell lines) leading to a differential response *in vivo.* Therefore, *in vitro* testing can only provide a pointer and actual chemopreventive potential must be evaluated through *in vivo* assay systems like animal models.

In vivo studies bridge the gap between *in vitro* testing and human situations by allowing us to take a closer look at signaling mechanisms and drug metabolism, forming an integral part of preclinical studies. In these assays, chemopreventive activity of an agent is generally investigated against carcinogen(s)-induced tumors or appropriate biomarkers in experimental animals [14-16]. However, a major drawback of assays employing animal models to study chemopreventive efficacies is shorter experimental duration than the inherent lifespan of animals. Due to this, certain adverse effects (if any) of chemopreventive agents exhibited at later time point may be missed. Several experimental studies have shown that some of the chemopreventive agent(s) have been shown to be carcinogenic under certain experimental conditions while some other agent(s) have been observed to be protective in one organ and enhance the risk in another organ [17]. Based on several of these observations, multi-organ model(s) for evaluation of chemopreventive activity of environmental agent(s) has been proposed [18]. Notably, rodents differ from humans in a number of general ways that are relevant to cancer such as mechanisms of oncogene signaling, length of telomeres, extent of karyotypic abnormalities, basal metabolic rate and non-epithelial origin of murine malignancies as compared to epithelial origin of human malignancies [19]. Therefore, it suggests that rodent models may not accurately reflect the cellular carcinogenesis processes and need extra caution in extrapolating data from murine neoplasia studies directly to humans. Nonetheless, animal studies are of prime importance not only as confirmatory studies employing various models with different dose regimes but also for better understanding of molecular pathways.

1.9.2 Clinical trials

After establishment of pre-clinical efficacy of an agent, it further undergoes phase I, II and III clinical trials to test their safety and efficacy in human situation [20, 21].

- ✓ ***Phase I trials***: These studies include evaluation of how a new drug should be given (by mouth, injected into the blood, or injected into the muscle), how often,

and what dose is safe. A phase I trial usually enrolls only a small number of patients.

- ✓ ***Phase II trials***: A phase II trial continues to test the safety of the drug, and begins to evaluate how well the new drug works. Phase II studies usually focus on a particular type of cancer.
- ✓ ***Phase III trials*:** These studies test a new drug, a new combination of drugs, or a new surgical procedure in comparison to the current standard. A participant will usually be assigned to the standard group or the new group at random (called randomization). Phase III trials often enroll large numbers of people and may be conducted at clinics and cancer centers nationwide.

Based on empirical experiments and clinical evaluations many compounds belonging to diverse chemical classes have been identified to elicit pronounced chemopreventive effects. These include vitamins, minerals, naturally occurring phytochemicals and synthetic compounds. Among various chemopreventive compounds, ***plant–derived natural compounds are receiving increasing attention as chemopreventives because of low toxicity and high tolerability***[6]. Figure 1.6 shows the representative chemopreventive phytochemicals and their dietary sources.

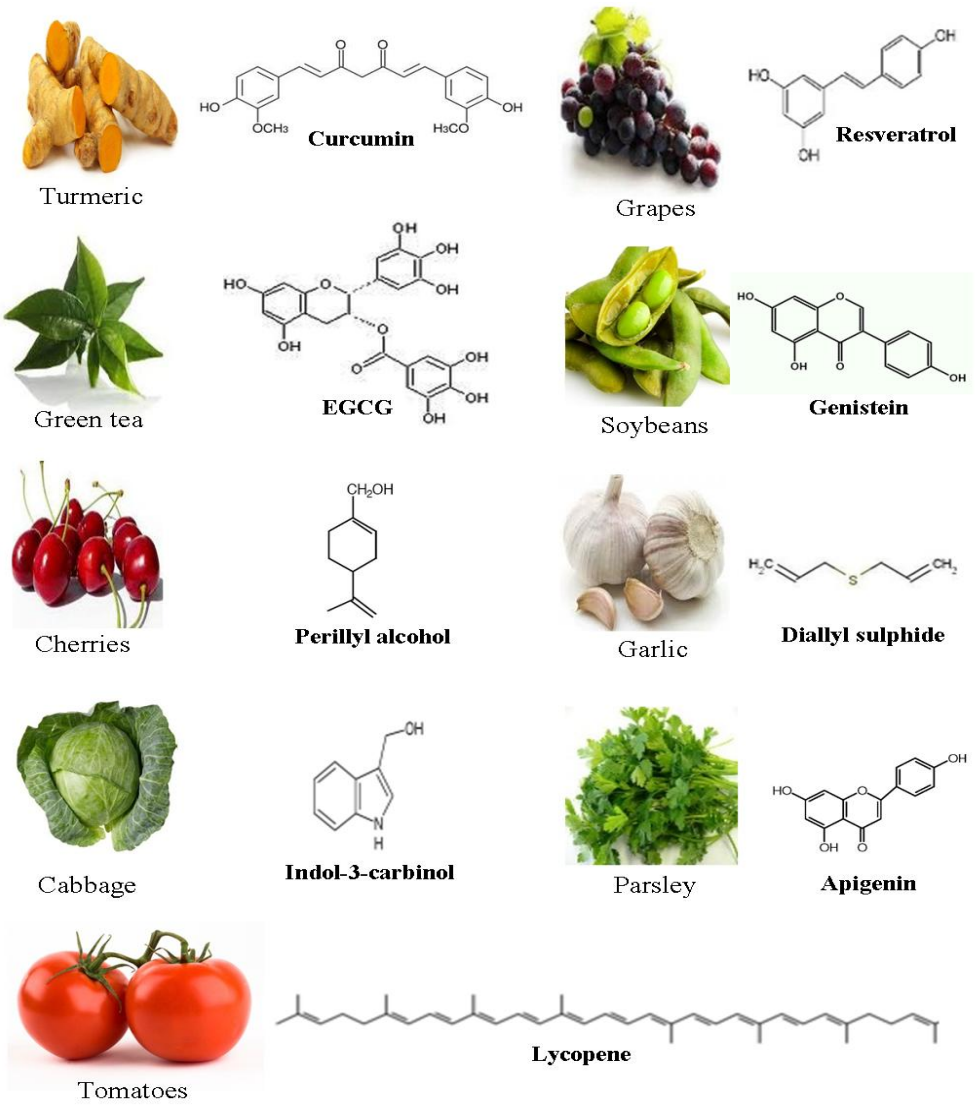

FIGURE 1.6: Representative chemopreventive phytochemicals and their dietary sources.

1.9.3 Current status and future perspectives of chemoprevention

Various epidemiological studies have indicated dietary agents to suppress and/or to prevent cancer of different organs [4]. However, most of the agents that have emerged highly promising after pre-clinical safety and efficacy studies, have failed in human trials [22]. These *failures* broadly can be grouped into two distinct outcomes:-

- ***Adverseeffects*** – inadequate knowledge about the safety of chemopreventive employed.
- ***Null effects***– These can be attributed to number of issues:
  - (a) individual differences in host susceptibility
  - (b) the choice of target population

(c) choice and dose of chemopreventive agents

(d) biomarkers / end point evaluated

(e) bioavailability problem

In particular, the failure of beta carotene trial for prevention of lungs cancer in high risk population has channelized rest of the preclinical studies on putative chemopreventive agents towards mechanistic aspects of the observed anticarcinogenic effects rather than focusing only on tumors as end points[22,23]. The advent of more sensitive assays like expressional arrays enables a bird's eye view of effect of particular chemopreventive agent at cellular, organ and entire organism level which will not only impart better understanding of the safety but also aid in identifying appropriate biomarkers [4,22].

Use of dietary agents for chemoprevention also emphasizes *nutritional studies*, which encompass certain aspects like interactions of chemopreventive supplements with normal diet and host factors [22,24,25]. Taken together, a better understanding of the mechanisms of the biological activity of dietary constituents will be pivotal for improving the chances of success for cancer-chemopreventive strategies. Also, since the existing plant-derived chemopreventive agents have attained limited success in clinical trials, there is increasing need to identify newer chemopreventive agents along with their mechanism of action. Figure 1.7 summarizes the path for optimum evaluation of dietary compounds as cancer chemopreventive agents with respect to current scenario.

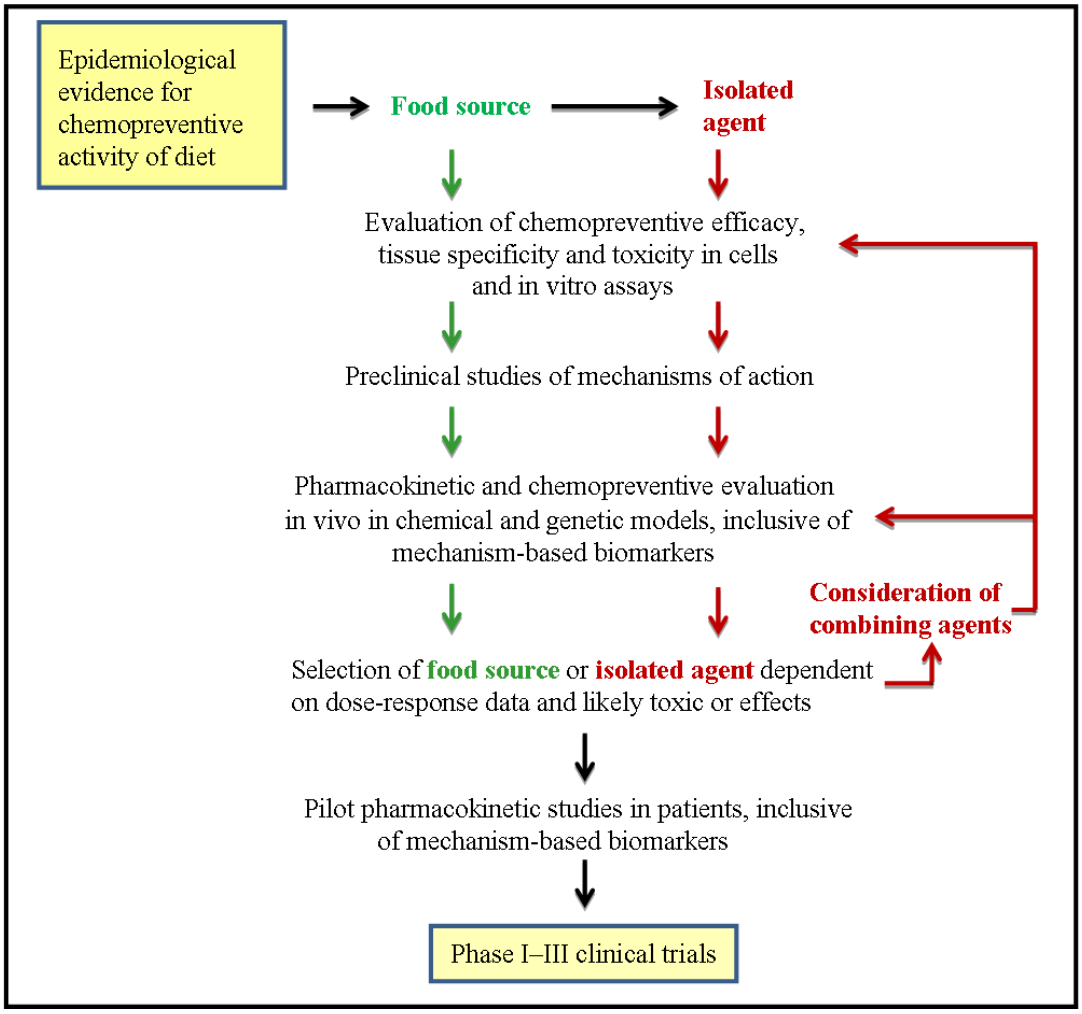

FIGURE 1.7: Path for optimum evaluation of dietary constituents as chemopreventive agents (Modified from Gescher et al., 2001, Lancet Oncology, 2, 371–79) [4].

Amongst number of dietary agents showing chemopreventive properties, turmeric/curcumin and/or tea are being considered for clinical development due to their chemopreventive properties and their perceived human safety following centuries of use in food and medicine.

1.10 TEA AND TEA POLYPHENOLS

Tea is one of the popular beverages consumed by over two third of the world population after water. Tea is an aqueous infusion prepared from the dried leaves, leaf buds and internodes of Camellia sinensis (an evergreen shrub of the Theaceae family). The tea shrub (genus *Camellia*, family Theaceae) [chromosome number (2n = 30)] is a perennial evergreen herb with its natural habitat in the tropical and sub-tropical forests of

the world. Historical references to tea dates back to 5,000 years. Tea was consumed even earlier by the indigenous people of China. Tea recorded as having medicinal value in a Chinese medical book. In Chinese and Indian traditional medicine, tea has been used for treatment of insomnia, calming effects, mental and visual clarity, thirst quenching, detoxifications of poisons, improving digestion, prevention of indigestion, breaking down oils, fats, body temperature regulation improving urination, speeding bowel evacuation, treatment of dysentery, loosening of phlegm, strengthening of teeth, treatment of epigastric pain, treatment of skin fungus, reducing hunger and longevity. Depending on the manufacturing process, tea is classified into three major types: green tea, black tea and oolong tea (Fig. 1.8). Out of total, 76-78% of tea produced and consumed (mainly consumed in Western and some Asian countries) is black tea, 20-22% is green tea (primarily in China, Japan and a few countries in North Africa and the Middle East) and 2% is oolong tea. Oolong tea production and consumption are confined to South-Eastern China and Taiwan [26,27]. Tea leaves contain more than 700 chemicals, among which the compounds closely related to human health are flavanoids, aminoacids, vitamins (C, E and K), caffeine and polysaccharides. Tea leaves also contain flavonols, such as quercetin and myricitin as well as the nitrogenous compounds, caffeine and theobromine [28].

Leaves of Camellia sinensis soon begins to wilt and oxidize if not dried quickly after picking. The leaves turn progressively darker because chlorophyll breaks down and tannins are released. This process, enzymatic oxidation, is called fermentation.

To produce green tea, freshly harvested leaves are rapidly steamed or pan-fried to inactivate enzymes, thereby preventing fermentation and producing a dry, stable product. In green tea (non-fermented), the polyphenol oxidase (PPO) enzyme present in the tea leaves is inactivated at the initial stage of tea processing to prevent oxidation of the leaf polyphenols.

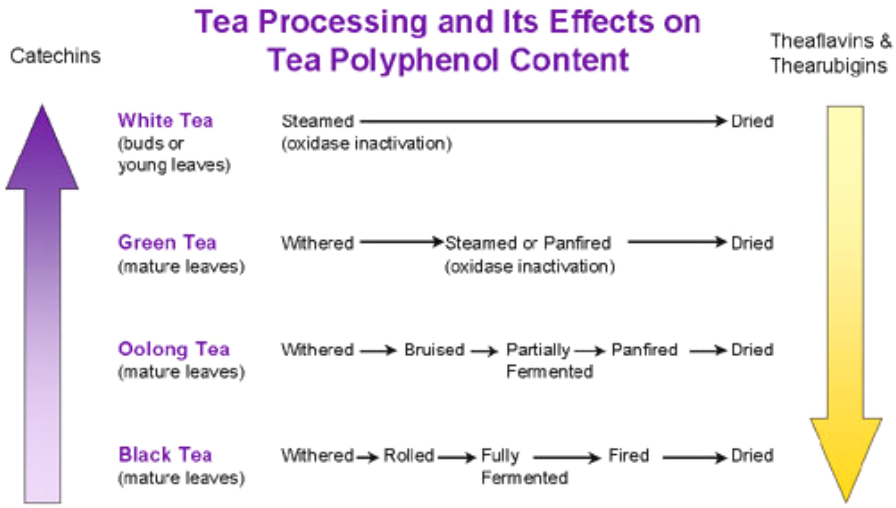

FIGURE 1.8: Methods of manufacturing process of different types of tea (Adapted from www.oregonstate.edu).

Polyphenols are the most significant group of components in tea, especially the catechin group of the flavanols. The major green tea polyphenols are: (-)-epigallocatechin-3-gallate (EGCG), (-)-epicatechin-3-gallate (ECG), (-)-epigallocatechin (EGC), (-)-epicatechin (EC), (+)-gallocatechin (GC), (+)-catechin which together may constitute 30–42% catechins of the dry leaf weight (Table 1.1) [29]. Among these, EGCG is the major polyphenol which accounts for 60% of total catechins and is believed to be the most protective agent in green tea. For the production of oolong and black teas, the fresh leaves are allowed to wither until their moisture content is reduced to <55% of the original leaf weight, which results in the concentration of polyphenols in the leaves. The withered leaves are then rolled and crushed, initiating fermentation of the polyphenols. Oolong tea is prepared by firing the leaves shortly after rolling to terminate the oxidation and dry the leaves. Normal oolong tea (semi-fermented) is considered to be about half as fermented as black tea. The fermentation process results in oxidation of simple polyphenols to more complex condensed polyphenols to give black and oolong teas their characteristic colors and flavors. During the manufacture of black tea, a major proportion of monomeric free catechins in the fresh green tea leaf undergo PPO-catalyzed oxidative polymerization, to form oligomers-theaflavins (TFs) (500-1000 Da) and polymers–polymeric black tea polyphenols (PBPs)/ thearubigins (TRs) (>1 kD) in a process commonly known as fermentation (Table 1.1) [30,31]. TFs are well characterized group of oligomeric compounds e.g. theaflavin (TF-1), theaflavin-3-gallate (TF-2a), theaflavin-3′-gallate (TF-2b) and theaflavin-3,3′-digallate (TF-3), whereas TRs are a group of

polymeric compounds and five different fractions (PBPs 1-5) have been isolated although poorly characterized[32-34] (for structures of BTPs see Fig. 1.9).

TABLE 1.1: Polyphenol content of green and black tea (Adapted from Kumar et al., 2010, MRMC, 10, 492-505) [29]

	Components	g % of dry solid extracted*	g % of total polyphenols content
Black Tea	Catechins	3-10	30
	Theaflavins	3-6	13
	Thearubigins/PBPs	12-18	47
Green tea	Catechins	30-42	90
	Theaflavins	-	-
	Thearubigins/PBPs	-	-

* % of solid extracted from black tea = 25-35%, PBPs = Polymeric black tea polyphenols

The precise composition of the tea leaves depends on a variety of factors, including climate, season, horticultural practices, type and age of the plant (nature of the green shoots used) and by the procedures employed in subsequent processing. Average caffeine levels in both black and green teas are 3-4% on a dry weight basis. The percentile differences in the different types of phenolics present in green and black tea are shown in figure 1.10 whereas the structures of the major polyphenolic compounds present in green and black tea are shown in figure 1.9. Comparative concentrations and types of polyphenols in green and black tea have been presented in table 1.1.

Extensive research on green tea/polyphenols has resulted in voluminous literature and evidence that they possess anti-bacterial, anti-viral, anti-oxidative, anti-mutagenic, anti-clastogenic, anti-inflammatory and anti-carcinogenic properties [28,35] and possess diverse mechanisms for observed chemopreventive actions [36-38]. The observed protective activity of green tea has been attributed to the powerful scavenging and anti-oxidative ability of monomeric catechins and their gallates [30,36].

Studies employing different *in vivo* animal models have demonstrated anti-initiating and anti-promoting activity of BTE and its components in both spontaneous and carcinogen-induced tumor models (Table 1.2). Oral and topical administration of BTPs has been shown to modulate incidence/multiplicity/ latency period or other degenerative changes at various organ sites in experimental animals (Table 1.2).

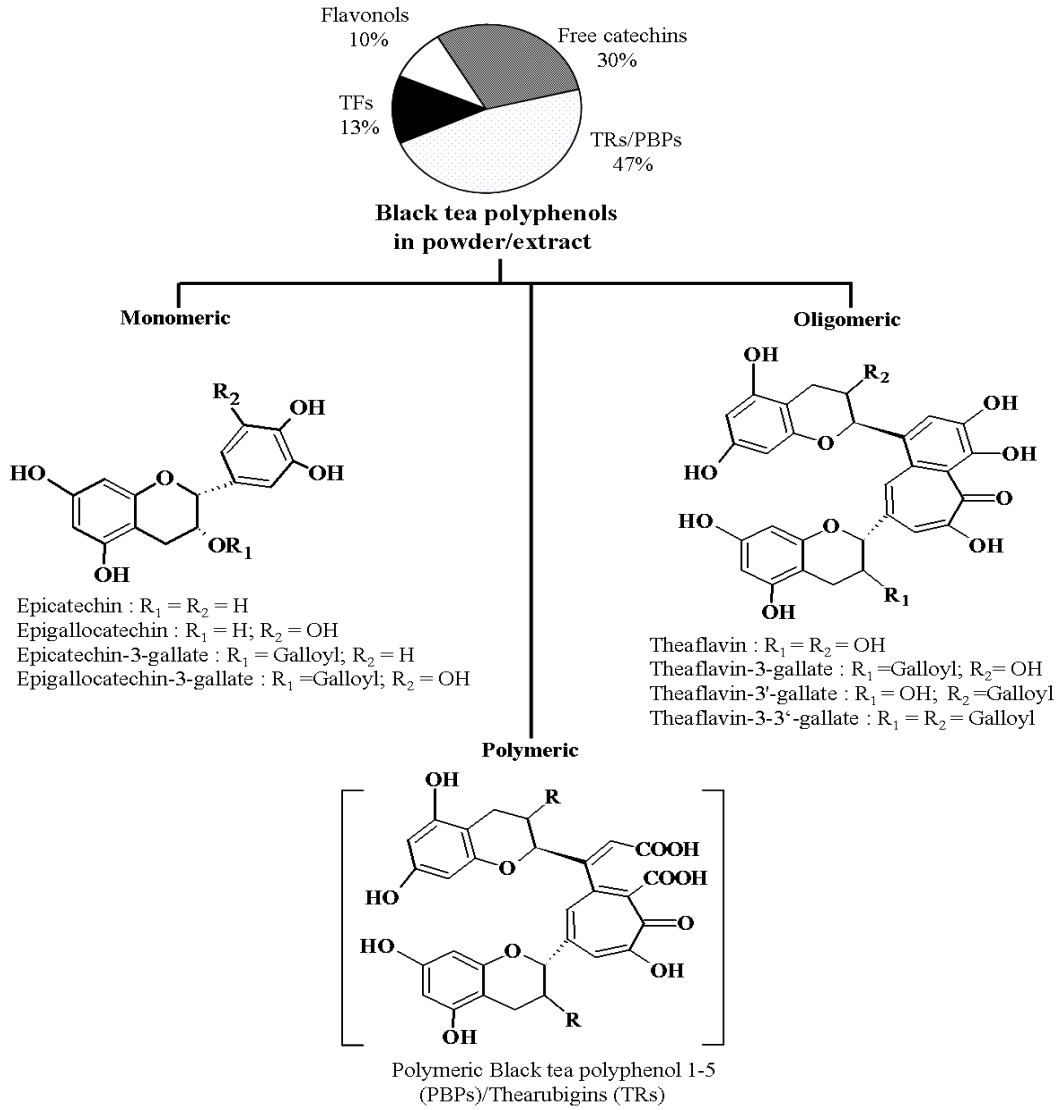

FIGURE 1.9: Structure of major polyphenols in green and black tea (Modified from Kumar et al., 2010, MRMC, 10, 492-505) [29].

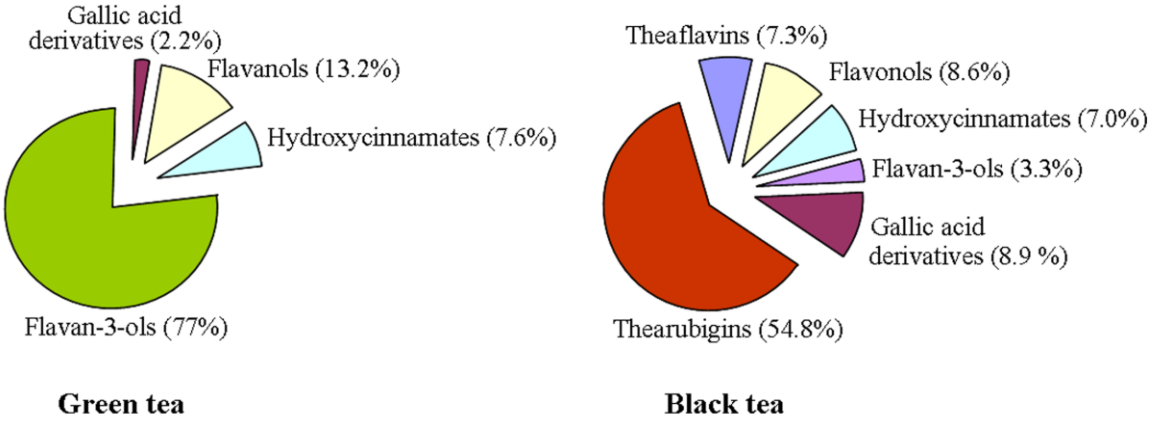

FIGURE 1.10: Percentile composition of the different classes of phenolics in the green and black tea (Modified from Rio et al., 2004, JAFC, 52 (10), 2807-15) [39].

TABLE 1.2:***In vivo*** **chemopreventive effects of black tea extract/polyphenols/constituents in different rodent models(**Adapted from Kumar et al., 2010, MRMC, 10, 492-505) [29]

S. No.	Animal Model	Organ	Carcinogen Dose / Route / Duration	Black tea extract / polyphenols Dose / Route / Duration	Salient observations	Ref.
Crude black tea extract						
1	SKH-1 mice	Skin	i) UVA - 1.8 x 10^{-3} W/cm^2, 5-15 mins/day, 5x/wk-30 wks ii) UVB - 2.4 x 10^{-4} W/cm^2, 5-15 mins/day, 5x/wk-30 wks iii) UVB - 180 mJ/cm^2, 5mins, 1x/day-2 days iv) UVB - 180 mJ/cm^2, single	i, ii) BTE - 1.25-2%, sole drinking fluid, 1 wk prior till end iii) SBTE - 0.8%, sole drinking fluid, 2 wks prior till end iv) SBTE, BTF1, BTF2 - 0.2 mg/ cm^2, 30 mins prior , topical	i, ii) Decreased multiplicity, increased latency period of skin tumors iii, iv) Decreased incidence, severity of erythema, skin fold thickness	[40,41]
2	SD rat	i) & ii) Mammary gland iii) Liver	i) DMBA – 5 mg, gavage, single on 49^{th} day ii) IQ a) 8.4 mg, gavage, 2x/ 1^{st} wk b) 14 mg, gavage, 2x/ 2^{nd}-5^{th} wks iii) DAB - 0.06%, diet-12 wks	i) & ii) BTE - 1.25% (w/v), sole drinking fluid, 1 wk prior till end iii) Polyphenon-B - 0.05%, diet-24 wks	i, ii) Decreased mammary gland tumor multiplicity, volume iii) Decreased pre-neoplastic, neoplastic lesions, oxidative stress. Modulation of XME	[42,43]
3	Swiss mice	Lung	DEN - 20 mg/kg BW, gavage, 1x/wk-8 wks	BTE - 1, 2, 4%, sole drinking fluid, simultaneously-20 wks	Decreased incidence, multiplicity of adenoma / adenocarcinoma	[44]
4	A/J mice	i) & ii) Lung, Rhabdomyosarcoma iii) Lung	i) & ii) Spontaneous tumors iii) NNK - 103 mg/kg BW, i.p., single	i) BT - 0.5, 1, 2%, sole drinking fluid-60 wks ii) Instant BT - 0.3-0.6%, sole drinking fluid-52 wks iii) BT - 0.6%, sole drinking fluid, starting 16 wks after NNK treatment till 52 wks	Decreased incidence, multiplicity, volume	[45,46]

5	i) CD-1 mice ii) Mouse	Skin	i) DMBA - 200 nmol, topical, single + TPA - 5 nmol , topical, 2x/wk - 24 wks ii) DMBA - 52 µg, topical, single + TPA - 5 µg, topical, 2x/wk	i) BT - 1.25%, sole drinking fluid, 11 wks post papilloma development ii) BTP a) 3 wks prior to DMBA application b) prior to each treatment of TPA	i) Decreased papilloma growth ii) Observed anti-initiating and anti-promoting activities	[47,48]
6	SKH-1 mice	Skin	UVB - 30 mJ/cm^2, 2x/wk, i) 35 wks, ii) 40 wks, iii) 45 wks	i) Caffeine - 0.072, 0.24%, sole drinking fluid-35 wks ii) LBT, LDBT - 0.9% , sole drinking fluid-40 wks iii) BT, DBT, DBT - 1.25% , 1.25%, 1.25% + Caffeine - 0.036%, sole drinking fluid-45 wks	Inhibited UVB-induced complete carcinogenesis, DBT < BT, caffeine alone had significant effect, addition of caffeine to DBT restored inhibitory effect	[49]
7	Syrian golden hamster	Buccal pouch	DMBA - 0.5%, topical, 3x/wk-14 wks	i) Polyphenon-B, BTF-35 - 0.05%, diet, 4 wks prior till end ii) Polyphenon-B - 0.05%, diet-14 wks	Decreased incidence, multiplicity, tumor burden, hyperplasia, dysplasia, inhibited DMBA-induced genotoxicity, development of HBP carcinomas by restoring normal cytokeratin expression, cell proliferation, induced apoptosis	[50-53]
8	SKH-1 mice	Skin	UVB - 30 mJ/cm^2, 25 secs, 2x/wk-2 wks	i) BT, DBT - 0.6%, Caffeine - 0.044% , LDBT + Caffeine - 0.6% + 0.044%, sole drinking fluid, 1 wk after UV treatments for 23 wks ii) BT - 6 mg/ml tea solids, sole drinking fluid, 11 wks post papilloma development	i) Caffeinated black teas, caffeine decreased tumor multiplicity, parametrial fat pads, thickness of dermal fat layer, decaffeinated tea was inactive ii)Decreased number of malignant, nonmalignant, tumors, BrdUr labeling, mitotic	[47,54]

					index, increased apoptotic index	
9	F344 rat	Colon, Small intestine	AOM - 7.4 mg/kg BW, s.c., 1x/wk-10 wks	BT - 50 mg/kg,1 wk after AOM for 16 wks	Decreased tumor incidence, multiplicity	[55]
Decaffeinated black tea						
10	A/J mice	Lung	NNK - 103 mg/kg BW, i.p., single	DBTE - 0.3, 0.6%, sole drinking water i) Starting 2 wk before, till 1 wk after NNK ii) Starting 1 wk after NNK treatment till end	Decreased tumor multiplicity without effect on incidence	[56]
11	C3H mice	Liver, Lung	DENA - 50 μg/kg BW,i.p., 1x/wk-8 wks	DBT - 1.25%, sole drinking fluid, 2 wks prior to & during 40 wks	Dose dependent decrease in multiplicity in lung and liver	[57]
12	SKH-1 mice	Skin	i) DMBA - 200 nmole, topical, single ii)UVB - 30 mJ/cm^2, 25 secs, 3 wks after DMBA treatment, 2x/wk-31 wks	DBTE, BT - 0.63% or 1.25%, sole drinking fluid, 2 wks prior to during 31 wks	Decreased incidence, multiplicity, volume of keratoacanthomas, carcinomas	[58]
13	SD rat	Esophagus	NMBzA - 2.5mg/kg BW, s.c., 2x/wk-5 wks	DBT - 0.6%, sole drinking fluid, during and after NMBzA treatments till 39 wks	Reduction in tumor incidence, mulitiplicity	[59]
Thearubigins						
14	Swiss bare mice	Skin	DMBA - 20 nmole, topical, single + TPA - 1.8 nmole, topical, 2x/wk-40 wks	PBPs - 1-5 - 200 μg , topical 20 mins prior to TPA treatment	Decreased multiplicity, incidence of skin papillomas, cell proliferation markers, transcription factors at 10-40 wks	[60]

15	SD rat	Colon	DMH - 40 mg/kg BW, s.c., 2x/wk-3wks	PBPE - 1.5%, sole drinking fluid, 15 days prior till end	Inhibited colorectal carcinogenesis by decreasing tumor volume, multiplicity, inhibited cell proliferation via Wnt / β-catenin pathway	[61]
Theaflavins						
16	Mice strain A	Lung	B(a)P - 4μg, s.c., single	TFs, EGCG and ECG - 0.02 mg, 0.01 mg and 0.004 mg, i.p., till end	Restricted lung carcinogenesis by differential modulation of expression of p53, H-ras, c-myc, cyclin-D1	[62]
17	A/J mice	i) Esophagus ii) Lung	i) NMBA - 3x/wk-5 wks, s.c. ii) NNK - 100 mg/kg BW, i.p., single	i) TFs - 360ppm, EGCG - 1200 ppm sole drinking fluid, 2 wks prior till end ii) TFs - 0.1%, sole drinking fluid, 2 days after NNK treatment for 16 wks	Decreased rate of tumor formation, only TFs decreased the multiplicity Decreased tumor incidence, multiplicity	[63, 64]

AOM = Azoxymethane; B(a)P = Benzo(a)pyrene; BrdUr = Bromodeoxyuridine ; BT = Black tea; BTE = Black tea extract; BTF1 = Ethyl acetate extractable; BTF2 = n-butanol extractable; BTF-35 = Black tea extract enriched with theaflavins and catechins; BTPs = Black tea polyphenols; BW = Body weight; DAB = ρ-Dimethylaminoazobenzene; DBT = Decaffeinated black tea; DBTE = Decaffeinated black tea extract; DEN = Diethyl nitrosamine; DMH = 1,2- dimethylhydrazine; DMBA = 7, 12-dimethylbenz (a) anthracene; ECG = (-)-Epicatechin-3-gallate; EGCG = (-)-Epigallocatechin-3-gallate; HBP = Hamster buccal pouch; i.p. = Intraperitoneal; IQ = 2-amino-3-methylimidazo[4,5-*f*]quinoline; LBT =Lyophilized black tea; LDBT = Lyophilized decaffeinated black tea; NNK = 4-(methylnitrosamino)-1-(3-pyridyl)-1-butanone; NMBA = N-nitrosomethyl-benzylamine; PBPs = Polymeric black tea polyphenols; PBPE = Polymeric black tea polyphenols rich extract; Polyphenon-B = mixture of different catechins, caffeine, oligomers and polymers of tea polyphenols; SBTE = Standardized black tea extract; s.c. = Subcutaneous; TF = Theaflavins; TPA = 12-*O*-tetradecanoyl phorbol-13-acetate; UV-A = Ultraviolet light (320-375 nm); UV-B = Ultraviolet light (280-320 nm); XMEs = Xenobiotic metabolizing enzyme.

1.11 TURMERIC

Turmeric, the powdered rhizome of the plant Curcuma longa Linn has been extensively used as a coloring agent, a food additive, preservative and in the treatment of inflammatory conditions and diseases [65]. Curcumin was first isolated in 1815 and its chemical structure was determined by Roughley and Whiting in 1973. The three main curcuminoids isolated from turmeric are curcumin, demethoxycurcumin and bisdemethoxycurcumin. Though principally cultivated in India, Southeast Asia, China, and other Asian and tropical countries and regions, turmeric is also common in other parts of the world [66].

1.11.1 Chemistry of turmeric

Turmeric contains protein (6.3%), fat (5.1%), minerals (3.5%), carbohydrates (69.4%) and moisture (13.1%). The essential oil (5.8%) obtained by steam distillation of rhizomes has *a*-phellandrene (1%), sabinene (0.6%), cineol (1%), borneol (0.5%), zingiberene (25%) and sesquiterpines (53%) [67]. Curcumin (diferuloylmethane) (3–5%) is responsible for the yellow color, and comprises curcumin, demethoxycurcumin and bisdemethoxycurcumin.

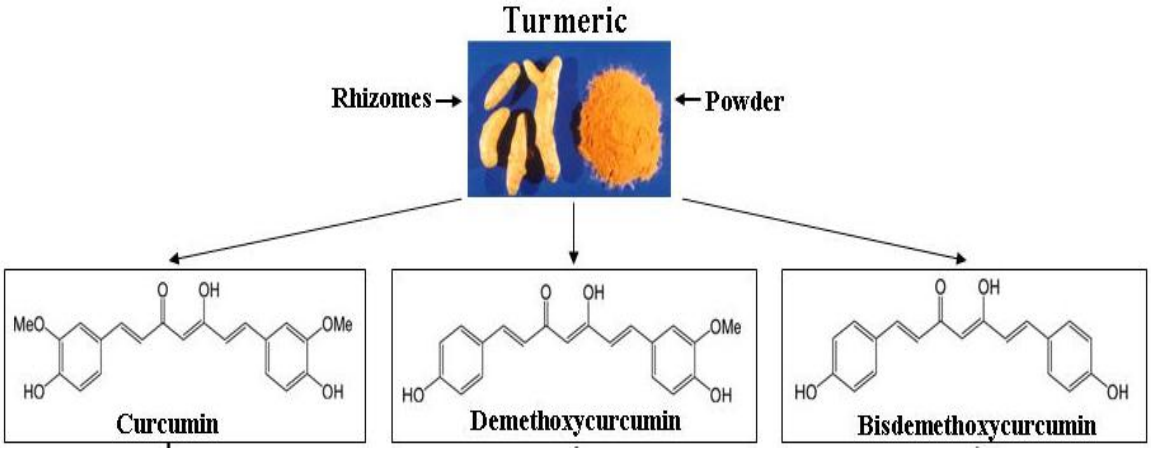

FIGURE 1.11: Chemical structures of curcumin(s)(Modified from Maru et al., 2010, Chapter Xth, Bioactive foods and Extracts Cancer treatment and Prevention, Edited by Ronald Ross Watson and Victor R. Preedy, CRC press 181-204) [97]

Curcumin has a melting point of 183°C, a molecular formula of $C_{21}H_{20}O_6$ and a molecular weight of 368.37 g/mol. It forms a reddish-brown salt with alkali and is soluble in ethanol, alkali, ketone, acetic acid and chloroform. Spectrophotometrically, the maximum absorption (λmax) of curcumin in methanol occurs at 430 nm and in acetone at 415–420 nm [68,69]. Curcumin appears brilliant yellow in color at pH 2.5–7 and red at

pH >7. Curcumin exists in enolic and β-diketonic forms. The fact that curcumin in solution exists primarily in its enolic form has an important bearing on the radical-scavenging ability of curcumin [70,71].

1.11.2 Pharmacokinetics and metabolism of curcumin

The food additive curcumin has the advantage of being a non-toxic natural product [72]. The kinetics of curcumin under various pH conditions and the stability of curcumin in physiological matrices have been reported [73]. Curcumin is stable at acidic pH but unstable at neutral and basic pH, under which conditions it is degraded to ferulic acid and feruloylmethane [73]. Most curcumin (>90%) is rapidly degraded within 30 min of placement in phosphate buffer systems of pH 7.2. Degradation of curcumin is extremely slow at pH 1–6, as normally encountered in the stomach. In contrast, one of the curcumin's major metabolites (tetrahydrocurcumin, or THC) is quite stable at neutral or basic pH [74] and still possesses antioxidant activities [75]. Curcumin is soluble in 0.1 M sodium hydroxide, although it remains stable for only 1–2 h.

The pharmacokinetic properties of curcumin have been investigated in mice (Pan *et al.*, 1999). It was reported that after i.p. administration of curcumin (0.1 g/kg) in mice, approximately 2.25 μg/ml of curcumin appeared in the plasma within first 15 min. After 1 h of administration, the levels of curcumin in intestine, spleen, liver and kidneys were 177.04, 26.06, 26.90 and 7.51 μg/g, respectively. Only traces (0.41 μg/g of tissue) were observed in the brain at 1 h. The chemical structure of the metabolites (Fig. 1.11), determined by mass spectrometry, suggested that curcumin is first biotransformed to dihydrocurcumin and tetrahydrocurcumin, or THC, and that these compounds are subsequently converted to monoglucuronide conjugates. Thus, curcumin-glucuronoside, dihydrocurcumin-glucuronoside, THC-glucuronoside, and THC are the major metabolites of curcumin *in vivo* [76].

The bioavailability of curcumin is low after oral ingestion [65,75]. However, it is interesting to note that the bioavailability of curcumin can be dramatically elevated by co-ingestion of piperine (a component of pepper) in both rats and humans [77]. Thus, the beneficial health effects of curcumin alone may be further magnified in the context of a mixture of dietary additives that are abundantly consumed as part of Asian diets [78]. A synergistic effect on cellular differentiation was observed when curcumin was combined

with all-*trans* retinoic acid or 1α, 25-dihydroxyvitamin D3 [79] and a chemopreventive synergism between epigallocatechin-3-gallate and curcumin is reported in normal, pre-malignant, malignant human oral epithelial cells [80]. Combinatorial studies of curcumin with drugs also reveal synergistic actions; e.g., curcumin enhances the anti-tumor effect of the widely used anticancer drug, cisplatin, when used in combination against fibrosarcoma [81]. Therefore, efficacy and the synergistic effects of curcumin in combination with other dietary constituents warrant further study to exploit its full potential.

1.11.3 Biological activities of curcumin

Curcumin is apparently a highly pleiotropic molecule that interacts physically with numerous targets. It binds to and inhibits the activity of enzymes, growth factor receptors, metals, albumin, and other molecules. It binds proteins such as P-glycoprotein [82], multidrug resistance proteins 1 and 2 (MRP1 and MRP2) (Wortelboer *et al.*, 2003), glutathione [83], protein kinase C and protein kinase A [84], ATPase[85], ErbB2 [86], and microtubulin [87] etc. By directly binding small β-amyloid species, curcumin blocks aggregation and fibril formation *in vitro* and *in vivo*[88]. Curcumin has also been shown to irreversibly bind CD13/aminopeptidase N (APN) and inhibits tumor invasion and angiogenesis [89].

Extensive research over the last five decades has indicated that curcumin reduces blood cholesterol, prevents LDL oxidation, inhibits platelet aggregation, suppresses thrombosis and myocardial infarction, suppresses symptoms associated with type II diabetes, rheumatoid arthritis, multiple sclerosis and Alzheimer, inhibits HIV replication, enhances wound healing, protects from liver injury, increase bile secretion, protects from cataract formation, is an anti-atherosclerotic etc. [68,69]. Comparison of structures of curcumin(s) with their activity profiles have suggested the importance of both parahydroxy (p-OH) and methoxy groups (-OCH3) for its biological activity[90]. The study also indicated that the presence of curcumin was essential for the inhibitory effect, as removal of curcumin resulted in restoration of cytochrome P450 activity and the levels of [^{3}H]-B(a)P-DNA adducts to control values [90].

1.11.4 Chemopreventive effects of curcumin

Curcumin has been shown to possess anti-inflammatory, antioxidant, anti-clastogenic, anti-viral, anti-fungal properties. Additionally, the hepato-protective, nephro-protective, thrombosis suppressing, myocardial-infarction protective, hypoglycaemic, anti-rheumatic effects of curcumin are also well documented [91]. Studies employing different *in vivo* systems have demonstrated anti-initiating/anti-promoting/anti-progressor activity of turmeric/curcumin in both chemical-induced and genetic models (Table 1.3). Oral and topical administration of turmeric/curcumin has been shown to modulate incidence/multiplicity/latency period or defer degenerative changes at various organ sites in experimental animals (Table 1.3).

1.12 TARGETS OF CHEMOPREVENTIVE AGENTS - PBPs AND/OR CURCUMIN

BTPs and/or Curcumin can act as blockers and/or suppressors by inhibiting carcinogenesis at initiation and/or promotion stages.

1.12.1 Mechanism(s) of anti-initiating action

Cellular metabolism plays a very crucial role in the process of initiation during carcinogenesis. Xenobiotics entering into the cellular environment are metabolized by xenobiotic metabolizing [phase I (functionalization) and phase II (conjugation)] enzymes (XMEs), rendering them into less toxic and more water soluble compounds. In all organisms, XMEs serve as an efficient defense mechanism against potential negative action of xenobiotics. Hence, these XMEs could be one of the probable targets for cancer chemoprevention.

1.12.1.1 Effects on carcinogen-activating phase I enzymes

Phase I enzymes predominantly cytochrome P450s (CYPs) are a diverse superfamily of heme-containing enzymes found in many organisms. CYP enzymes are integral membrane proteins located in endoplasmic reticulum and mitochondria in various tissues. More than fifty CYP isozymes, classified into 17 families and 39 subfamilies based on amino acid sequence similarities are known to exist in humans. Phase I enzymes play an important role in the very first step of metabolism, where xenobiotics are processed to more electrophilic moieties by addition of functional groups for further

detoxification by phase II enzymes. Among the different reactions catalyzed by CYPs, hydroxylation at the vacant position of an aromatic ring is considered to be the hallmark for the initiation of carcinogenesis. These electrophilic moieties will further react with cellular macromolecules to form adduct, there by marking the process of initiation. Thus, decreased activation of carcinogens due to modulation of CYPs could be one of the main targets for prevention of the cancer initiation process. CYP1A, which are primarily involved in the metabolic bioactivation of polycyclic aromatic hydrocarbons, in general, are regulated by a basic helix-loop-helix cytosolic protein, aryl hydrocarbon receptor (AhR). Upon ligand binding, AhR translocates to the nucleus, where it heterodimerizes with aryl hydrocarbon receptor nuclear translocator (ARNT) protein and binds to the xenobiotic response element (XRE) flanking CYP1A1 gene, thereby activating its transcription [92]. CYP1A1 and CYP1A2 are mainly involved in the metabolic activation of polycyclic aromatic hydrocarbon (PAH), some of which are found in cigarette smoke for example, benzo(a)pyrene (BP); while CYP1B1 and CYP2E1are involved in activation of nitrosamines and alcohol metabolism, respectively.

1.12.1.2 Effects on anti-oxidant and detoxifying phase II enzymes

Phase II enzymes play an important role in the detoxification of activated carcinogens by eliminating the reactive intermediates from cellular environment resulting in the decrease in the DNA and protein adducts. Phase II enzymes catalyze conjugation reactions such as glucuronidation, sulfation, methylation, acetylation and mercapture formation wherein phase I introduced functional groups are conjugated with endogenous, polar products (glutathione, glucuronic acid) rendering them less toxic and more water soluble. Therefore, chemopreventive agents altering the activity and / or levels of phase II enzymes would play an important role in blocking the initiation process. The expression of phase II enzymes is governed by a cis-acting regulatory element named the anti-oxidant response element (ARE). ARE containing gene is regulated by nuclear transcription factor erythroid 2 p45–related factor2 (Nrf2), a member of the cap ‘n’ collar family basic-leucine-zipper family of transcription factors via ARE. In an inactive state, the Nrf2 is sequestered in cytoplasm by kelch-like-ECH-associated protein 1 (keap 1), which in turn is bound to actin cytoskeleton. Upon activation, Nrf2 dissociates from keap1 and translocates to nucleus where it heterodimerizes with other leucine zipper proteins to transcriptionally activate the downstream genes [93].

1.12.1.3 Effects on xenobiotics-induced DNA damage

Most environmental carcinogens entering into the cellular environment undergo bio-activation during which pro-carcinogens get converted to electron deficient reactive intermediate(s). These intermediate(s) in turn can form chemical adduct(s) with nucleophilic moieties in DNA, RNA and proteins [94]. In addition, changes like DNA single/double strand breaks, cross linkages, depurination/depyrimidation, dimerization of pyrimdines and structural modification of DNA bases/deoxyribose, etc. may also result. Products of oxidative damage to macromolecules have been identified in biological materials such as plasma, urine and tissue/blood cells and may serve as biomarkers for oxidative damage.

1.12.2 Mechanism(s) of anti-promoting action

The tumor promotion involves the clonal expansion of initiated cells to give rise to tumor comprised of pre-neoplastic cells. This stage is largely characterized by two important cellular events viz. cellular proliferation and apoptosis. Evidence suggests that in response to various extracellular stimuli, cellular kinases including PKC, PI3K, mitogen-activated protein kinases (MAPKs) [extracellular signal-regulated kinase (ERK), p38, c-Jun N-terminal kinase (JNK)] are activated, which in turn regulate the transcription factors [jun, fos, nuclear factor kappa B (NF-κB)] thereby modulating the downstream effector molecules associated with various cellular responses such as cell proliferation, inflammation, differentiation, apoptosis, etc. This therefore suggests that modulation of these signaling effector molecules to either suppress cell proliferation or to induce apoptosis would be one of the important strategies by which a potential chemopreventive could inhibit promotion phase of carcinogenesis.

1.12.2.1 Effects on cellular kinases

Tumor promotion is an important process in carcinogenesis and 12-*O*-tetradecanoylphorbol 13-acetate (TPA) has been used as a model tumor promoter. Studies have shown that primary site of action of TPA is PKC, located on cell membranes. PKC plays an important role in transducing the signal from mediators across the membrane and in tumor promotion [95,96]. It has also been shown that TPA induces cell proliferation by decreasing activation of signaling kinases (c-Jun, ERK, p38, AKT), transcription factors [activator protein-1(AP-1), NF-κB] and inflammatory protein (cox-2). Therefore, an agent

that is able to block tumor promoter-mediated cellular responses is likely to be an effective anti-tumor promoter.

The MAPK proteins are important upstream regulators of transcription factor activities and their signaling is critical to the transduction of a wide variety of extracellular stimuli into intracellular events. The MAPK family proteins like ERK1/2, JNK and p38 are thought to interplay in the control of cellular events like proliferation, differentiation and apoptosis in response to external stimuli and have been implicated in multi-stage skin carcinogenesis. MAPKs have received increasing attention as target molecules for cancer prevention and therapy. It has been reported that activation of the MAPK pathways may cause the induction of phase II detoxifying enzymes, and inhibition of MAPK pathways may inhibit AP-1-mediated gene expression. MAPK pathway consists of a three-tiered kinase core where a MAP3K activates a MAP2K that activates a MAPKs (ERK, JNK, and p38), resulting in the activation of NF-κB, cell growth, and cell survival [29,97]. ERK and p38 MAPKs are involved in upregulation of cox-2 expression via NF-kB signaling in TPA-stimulated mouse skin [98,99].

1.12.2.2 Effects on transcription factors and oncogenes

It has been well accepted that transcription factors play important roles in the control of cell growth, apoptosis, inflammation, stress response, and many other physiological processes. AP-1 family of transcription factors is composed of homo- and hetero-dimers of the Fos (c-Fos, FosB, Fra-1, Fra-2) and Jun (c-Jun, JunB, JunD) families. After dimerization, they bind to TPA-responsive elements in the promoter and enhancer region of target genes that have been shown to be important mediators in oncogenic transformation. Likewise, Rel/NF-κB, a widely distributed transcription factor, is associated with many physiological processes including inflammation, cellular proliferation and cancer. In an inactive state, NF-κB remains sequestered in the cytoplasm by an inhibitory protein, IκB-α. Upon stimulation by agents such as cytokines, phorbol esters, mitogens, bacterial products, oxidative stress, ultraviolet light, etc., IκB kinases (IKKs) mediate the phosphorylation of IκB-α, leading to its proteosomal degradation, and facilitating the release of NF-κB into the nucleus. There are several important molecules such as NF-κB, IκB-α, IKK, within NF-κB signalling pathway. However, NF-κB is the key protein in the pathway, and has been described as a major cause and a therapeutic target in cancer [29,97].

NF-κB also plays a key role in the regulation of many genes that are involved in cell proliferation, differentiation, inflammation, cell survival, cell death, angiogenesis, etc.[100].

1.12.2.3 Effects on cellular response markers

Cell proliferation

In normal condition, cell proliferation is regulated by proliferation signals, however in transformed cells they are over ridden to cause hyper proliferation under the influence of certain promotion signals. Promotion can be initiated by mitogenic stimuli like growth factors, oxidative stress, hormones etc.

Uncontrolled cell proliferation is a hallmark of malignancy and may arise from stepwise increase in mitogenic stimuli that are otherwise involved in normal cell growth. In normal condition, cell proliferation is regulated by proliferation signals, however in transformed cells they are over ridden to cause hyper proliferation under the influence of certain promotion signals. Promotion can be initiated by mitogenic stimuli like growth factors, oxidative stress, hormones etc.

Inflammation

Chronic inflammation is closely linked to tumor promotion and substances with anti-inflammatory activities are anticipated to exert chemopreventive effects particularly during the promotion stage. Cox-2 and nitric oxide synthase are important enzymes that mediate inflammatory processes and are known to be up-regulated during tumorigenesis.

Apoptosis

Apoptosis is characterized by cell shrinkage, membrane blebbing, chromatin condensation and DNA fragmentation. Induction of apoptosis or cell cycle arrest by elimination of cells under stress or genetically damaged cells may represent a protective mechanism by which chemopreventive agent can inhibit promotion / progression stages of carcinogenesis [94].

p53 is a tumor suppressor and transcription factor. It is a critical regulator in many cellular processes including cell signal transduction, cellular response to DNA-damage, genomic stability, cell cycle control, and apoptosis. As a tumor suppressor, functional p53 activates the transcription of downstream genes such as p21WAF1 and Bax to induce apoptosis leading to inhibiting the growth of DNA damaged cells or cancer cells. The

status of p53 is thought to be an important mediator in the cellular response to chemotherapy. It is to note that all of these investigations with polyphenols have been made in immortalized or transformed cells *in vitro*. The doses employed in different experiments are much higher than regularly consumed by humans. Along with this, activity shown is due to parent compound(s) or its metabolite(s) is unknown. However, information on its effects on malignant and non-malignant cells in animal models *in vivo* is limited [29,97-99].

Tea polyphenols have been shown to induce apoptosis in many cells *in vitro*; however, information on its effect on malignant and non-malignant cells in animal models *in vivo* is limited.

TABLE 1.3: *In vivo* chemopreventive effects of turmeric/curcumin in different rodent models (Modified from Maru et al., 2010, Chapter Xth, Bioactive foods and Extracts Cancer treatment and Prevention, 181-204) [97]

S. No.	Animal Model	Organ	Carcinogen Dose/Route/Duration	Curcumin/Turmeric Dose/Route/Duration	Observations	Ref.
1	CD-1 Mice	Skin	DMBA - 200 nmol, topical, single + TPA - 5 nmol, topical, 2x/wk-20 wks	Curcumin - 1,3,10 μmol or 1-100, 3000 nmol, DMC, BDMC, THC - 1,3,10 μmol, topical, during promotion	Dose-dependent inhibition of TPA-induced promotion (tumor multiplicity / volume) especially with pure curcumin and DMC	[101-103]
2	CD-1 Mice	Skin	i) B(a)P - 20 nmol, topical, 1x/wk, 10 wks + TPA - 15 nmol, topical, 2x/wk-21 wks ii) DMBA - 2 nmol, topical, 1x/wk-10 wks + TPA - 15 nmol, topical, 2x/wk-15 wks	Curcumin i) & ii) 3 or 10 μmol, topical, during initiation	Decrease in the multiplicity / incidence of tumors	[104]
3	Swiss Mice	Skin	i) DMBA - 100 nmol, topical, 2x/wk-8 wks ii) DMBA - 100 μg, topical, single + TPA - 2.5 μg, topical, 2x /wk-26 wks	i) Turmeric - 2-5%, diet, during initiation, post-initiation and until end ii) Curcumin - 1%, diet, during initiation and until end	Decrease in tumor volume, multiplicity / incidence	[105,106]
4	i) Swiss Mice ii) A/J Mice	Fore-stomach	B(a)P i) 1mg, gavage, 2x/wk - 4wks ii) a) & b) 1.5 mg, gavage, 1x /wk-4wks	i) AqTE - 3 mg/day, curcumin - 1 mg/day, gavage; ETE - 0.0-0.25%, Turmeric - 0.2-5%, diet, during initiation, post-initiation and until end ii) Curcumin, a) 0.5-4.0%, diet, during initiation, post-initiation and until end b) 2%, diet, during initiation	Significant decrease in multiplicity/ incidence of forestomach tumors	[105,107-110]

5	Wistar Rats	Stomach	MNNG - 100 ppm, drinking water- 8 wks + NaCl - 5%, diet-8 wks	Curcumin - 0.05-0.2%, diet, during promotion	Decrease in incidence /multiplicity of glandular stomach hyperplasia and adenocarcinomas	[111]
6	C57Bl/6 Mice	Duodenum	ENNG - 120 mg/l, drinking water-4 wks	Curcumin (commercial grade) - 0.5-4.0%, diet, post-initiation until end	Decrease in tumor size, multiplicity / incidence	[109]
7	CF-1 Mice	Colon	AOM - 10 mg/kg BW, s.c., 1x/wk-6 wks	Curcumin (commercial grade) - 0.5-4.0%, diet, during initiation, post-initiation and until end	Decrease in tumor size, multiplicity / incidence	109]
8	F344 Rats	Colon	AOM i) a), b), & c) 15 mg kg BW, s.c., 1x/wk-2 wks, after curcumin ii) 30 mg/kg BW, s.c., single,	Curcumin, i) a) & b) 2000 ppm, diet, during initiation and until end c) 0.2-0.6% , diet, during initiation, post-initiation and promotion until end ii) 8-16 g/kg diet-45 wks	Decrease in tumor volume, multiplicity/ incidence of preneoplasia and invasive/ non-invasive colon tumors	[112-115]
9	B6C3F1 Mice	Colon	DMH - 20 mg/kg BW, s.c., 2x /wk-3 wks	Curcumin, THC - 0.5%, diet, post-initiation	Decrease in preneoplastic aberrant crypt foci	[116]
10	Wistar Rats	Colon	DMH - 20 mg/kg BW, s.c., 1x /wk-15 wks	Curcumin, BDMC - 80 mg/kg BW, i.g., during initiation and post-initiation	Reduction in number /size of colon tumors	[117]
11	C57Bl/6 J-(Min/+) Mice	Colon	Spontaneous intestinal tumors	Curcumin, 0.1-0.5%, diet-15 wks	Reduction in multiplicity of colon adenomas	[118]
12	C57Bl/6 J-Mice	Intestine	Spontaneous intestinal tumors	Curcumin - 0.1%, diet, started at 5 wk of age up to 110 days of age	Decreased intestinal adenomas	[119]
13	F344 Rats	Mammary gland	DMBA - 12 mg/rat, gavage, single, 1 wk after start of curcumin	Curcumin -10-20 g/kg diet, during initiation and until end	No alterations in incidence/ multiplicity of mammary tumors	[115]

14	Sencar Mice	Mammary gland	DMBA - 1 mg, gavage, 1x/wk-5 wks	i) Curcumin - 2% ii) Dibenzoyl methane (β-diketone analogue of curcumin) - 1% diet, during initiation and post-initiation	i) Little or no effect on incidence of mammary tumors; Reduction in the incidence of lymphoma/ leukemia ii) Decrease in multiplicity /incidence of mammary tumor	[120,121]
15	Sprague Dawley Rats	Mammary gland	DMBA i) 15 mg, gavage, single on day 55 ii) 30 mg/kg, i.g., single, at 50 days of age	i) Turmeric - 1%, ETE - 0.05%, diet, during initiation and post- initiation ii) Curcumin - 1%, diet, 2 wk pre-initiation	i) Significant reduction in tumor multiplicity/incidence /burden ii) No significant effect on mammary tumor development	[122,123]
16	Wistar-MS Rats	Mammary gland	γ-rays (2.6 Gy) day 20 of pregnancy - DES pellet implantation after weaning until end (0.38μg/day)	Curcumin - 1%, diet, during initiation	Significant reduction in incidence /multiplicity of mammary tumors, Increase in latency period	[124,125]
17	i a, b, c) Wistar Rats ii) C3H/He N Mice	Liver	i a) DEN -150 mg/kg, i.p., 1x/wk-4wks i b) DEN - 200 ppm, drinking water- 4 wks i c) DEN - PB, 200 mg/kg, i.p., single - PB , 0.05%, drinking water-13 wks ii) DEN - 20 μg/g BW, i.p., single	Curcumin i a) 200-600 mg/kg, gavage, pre-initiation i c) 100 mg/kg/day, gavage, pre-initiation and until end I c) 0.2%, diet, during initiation and until end ii) Turmeric - 0.2-5%, diet, during initiation and post-initiation	i a) Suppression of DEN-induced inflammation and hyperplasia i b) Decrease in incidence of focal dysplasia and HCC i c) Prevention of hepatic hyperplastic nodules ii) Reduction in multiplicity /incidence of HCC	[126-129]
18	LEC Rats	Liver, Kidney	Copper - ~300 μg/rat/day, diet & drinking water, lifespan	Curcumin - 0.5%, diet, life span	No decrease in copper-induced liver or kidney tumor incidence; Reduction in overall cancer formation and metastasis	[130]
19	A/J Mice	Lung	B(a)P + NNK, 3 μmol each, gavage, 1x /wk-8wks	Curcumin - 2000 ppm, diet, post-initiation	No effect on lung tumor multiplicity	[131]

20	CCSP-rtTA/Ki-ras TG Mice	Lung	DOX - 500 µg/ml, drinking water, BHT - 150 mg/kg, i.p., 1x /wk-6 wks	Curcumin - 8000 ppm, diet, post-initiation	No change in tumor multiplicity and progression to later lesions	[132]
21	Syrian Golden Hamsters	Cheek pouch	DMBA - 0.5%, topical, 3x /wk – i) 6wks; ii) 12wks; iii) 14wks	i) Curcumin - 10 µmol, topical, post-initiation ii) Turmeric - 1%, diet, during initiation iii) Curcumin - 80 mg/kg BW, gavage,14 wks, during initiation	i) Decrease in incidence of SCC and tumor volume, inhibited angiogenesis in papillomas and SCC ii) Decrease in tumor burden/ multiplicity, increase in latency period iii) Prevented formation of oral carcinoma, but showed hyperplasia and dysplasia	[133-135]
22	F344 Rats	Esophagus	NMBA - 0.5 mg/kg BW, i.p., 3x/wk-5 wks	Curcumin - 500 ppm, diet, during initiation and post-initiation	Reduction in incidence / multiplicity of esophageal tumors and preneoplastic lesions	[136]
23	F344 Rats	Prostate	i) DMAB - 50 mg/kg BW, s.c., 10x 2wk intervals-20 wks ii) PhIP - 100 mg/kg BW, i.g., 2x/wk-20 wks	Curcumin i) 500 ppm, diet, during initiation and post-initiation ii) 500 ppm, diet, post-initiation	Inhibition of DMAB induced prostate carcinomas, no effect on PhIP-induced tumors	[137]

AqTE = Aqueous turmeric extract; AOM = Azoxymethane; B(a)P = Benzo(a)pyrene; BDMC = Bisdemethoxycurcumin; BHT = Butylated hydroxytoluene; DEN = Diethylnitrosamine; DES = Diethylstilbestrol; DMAB = 3,2'-Dimethyl-4-aminobiphenol; DMBA = 7,12-Dimethylbenz(a)anthracene; DMC = Demethoxycurcumin; DMH = 1,2-Dimethylhydrazine; DOX = Doxycycline; ENNG = N-Ethyl-N'-nitro-N-nitrosoguanidine; ETE = Ethanolic turmeric extract; HCC = Hepatocellular carcinoma; MNNG = N-Methy[-N'-nitro-N-nitrosoguanidine; NaCl = Sodium chloride; NMBA = N-Nitrosomethylbenzylamine; NNK = 4-(methylnitrosamino)-1-(3-pyridyl)-1-butanone; NQO = 4-Nitroquinoline 1-oxide; PB = Phenobarbitone; PhIP = 2-amino-1-methyl-6-phenylimidazo [4,5-b] pyridine; SCC = Squamous cell carcinoma; THC = Tetrahydrocurcumin; TPA = 12-*O*-tetradecanoylphorbol-13-acetate.

1) To investigate the mechanism(s) of anti-promoting activity of PBPs on 12-*O*-tetradecanoylphorbol-13-acetate (TPA)-induced biochemical alterations in mouse skin.

2) To evaluate the effects of dietary turmeric post-treatment on tumor growth, markers of cell proliferation and apoptosis in DMBA-induced hamster buccal pouch (HBP) model.

3) To evaluate the effect(s) of dietary curcumin post-treatment on the disappearance/persistence of B(a)P-derived DNA adducts and apoptosis of cells in liver and lungs of mice.

4) To evaluate the chemopreventive efficacy and mechanisms of dietary-curcumin mediated chemoprevention in B(a)P-induced lung tumorigenesis in A/J mouse.

3.1 MATERIALS

Chemicals/reagents/consumables	Source
7, 12-dimethyl-benz(a)anthracene (DMBA, purity ~95%)	Sigma Chemical Co., USA
12-O-tetradecanoylphorbol-13-acetate (TPA, purity ~95%)	Sigma Chemical Co., USA
Acrylamide (MB grade)	Sisco Research Laboratories, India
Ammonium persulphate (APS, AR grade)	Sisco Research Laboratories, India
Aprotinin	Sigma Chemical Co., USA
Benzo(a)pyrene [B(a)P, purity ~98%]	Sigma Chemical Co., USA
Bis-acrylamide (AR grade)	Sisco Research Laboratories, India
Black tea powder (Brooke Bond Red Label)	Brook bond red label, India
β-Mercaptoethanol	Sigma Chemical Co.,USA
Bovine serum albumin (BSA)	Sigma Chemical Co.,USA
Bromophenol blue (BPB)	Sigma Chemical Co.,USA
Caffeine	Sigma Chemical Co.,USA
Catechin	Sigma Chemical Co.,USA
Coomassie brilliant blue R 250	Sigma Chemical Co.,USA
Copper sulphate (AR grade)	Sisco Research Laboratories, India
Curcumin (purity 65-70%)	Sigma Chemical Co.,USA,
Dithiothreitol (DTT)	Sigma Chemical Co.,USA
Epicatechin	Sigma Chemical Co.,USA
Epicatechin gallate	Sigma Chemical Co.,USA
Epigallocatechin	Sigma Chemical Co.,USA
Gallocatechin gallate	Sigma Chemical Co.,USA
Folin and Ciocalteu's phenol reagent (AR grade, 2N)	Sisco Research Laboratories, India
(N-[2-Hydroxyethyl]piperazine-N'-[2-ethanesulfonic acid]) sodium salt (HEPES)	Sigma Chemical Co.,USA
PageRuler prestained protein ladder	Fermentas Life Sciences, USA
Phenylmethylsulfonyl fluoride (PMSF)	Sigma Chemical Co.,USA

Poly-L-lysine (0.1% w/v)	Sigma Chemical Co.,USA
Polyvinylidene difluoride (PVDF) membrane	Amersham Biosciences, UK
Ponceau S	Sigma Chemical Co.,USA
Protein A-sepharose beads	Amersham Biosciences, UK
Restore western blot restriping buffer	Thermo Scientific, USA
Skimmed milk powder	Sagar milk, India
Sodium fluoride (AR grade)	Sigma Chemical Co.,USA
Sodium orthovanadate	Sigma Chemical Co.,USA
N,N,N',N'-tetramethylethylenediamine (TEMED)	Sigma Chemical Co.,USA
Tris (MB grade)	Amersham Biosciences, UK
Triton X 100	Sigma Chemical Co.,USA
Tween-20	USB, USA
Sodium carbonate (AR grade)	Sisco Research Laboratories, India
Sodium hydroxide (AR grade)	Sisco Research Laboratories, India

Solvents	**Source**
Acetone (ultra pure analytical grade [AR])	Merck Limited, India
Butanol (AR grade)	S.D. Fine Chemicals Co., India
Chloroform (AR grade)	S.D. Fine Chemicals Co., India
Diethyl ether (AR grade)	S.D. Fine Chemicals Co., India
Distilled water (Milli Q)	Millipore assembly set up in ACTREC
Ethyl acetate (AR grade)	S.D. Fine Chemicals Co., India
Ethanol absolute 99.9%	S.D. Fine Chemicals Co., India
Formaldehyde (37-41% w/v)	Sisco Research Laboratories, India
Glacial acetic acid (AR aldehyde free)	S.D. Fine Chemicals Co., India
Glycerol (extra pure AR)	Sigma Chemical Co.,USA
Hexane (HPLC grade)	S.D. Fine Chemicals Co., India
Hydrochloric acid (35-38% AR)	S.D. Fine Chemicals Co., India
Hydrogen peroxide (30% AR)	S.D. Fine Chemicals Co., India
Isopropanol (AR)	S.D. Fine Chemicals Co., India
Methanol (AR)/ (LR)/(HPLC)	S.D. Fine Chemicals Co., India
Orthophosphoric acid (ExcelaR)	Qualigens Fine Chemicals Co., India
Sulphuric acid (98% AR)	S.D. Fine Chemicals Co., India
Toluene (HPLC grade)	S.D. Fine Chemicals Co., India

Enzymes	Source
Deoxyribonuclease I (DNase I)	Ambion, USA
Proteinase K	Sigma Chemical Co., USA
Ribonuclease A (RNase A)	Sigma Chemical Co., USA

Immunochemical reagents / Kits	Company
Goat anti-mouse AKT1/2 primary antibody	SantaCruz Biotechnology Inc., USA
Goat anti-mouse β-actin primary antibody	SantaCruz Biotechnology Inc., USA
Goat anti-mouse Cox-2 primary antibody	SantaCruz Biotechnology Inc., USA
Goat anti-mouse ERK 1/2 primary antibody	SantaCruz Biotechnology Inc., USA
Mouse monoclonal BPDE-DNA adduct (clone 5D11) primary antibody	Hycult Biotechnology (Uden, Netherlands)
Mouse monoclonal PCNA (PC 10) primary antibody	BD Pharmingen, USA
Mouse monoclonal PKC isozymes (β, γ, ε, η) primary antibodies	BD Transduction Laboratories, USA
Rabbit anti-mouse AKT1 (pS473) primary antibody	Abcam, USA
Rabbit anti-mouseAKT1 (pT308) primary antibody	Abcam, USA
Rabbit anti-mouse Bax primary antibody	SantaCruz Biotechnology Inc., USA
Rabbit anti-mouse Bcl-2 primary antibody	SantaCruz Biotechnology Inc., USA
Rabbit anti-mouse Caspase 3 primary antibody	Abcam, USA
Rabbit anti-mouse Caspase-9 primary antibody	SantaCruz Biotechnology Inc., USA
Rabbit anti-mouse c-fos primary antibody	SantaCruz Biotechnology Inc., USA
Rabbit anti-mouse c-jun primary antibody	SantaCruz Biotechnology Inc., USA
Rabbit anti-mouse Cox- 2 primary antibody	Cell Signaling Technology Inc., USA
Rabbit anti-mouse Cytochrome c primary antibody	Cell Signaling Technology Inc., USA
Rabbit anti-mouse Histone primary antibody	SantaCruz Biotechnology Inc., USA
Rabbit anti-mouse IκBα primary antibody	SantaCruz Biotechnology Inc., USA
Rabbit anti-mouse IKK primary antibody	Cell Signaling Technology Inc., USA
Rabbit anti-mouse NF-κB primary antibody	Abcam, USA
Rabbit anti-mouse p21 primary antibody	SantaCruz Biotechnology Inc., USA
Rabbit anti-mouse p38 primary antibody	SantaCruz Biotechnology Inc., USA
Rabbit anti-mouse p53 primary antibody	SantaCruz Biotechnology Inc., USA
Rabbit anti-mouse p-ERK primary antibody	Cell Signaling Technology Inc., USA

Rabbit anti-mouse PDK1 primary antibody	Abcam, USA
Rabbit anti-mouse PI3K primary antibody	Cell Signaling Technology Inc., USA
Rabbit anti-mouse pIκB-α primary antibody	Cell Signaling Technology Inc., USA
Rabbit anti-mouse p-JNK primary antibody	Cell Signaling Technology Inc., USA
Rabbit anti-mouse PKCα primary antibody	Abcam, USA
Rabbit anti-mouse PKCα (pT497) primary antibody	Abcam, USA
Rabbit anti-mouse PKCα (pS657 +Y658) primary antibody	Cell Signaling Technology Inc., USA
Rabbit anti-mouse PKC PAN (βII S660) primary antibody	Cell Signaling Technology Inc., USA
Rabbit anti-mouse PKCα/βII(pT638/641) primary antibody	Cell Signaling Technology Inc., USA
Rabbit anti-mouse PKCδ primary antibody	SantaCruz Biotechnology Inc., USA
Rabbit anti-mouse PKCζ primary antibody	SantaCruz Biotechnology Inc., USA
Rabbit anti-mouse pNF-κB primary antibody	Cell Signaling Technology Inc., USA
Rabbit anti-mouse p-p38 primary antibody	Cell Signaling Technology Inc., USA
Rabbit anti-mouse Survivin primary antibody	Cell Signaling Technology Inc., USA
Horse-radish peroxidase conjugated secondary antibodies (anti-goat/mouse/rabbit)	Amersham Biosciences, UK
ECL chemiluminescence detection kit	Amersham Biosciences, UK;
Vectastain ABC kit	Vector Laboratories, USA
PGE-2 enzyme-immuno assay kit	Cayman Chemical Company, USA
Protein kinase C biotrak enzyme assay kit	Amersham Biosciences, UK
In-situ TUNEL assay kit	Promega, USA

Instruments	Model	*Company*
Spectrophotometer	UV – 160 A, UV – 240	*Shimadzu, Japan*
	U – 2001	*Hitachi, Japan*
	Biophotometer 6131	*Eppendorf, Germany*
Spectrofluorophotometer	RF-1501	*Shimadzu, Japan*
Centrifuges		
High – speed	Rota 4-R, Superspin R -V FA	*Plasto Crafts, India*
	Sorvall RC5C, Sorvall RC – 5C plus	*DuPont, USA*
Ultracentrifuge	Sorvall Ultra 80; Centrikon T – 1065	*DuPont, USA* *Kontron, USA*
Tabletop ultracentrifuge	TL – 100, Optima TLX	*Beckman, USA*
Microfuge	Spinwin	*Tarsons, India*
Liquid scintillation counter	Tri-Carb 2300 TR	*Packard, USA*
Lyophilizer	FreeZone 12	*Lab Conco, USA*
Speedvac concentrator	SVC 1000, AES 1000	*Savant, USA*
Homogenizer	CH – 6010	*Kinematica, Germany*
Upright microscope	Axioimager.Z1	*Zeiss, Germany*
	Eclipse 50i	*Nikon, Japan*
Confocal microscope	LSM 510 Meta	*Zeiss, Germany*
Microtome	RM2145	*Leica Instruments, Germany*
X-ray film developing machine	Optimax	*Protec, Germany*
pH meter	APX 175E	*Ingold, Germany*
Vertical electrophoresis assembly	Monokin, Minikin, Macrokin	*Techno Source, India*
Electroblot transfer assembly	Technoblot Trans – Blot Cell	*Techno Source, India* *Bio – Rad, USA*
Power packs	Gativaan Power pac 2000	*Techno Source, India;* *Bio – Rad, USA*
Radioactivity contamination detection monitor	GM -2	*Research Products International Corp, USA*
ELISA reader	*Spectra Max 190*	*Molecular Devices, USA*

3.2 DIET PREPARATION

Turmeric rhizomes were purchased from the local market of Mumbai, washed with deionised water, sun dried and powdered in a grinding mill. The resultant turmeric powder was stored in an air-tight container at room temperature throughout the experiments.

The standard laboratory diet prepared in ACTREC animal house was collected in the powdered form. The composition of diet is 41% cracked wheat, 50% roasted Bengal gram powder, 5% casein powder, 1% refined oil, 1% skimmed milk powder, 0.5% yeast powder and 0.5% common salt. The moisture content of the diet is 17.47%, fat 4%, protein 21.6%, crude fiber 0.95%, carbohydrate 57.2% and ash 3.38%. The total caloric content is 3330 Kcal. Quantities of turmeric/curcumin (Sigma) powder required for preparation of 1% turmeric and 0.05% curcumin diet were weighed and added to the pre-weighed standard laboratory diet. Turmeric/curcumin powder was thoroughly mixed in the diet while adding aldehyde-free distilled ethanol (upto 2% concentration) to ensure its uniform distribution. Aldehyde-free distilled ethanol was also added to the standard laboratory diet (control diet). Ethanol from control as well as experimental diets (with turmeric/curcumin) was allowed to evaporate completely and then, the diets were used. Control and experimental diet(s) were prepared twice a month. Food cups were replenished with fresh diet every alternate day.

3.3 ANIMALS

All animal studies were conducted after approval from the Institutional Animal Ethics Committee as per the Committee for the Purpose of Control and Supervision of Experiments on Animals (CPCSEA, Government of India) guidelines. Inbred female Swiss albino (S/RV/Cri Swiss) mice, female Swiss bare (S/RV/Cri-ba) mice, male Syrian hamsters and female A/J mice, 6-8 weeks old were obtained from animal house, ACTREC, India. They were randomly distributed into various groups, housed in polypropylene cages (4-5 per cage) and maintained under standard conditions of 22 ± 2 °C, 45 ± 10 % relative humidity and 12 h light/dark cycles. Drinking water was passed through Aquaguard® for UV sterilization. Specific-pathogen-free animals were used for all the studies. Details of animal treatments for different objectives have been described separately under each chapter. Animals were sacrificed generally employing CO_2 as a euthanasia agent or by cervical dislocation when

chemical or CO_2 use was not permitted by experimental requirements.A portion of the tissue was fixed in 10% buffered formalin for histopathological evaluation and immunohistochemical staining while rest of the tissue was snap frozen in liquid nitrogen and stored at -80 °C until used. Mice belonging to the various treatment groups were observed once a week for net body weight gain/loss, survival, and signs of toxicity, such as changes in fur color or texture, motor and behavioral abnormalities and palpable masses during the experimental period.

3.4 PREPARATION OF VARIOUS CELLULAR FRACTIONS

3.4.1Total cell lysatepreparation

Total cell lysate from mouse (liver, lungs, and skin epidermis) and hamster (cheek pouch) tissues were prepared as described [138]. Epidermis was gently separated from skin using Watson's skin grafting knife with suitably adjusted cutting angle. Skin of animals belonging to the various treatment groups were washed with acetone, since this facilitates the removal of color of curcumin/PBPs from the skin before separation of the epidermis. This was done to avoid color interference if any, in spectrophotometric determinations. All steps were carried out at 0-4 °C. Tissues were weighed (liver ~ 0.15 g, lungs ~ 0.2 g, skin epidermis from 1 animal, 0.25 g cheek pouch) and homogenized in 1-3 ml of ice-cold lysis buffer with freshly added protease and phosphatase inhibitors***** (Table 3.1). The homogenate was incubated on ice for 30 min with intermittent tapping to allow complete lysis to occur. Homogenate was then, centrifuged at 14,000 x g for 30 min and the supernatant (total cell lysate) was collected, aliquotised, protein content determined, and stored at -80 °C.

TABLE 3.1: Lysis buffer (for total cell lysate) composition

S. No.	Component	Stock conc.	Working conc.	For 25 ml buffer
1	Tris-HCl, pH 7.4	1 M	50 mM	1.25 ml
2	NaCl	1 M	150 mM	3.75 ml
3	EGTA	0.2 M	1 mM	0.125 ml
4	EDTA	0.5 M	1 mM	0.05 ml

5	NaF*	0.5 M	20 mM	1 ml
6	Na_3VO_4*	0.5 M	100 mM	5 ml
7	NP-40	100%	0.5%	0.125 ml
8	Triton X-100	100%	1%	0.25 ml
9	PMSF*	200 mM	1 mM	0.125 ml
10	Aprotinin*	4 mg/ml	10 μg/ml	0.0625 ml
11	Leupeptin*	4 mg/ml	10 μg/ml	0.0625 ml
12	β-glycero phosphate	1 M	10 mM	0.25 ml
13	Chilled distilled water (D/W)	-	-	12.95 ml

The stock solutions of Tris-HCl, pH 7.4 and NaCl were autoclaved and stored at 4 °C whereas other component of lysis buffer were filter sterilized and stored at -20 °C (except EDTA, stored at 4 °C). Always fresh lysis buffer was prepared using individual components at the time of use.

3.4.2 Cytosolic and crude nuclear lysate preparation

Cytosolic and nuclear (crude) lysates from mouse (lungs, skin epidermis) and hamster (cheek pouch) tissues were prepared as described [138]. All steps were carried out at 0-4 °C. Tissues were weighed (liver ~ 0.4 g; lungs ~ 0.4 g; pooled scraped epidermis from 2 animals; 0.4 g cheek pouch) and homogenized in 1-3 ml of ice-cold buffer A with freshly added protease inhibitors* (Table 3.2). After homogenization, the homogenates were incubated on ice for 30 min, with intermittent tapping and then, centrifuged at 25,000 x g for 10 min. The supernatant was collected as cytosolic lysate and stored at -80 °C. The nuclear pellet was resuspended in 0.3-0.5 ml of chilled buffer B (Table 3.3). The suspension was gently shaken for 30 min at 4 °C. After centrifugation at 25,000 x g for 10 min, supernatant was collected as nuclear extract, aliquotised and quickly frozen at -80 °C.

TABLE 3.2: Composition of buffer A (for cytosolic fraction)

S. No.	Component	Stock conc.	Working conc.	For 25 ml buffer
1	HEPES, pH 7.9	1 M	10 mM	0.25 ml
2	$MgCl_2$	1 M	2 mM	0.05 ml
3	KCl	1 M	10 mM	0.25 ml
4	DTT	0.1 M	1 mM	0.25 ml
5	EDTA	0.5 M	0.1 mM	0.002 ml
6	NaF*	0.5 M	20 mM	1 ml
7	Na_3VO_4*	0.5 M	10 mM	0.05 ml
8	PMSF*	200 mM	1 mM	0.125 ml
9	Aprotinin*	4 mg/ml	10 μg/ml	0.0625 ml
10	Leupeptin*	4 mg/ml	10 μg/ml	0.0625 ml
11	β-glycero phosphate	1 M	10 mM	0.25 ml
12	Chilled D/W	-	-	22.648 ml

TABLE 3.3: Composition of buffer B (for nuclear fraction)

S. No.	Component	Stock conc.	Working conc.	For 10 ml buffer
1	HEPES, pH 7.9	1 M	10 mM	0.1 ml
2	NaCl	1 M	300 mM	3 ml
3	KCl	1 M	50 mM	0.5 ml
4	DTT	0.1 M	1 mM	0.1 ml
5	EDTA	0.5 M	0.1 mM	0.002 ml
6	Glycerol	100%	10%	1 ml
7	NaF*	0.5 M	20 mM	0.4 ml
8	Na_3VO_4*	0.5 M	10 mM	0.02 ml
9	PMSF*	200 mM	1 mM	0.05 ml
10	Aprotinin*	4 mg/ml	10 μg/ml	0.025 ml
11	Leupeptin*	4 mg/ml	10 μg/ml	0.025 ml
12	β-glycerophosphate	1 M	10 mM	0.1 ml
13	Chilled D/W	-	-	4.678 ml

3.4.3 Cytosolic and particulate lysate preparation

Cytosolic and particulate lysate from mouse epidermis were prepared as described[139]. All steps were carried out at 0-4 °C. Tissues of animals belonging to the various treatment groups were washed with acetone, since this facilitates the removal of color of curcumin/PBPs from the skin before separation of the epidermis. This was done to avoid color interference if any, in spectrophotometric determinations. Epidermis was gently separated from skin using Watson's skin grafting knife with suitably adjusted cutting angle. Briefly, dissecting out epidermis (pooled from 2 mice) was homogenized in 1 ml of ice-cold buffer A with freshly added protease inhibitors***** (Table 3.4), centrifuged at 100,000 x g for 1 h at 4°C. The supernatant was collected as cytosolic fraction. Pellet was resuspended in 0.4 ml of tissue extraction buffer A supplemented with 0.5% Triton X-100; incubated on ice for 30 min with intermittent tapping and then centrifuged at the same speed. The supernatant was collected as particulate fraction. Both cytosolic and particulate lysates were aliquotised, their protein content determined and stored at -80°C.

TABLE 3.4: Composition of buffer

S. No.	Component	Stock conc.	Working conc.	For 25 ml buffer
1	Tris-HCl, pH 7.4	1 M	20 mM	1.25 ml
3	EGTA	0.2 M	1 mM	0.125 ml
4	EDTA	0.5 M	2 mM	0.05 ml
6	Sucrose	2 M	300 mM	3.75ml
7	DTT	0.1 M	1 mM	0.25ml
10	Aprotinin*****	4 mg/ml	10 μg/ml	0.0625 ml
11	Leupeptin*****	4 mg/ml	10 μg/ml	0.0625 ml
5	NaF*****	0.5 M	20 mM	1 ml
9	PMSF*****	200 mM	1 mM	0.125 ml
6	Na_3VO_4*****	0.5 M	100 mM	5 ml
12	β-glycero phosphate	1 M	10 mM	0.25 ml
13	Chilled D/W	-	-	13.075 ml

3.5 DETERMINATION OF PROTEIN CONTENT

Determination of the protein content of various cellular fractions prepared was done according the previously detailed procedure [140]. 1 ml of distilled water was taken in test tubes and 5 µl of blanks/standards (5–40 µg BSA solution)/samples (tissue homogenates/ extracts/lysates) (1:5 diluted for liver, 1:2 for lungs, skin epidermis and hamster buccal pouch) were added in test tubes. To this 1 ml of freshly prepared CTC (Copper Tartrate Carbonate) mixture solution***** was added and vortexed. After an incubation of 10 min at RT, 500 µl of Folin Ciocalteau (FC) reagent (1 in 6 times diluted, 0.33N) was added and tubes were vortexed and incubated in dark for 30 min at RT. All samples and standards were run in duplicates. Absorbance at 750 nm was measured in a spectrophotometer. A standard curve was prepared using 5–40 µg of BSA. Concentration of protein in samples was determined from the standard curve.

[***CTC mixture** = CTC: 0.8 N NaOH: 10% Sodium-dodecyl-sulphate (SDS): D/W].

[**CTC =** 0.1% $CuSO_4$ + 0.2% Sodium potassium tartrate + 10% Na_2CO_3]

3.6 PROTEIN IMMUNOBLOTTING

To study the expression of various proteins in cellular fractions that were prepared, SDS-PAGE followed by western blot analysis was employed [141].

3.6.1 Sodium-dodecyl-sulphate (SDS) polyacrylamide gel electrophoresis (PAGE)

Polyacrylamide gels are formed by cross linking monomeric acrylamide with N,N'-methylene bisacrylamide. Cross-links add rigidity and tensile strength and form pores through which the proteins to be separated must pass. The size of these pores decreases as the bisacrylamide:acrylamide ratio increases.

TABLE 3.5: Effective range of separation of SDS-polyacrylamide gels

Acrylamide concentration (%) (usually with 0.2%-0.5% bisacrylamide)	Linear range of separation (kD)
15	*10 - 43*
12	*12 - 60*
10	*20 - 80*
8	*36 - 94*
5.0	*57 – 212*

3.6.2 Resolving gel preparation

Firstly, the glass plates were assembled with 1.5 mm spacers in between. The two sides and bottom of the glass plate assembly were sealed with 1% molten agar. Simultaneously resolving gel was prepared as below.

TABLE 3.6: Composition of resolving gel

Components	8%	10%	12%
30% Acrylamide solution (Acrylamide : Bisacrylamide = 29 : 1)	8 ml	10 ml	12 ml
Tris-HCl pH 8.8 (1.5 M)	7.5 ml	7.5 ml	7.5 ml
10% SDS	0.3 ml	0.3 ml	0.3 ml
Distilled water	13.87 ml	11.87 ml	9.87 ml
10% Ammonium presulfate (APS, freshly prepared)	0.3 ml	0.3 ml	0.3 ml
TEMED (added just before pouring the gel)	0.030 ml	0.030 ml	0.030 ml
Total volume	30 ml	30 ml	30 ml

Resolving gel was poured into the slot between the two glass plates (upto $3/4^{th}$ their height). A layer of distilled water was poured above the gel; this facilitates the formation of

an even upper surface of the gel and prevents the air (oxygen) from affecting the polymerization of the gel. The gel polymerizes in 20-30 min.

3.6.3 Stacking gel preparation

TABLE 3.7: Composition of stacking gel

Components	6%
30% Acrylamide solution (Acrylamide : Bis acrylamide = 29 : 1)	4.0 ml
Tris-HCl pH 6.8 (0.5 M)	5.0 ml
10% SDS	0.200 ml
Distilled water	10.58 ml
10% APS (freshly prepared)	0.200 ml
TEMED (added just before pouring the gel)	0.020 ml
Total volume	20 ml

After removing the water layer from above the resolving gel, stacking gel was poured and appropriate comb was immediately inserted. Polymerization takes place in about 20-30 min. Comb was then carefully removed and the wells were washed with distilled water to remove any polymerized/unpolymerized acrylamide therein. The unit was then filled with tank buffer (at a final conc. of 1X, Table 3.8).

3.6.4 Sample preparation and gel electrophoresis

While the gels were polymerizing, protein samples were prepared. Appropriate concentrations of proteins from different cellular fractions were taken. Protein samples were mixed with 3X gel loading dye (Table 3.8) to a final concentration of 1X. The eppendorfs were sealed with parafilm and pulse centrifuged. Samples were denatured by keeping on a float in boiling water bath (100 °C) for 10 min. Samples were then loaded into the wells of polyacrylamide gel and electrophoresed at a constant current of 30 mA for 2-3 h at room temperature (RT). In one of the lane along-side the samples; molecular weight marker was

also run so as to determine the mobility and molecular weights of the various proteins in a particular lysate. To check the resolution of proteins and the band pattern of a particular type of lysate, the gel (after the run) was stained with Coomassie blue solution (0.2% Coomassie blue in destainer) overnight with gentle rocking. The gel was destained the next day by giving several changes of destaining solution (methanol: glacial acetic acid: water = 5:1:4).

TABLE 3.8: Buffer compositions for SDS-PAGE

5X Tank Buffer

Component	Working Conc.	Amount
Tris	125 mM	15.1 g
SDS	5%	5 g
Glycine	960 mM	72 g
D/W		to 1000 ml

Transfer Buffer

Component	Working Conc.	Amount
Tris	24.7 mM	12 g
Glycine	190 mM	57.2 g
Methanol	20%	800 ml
D/W		to 4000 ml

3X Loading Dye

Component	Working Conc. (3X)	For 10 ml (3X)	Working Conc. (1X)	For 10 ml (1X)
Tris, pH 6.8 (1M)	0.19 M	1.9 ml	0.063 M	0.63 ml
Glycerol	30%	3 ml	10%	1 ml
20% SDS	6%	3 ml	2%	1 ml
1% Bromophenol blue (BPB)	0.06%	0.006 gm	0.02%	0.002gm
D/W	-	to 8.5 ml	-	to 9.5 ml
β-mercaptoethanol (BME)*	15%	0.15 ml	5%	0.05 ml

* Make up the volume to 8.5 ml (for 3X) or 9.5 ml (for 1X) with D/W. Before use, to 850 µl (for 3X) or 950 µl (for 1X) of buffer add 150 µl (for 3X) or 50 µl (for 1X) of BME.

3.6.5 Transfer of proteins (electro blotting, western blot analysis)

Alternatively, proteins separated by SDS-PAGE were identified by blotting onto an adsorbent porous Polyvinylidene difluoride (PVDF) membrane, which gives a mirror image

of the gel. Proteins were transferred at 4 °C, employing a constant voltage of 100V, for 45-50 min. A cassette clamping the gel and membrane tightly together in between the two scotch-brite pads was put in the transfer apparatus containing transfer buffer (Table 3.8). A current is applied from electrodes situated at either side of the cassette. The buffer is often chilled to avoid heating effects.

Following electro-blotting, to check for the transferred proteins the nitrocellulose/ PVDF membrane was stained with Ponceau S or Fast green (0.1% in destaining solution). The efficiency of transfer was also checked by staining the transferred-gel with Coomassie blue to detect any residual protein in the gel.Subsequently the membrane was washed with TTBS (20 mM Tris-HCl, 500mM NaCl, 0.1% (v/v) Tween 20, pH 7.4) for ~ 5 min to remove the color of Ponceau S or Fast green. After blocking with 5% non-fat skimmed milk or 5% BSA in TTBS (depending upon the protein), membranes were probed with 1:500-1:2000 dilutions of appropriate primary antibody at 4 °C, overnight (*antibody dilutions were made in 2.5% milk in TTBS or 3% BSA). Next day, blots were washed with TTBS (15 min x 3) and incubated with 1:2000-1:10000 dilutions of anti-rabbit or anti-goat or anti-mouse horse radish peroxidase conjugated-secondary antibodies* at RT for 1h. Membranes were then washed with TTBS (15 min x 2), followed by a wash with TBS for 15 min. Immunoreactive bands were then visualized with enhanced chemiluminescence reagent or femto west (Pierce) as per the manufacturer's instructions followed by autoradiography. Further, for loading controls the blots were washed with TTBS (10 min x 2), followed by incubating with 2-3 ml of restore western blot restriping buffer (Thermo Scientific) at 37 °C for 10-15 min. The blots were then again rigorously washed with TTBS (10 min x 5), until smells of BME is eliminated from the washing buffer. Blots were then re-probed with appropriate primary antibody for loading control proteins (β-actin for total cell or cytosolic proteins, Histone H1 for nuclear proteins) and processed as described above. Densitometry of various analyte proteins was performed using Image J 1.43 (NIH) software by inverting the blot image, subtracting the background, and then calculating the mean intensity of each band in a single blot by drawing/selecting the largest band area. Similarly, the intensity of the respective loading controls from the same blot was determined. The intensity of the analyte protein was divided by that of the respective loading control to get normalized relative optical density.

Data i.e. mean ± SE of three to five independent samples in each group, were compared and presented.

3.7 IMMUNOPRECIPITATION

The protein modifications and/or associations (e.g. PKCα/AKT1/2 phosphorylation) were investigated by immuno-precipitation analyses.

3.7.1 Preparing 50% slurry of protein-A sepharose beads

0.5 g protein-A beads were suspended in 50 ml NETN buffer (20 mM Tris, 1 mM EDTA, 100 mM NaCl, 0.5% NP40) overnight at 4 °C. Next day, the supernatant containing the broken beads was removed, and beads were washed twice with NETN buffer, with each change after 2 h at 4 °C. Then, finally the beads were resuspended in appropriate amount of NETN buffer so as to make 50% slurry (i.e. depending on how much the beads have swollen, equal amount of NETN buffer was added).

3.7.2 Preclearing of lysate

Particulate lysate (500 µg protein) was incubated with 20 µl of protein-A beads and NETN buffer in a final volume of 0.5 ml for 2 h at 4 °C with gentle rocking. Cleared lysate was collected as supernatant after a centrifugation at 5,000 x g for 10 min at 4°C.

3.7.3 Immunoprecipitation

The cleared lysate was then, incubated with 2-8 µg protein of primary antibody (anti-phospho-threonine or anti-PI3K) overnight at 4 °C with gentle rocking. After addition of 20 µl protein-A beads, the complexes were rotated for additional 2 h at 4°C. Samples were centrifuged at 5,000 x g for 10 min at 4 °C to pellet out the immuno-precipitated complex. Immunoprecipitated proteins were washed three times with TTBS and resuspended in SDS sample buffer. The samples were boiled, resolved through SDS-PAGE and analyzed by immunoblotting using PKCα or AKT1/2 or PI3K antibody as described above in section 3.6.

3.8 PROTEIN KINASE C ACTIVITY AND PROTEIN LEVEL MEASUREMENTS

3.8.1 Determination of protein levels of PKC isozymes

To study the cellular distribution of PKC isozymes (α, β, γ, ε, η, δ, ζ) known to be expressed in mouse skin, 50 µg of cytosolic and particulate proteins were prepared and separated on an 8% SDS-PAGE and immunoblotted using isozyme-specific antibodies as described above in section 3.7. After western blotting, the membrane was stained with Coomassie Brilliant Blue R-250 (CBB) which served as control for equal loading. Densitometry of various analytes protein and loading control were performed using Image J 1.43 (NIH) software. Optical density of analytes protein was divided by optical density of respective loading control to get normalized relative optical density. Data i.e. mean ±SE of three to five independent samples in each group have been compared and presented.

3.8.2 PKC activity measurement

PKC activity incytosolic and particulate fractions was measured using protein kinase C biotrak enzyme assay kit (Amersham Biosciences, UK) as per the manufacturer's instructions, wherein PKC present in the samples catalyzed the transfer of γ-phosphate group of radiolabeled adenosine-5'-triphosphate to a peptide which is specific for PKC. The extent of phosphorylation thus, represents the PKC activity and results were expressed as pmol/min/mg protein. Briefly, the calcium buffer (12 mM calcium acetate, initial concentration), lipid (0.3 mg/ml Lα-phosphatidyl-L-serine, 24 µg/ml TPA), peptide buffer (900 µM peptide), and DTT buffer (30 µM dithiothreitol) (kit components) were mixed in equal volumes. 25 µl of this component mixture was used per assay and added to each of the tubes containing 25 µl of samples (for blank, sample buffer was used). Reaction was started following the addition of 5 µl of magnesium [^{32}P] ATP buffer (1.2 mM ATP, 30 mM HEPES, 72 mM $MgCl_2$, pH 7.4), consisting of [^{32}P] ATP at a concentration of 40 µCi/ml i.e. 0.2 µCi per tube. The tubes were incubated for 30 min in a shaking water bath at 37°C. Reaction was terminated by the addition of 10 µl of stop reagent. 35 µl of the terminated reaction mixture was spotted on to the peptide binding paper disc (provided with the kit). The spots were allowed to dry for 5 min. The paper discs were then washed five times with 75

mM orthophosphoric acid in a tray, with a change after every 10 min. The discs were transferred to vials containing 6 ml scintillation cocktail (PPO = 0.5 g and POPOP = 7 g was added in 1 l of toluene and mixed overnight over magnetic stirrer in amber color bottle) and radioactivity in the disc was counted. The extent of phosphorylation was determined by scintillation counting. It was confirmed that the assay was linear with regards to time and protein amounts used. The method has been optimized to exhibit maximum PKC activity. In appropriate controls, peptide buffer or sample proteins were replaced by buffer or heat inactivated sample protein to exclude the contribution of background, endogenous phosphorylation and adsorption of radioactivity to proteins.

3.9 IMMUNOHISTOCHEMICAL STAINING

The expression of Bax, Bcl-2, p53, survivin, cox-2, PCNA, cyclin D1, KI-67, AKT (pS473) and AKT (pT308) in mice lungs and hamster buccal pouch of animals belonging to the various treatment groups were determined by the immunohistochemical staining in formalin-fixed, paraffin-embedded, 5 μm thick tissue sections mounted on poly-L-lysine coated glass slides. Sections were deparaffinised with xylene and rehydrated through a graded series of alcohol and finally washed with distilled water and 1X PBS as described above in section 3.9. To quench the endogenous peroxidase activity of the tissues, sections were incubated with 3% H_2O_2 in methanol for 30 min in dark. Excess of methanol was removed by three successive washes with 1X PBS for 5 min each. Non-specific binding was blocked by 1% horse or goat serum (from Vectastain Elite kit) for 1 h at 37 °C in humidified chamber. Sections were then, incubated with primary antibodies for PCNA (dilution 1:50)/cox-2 (dilution 1:25)/survivin (dilution 1:100)/p53 (dilution 1:25)/Bax (dilution 1:25) and Bcl-2 (dilution 1:25) overnight at 4 °C. The following day, after two washes with 1X PBS (5 min each), sections were incubated with biotinylated anti-horse or anti-goat secondary antibody (from Vectastain Elite kit) for 30 min at 37 °C for 1 h in a humidified chamber. Before and after incubating with Vectastain ABC reagent system for 30 min at 37 °C for 1 h, slides were washed with 1X PBS. This was followed by the detection using diaminobenzidine (DAB) as the chromogen and slides were counterstained with Mayer's haematoxylin. Images were captured with Zeiss Microscope (at magnification X100 and

X400), with Axiocam MRc5 digital camera attached. For negative or isotype controls, the primary antibody was replaced with PBS/ TBS or respective antibody serum (used at respective antibody concentration). In each batch slides with positive control(s) (p53, survivin and PCNA) were also processed simultaneously. For nuclear staining of protein, semi quantitative analysis was done by Image J 1.43 (NIH) software. PCNA labeling (Mitotic) index/survivin labeling index/p53 labeling index was calculated by counting the number of positively stained cells × 100/total number of cells in photomicrographs of at least 10 different randomly selected fields/section/animals, with at least five animals per group. More than 1000 cell were counted/section /animals.

3.10 TERMINAL DEOXYNUCLEOTIDYL TRANSFERASE BIOTIN-dUTP NICK END LABELING (TUNEL) ASSAY FOR MEASURING APOPTOTIC INDEX

Apoptosis in mouse (liver and lungs) and hamster (buccal pouch) tissues was assayed, as per the guidelines of *in-situ* TUNEL assay kit, in formalin-fixed, paraffin-embedded 5 µm tissue sections. The tissue sections were deparaffinised with xylene and rehydrated through a graded series of alcohol and finally washed with distilled water and 1X PBS as described in section 3.9. Slides were washed by immersing in 0.85% NaCl for 5 min and then with 1X PBS. Tissue sections were fixed by immersing the slides in 10% buffered formalin in PBS for 15 min at RT. Slides were then washed twice with 1X PBS, 5 min each. Tissue sections were permeabilised by incubating with 20 µg/ml proteinase K solution in PBS for 30 min at RT. After washing with 1X PBS, sections were refixed by immersing the slides in 10% buffered formalin in PBS for 5 min at RT and then, washed twice with 1X PBS. Sections were then equilibrated for 10 min with equilibration buffer. The fragmented DNA of apoptotic cells was then, labeled with the help of terminal deoxynucleotidyl transferase, recombinant, (rTdT) enzyme and biotinylated nucleotides (supplied with the TUNEL assay kit). The sections were incubated with rTdT mix (i.e. a mixture of equilibration buffer, biotinylated nucleotide mix and rTdT enzyme) for 1 h at 37 °C in a humidified chamber. For negative controls, a control incubation buffer without rTdT enzyme (i.e. a mixture of equilibration buffer, biotinylated nucleotide mix and autoclaved water) was prepared. Reaction was terminated by immersing the slides in 2X SSC buffer for 15 min at RT. Slides

were then washed three times with 1X PBS, 5 min each, to remove unincorporated biotinylated nucleotides. Endogenous peroxidase activity was blocked by incubating the sections with 3% H_2O_2 in methanol for 30 min in dark. Slides were then washed with 1X PBS and incubated with Streptavidin HRP solution (1:500 in PBS) for 30 min at 37 °C in a humidified chamber and then washed twice with 1X PBS before proceeding for DAB staining. For DAB step, 5 µl DAB substrate (provided with the kit) to be added to 95 µl of deionized autoclaved D/W. Further, 5 µl DAB (20X) chromogen and 5 µl H_2O_2 (20X) (provided with the kit) were added in the DAB mixture. Slides were counterstained with haematoxylin and then dehydrated, cleared in serial ethanols and xylenes and mounted with D.P.X. The nuclei of the apoptized cells were stained brown in color. Apoptotic index was calculated by counting the number of positively stained cells × 100/total number of cells in photomicrographs of at least 10 different randomly selected fields/section/animals, with at least five animals per group. More than 1000 cell were counted/section /animals.

3.11 HISTOPATHOLOGICAL ANALYSIS

The histopathological analysis of mouse (liver, lungs or skin) and hamster (buccal pouch) tissues was performed on formalin-fixed, paraffin embedded 5 µm tissue sections stained with haematoxylin and eosin.

3.12 CONFOCAL MICROSCOPY

To detect expression and translocation of PKCα and PKCδ isoforms, epidermal layer was manually extracted from skin as described above and fixed in 10% buffered formalin, which was further processed for making 5 µm paraffin-embedded tissue section on glass slides. The tissue sections were deparaffinised with xylene and rehydrated through a graded series of alcohol and finally washed with distilled water and 1X TBS as described above in section 3.9. Antigen unmasking was performed in Tris-EDTA buffer (10 mM Tris, 2 mM EDTA) in pressure cooker for 6 min. Sections were washed twice with TBS for 5 min and treated with freshly prepared 1% sodium borohydrate in distilled water for 30 min at RT in dark. Sections were subsequently incubated with 1% BSA in TBS for 30 min to prevent non-specific binding. Sections were incubated with PKCα and anti-rabbit Alexa fluor 488 (Molecular Probes) for 30 min followed by PKCδ and anti-goat Alexa fluor 568 (Molecular

Probes) treatment. Slides were washed three times for 10 min with TTBS and then incubated with 4',6-diamidino-2-phenylindole (DAPI; 100 ng/ml) for 20 min. The slides were mounted with Vectashield mounting medium (Vector Laboratories, Burlingame, CA, USA) with cover slips and sealed with nail enamel. Confocal images were obtained using an LSM 510 Meta Carl Zeiss Confocal system with argon 488 nm and helium/neon 543-nm lasers. The images were obtained using an Axio Observer Z.1 microscope at a magnification of 630X with 1X optical zoom. Results were expressed as mean fluorescence intensity of PKCα/PKCδ/area (μm^2) of epidermal cells from skin tissue sections.

3.13 CELL CULTURE EXPERIMENTS

The human transformed HaCat cells were cultured as monolayers at 37 °C in a 5% CO_2 atmosphere in Dulbecco's modified Eagle's medium (DMEM) containing 5-10% fetal bovine serum (FBS). Initially, monolayer-cultured HaCat cells were treated with dimethyl sulfoxide (DMSO; vehicle control) or different concentration of TPA (100, 200, 400, 600 ng/ml of media) for 1 h for evaluation of translocation of PKCα by western blot. HaCat cells were pretreated with PBP-3 or PBP-5 (200 µg/ml of media) for 20 min followed by TPA treatment (200 ng/ml of media) for 1 h. Further, treated cells were washed with PBS, trypsinized, collected by centrifugation (1500 x g for 5 min), washed with PBS and pelleted again. Cytosolic and particulate protein fractions were prepared as described [142]. All steps were carried out at 0-4 °C. Briefly, pellet down cells (approximately 8 million) was sonicated (5 cycles of 5sec at 30-40 Hz with intervals of 30 sec) in 800 µl of extraction buffer A [20 mM Tris-HCl (pH 7.5), 10 mM EGTA, 5 mM EDTA and 0.3% BME with freshly added protease and phosphatase inhibitors (20 µg/ml aprotinin, 10 µg/ml leupeptin, 20 mM NaF, 10 mM Na_3VO_4, 10 mM β-glycerophosphate)]; centrifuged at 100,000 x g for 45 min at 4°C. The supernatant represented the cytosolic fraction. Pellet was resuspended in 0.3 ml of tissue extraction buffer A supplemented with 0.5% Triton X-100; sonicated at same frequency, incubated on ice for 30 min with intermittent tapping and then centrifuged at 100,000 x g for 45 min at 4°C. The supernatant was collected as the particulate fraction. Both cytosolic and particulate lysates were aliquotised, their protein content determined and stored at -80°C.

3.14 IMMUNOSTAINING OF CELLS

To detect the expression and translocation of PKCα and PKCδ isoforms, immunostaining was performed on HaCat cells. For this, cells were plated on cover slips and grown overnight. The next day, cells were treated as described above with PBP-3 or PBP-5 followed by TPA for immmunostaining. To detect the expression and translocation of PKCα and PKCδ isoforms, immunostaining was performed on HaCat cells grown on cover slips. After treatment (as described above), the cells were fixed by freshly prepared 4% paraformaldehyde at 37 °C for 20 min followed by a PBS wash. The cells were permeabilized with 0.3% Triton X-100 for 3 min, followed by 1 h 5% BSA blocking and PKCα antibody treatment in a humidified chamber. After incubation, the cover slips were washed twice for 10 min with PBS and incubated with anti-rabbit Alexa fluor 488(Molecular Probes) for 1 h at RT. The cover slips were further treated with PKCδ antibody for 1 h in humified chamber followed by incubation with anti-goat Alexa fluor 568 (Molecular Probes) for 1 h. The cover slips were washed three times for 10 min with PBS and then incubated with DAPI for 20 min. They were then mounted with Vectashield mounting medium on slides and sealed with nail enamel. Non-specific staining was determined by processing the cells without primary antibody. Each experiment was repeated three times and atleast 50 cells were examined in each group. Confocal images were obtained as described above at a magnification of 630X with 3X optical zoom. The translocation of PKCα from cytosol to membrane was determined using the mean fluorescence intensity of plasma membrane, calculated by subtracting the mean fluorescence intensity (PKCα/PKCδ) of the cytosol from the whole cell.

3.15 PI3K ACTIVITY

PI3K activity inparticulate fractions was measured using PI3K ELISA kit (K-1000s, Echelon Biosciences, Salt lake City, UT, USA) as per the manufacturer's instructions. PI3K activity was compared in immunoprecipitated proteins (500 μg) from particulate fractions in different treatment groups. The assay is a competitive ELISA in which the signal is inversely propotional to the amount of phosphatidyl-inositol (3,4,5) triphosphate [PI(3,4,5)P_3]produced. This kit measures PI3K activity in terms of conversion of

phosphatidyl-inositol 4,5-bisphosphate [PI(4,5)P_2] into PI(3,4,5)P3. It was confirmed that the assay was linear with regards to time and protein amounts used. Briefly, particulate fraction (500 µg protein) from different treatment groups wasprecleared, immunoprecipitated with anti-PI3K antibody as described above in section 3.8. After centrifugation and washing, precipitate/immunoprecipitate were collected and 30 µl of KBZ reaction buffer and 30 µl of 10 µM PI(4,5)P_2 substrate (300 pmol) were added. For enzyme only controls, 30 µl substrate was replaced with 30 µl of KBZ reaction buffer. The tubes were incubated for 4 h in a water bath at 37 °C for kinase reaction. Reaction was terminated by the addition of 90 µl of kinase stop solution, pelleting the beads by centrifugation and transferring the 60 µl reaction mixture to the incubation plate and incubated for 1 h with a PI(3,4,5)P3 detector (60 µl), then added to the PI(3,4,5)P3-coated microplate for 1 h for competitive binding. In parallel, a standard was run to measure the pmol of PI(3,4,5)P3 formed. A peroxidase-linked secondary detection reagent and colorimetric detection was used to detect PI(3,4,5)P3 detector protein binding to the plate. The colorimetric signal is inversely proportional to the amount of PI(3,4,5)P3 produced by PI3K. Absorbance values were measured at 450 nm using an ELISA reader. The enzyme activity was expressed as pmol of PI(3,4,5)P3 formed/mg protein.

3.16 ISOTHERMAL TITRATION CALORIMETRY (ITC)

To determine the interaction between TPA and PBP-3 or PBP-5 if any, TPA (3µg/100µl), PBP-3 or PBP-5 (30µg and 60 µg/100µl) were dissolved in 50 mM Tris HCl buffer (pH 7.4) containing 1% DMSO. An ITC experiment was carried out (at 20 °C and 37 °C) with a MicroCal ITC 200 (GE Healthcare, UK) where TPA in calorimeter cell was titrated with PBP-3 or PBP-5 in syringe. In this, binding equilibrium was measured by determining the heat change if occurs due to interaction between partners. Prior to sample analysis, a control experiment was performed. PBP-3 or PBP-5 (in the syringe) was injected into TPA (in the cell) at a cell temperature of 20 °C or 37 °C using 25 or 20 injections of 2 µl (4 s), injection intervals of 100 or 120 s, a reference power of 10 or 8 µcal/s, and a stirring speed of 1,000 rpm. Instrumental baseline was subtracted from the raw exothermic heat pulse data from each injection to obtain normalized integrated heat. Thermograms were evaluated using Origin (version 7; OriginLab).

3.17 UV ABSORPTION SPECTRA AND MASS SPECTROMETRY

To determine the interaction between TPA and PBP-3 or PBP-5 if any, TPA (3µg/100µl), and PBP-3 (200µg/100µl) and PBP-5 (200µg/100µl) were dissolved in acetone. TPA, PBP-3, PBP-5 and mixture containing PBP-3 + TPA and PBP-5 + TPA were incubated for 20 min at 37 °C. UV absorption spectra were recorded at 200-600 nm in a range of 0-2 absorbance using Jasco V-650 spectrophotometer after diluting the sample in acetone at a ratio of 1:50.

Further, the same samples were analyzed by Mass spectrometry (MS), where 2µl of diluted samples (1:2 v/v in α-Cyano-4-hydroxycinnamic acid) were loaded on MTP 384 ground steel ground plate (Bruker Daltonik, Germany). Mass calibration was carried out using peptide mixture of five known peptides spanning mass range of 500–4400 m/z and error was kept to less than 10 ppm. Accelerating voltage of 25 kV was applied to the first time of flight tube. The MS data were acquired using a solid state NdYAG laser at 337 nm. The resulting MS data was analyzed using Flex analysis 3.0 software (Bruker Daltonik, Germany).

3.18MEASUREMENT OF GSH/GSSG RATIO IN EPITHELIAL CELL EXTRACTS

Freshly collected epithelial cells from animals belonging to various treatment groups were used for the measurement of reduced glutathione (GSH) and oxidized glutathione (GSSG) levels as described [143]. Briefly, total cell lysate from mouse skin was prepared [138] as described above in section 3.5.1. From this, an aliquot of 50µl has taken for measuring the protein and DNA content in tissue lysate. Remaining lysate was diluted with 25% of metaphosphoric acid (HPO_3) (4:1 ratio) and centrifuge at 100,000 x g for 30 min. The supernatant was collected. An equal aliquot of supernatant (0.5 ml) were used for measuring the levels of GSH and GSSG. For measuring GSH, supernatant was diluted ten times with 0.1 M sodium phosphate-0.005M EDTA buffer (pH 8.0). In parallel, GSH standard [10ng to 5µg in 100µl of phosphate EDTA buffer (pH 8)] was made to calculate the GSH levels in samples from various treatment groups. Further, 1.8 ml of phosphate EDTA buffer (pH 8) and 100 µl of freshly prepared o-phthalaldehyde (OPT) (in methanol)

was added to the 100 µl of diluted supernatant sample/standard and incubated for 15 min at RT. Fluorescence intensity was measured at 420 nm (excitation was at 350nm). The fluorescence intensity for the OPT-GSH reaction was directly related to the GSH concentration and was linear over the concentration of 10ng to 2µg.

However, for GSSG measurement 0.2 ml of 0.04M N-ethylmaleimide (NEM) was added to 0.5 ml of original 100,000 x g supernatant for 30 min at RT in dark. To this, 4.3 ml of 0.1 N NaOH was added. In parallel, GSSG standard (5ng to 2µg in 100µl of 0.1 N NaOH) was made to calculate the GSSG levels in samples from various treatment groups. Further, 1.8 ml of 0.1 N NaOH and 100 µl of freshly prepared OPT was added to the 100 µl of diluted supernatant sample/standard and incubated for 15 min at RT. Fluorescence intensity was measured at 420 nm (excitation was at 350nm). The levels of GSH and GSSG in ng per µg DNA were used for the calculation of GSH/GSSG ratio. mean ± SE of two independent samples have been presented.

3.19 MEASUREMENT OF DNA IN EPITHELIAL CELL EXTRACTS

Freshly prepared total cell extracts of epithelial cells from animals belonging to various treatment groups were used for the measurement of DNA as described [144]. Briefly, calf thymus DNA was used as a standard. A stock solution was prepared by dissolving DNA at about 0.4 mg/ml in 5 mM NaOH. From this, working standards were prepared (every three weeks) by mixing an equal volume of $HClO_4$ and heating at 70 °C for 15 min. Diphenylamine (DPA) reagent was prepared by dissolving 1.5 g of DPA in 100 ml of distilled acetic acid and adding 1.5 ml of conc. H_2SO_4. The DPA reagent was stored in dark. On the day of use, 0.1 ml of aqueous acetaldehyde (16 mg/ml) was added for each 20 ml.Total cell lysate extracts containing nucleic acid was diluted with 0.5 N $HClO_4$. DNA standard and diluted total cell extracts were mixed with 2 volumes of DPA reagent containing acetaldehyde. Tubes containing known amount of standard DNA and a blank containing 0.5 N $HClO_4$ but no DNA was also prepared. It was confirmed that the assay was linear with regards to DNA amounts used. The color was developed by incubating at 30 °C for 16-20 h. The optical density at 600 nm was measured against the blank and compared with the values obtained with the standard DNA.

3.20 STATISTICAL ANALYSIS

Densitometry and cell counting were carried out using Image J 1.43 (NIH) software. Densitometry of western blots or various analyte proteins was carried out using Image J 1.43 (NIH) software as described in section 3.6.5. Statistical analysis was performed using SPSS 15.0 software. Data are presented as mean ± SE. Means of all data were compared by ANOVA with post-hoc Bonferroni's test. $p \leq 0.05$ was considered statistically significant.

4.1 INTRODUCTION

Chemoprevention by plant-derived antioxidants is gaining increased attention because of their high tolerability and low toxicity. Many dietary- and beverage-derived compounds have demonstrated anti-initiating and/or anti-promoting activities in several *in vitro* and *in vivo* experimental model systems and emerged as promising chemopreventive agents [145]. Tea is fast emerging as a potential chemopreventive beverage and tea polyphenols such as (-)-epigallocatechin-3-gallate (EGCG, the most effective monomeric catechin in green tea) and TFs (oligomeric black tea polyphenols) have reached clinical trials after their chemopreventive efficacies were established by various preclinical studies [146,147]. However, similar studies on PBPs, which are the most abundant polyphenols, although structurally and chemically ill defined [32,148] are limited. Our earlier studies have shown PBPs to possess anti-initiating activities as judged by their ability to inhibit carcinogen-induced DNA adduct formation *in vitro* and in mouse skin, inhibit benzo(a)pyrene [B(a)P]-induced activation of phase I enzymes such as cytochrome P450 1A1 and 1A2, and/or enhance the levels/activities of phase II enzymes [61,93,149,150]. Furthermore, PBPs were observed to possess anti-promoting effects in two-stage skin carcinogenesis [60]. However, their mechanisms of actions are not fully elucidated. Hence in this study, the mechanisms of PBP-mediated anti-promoting effects were investigated in mice employing 12-*O*-tetradecanoylphorbol-13-acetate (TPA), a potent tumor-promoting phorbol ester.

TPA activates protein kinase C (PKC) by mimicking diacylglycerol (DAG), a natural ligand and activator of PKC, for binding to specific motifs in its regulatory domain [95]. The PKCs, a family of phospholipid-dependent serine/threonine kinases, play an important role in tumor promotion and transducing the signal from mediators across the membrane [151]. Before responding to lipid second messengers for activation and translocation, the PKC must first be properly processed by three ordered phosphorylations: activation-loop phosphorylation (Thr497/500), turn-motif phosphorylation (Thr638/641), and hydrophobic-motif phosphorylation (Ser657/660) [152,153]. PDK1 and some AGC kinases such as AKT1/2 are mainly responsible for phosphorylation of PKC [151,154,155]. Furthermore, PDK1 also mediates the first of three ordered phosphorylations of PKC as well as phosphorylation of AKT at Thr308 [156]. PDK1 translocates to the membrane and binds lipid vesicles containing phosphatidylinositol 3,4,5-triphosphate [PI(3,4,5)P3] and phosphatidylinositol 3,4-bisphosphate [PI(3,4)P2], whose formation is dependent upon phosphatidylinositol 3-

kinase (PI3K). Upon stimulation, PKC translocates to the plasma membrane where it interacts with DAG and phosphatidylserine. Several *in vitro* and *in vivo* studies have documented the involvement of PKC in regulating target proteins associated with proliferation, differentiation, apoptosis, angiogenesis, invasion, or metastasis, because of which it has attracted considerable interest as a potential target for cancer prevention and chemotherapy.

Considering the central role of common upstream protein kinases such as PI3K/AKT/PDK in phosphorylation of PKC resulting in translocation of PKC from cytosol to membrane and subsequent PKC-mediated cascade of phosphorylation resulting in activation of transcription factors such as NF-κB and AP-1 in TPA-mediated cellular responses and tumor promotion, the mechanisms of PBP-mediated anti-promoting effects were investigated by studying the modulation of these processes in mouse skin. The study highlights the effects of pre-treatment with PBPs on TPA-mediated perturbations in the levels/activities/phosphorylation status of upstream protein kinases and PKC and its localization and the correlation of TPA-induced modulation of PKC activation with that of TPA-induced response markers, i.e., activation of transcription factors related to cell proliferation, apoptosis, inflammation, etc.

4.2 METHODS

4.2.1 Isolation of PBP fractions using Soxhlet continuous extractor

To study the mechanism(s) of anti-promoting activity of PBPs on TPA-induced biochemical alterations in mouse skin, five PBP fractions were isolated from a popular brand of black tea powder (Brooke Bond Red Label, India) in our laboratory via well established and reported protocol, employing a Soxhlet extractor [33].

Briefly, black tea powder (450 g) in a thimble was decaffeinated with chloroform (2.5 l) in a Soxhlet continuous extractor, until no color was present in the solvent (~48 h). Air-dried black tea powder (~445 g) in a thimble was further Soxhlet-extracted with ethyl acetate (2.5 l, 48 h). The ethyl acetate extract was dried *in vacuo*, while air-dried black tea powder (~415 g) in a thimble was further Soxhlet extracted with n-butyl alcohol (2.5 l, 24 h) to obtain n-butyl alcohol extract, which was dried *in vacuo*. The dried ethyl acetate extract was dissolved in acetone (200 ml) and precipitated with 8 volumes of diethyl ether, three times, to obtain precipitate of PBP-1. Subsequently, the dried n-butyl alcohol extract was dissolved in methanol (130 ml) and precipitated three times with 10 volumes of diethyl ether to yield PBP-2 precipitate. The filtrates obtained were dried, dissolved in

acetone (100 ml) and precipitated three times with 10 volumes of diethyl ether to yield PBP-3 precipitate. Next, the residual air-dried black tea powder (~351.8 g) was boiled with distilled water (1.5 l) for 20 min to obtain an aqueous solution, which after filtration was acidified with 3.5N sulfuric acid (75 ml). This acidified aqueous solution was then extracted with equal volumes of n-butyl alcohol, until the upper n-butyl alcohol layer became colorless (~7 times), following which the n-butyl alcohol extracts were pooled, dried *in vacuo* and processed in same way as for PBP-2 and PBP-3, to obtain PBP-4 and PBP-5. The above procedures were carried out in a chemical safety hood with necessary protective gadgets and precautions. The schematic presentation of the above mentioned method is presented in figure 4.1.

To prevent any light-mediated effect(s), containers were covered with brown paper and/or aluminium foil during the course of extraction. All the PBP fractions were dried *in vacuo* employing a rotary flash evaporator, to remove any residual organic solvent, and stored at -20°C for later use.

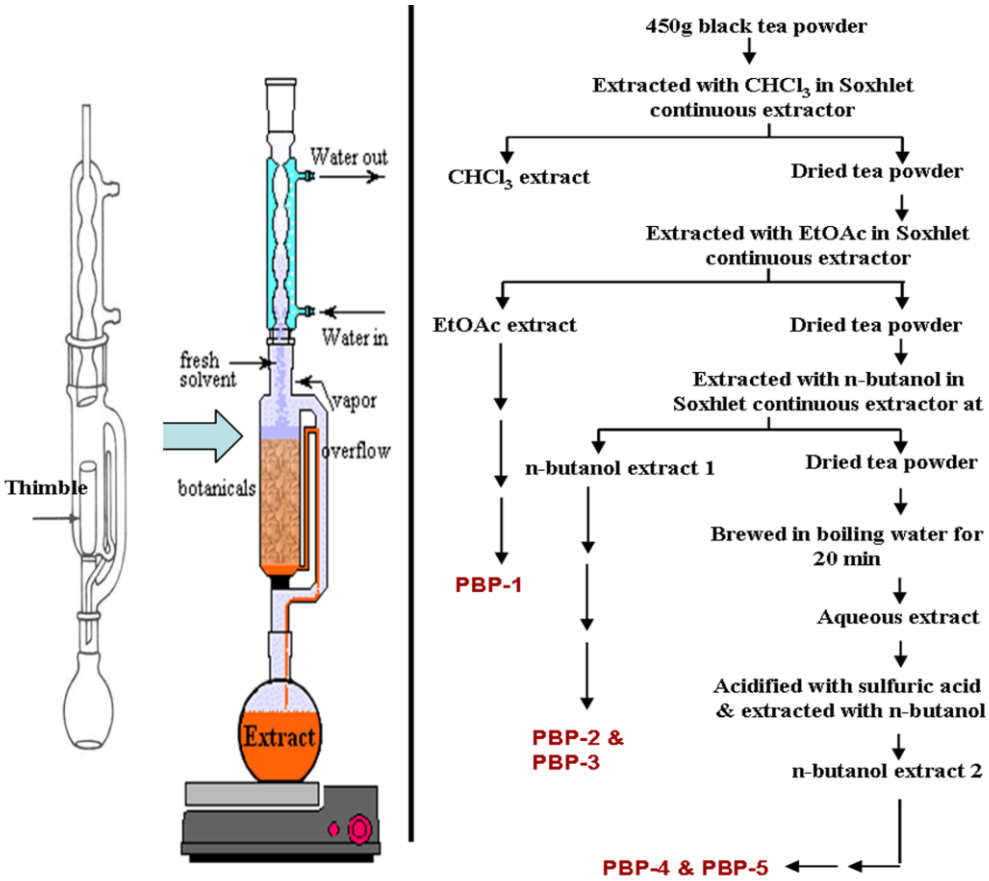

FIGURE 4.1: Solid (tea powder) – liquid extraction of polymeric black tea polyphenols (PBPs), employing the Soxhlet continuous extractor.

4.2.2 Determination of contamination by other black tea components

To ascertain that PBP fractions were free from other known biologically active, mobile components present in black tea such as caffeine, free catechins [C, EC, ECG, EGC, EGCG, GCG] or TFs, 20-40 µl of each PBP fraction (5 mg dissolved in 1 ml acetone) were spotted on pre-coated silica gel plates containing 254 nm fluorescent indicator and developed in chloroform: ethyl acetate: formic acid (6:4:1) and visualized under UV light. The authentic standards for caffeine and free catechins were also spotted on the same plate for comparison. After confirming the purity, these extracted PBPs were used for all further experiments.

4.2.3 Animal treatment

Six to eight weeks old female Swiss bare mice (Generation used 12^{th}-26^{th}) were randomized into eighteen different treatment groups (each group with at least five animals), viz., vehicle control (acetone), TPA (5 nmol), PBPs 1-5 each/ EGCG (200 µg), curcumin (10 µmol) and Ro-31-8220 (PKC inhibitor, 1 nmol) treated group, test groups [topically pretreated with PBPs 1-5/EGCG/curcumin/Ro-31-8220 and subsequently with TPA after 20 min]. For all groups, the mice were killed 4 h after TPA application. For upstream kinase study, animals were pretreated with inhibitors (2 µmol) for various kinases (BAG 956 - PDK and PI3K inhibitor; OSU-03012 - PDK1 inhibitor; PDK1/AKT/Fit dual inhibitor - PDK1 and AKT inhibitor; Wortmannin - PI3K inhibitor and mixture of all above four inhibitors- each 500 nmol) for 20 min followed by TPA (5 nmol) treatment for 4 h. The epidermis was gently separated from the skin using a Watson skin grafting knife with suitably adjusted cutting angle. Tissues of animals belonging to the various treatment groups were washed with acetone, because this facilitates the removal of the color of curcumin/PBPs from the skin before separation of the epidermis. This was done to avoid color interference in spectrophotometric determinations.

4.2.4 PKC enzyme assays and levels

For assaying PKC activity and expression of its isozymes known to be expressed in mouse skin (α, β, γ, ε, η, δ, ζ), cytosolic and particulate/membrane fractions were prepared as described in Materials and methods (Chapter 3; sections 3.4.3) [139]. PKC activity in cytosolic and particulate/membrane fractions was measured using PKC biotrak

enzyme assay kit (RPN-77; Amersham Biosciences, Little Chalfont, UK) as described in Materials and methods (Chapter 3; section 3.8.2), wherein PKC present in the samples catalyzed the transfer of γ-phosphate group of adenosine-5'-triphosphate to a peptide which is specific for PKC. The extent of phosphorylation thus, represents the PKC activity and results were expressed as pmol/min/mg protein. To study the cellular distribution of PKC isozymes (α, β, γ, ε, η, δ, ζ), 50 µg of cytosolic and particulate proteins were separated on an 8% SDS-PAGE and immunoblotted using isozyme-specific antibodies as described in Materials and methods (Chapter 3; section 3.6). After western blotting, the membrane was stained with Coomassie Brilliant Blue R-250 (CBB) which served as control for equal loading. Densitometry of various analyte proteins and their respective loading controls from the same blots was performed using Image J 1.43 (NIH) software. Densitometry of analytes protein was divided by densitometry of respective loading control to get normalized relative optical density. Data i.e. mean ±SE of three to five independent samples in each group have been compared and presented.

4.2.5 Protein immunoblotting

Total cell extracts and cytosolic and nuclear extracts were prepared from the epidermis by a previously described cell fractionation protocol in Materials and methods (Chapter 3; sections 3.4.1 and 3.4.2) [138]. The expression of various proteins in different lysates was studied by SDS-PAGE followed by immunoblotting as described in Materials and methods (Chapter 3; section 3.6). All primary and secondary antibodies were first standardized for their dilutions and then used accordingly. β-actin or Histone H1 or total lane density of fast green stained membrane was used as loading control for respective protein depending upon the fraction. Densitometry of various analyte proteins was performed using Image J 1.43 (NIH) software as described in Materials and methods (Chapter 3; section 3.6.5).

4.2.6 Immunoprecipitation

Particulate fraction (500 µg protein)waspre-cleared, immunoprecipitated with anti-phosphothreonine antibody and blotted with PKCα and AKT1/2 as described in Materials and methods (Chapter 3; section 3.7) to study the levels of PKCα and AKT1/2 phosphorylations at threonine positions.

Protein	% gel	Amount of protein	Primary antibody dilution	Secondary antibody dilution
AKT1 (pS473)	10%	Particulate lysate, 50 µg	1:1000	1:4000
AKT1 (pT308)	10%	″	1:1000	1:4000
AKT1/2	10%	″	1:2000	1:8000
β-actin	10%	Total cell lysate, 50 µg	1:1000	1:5000
Bax	12%	″	1:1000	1:5000
Bcl-2	12%	″	1:1000	1:5000
Cox-2	8%	″	1:2000	1:5000
Cyclin D1	10%	″	1:500	1:4000
Histone H1	12%	Nuclear lysate, 50 µg	1:1000	1:5000
IKKα	8%	Cytosolic lysate, 50 µg	1:1000	1:5000
IκB-α	12%	″	1:1000	1:5000
pIκB-α	12%	″	1:500	1:5000
NF-κB	10%	Nuclear lysate, 50 µg	1:1000	1:5000
pNF-κB	10%	″	1:1000	1:5000
PCNA	12%	Total cell lysate, 50 µg	1:1000	1:5000
PDK1	10%	Particulate lysate, 50 µg	1:1000	1:4000
PDK1 (pS241)	10%	″	1:1000	1:4000
PI3K	8%	Particulate lysate, 50 µg	1:1000	1:4000
PKCα	8%	Cytosolic & particulate lysate, 50 µg	1:1000	1:6000
PKCα (pT497)	8%	Particulate lysate, 50 µg	1:1000	1:4000
PKCα (pS657 +Y658)	8%	″	1:1000	1:6000
PKC PAN (βII S660),	8%	″	1:1000	1:6000
PKCα/βII(pT638/ 641)	8%	″	1:1000	1:4000
PKCß	8%	Cytosolic & particulate lysate, 50 µg	1:1000	1:4000
PKCδ	8%	″	1:500	1:4000
PKCη	8%	″	1:1000	1:4000
PKCγ	8%	″	1:1000	1:4000
PKCζ	8%	″	1:500	1:4000
PKCε	8%	″	1:1000	1:4000

4.2.7 Confocal microscopy

The epidermal layer was manually extracted from skin as described above and fixed in 10% buffered formalin, which was further processed for making 5 µm paraffin-embedded tissue section on glass slides. Initially, tissue sections were collected after varying time period of TPA treatment (15 min, 30 min, 1 h, 2 h, 4 h) to select the suitable sampling time for optimal signal detection. Signal detection is expressed by calculating

the mean fluorescence intensity of PKCα/PKCδ/area of epidermal cells. PKCα is one of the isoforms that are altered and highly abundant in skin and key regulator of the initiation of differentiation, whereas PKCδ is not altered in any of the treatment groups. The mean fluorescence intensity of PKCα and PKCδ were determined in epidermal layer of mouse skin as described in Materials and methods (Chapter 3; section 3.12). Confocal images were obtained using a LSM 510 Meta Carl Zeiss Confocal system with argon 488 nm and helium/neon 543 nm lasers. The images were obtained using an Axio Observer Z.1 microscope at a magnification of 630X with 1X optical zoom. Results were expressed as mean fluorescence intensity of PKCα/PKCδ/area (μm^2) of epidermal cells from skin tissue sections.

4.2.8 Cell culture experiments

The human transformed HaCat cells were cultured as monolayers at 37 °C in a 5% CO2 atmosphere in DMEM containing 5-10% FBS. Initially, monolayer-cultured HaCat cells were treated with DMSO (vehicle control) or TPA (100, 200, 400, 600 ng/ml of media) for 1 h for evaluation of translocation of PKCα by western blot. HaCat cells were pretreated with PBP-3 or PBP-5 (200 µg/ml of media) for 20 min followed by TPA treatment (200 ng/ml of media) for 1 h. Further, treated cells were washed with PBS, trypsinized, collected by centrifugation, washed with phosphate buffer saline (PBS) and pelleted again. Cytosolic and particulate protein fractions were prepared as described [142]. Protein content was determined as described in Material and methods (Chapter 3, section.3.5)

In another series of experiments, the cells were plated on coverslips and grown overnight. The next day, the cells were treated as described above with PBP-3 or PBP-5 followed by TPA for immmunostaining evaluations.

4.2.9 Immunostaining of cells

To detect the expression and translocation of PKCα and PKCδ isoforms, immunostaining was performed on HaCat cells grown on cover slips. After treatment (as described above), the cells were fixed and permeabilized. The mean fluorescence intensity of PKCα and PKCδ was determined on HaCat cells grown on cover slips as described in Materials and methods (Chapter 3; section 3.14). Non-specific staining was determined by processing the cells without primary antibody. Each experiment was

repeated three times and atleast 50 cells were examined in each group. Confocal images were obtained as described above at a magnification of 630X with 3X optical zoom. The translocation of PKCα from cytosol to membrane was determined using mean fluorescence intensity of plasma membrane, calculated by subtracting the mean fluorescence intensity (PKCα/PKCδ) of cytosol from the whole cell.

4.2.10 PI3K activity

PI3K activity was compared in immunoprecipitated proteins (500 µg) from particulate fractions in different treatment groups employing a PI3K ELISA kit (K-1000s, Echelon Biosciences, Salt lake City, UT, USA) as described in Materials and methods (Chapter 3; section 3.15). This kit measures PI3K activity in terms of conversion of phosphatidyl-inositol 4,5-bisphosphate [PI(4,5)P2] into phosphatidyl-inositol (3,4,5) triphosphate [PI(3,4,5)P3]. Absorbance values were measured at 450 nm using an ELISA reader. The enzyme activity was expressed as pmol of PI(3,4,5)P3 formed/mg protein.

4.2.11 Determination of *in vitro* interaction between TPA and PBP-3 or PBP-5

4.2.11.1 Isothermal titration calorimetry (ITC)

TPA (3µg/100µl) and PBP-3 or PBP-5 (30µg and 60 µg/100µl) were dissolved in 50 mM Tris HCl buffer (pH 7.4) containing 1% DMSO. An ITC experiment was carried out (at 20 °C and 37 °C) with a MicroCal ITC 200 (GE Healthcare, UK) wherein TPA in calorimeter cell was titrated with PBP-3 or PBP-5 in a syringe as described in Materials and methods (Chapter 3; section 3.19). Instrumental baseline was subtracted from the raw exothermic heat pulse data from each injection to obtain normalized integrated heat. Thermograms were evaluated using Origin (version 7; OriginLab).

4.2.11.2 UV absorption spectra and mass spectrometry

TPA (3µg/100µl), and PBP-3 (200µg/100µl) and PBP-5 (200µg/100µl) were dissolved in acetone. TPA, PBP-3, PBP-5 and mixture containing PBP-3 + TPA and PBP-5 + TPA were incubated for 20 min at 37°C. UV absorption spectra were recorded at 200-600nm in a range of 0-2 absorbance using Jasco V-650 spectrophotometer after diluting the sample in acetone at a ratio of 1:50.

Further, the same samples were analyzed by Mass spectrometry (MS) as described in Materials and methods (Chapter 3; section 3.17). Mass calibration was carried out

using peptide mixture of five known peptides spanning mass range of 500–4400 m/z and error was kept to less than 10 ppm. The MS data were acquired using a solidstate NdYAG laser at 337 nm. The resulting MS data was analyzed using Flex analysis 3.0 software (Bruker Daltonik, Germany).

4.2.11.3 Measurement of GSH/GSSG ratio in epithelial cell extracts

Freshly collected epithelial cells from animals belonging to various treatment groups were homogenized and the extracts were used for the measurement of reduced glutathione (GSH) and oxidized glutathione (GSSG) levels as described in Materials and methods (Chapter 3; section 3.18). The levels of GSH and GSSG in nanograms per microgram DNA were used for calculation of GSH/GSSG ratio. The mean ± SE of two independent samples were presented.

4.2.12 Statistical analysis

Statistical analysis was performed using SPSS 15.0 software. Data are presented as the mean ± SE. Means of all data were compared by ANOVA with post hoc Bonferroni's test. Considering multiple group comparisons the most commonly used Bonferroni's post hoc test was employed for statistical analysis wherein numbers of family wise error rates are compensated. $p \leq 0.05$wasconsideredstatistically significant.

4.3 RESULTS

4.3.1 Isolation of PBP fractions using Soxhlet continuous extractor

As mentioned in methods section 4.2.1, the isolation of the PBP fractions was carried out by successive extraction of the black tea powder with chloroform, ethyl acetate and n-butanol using Soxhlet continuous extractor (Fig. 4.1). This process yielded five main polymeric black tea polyphenol fractions, namely, PBP-1, PBP-2, PBP-3, PBP-4 and PBP-5. This method yielded 10.3% of total PBPs, of which 2.68%, 3.79%, 1.34%, 2.20% and 0.32% (w/ w) were the individual yields of PBP-1 to PBP-5, respectively (Fig. 4.2). The PBP fractions were isolated in big batches and yields of PBP fractions obtained during each extraction were similar to those reported.

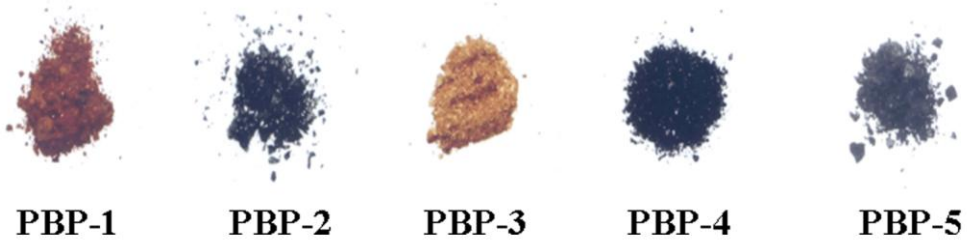

FIGURE 4.2: Polymeric black tea polyphenol (PBPs) fractions.

4.3.2 Determination of contamination by other black tea components

Thin-layer chromatographic evaluation of PBPs (PBP 1-5) showed that all PBP fractions (PBP 1-5) were free from contamination by other known biologically active mobile components in black tea (Fig. 4.3), as suggested by the absence of spots corresponding to caffeine, free catechins or TFs. PBPs were retained at the origin, showing strong solid matrix reactivity whereas free catechins and caffeine from green tea migrated as expected and so did TFs from black tea. These results show that PBPs isolated from black tea were free from other known biologically active components of black tea.

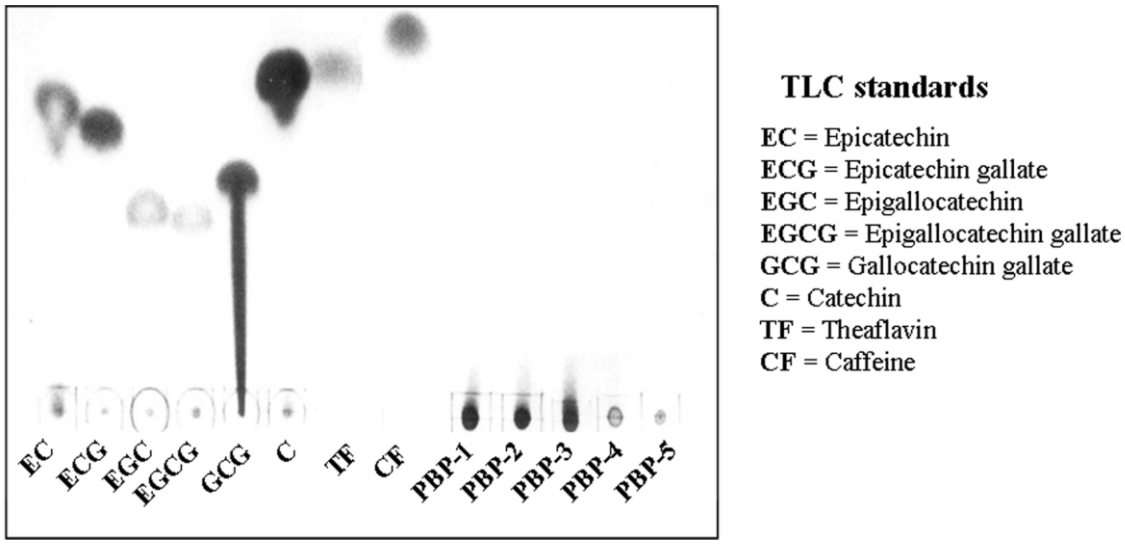

FIGURE 4.3: Thin layer chromatogram of different green and black tea polyphenols for confirming the purity of PBPs fractions.

4.3.3 PBP pre-treatment inhibits TPA-induced PKC translocation

4.3.3.1 Measurement of PKC protein level and activity

Compared to controls, topical application of TPA (5 nmol) onto the dorsal skin of Swiss bare mice enhanced the translocation of PKC isozymes (α, β, η, γ, ε) from cytosolic to the particulate membrane, as evident from their relative protein levels in the two compartments (Figs. 4.4, 4.5, 4.6 and 4.7). In concordance with the protein levels, TPA

treatment resulted in a relative decrease in PKC activity in the epidermal cytosolic fraction, whereas the activity increased significantly in the particulate fraction (Fig. 4.8). However, TPA treatment did not alter the levels of PKCs δ and ζ in the two compartments (Figs. 4.4, 4.5, 4.6 and 4.7). PKC levels as well as the activity in both the compartments of mouse skin treated with PBPs 1-5 (200 μg), EGCG (200 μg), or curcumin (10 μmol) (positive control) alone were comparable with those of acetone (vehicle control)-treated animals (Figs. 4.4, 4.5, 4.6, 4.7 and 4.8). Topical application of PBPs 1-3, EGCG, or curcumin before TPA significantly decreased the TPA-induced translocation of PKC isozymes (α, β, η, γ, ε) from cytosol to membrane, measured in terms of protein levels (Figs. 4.4, 4.5, 4.6 and 4.7). However, no such decrease in translocation of TPA-induced PKC was observed on pre-treatment with PBP-4 and PBP-5 (Figs. 4.6 and 4.7). This was further correlated with the effects on enzyme activity, wherein PBP 1-3, EGCG, and curcumin pre-treatment significantly reduced both the TPA-mediated decrease in cytosolic PKC activity and the increase in particulate PKC activity, whereas PBP-4 and PBP-5 did not have any significant effect (Fig. 4.8). Topical application of Ro-31-8220 (1 nmol) (PKC inhibitor) alone attenuated the PKC activity in both cytosolic and particulate fractions compared to controls (Fig. 4.8B) but did not alter the protein levels of PKC isozymes (Figs. 4.6 and 4.7). Interestingly, although pre-treatment of mouse skin with Ro-31-8220 inhibited PKC activity in both compartments (Fig. 4.8B), TPA-induced translocation of protein remained unaltered, resulting in levels of proteins similar to those observed in animals treated with TPA alone (Figs. 4.6 and 4.7).

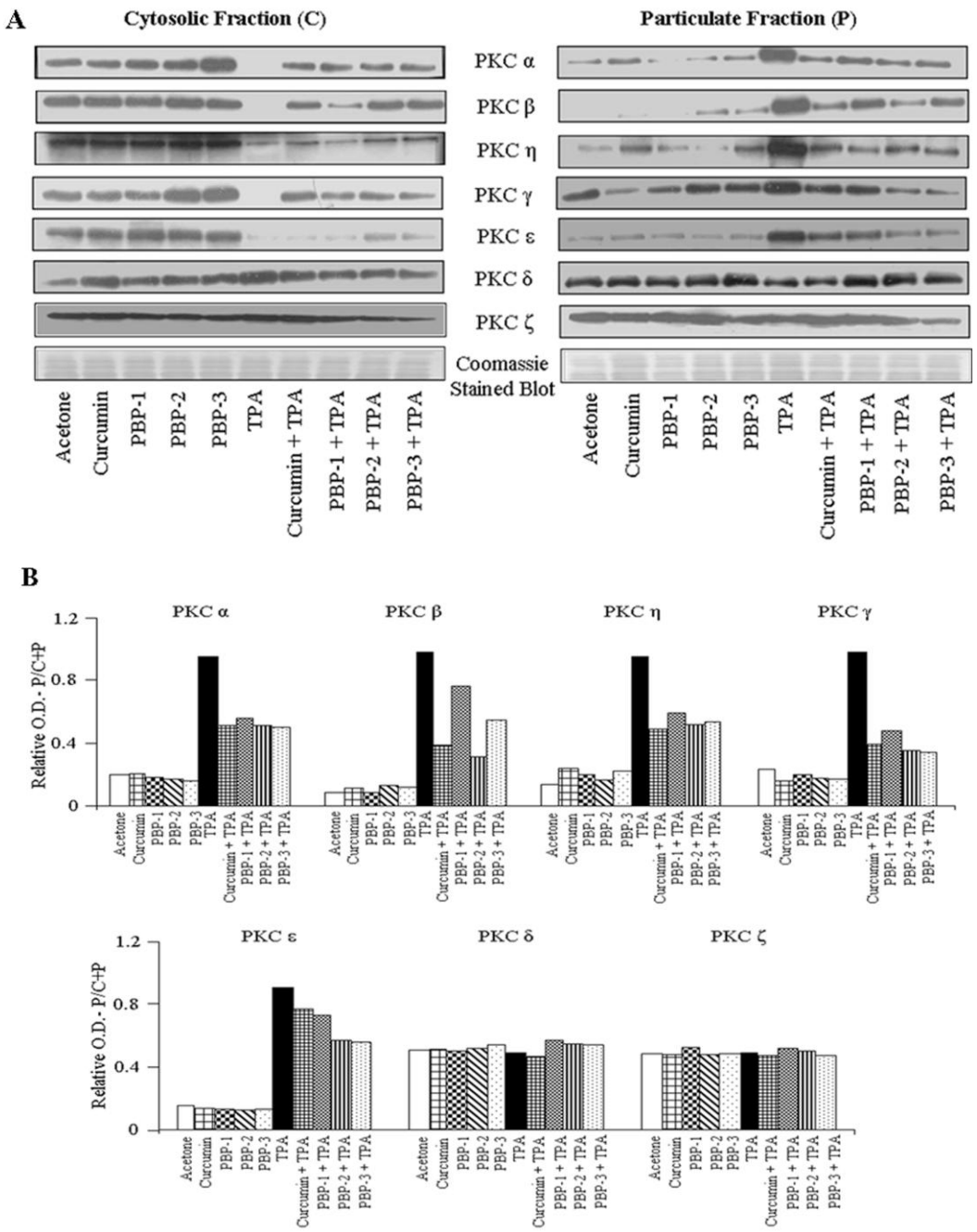

FIGURE 4.4: Effect of PBPs 1-3 and curcumin on the levels of TPA-induced PKC isoforms in cytosolic and particulate cell lysates from mouse skin epidermis. (A)*Representative blots, and***(B)** *Relative levelsof PKC isozymes (α, β, η, γ, ε, δ, ζ) protein levels in cytosolic (50 µg) and particulate (50 µg) fractions of curcumin or PBPs 1-3 alone or before TPA treated groups by western blotting using specific antibodies. Quantification was done by normalizing the band density to that of total lane density in the same membrane stained with Coomassie Brilliant Blue (CBB) after western blotting. Relative optical density of particulate fraction (P)/cytosolic + particulate fraction (C+P) is shown. Data represent mean ± SE of five observations. Differences among groups were determined by one-way ANOVA followed by Bonferroni's test, $p \leq 0.05$. '*' significant when compared with TPA; '#' significant when compared with acetone; '¥' significant when compared with respective controls.*

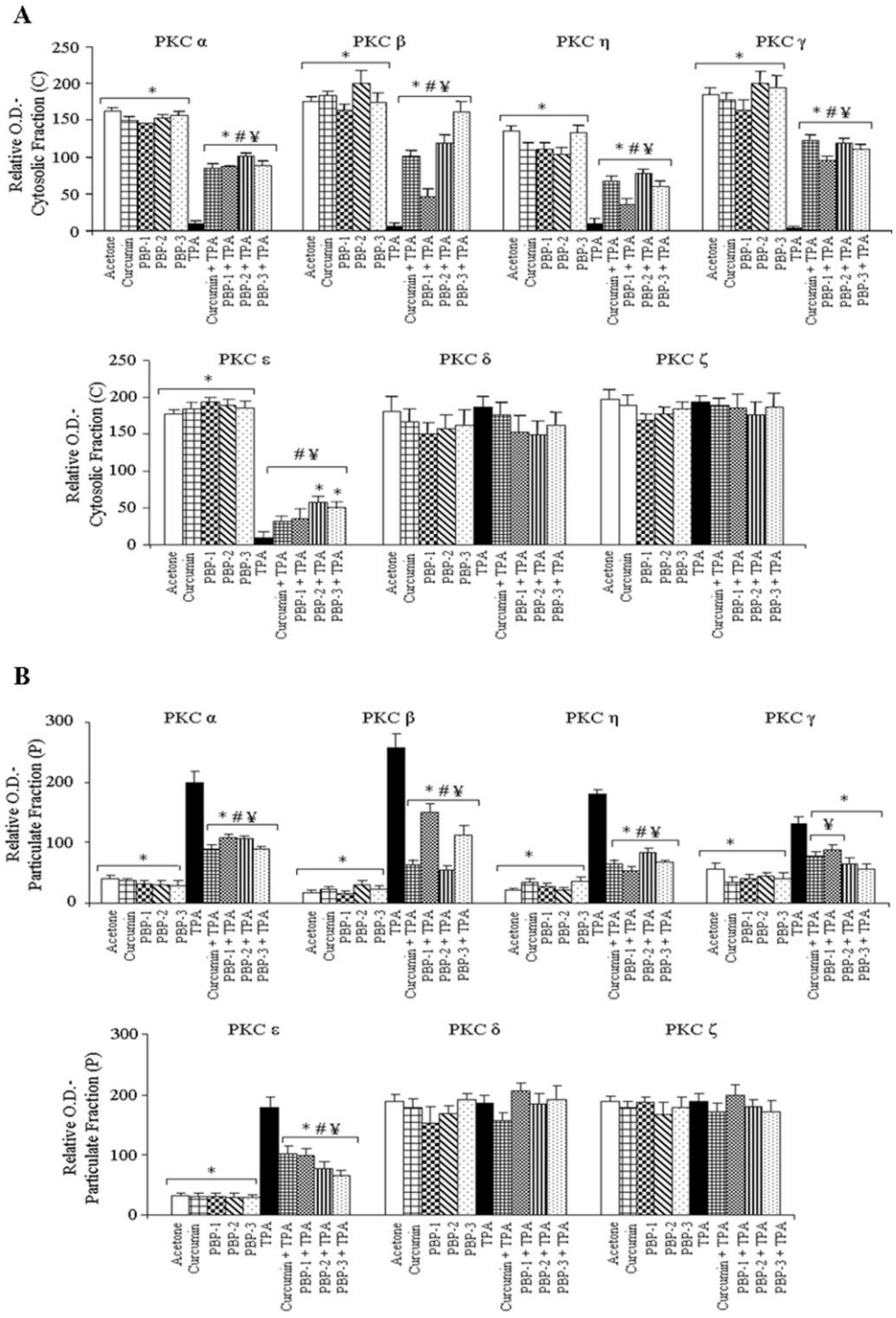

FIGURE 4.5: Effect of PBPs 1-3 and curcumin on the levels of TPA-induced PKC isoforms in cytosolic and particulate cell lysate from mouse skin epidermis. (A) *Relative optical density of cytosolic fraction.* **(B)** *Relative optical density of particulate fraction. Quantification was done by normalizing the band density of PKC isozymes (α, β, η, γ, ε, δ, ζ) protein levels in cytosolic and particulate fractions to that of total lane density of same membrane stained with CBB after western blotting. Data represent mean ± SE of five observations. Differences among groups were determined by one-way ANOVA followed by Bonferroni's test, $p \leq 0.05$. '*' significant when compared with TPA; '#' significant when compared with acetone; '¥' significant when compared with respective controls.*

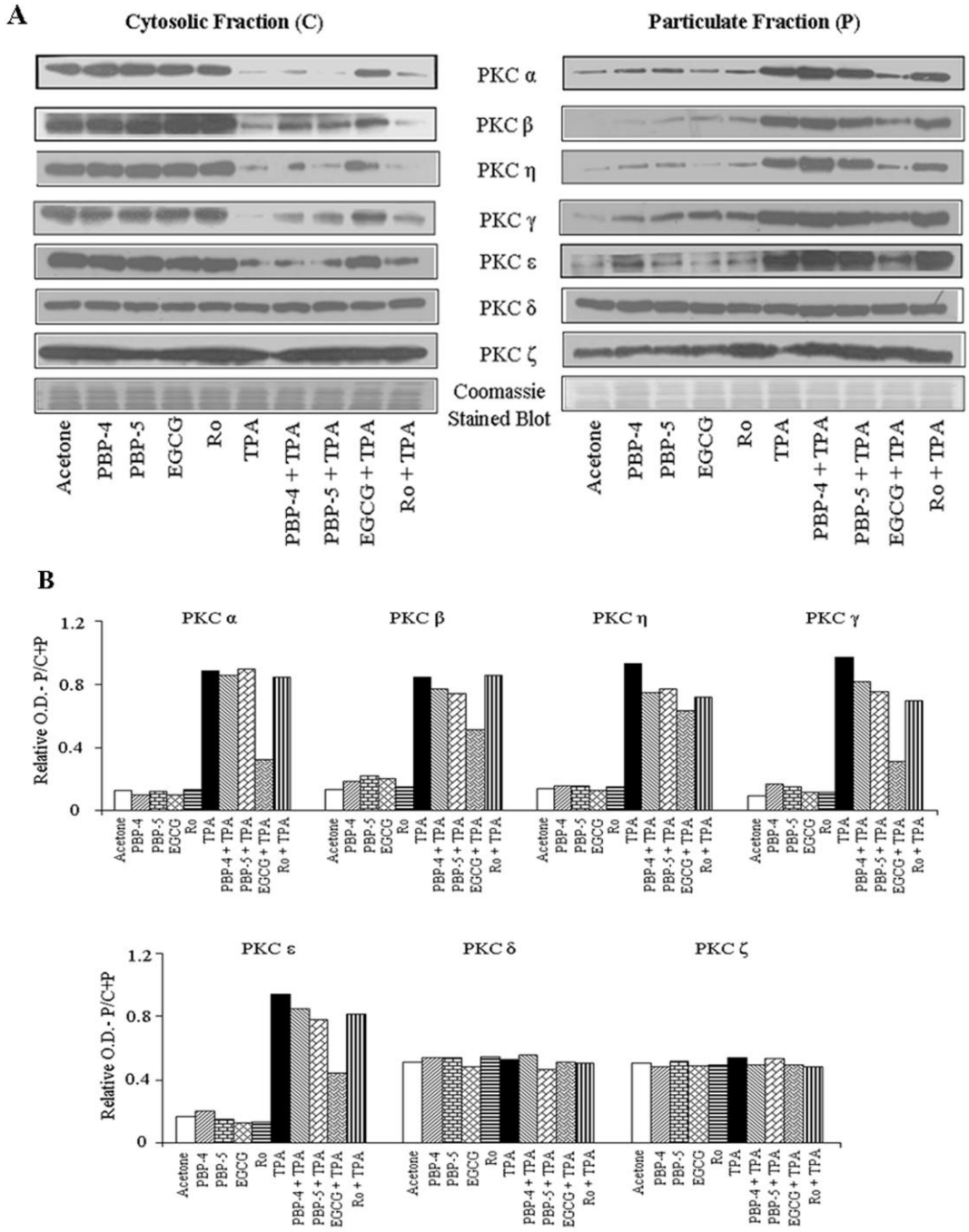

FIGURE 4.6: Effect of PBPs 4 and 5, EGCG and Ro-31-8220 on the levels of TPA-induced PKC isoforms in cytosolic and particulate cell lysate from mouse skin epidermis.(A)*Representative blots, and***(B)** *Relative levels of PKC isozymes (α, β, η, γ, ε, δ, ζ) measured in cytosolic (50 µg) and particulate (50 µg) fractions of PBP-4 or PBP-5 or EGCG or Ro-31-8220 alone or before TPA treated groups by western blotting using specific antibodies. Quantification was done by normalizing the band density to that of total lane density of same membrane stained with CBB after western blotting. Relative optical density of particulate fraction (P)/cytosolic + particulate fraction (C+P) is shown. Data represent mean ± SE of five observations. Differences among groups were determined by one-way ANOVA followed by Bonferroni's test, p ≤ 0.05. '*' significant when compared with TPA; '#' significant when compared with acetone; '¥' significant when compared with respective controls.*

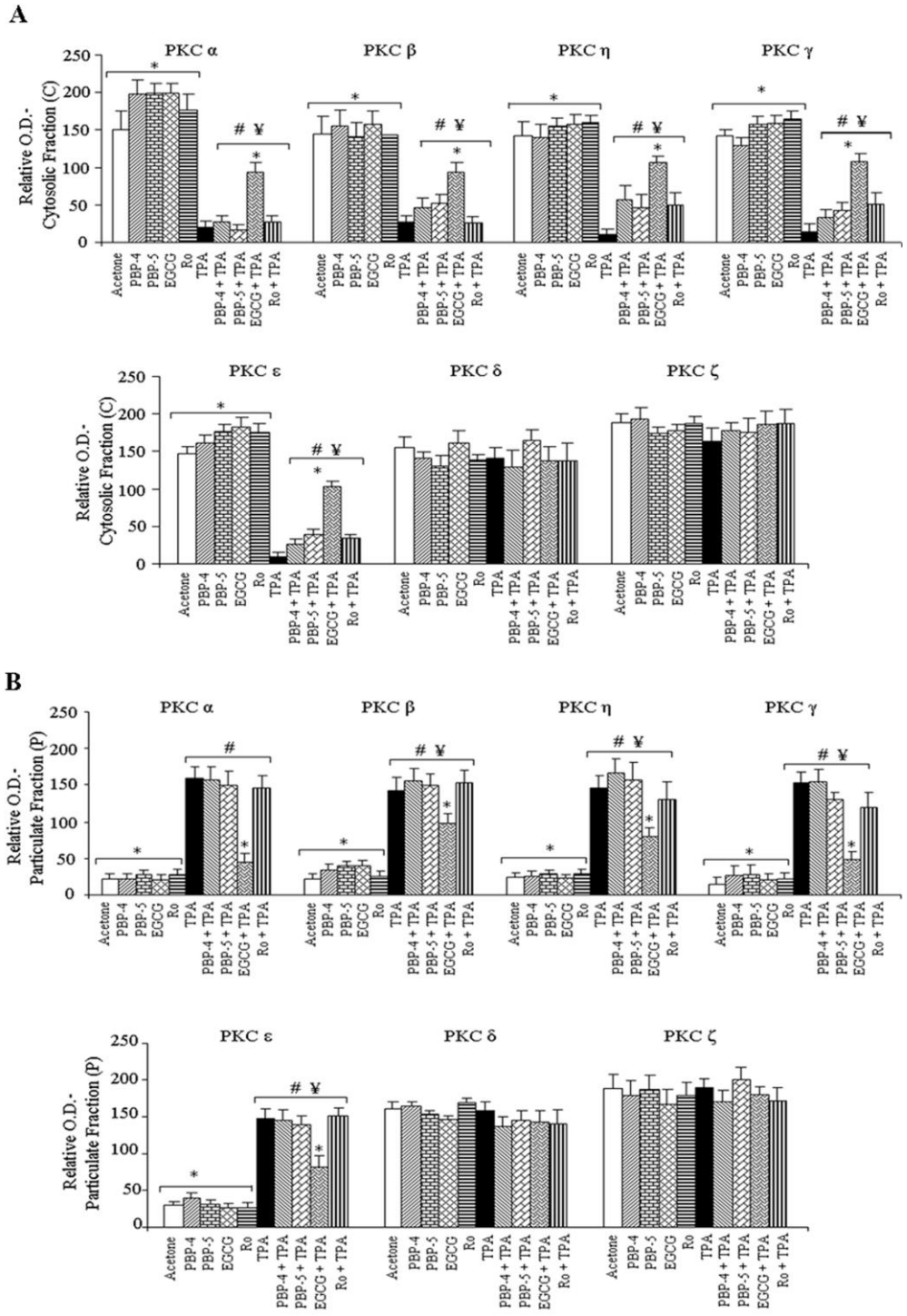

FIGURE 4.7: Effect of PBPs 4 and 5, EGCG and Ro-31-8220 on the levels of TPA-induced PKC isoforms in cytosolic and particulate cell lysate from mouse skin epidermis.(A) *Relative optical density of cytosolic fraction.***(B)** *Relative optical density of particulate fraction. Quantification was done by normalizing the band density of PKC isozymes (α, β, η, γ, ε, δ, ζ) protein levels in cytosolic and particulate fractions to that of total lane density of same membrane stained with CBB after western blotting. Data represent mean ± SE of five observations. Differences among groups were determined by one-way ANOVA followed by Bonferroni's test, $p \leq 0.05$. '*' significant when compared with TPA; '#' significant when compared with acetone; '¥' significant when compared with respective controls.*

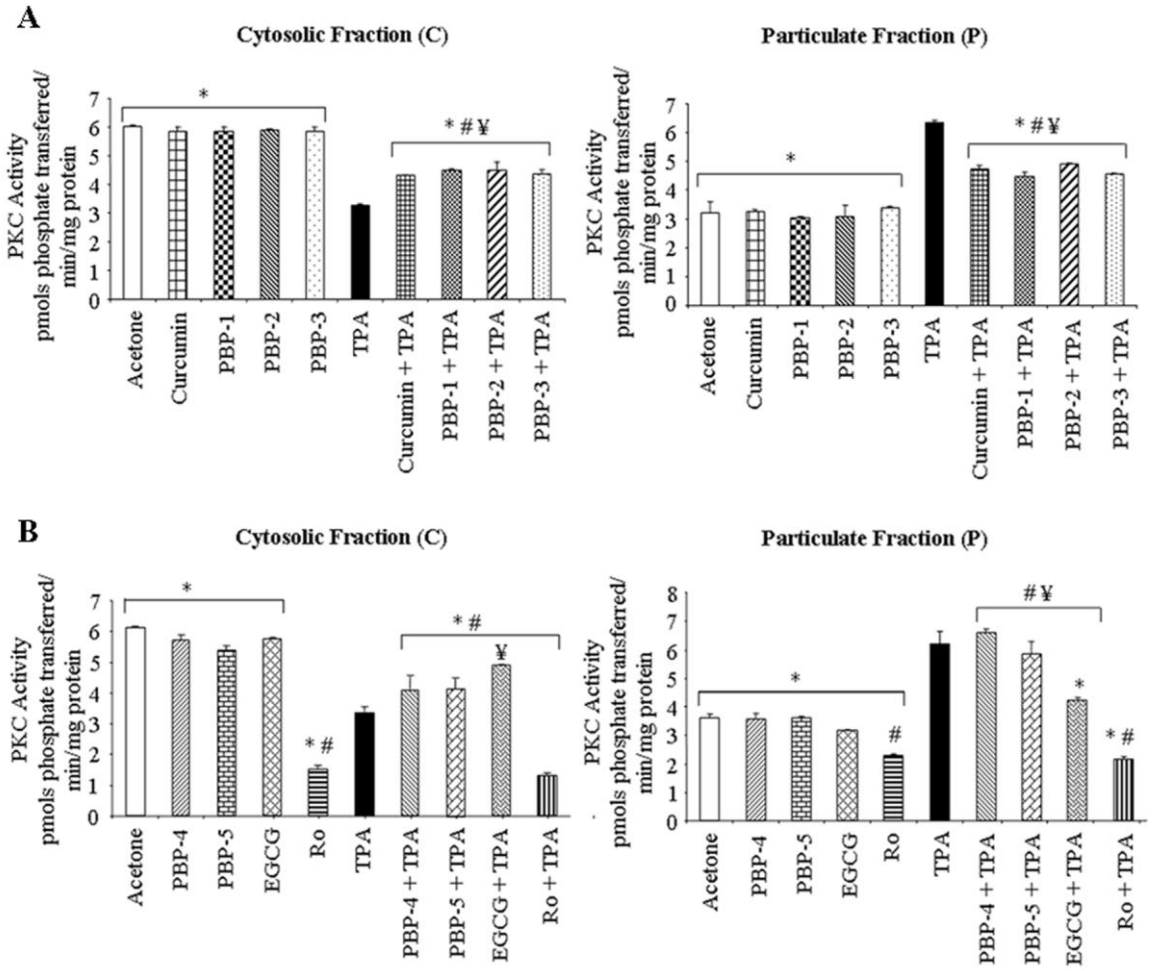

FIGURE 4.8: Effect of PBPs 1-5, curcumin, EGCG and Ro-31-8220 on PKC activity in cytosolic and particulate cell lysate from mouse skin epidermis. *PKC activity in cytosolic and particulate fractions of* **(A)** *Curcumin or PBPs 1-3 alone or before TPA treated groups.* **(B)** *PBPs 4 and 5 or EGCG or Ro-31-8220 alone and before TPA treated groups. Data represent mean ± SE of at least three observations. Differences among groups were determined by one-way ANOVA followed by Bonferroni's test, $p \leq 0.05$. '*' significant when compared with TPA; '#' significant when compared with acetone; '¥' significant when compared with respective controls.*

4.3.3.2 Measurement of localization of PKC isoforms (α and δ) by confocal microscopy

To complement the results from western blot analysis, confocal microscopic evaluations of treated skin sections from above referenced treatment groups were undertaken. For selection of the optimal time point for signal detection, the mean fluorescence intensity of PKCα (calculated by PKCα-green/PKCδ-red/area) of epidermal layer of mouse skin was detected at various times of TPA treatment (15 min, 30 min, 1 h, 2 h, 4 h). It was observed that at 1 h mean fluorescence intensity of PKCα was relatively higher in TPA-treated sections compared to those at other time points (Fig. 4.9A).

Subsequently 1 h post-TPA treatment was employed in all further experiments. Moreover, the effects of pre-treatment with PBP-3, PBP-5, EGCG and Ro-31-8220 on the localization/distribution of TPA-induced changes on PKC isoforms (α, δ) were compared employing the mean fluorescence intensity of PKCα of the epidermal layer of mouse skin belonging to the various treatment groups. Compared with control, topical application of TPA resulted in an increase in mean fluorescence intensity of PKCα on the membrane (Figs. 4.9B, 4.10 and 4.11). In contrast, the levels of mean fluorescence intensity of PKCα in PBP-3-, PBP-5-, EGCG- and Ro-31-8220- treated controls were similar to that in acetone-treated cells (Figs. 4.9B, 4.10 and 4.11). However, topical pre-treatment with PBP-3 and EGCG before TPA application caused a decrease in mean fluorescence intensity of PKCα on membranes as compared to the TPA-treated group (Figs. 4.9B and 4.10), whereas animals pretreated with PBP-5 and Ro-31-8220 did not show such significant decrease (Figs. 4.9B and 4.11).

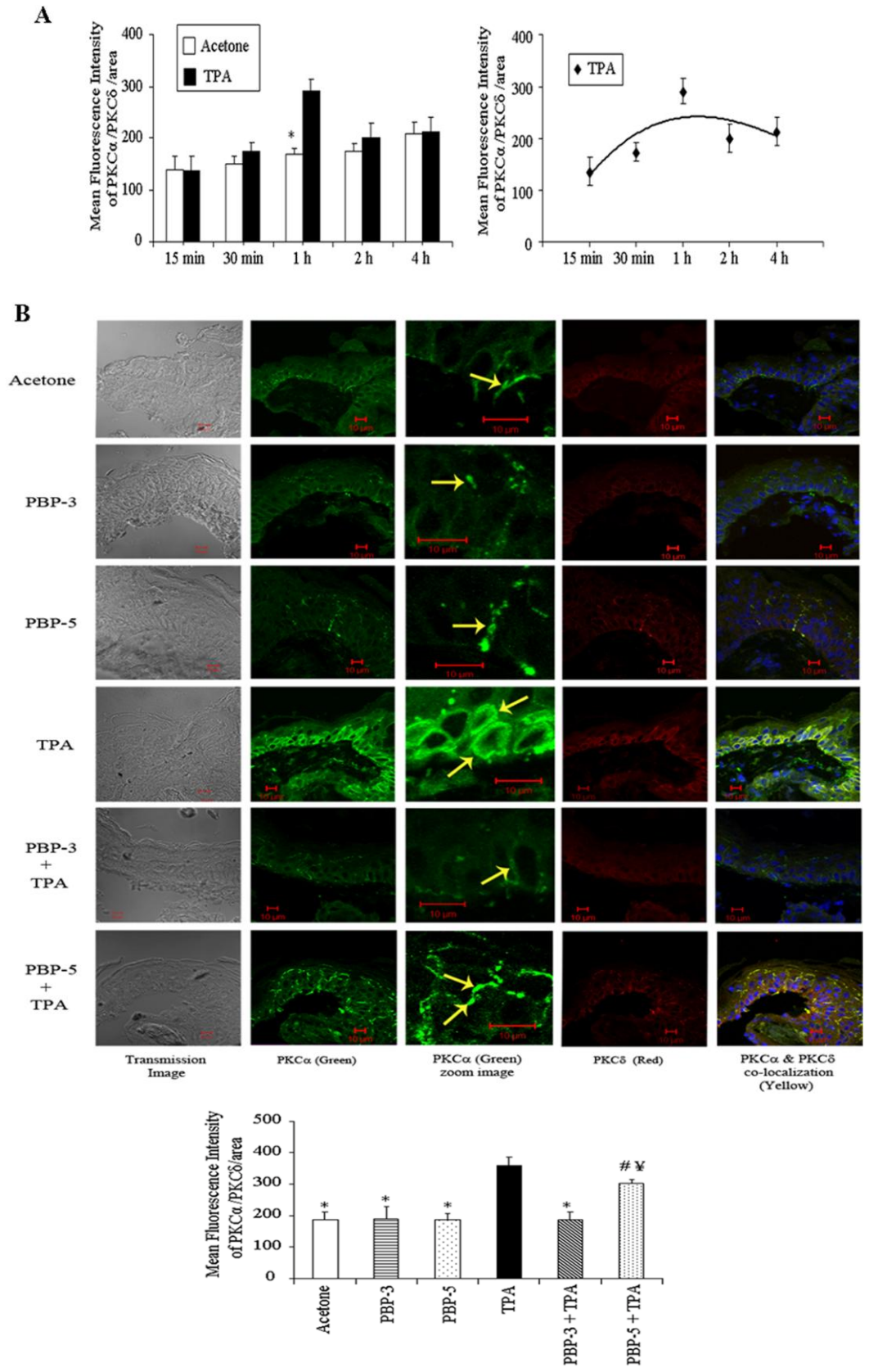

FIGURE 4.9: Effect of PBP-3 or PBP-5 on TPA-induced localization of PKC isoforms (α and δ) in the epidermal layer of mouse skin by confocal microscopy. (A) *Analysis of suitable sampling time for optimal signal detection on localization of TPA-induced PKC isoforms (α and δ) in epidermal layer of mouse skin sections at different*

time points (15 min, 30 min, 1 h, 2 h, 4 h). Differences among groups were determined by Non-Parametric test followed by Mann-Whitney test, p ≤ 0.05. '' significant when compared with TPA.* **(B)** *Confocal images comparing the TPA-induced localization of PKC isoforms (α and δ) in epidermal layer of mouse skin. Scale bars, 10 μm. Mean fluorescence intensity shown at the bottom panel was calculated by PKCα/ PKCδ/area of at least 10 randomly selected fields per section/animal. Data represent mean ± SE of three observations. Differences among groups were determined by one-way ANOVA followed by Bonferroni's test, p ≤ 0.05. '*' significant when compared with TPA; '#' significant when compared with acetone; '¥' significant when compared with respective controls.*

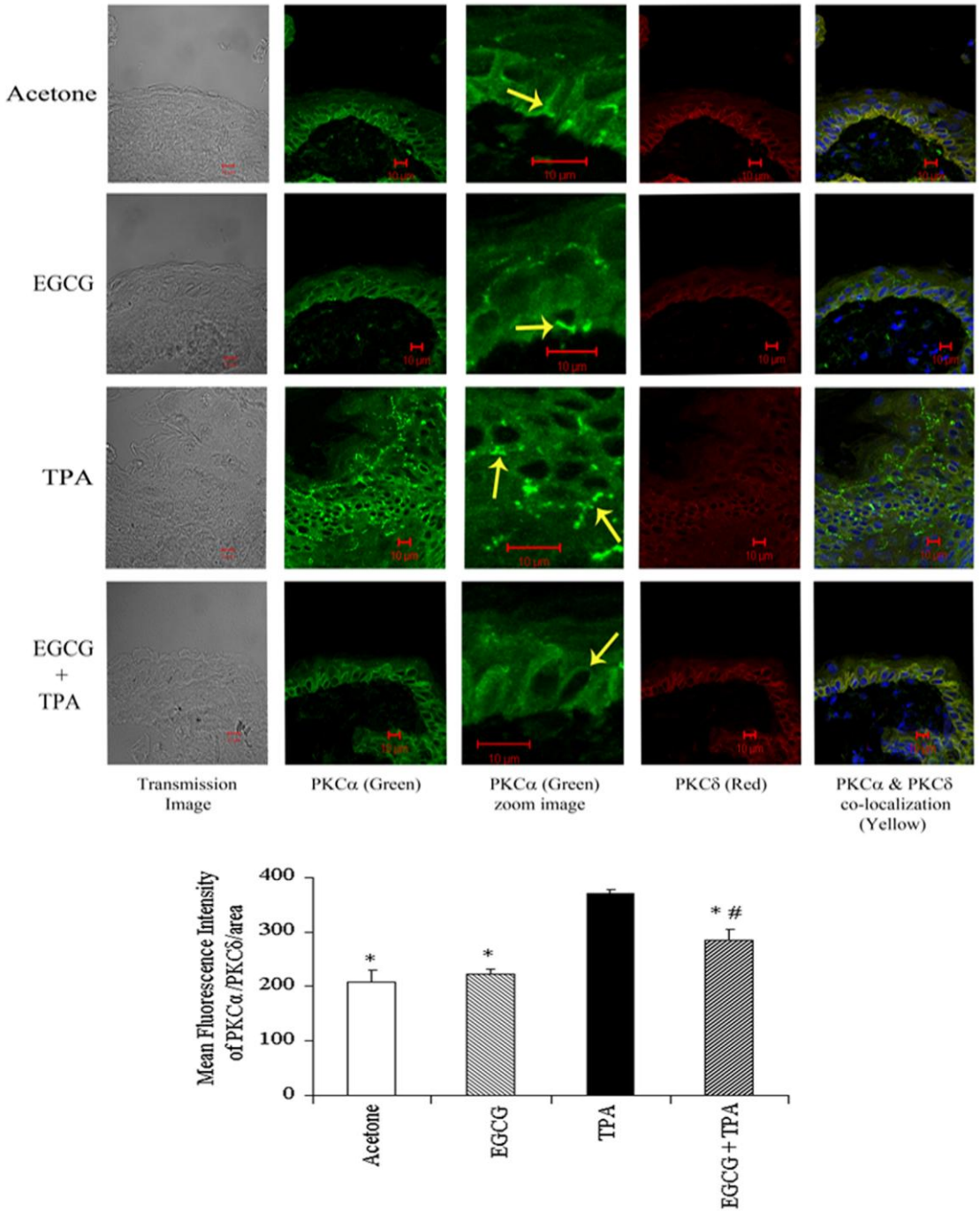

FIGURE 4.10: Effect of EGCG on TPA-induced localization of PKC isoforms (α and δ) in epidermal layer of mouse skin by confocal microscopy. *Confocal images comparing the TPA-induced localization of PKC isoforms (α and δ) in epidermal layer of mouse skin sections of EGCG treated groups. Scale bars, 10 µm. Mean fluorescence intensity shown at the bottom panel is calculated by PKCα/PKCδ/area of at least 10 randomly selected fields per section/animal. Data represent mean ± SE of three observations. Differences among groups were determined by one-way ANOVA followed by Bonferroni's test, $p \leq 0.05$. '*' significant when compared with TPA; '#' significant when compared with acetone.*

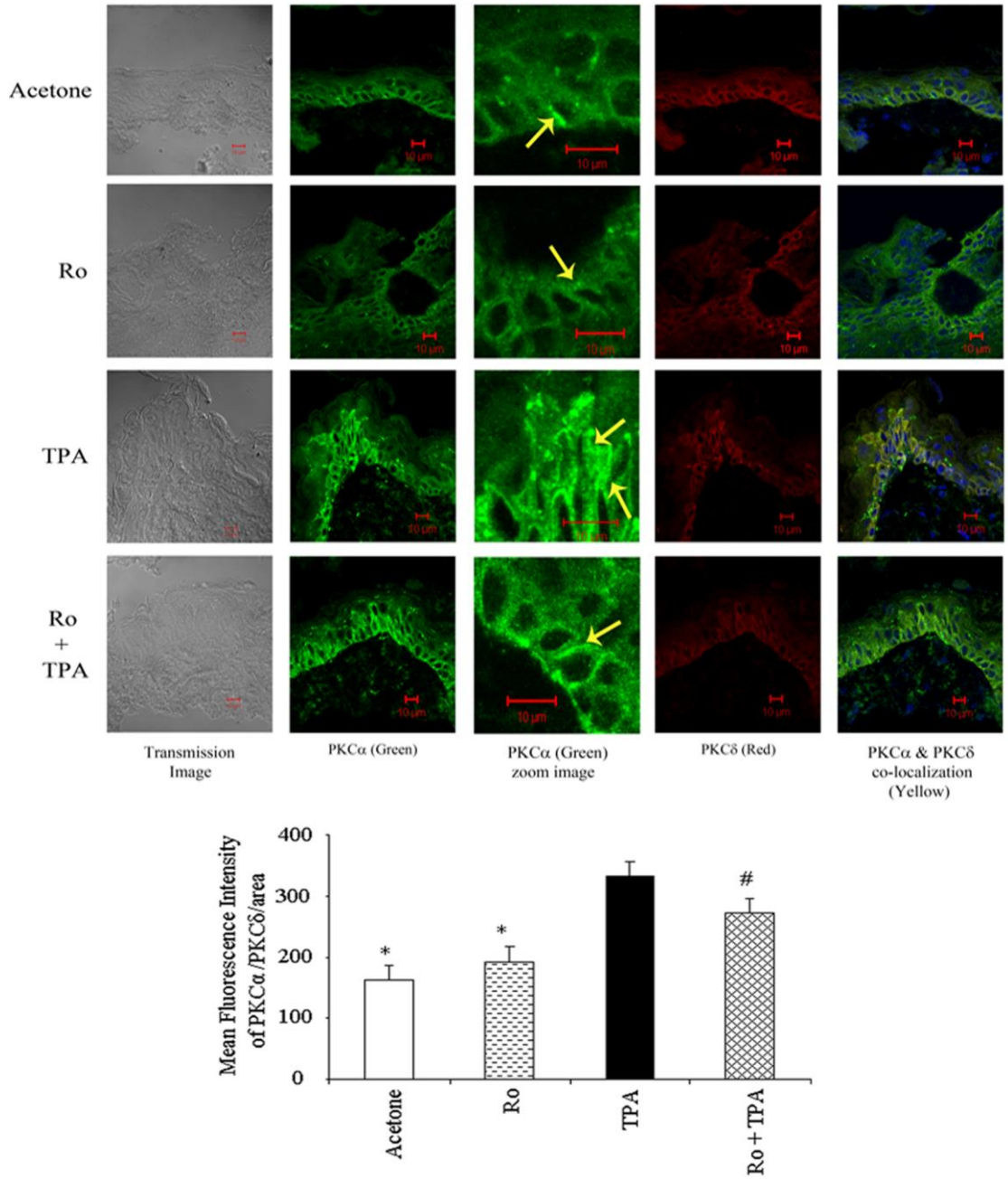

FIGURE 4.11: Effect of Ro-31-8220 on TPA-induced localization of PKC isoforms (α and δ) in epidermal layer of mouse skin evaluated by confocal microscopy.*Confocal images comparing the TPA-induced localization of PKC isoforms (α and δ) in epidermal layer of mouse skin sections of Ro-31-8220 treated groups. Scale bars, 10 µm. Mean fluorescence intensity shown at the bottom panel is calculated by PKCα/PKCδ/area of at least 10 randomly selected fields per section/animal. Data represent mean ± SE of three observations. Differences among groups were determined by one-way ANOVA followed by Bonferroni's test, p ≤ 0.05. '*' significant when compared with TPA; '#' significant when compared with acetone.*

Further, to complement and confirm the effects on localization observed in tissue/sections *in vivo* on a cell basis, monolayer-cultured HaCat cells were evaluated for

translocation of PKC. Western blot analysis and confocal microscopy results (data not shown) showed that application of TPA at a dose of 200 ng/ml resulted in maximum translocation of PKCα on membrane compared to control (Fig. 4.12A) and this dose was further used for all subsequent experiments.

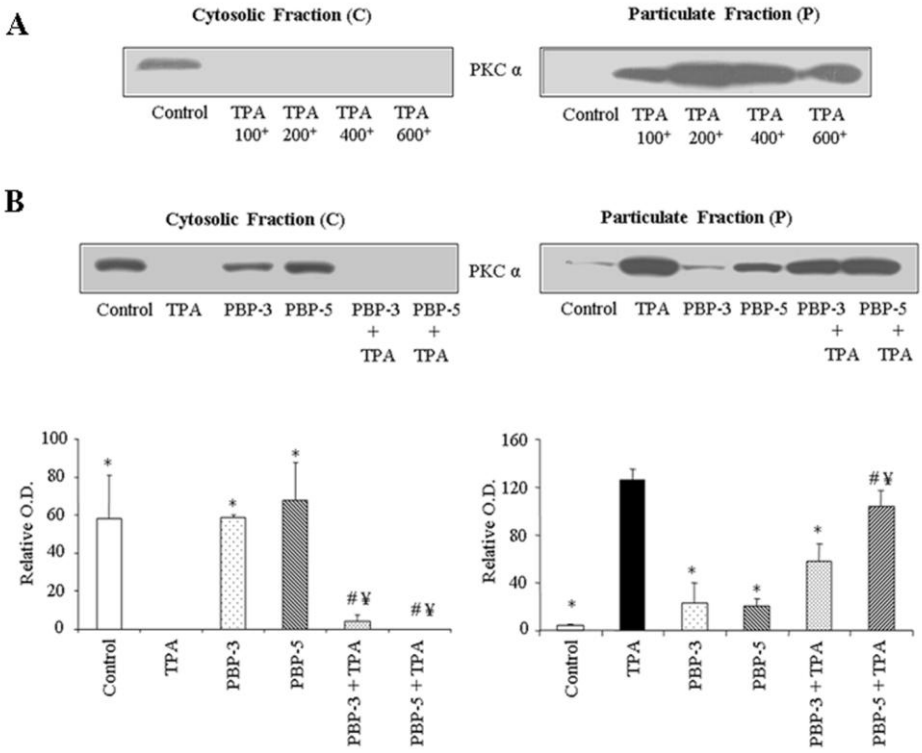

FIGURE 4.12: Effect of PBP-3 or PBP-5 on the levels of TPA-induced PKCα in cytosolic and particulate cell lysate from HaCat cells.*Representative blots and relative levels of PKCα in* **(A)** *TPA treatment groups at varying concentrations.* **(B)***PBP-3 or PBP-5 alone or before TPA treated groups. Quantification was done by normalizing the band density to that of total lane density in the same membrane stained with fast green after western blotting. Data represent mean ± SE of three observations. Differences among groups were determined by one-way ANOVA followed by Bonferroni's test, p ≤ 0.05. '*' significant when compared with TPA; '#' significant when compared with acetone; '¥' significant when compared with respective controls.*

To check the effect of PBPs, HaCat cells were grown on coverslips and treated with PBP-3 (200 µg/ml) for 20 min followed by 1 h TPA treatment. Topical application of TPA resulted in an increase in mean fluorescence intensity of membrane PKCα (translocates from cytosol to membrane), compared with control (where PKCα is mainly present in cytosol) (Fig. 4.13). In contrast, the levels of mean fluorescence intensity of PKCα in PBP-3 and PBP-5 treated controls were similar to that in the vehicle control (Fig. 4.13). However, pre-treatment with PBP-3 before TPA significantly decreased the TPA-induced mean fluorescence intensity of PKCα on the membrane, whereas PBP-5 pre-treatment did not significantly alter the TPA-induced effect on PKCα (Fig. 4.13).

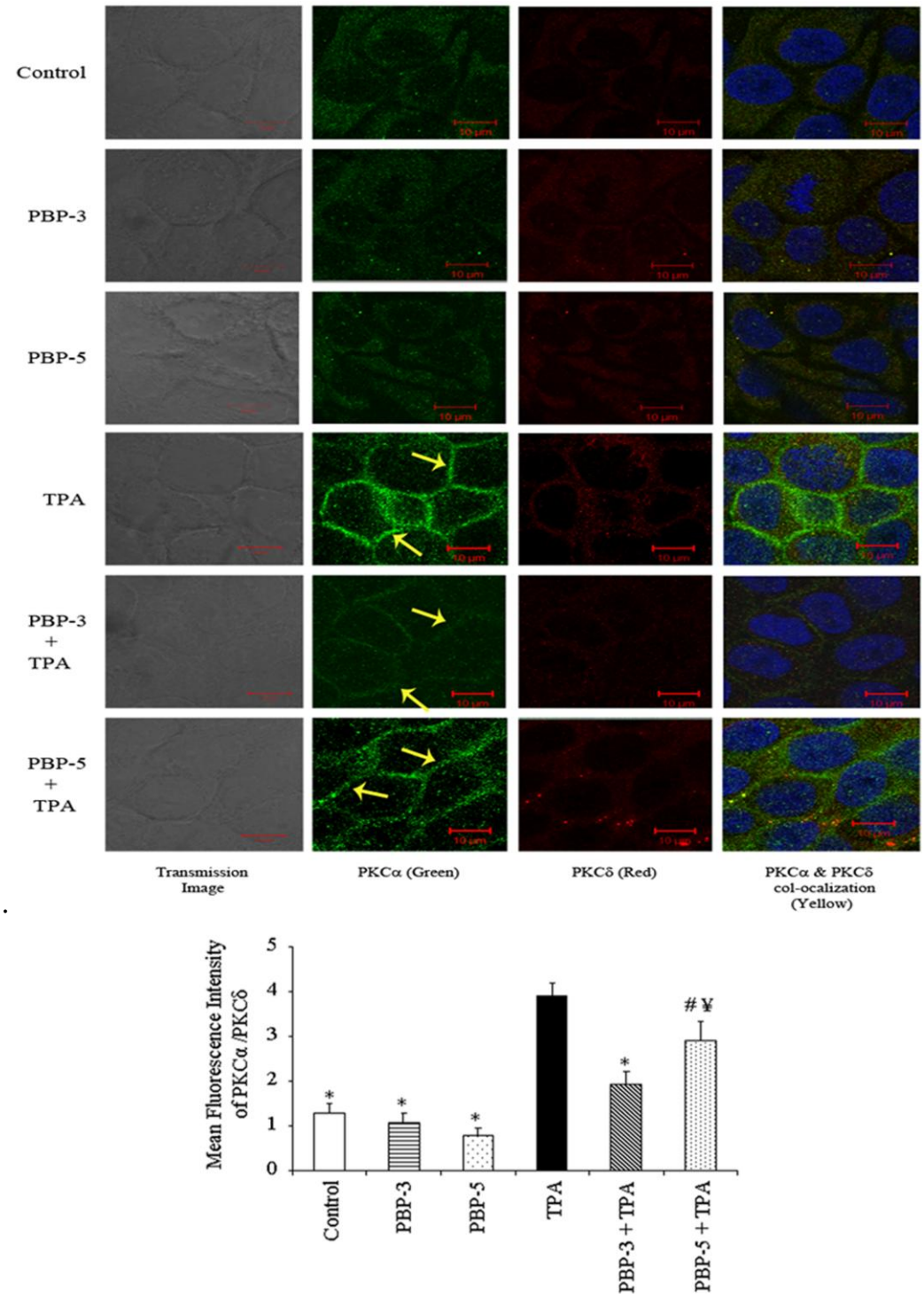

FIGURE 4.13: Effect of PBP-3 or PBP-5 on TPA-induced localization of PKC isoforms (α and δ) in HaCat cells by confocal microscopy. *Confocal images comparing the TPA-induced localization of PKC isoforms (α and δ) in HaCat cells, in different treatment groups. Scale bars, 10 µm. Mean fluorescence intensity shown at the bottom panel is calculated by PKCα/ PKCδ of 50 cells per group. Data represent mean ± SE of three observations. Differences among groups were determined by one-way ANOVA followed by Bonferroni's test, p ≤ 0.05. '*' significant when compared with TPA; '#' significant when compared with acetone; '¥' significant when compared with respective controls.*

4.3.4 Inhibition of TPA-induced phosphorylation of PKC by kinase inhibitors and PBP-3 or PBP-5

To confirm the effects of TPA on phosphorylation of PKCα and effects of PBP-3 and PBP-5 pre-treatment on TPA-induced phosphorylation of PKCα, particulate lysates were analyzed and compared. For this, phosphothreonine protein was immunoprecipitated from particulate fractions and probed with PKCα and AKT1/2. Western blot analyses showed that, compared to control, topical application of TPA significantly increased the expression of phosphothreonine PKCα and AKT1/2 on the membrane. However, pre-treatment with PBP-3 and PBP-5 decreased the TPA-induced phosphothreonine-PKCα on the membrane (Fig. 4.14). Similarly, western blot analysis of AKT1/2 after immunoprecipitation of phosphothreonine proteins from particulate fraction showed that pre-treatment with PBP-3 decreased the TPA-induced level of phosphothreonine AKT1/2 on membrane (Fig. 4.14). However, PBP-5 did not have any significant effect on the level of phosphothreonine AKT1/2 (Fig. 4.14). Thus, results suggest that PBP-3 is decreasing the level of AKT1/2 protein phosphorylated at threonine, whereas PBP-5 did not have any effect on AKT1/2 protein phosphorylation at threonine residues.

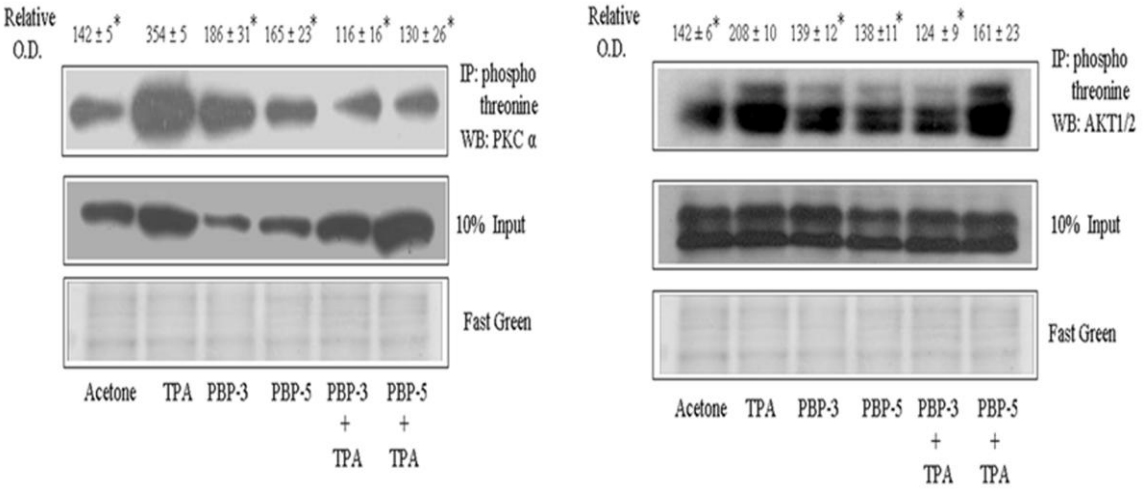

FIGURE 4.14: Effect of PBP-3 or PBP-5 on TPA-induced levels of PKC and AKT in particulate cell lysate from mouse skin epidermis. *Particulate extracts from epidermal cells of mouse skin belonging to the various treatment groups were immunoprecipitated with phospho-threonine antibody followed by immunoblotting with PKCα and AKT1/2, antibody in different treatment groups. Quantification was done by normalizing the band density to that of total lane density of membrane stained with fast green. Data represent mean ± SE of three observations. Differences among groups were determined by one-way ANOVA followed by Bonferroni's test, $p \leq 0.05$. '*' significant when compared with TPA; '#' significant when compared with acetone; '¥' significant when compared with respective controls.*

To check the role of upstream kinases in TPA-induced phosphorylation of PKC and its modulation by PBP-3 and PBP-5, phosphospecific antibodies and specific inhibitors (single or dual) of upstream kinases as detailed under Materials and methods (Chapter 3, section 3.17) were employed. Western blot analysis of the particulate (membrane) fraction employing phosphospecific antibodies of PKCα showed that, compared to control, topical application of TPA significantly induced the phosphorylation of PKC at specific positions i.e. it increased the level of phosphorylatedPKCα (pT497), PKCα/βII (pT638/641),PKCα (pS657 + Y658) and PKC PAN (βII pS660) (Fig. 4.15). In contrast, the level of these phosphorylated PKCs at all three specific positions in PBP-3- and PBP-5- treated controls was comparable to that of acetone (vehicle control)- treated animals (Fig. 4.15). However, pre-treatment with PBP-3 significantly decreased the TPA-induced phosphorylation of PKCα (pT497), PKCα/βII (pT638/641), and PKCα (pS657 + Y658), and PKC PAN (βII pS660), similar to individual kinase inhibitors of upstream kinases (PDK1, AKT and PI3K) and their combination in membrane, whereas PBP-5 did not have any significant effect on phosphorylation at these sites (Fig. 4.15). Results of western blotting and immunoprecipitation suggest that PBP-3 decreased the phosphorylation of PKCα at both specific (Thr497 and Thr638/641) and nonspecific positions of threonine, whereas PBP-5 decreased the phosphorylation of PKCα only at nonspecific positions (Figs. 4.14 and 4.15).

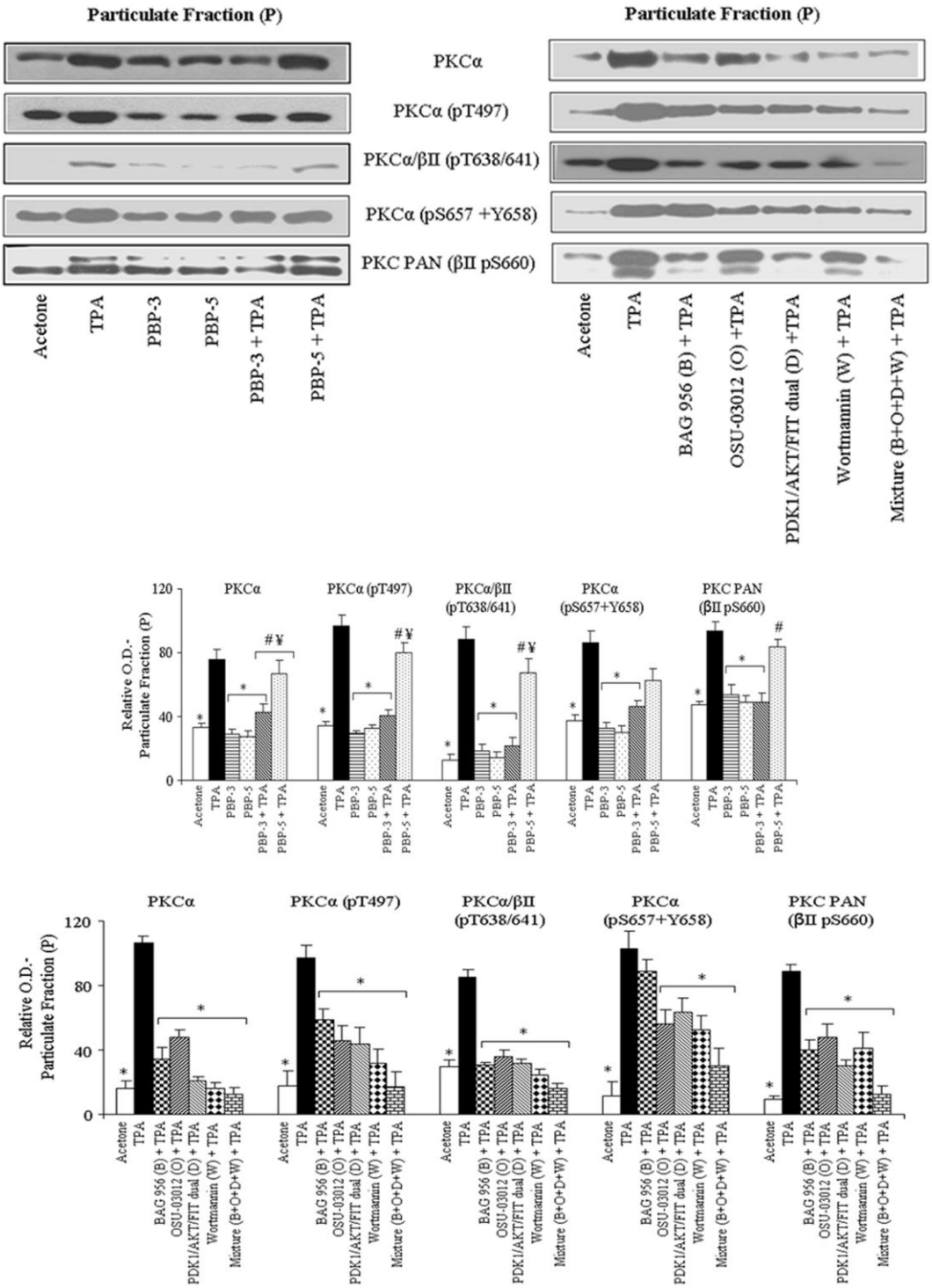

FIGURE 4.15: Effect of PBP-3 or PBP-5 on TPA-induced levels and activity of PKC in particulate cell lysate from mouse skin epidermis.*Representative blots and relative levels of PKCα, PKC PAN (βII pS660), PKCα/βII (pT638/641), PKCα (pT497), PKCα (pS65 + Y658) in particulate fraction of epidermis of mice belonging to the different treatment groups. Quantification was done by normalizing the band density to that of total lane density of membrane stained with fast green. Relative optical density is shown at the lower panel. Data represent mean ± SE of three observations. Differences among groups were determined by one-way ANOVA followed by Bonferroni's test, $p \leq 0.05$. '*' significant when compared with TPA; '#' significant when compared with acetone; '¥' significant when compared with respective controls.*

Because phosphorylation of PKC is mediated by PDK1 and AKT, the effects of PBP-3 and PBP-5 along with kinase inhibitors were evaluated by studying the protein levels and activity of PDK1 and AKT. Compared to controls, a single topical application of TPA to skin increased the level of PDK1, whereas it did not have any effect on the level of AKT1/2 in the particulate (membrane) fraction (Fig. 4.16). Furthermore, TPA application increased the levels of phosphorylated AKT1 (pS473; pT308) in the particulate fraction (Fig. 4.16). In contrast, the levels of PDK1 and AKT1 and their phosphorylated forms in PBP-3- and PBP-5- treated controls were comparable to those of acetone treated animals (Fig. 4.16). PBP-3 pre-treatment decreased the TPA-induced levels of PDK1. It did not have any effects on AKT1/2, whereas it decreased the TPA-induced levels of phosphorylated AKT1 (pS473; pT308) in membrane as in the case of individual kinase inhibitors and their combination in membrane (Fig. 4.16). PBP-5 pre-treatment decreased the TPA-induced levels only of phosphorylated AKT1 (pS473) on membrane, whereas it did not influence the TPA-induced levels of PDK1 and AKT1/2 or phosphorylation of AKT1 (pT308) (Fig. 4.16). PDK1 phosphorylation at the Ser241 position is an autophosphorylation that occurs after translocation of PDK1 to the membrane. To check the effects of PBP-3, PBP-5 and kinase inhibitors on the autophosphorylation of PDK1 at the Ser 241 position, the levels of PDK1 and phosphorylatedPDK1 (pS241) were evaluated after equal loading of PDK1 in the various treatment groups using specific antibodies. Our results suggest that pre-treatment with PBP-3/PBP-5/individual kinase inhibitors did not have any effect on phosphorylated PDK1 (pS241). However, the difference in the band intensity in (Fig. 4.16) is due to decreased translocation of PDK1 further resulting in decreased phosphorylation, rather than its effects on phosphorylation. Activity of PDK1 has been measured by comparing the levels of phosphorylated PKC and AKT (T308). Our results indicate that PBP-3 pre-treatment decreased the TPA-induced PDK activity as shown by a decrease in phosphorylation of PKC and AKT (T308) on membrane (Figs. 4.15 and 4.16).

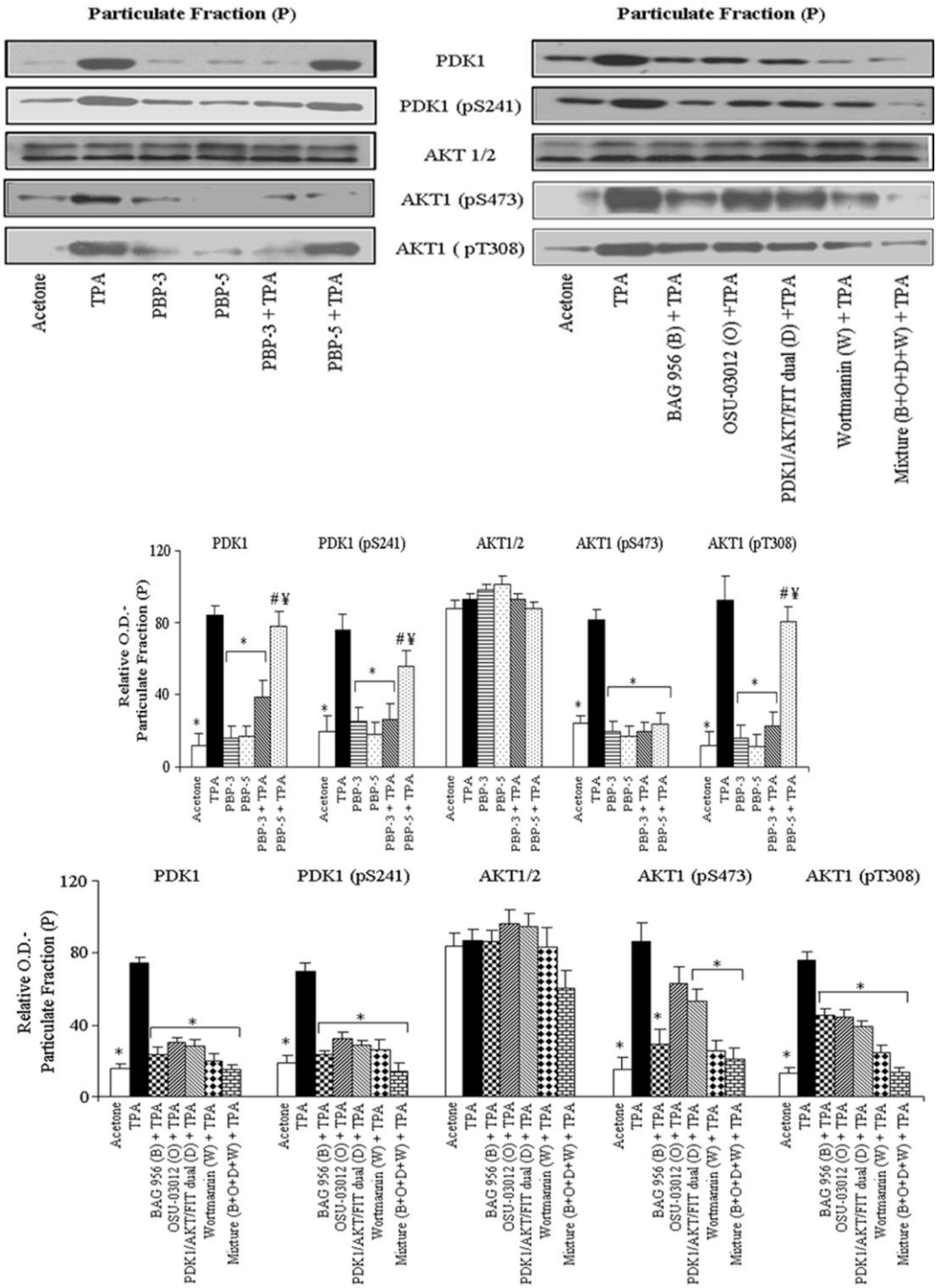

FIGURE 4.16: Effect of PBP-3 or PBP-5 on TPA-induced levels and activity of PDK1 and AKT1 in particulate cell lysate from mouse skin epidermis.*Representative blots and relative levels of PDK1, PDK1 (pS241), AKT1/2, AKT1 (pS473), AKT1 (pT308) in particulate fraction of epidermis of mice belonging to the different treatment groups. Quantification was done by normalizing the band density to that of total lane density of membrane stained with fast green. Relative optical density is shown at the lower panel. Data represent mean ± SE of three observations. Differences among groups were determined by one-way ANOVA followed by Bonferroni's test, $p \leq 0.05$. '*' significant when compared with TPA; '#' significant when compared with acetone; '¥' significant when compared with respective controls.*

The effects of PBP-3 and PBP-5 pre-treatment on TPA-induced PI3K level and activity were also analyzed, as AKT and PDK1 are known to be modulated by PI3K. Topical application of TPA significantly increased the PI3K protein level and activity, compared to acetone (Fig. 4.17). In contrast, PI3K protein level and activity in PBP-3- and PBP-5-treated controls were similar to those in vehicle control (Fig. 4.17). However, pre-treatment with PBP-3 and PBP-5 before TPA significantly decreased the TPA-induced PI3K protein level as in the case of individual kinase inhibitors and their combination (Fig. 4.17A). Pre-treatment with PBP-3 significantly decreased the TPA-induced PI3K activity also, whereas PBP-5 was not as effective ($p \leq 0.057$) (Fig. 4.17B). Results thus suggest that PBP-3 and PBP-5 mimics the effects of kinase inhibitors and that PBP-3 is more effective than PBP-5.

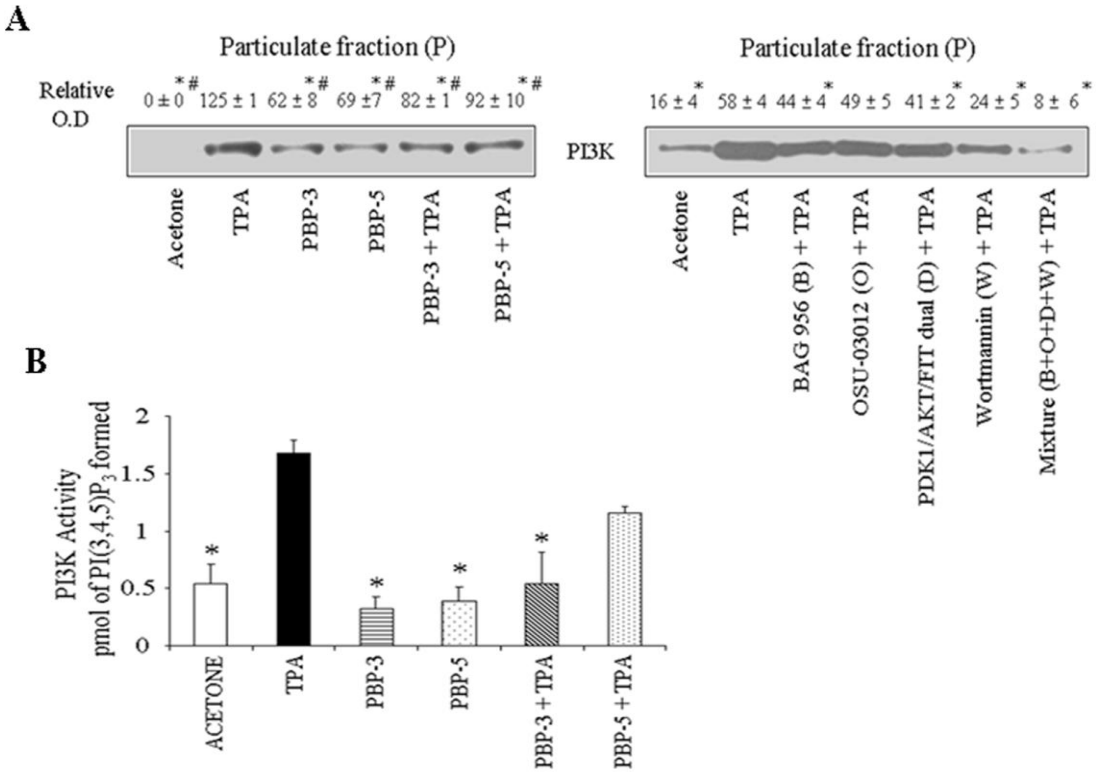

FIGURE 4.17: Effect of PBP-3 or PBP-5 on TPA-induced levels and activity of PI3K in particulate cell lysate from mouse skin epidermis.(A) *Representative blots and relative levels of PI3K in particulate fraction of mice epidermis belonging to different treatment groups.***(B)** *PI3K activity in particulate fraction of mice epidermis belonging to different treatment groups. Quantification was done by normalizing the band density to that of total lane density of membrane stained with fast green. Data represent mean ± SE of three observations. Differences among groups were determined by one-way ANOVA followed by Bonferroni's test, $p \leq 0.05$. ''*' significant when compared with TPA; '#' significant when compared with acetone; '¥' significant when compared with respective controls.*

4.3.5 Modulation of TPA-induced cell proliferation and apoptosis markers by PBP-3 or PBP-5

The effects of PBPs on modulation of the TPA-responsive markers (the downstream targets of PKC) in mouse skin were evaluated. Compared to acetone (vehicle control) treatment, topical application of TPA significantly increased the expression of cyclin D1 and PCNA (proliferation marker), cox-2 (cell inflammation marker) and Bcl-2 (anti-apoptotic protein), whereas it decreased the levels of pro-apoptotic protein, Bax in mouse epidermis (Fig. 4.18A). Importantly, pre-treatment with PBP-3 in mouse skin significantly abrogated the TPA-induced expression of anti-apoptotic protein, Bcl-2 and increased the expression of Bax, the pro-apoptotic marker (Fig. 4.18A), whereas PBP-5 was less effective. PBP-3 mediated inhibition of TPA-induced anti-apoptotic response was also reflected in increased Bax/Bcl-2 ratio (Fig. 4.18B). Further, topical pre-treatment with PBP-3 and PBP-5 significantly decreased the TPA-induced protein expressions of cox-2 (Fig. 4.18A), thereby suggesting PBP-3 and PBP-5 protection against TPA-induced inflammation. This was further complemented by immunoblot analysis of cell proliferation markers, showing a significant decrease in TPA-induced protein levels of cyclin D1 and PCNA upon PBP-3 pre-treatment in skin epidermis (Fig. 4.18A). However, PBP-5 decreased the TPA-induced protein levels of PCNA, whereas it was less effective in modulating TPA-induced cyclin D1 (Fig. 4.18A).

Furthermore, the effects of PBP-3 and PBP-5 on NF-κB family proteins in mouse skin as well as HaCat cells were investigated. Compared to control, TPA significantly increased the levels of NF-κB, p-NF-κB, IKKα and pIκB-α in both mouse skin and HaCat cells (Fig. 4.19), whereas it decreased the levels of IκB-α. In contrast, the levels of NF-κB, p-NF-κB, IKKα, pIκB-α in PBP-3 and PBP-5 treated controls were comparable to respective vehicle control in both mouse skin and HaCat cells (Fig. 4.19). However, pre-treatment with PBP-3 significantly decreased the TPA-induced levels of NF-κB and p-NF-κB (Fig. 4.19). In addition, PBP-3 blunted the TPA-mediated increase in pIκB-α protein expression, which in turn accounts for the reduced TPA-mediated degradation of IκB-α protein and further decrease in the TPA-mediated increase in IKKα (Fig. 4.19). PBP-5 pre-treatment significantly decreased the TPA-induced level of IKK, whereas it did not influence the TPA-mediated levels of NF-κB, p-NF-κB, pIκB-α and IκB-α (Fig. 4.19).

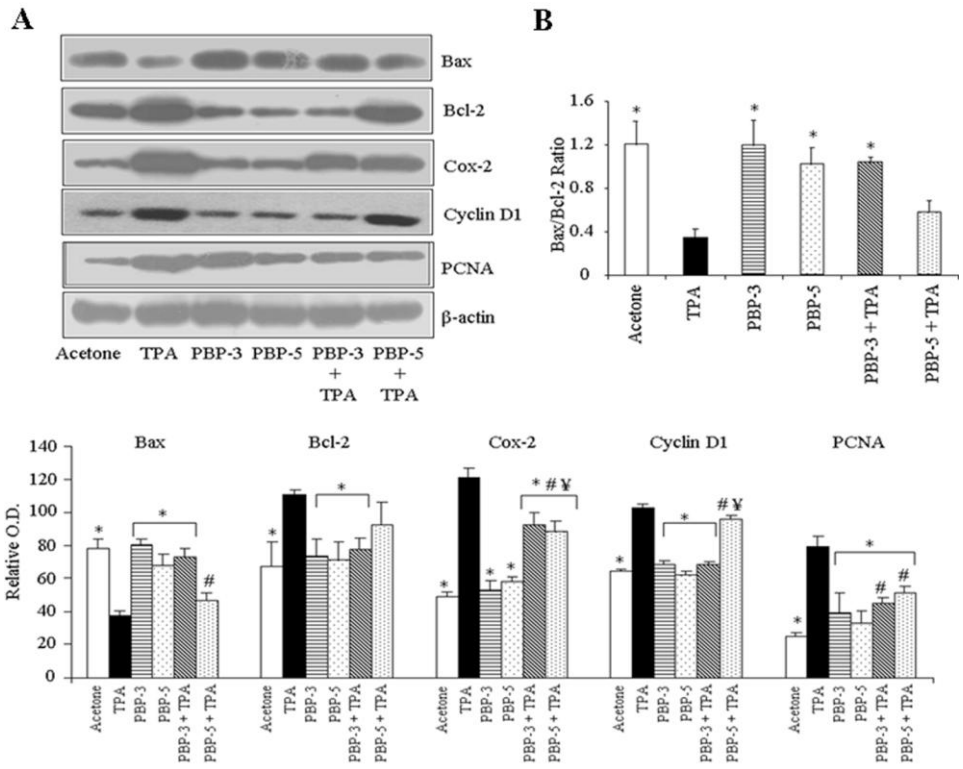

FIGURE 4.18: Effect of PBP-3 or PBP-5 on TPA-responsive markers in cell lysate from mouse skin epidermis. (A) *Representative blots and relative levels of Bax, Bcl-2, cox-2, cyclin D1 and PCNA in total cell lysate of mice epidermis belonging to different treatment groups. β-actin was used as loading control. Quantification of proteins was done by normalizing the band density to that of β-actin in respective cellular compartments.***(B)** *Extent of apoptosis was determined in terms of Bax/Bcl-2 ratio. Data represent mean ± SE of three observations. Differences among groups were determined by one-way ANOVA followed by Bonferroni's test, p ≤ 0.05. '*' significant when compared with TPA; '#' significant when compared with acetone; '¥' significant when compared with respective controls.*

4.3.6 Lack of interaction between TPA and PBP-3 or PBP-5

Evaluation of solutions of TPA, PBP-3, and PBP-5, individually or in combination, by UV absorption spectra, mass spectrometry and ITC showed a lack of binding between PBP-3 or PBP-5 and TPA as judged by the absence of changes in UV spectra, mass of compounds detected, and heat (Fig. 4.20 and 4.21).

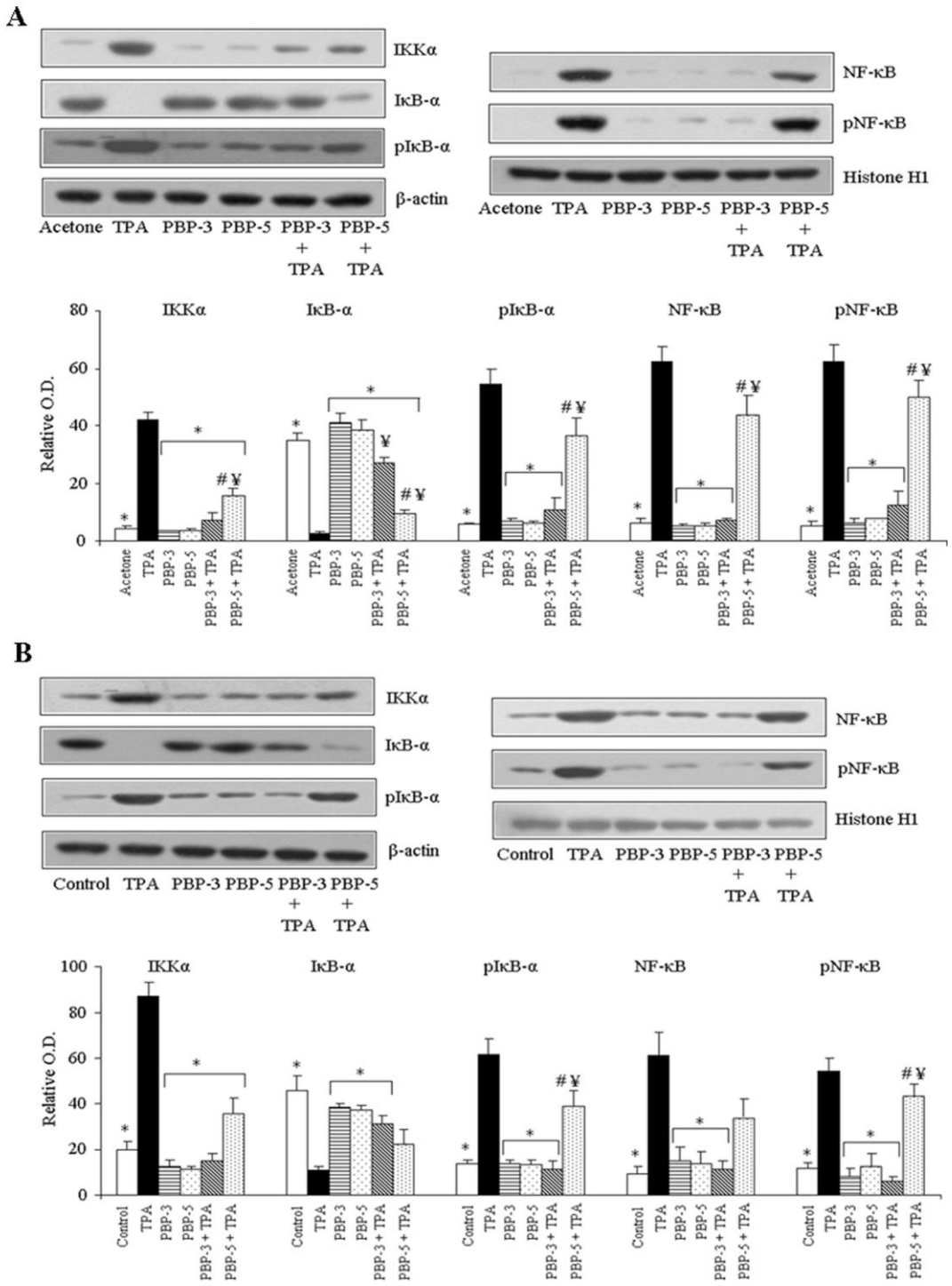

FIGURE 4.19: Effect of PBP-3 or PBP-5 on TPA-induced activation of nuclear transcription factor related proteins in mouse skin epidermis and HaCat cells.*Representative blots and relative levels of IKK, pIκB-α and IκB-α measured in cytosolic extracts, while levels of NF-κB and pNF-κB measured in nuclear extracts from different treatment groups in* **(A)** *epidermal cells of mouse skin. (***B)** *HaCat cells. Quantification of proteins was done by normalizing the band density to that of β-actin and Histone H1 in respective cellular compartments. Data represent mean ± SE of three observations. Differences among groups were determined by one-way ANOVA followed by Bonferroni's test, $p \leq 0.05$. '*' significant when compared with TPA; '#' significant when compared with acetone; '¥' significant when compared with respective controls.*

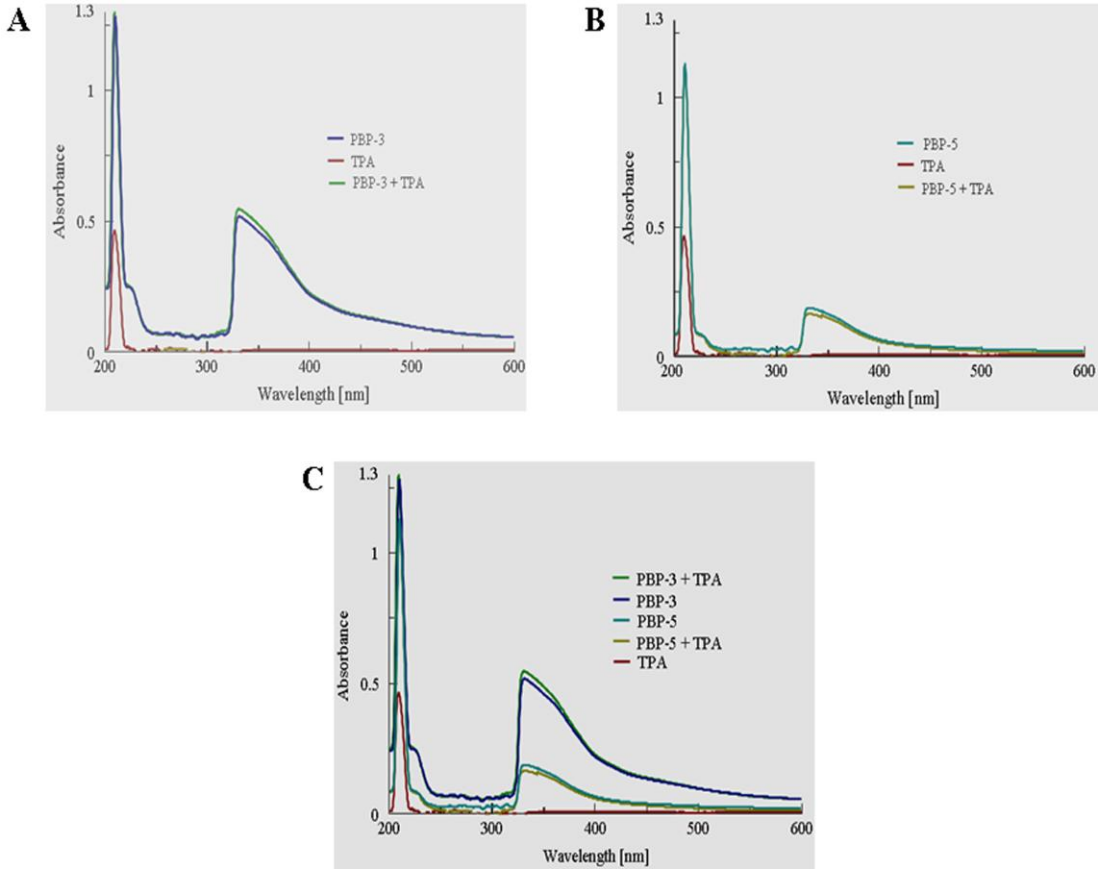

FIGURE 4.20: UV-Vis spectra of PBP-3 or PBP-5 or TPA and their mixtures. *TPA, PBP-3, PBP-5, and mixtures containing PBP-3 + TPA and PBP-5 + TPA were incubated for 20 min at 37 °C. UV absorption spectra of* **(A)** *PBP-3, TPA and PBP-3 + TPA.***(B)** *PBP-5, TPA and PBP-5 + TPA.* **(C)** *PBP-3, PBP-5, TPA, PBP-3 + TPA and PBP-5 + TPA, were recorded at 200- 600 nm in a range of 0–2 absorbance using a JascoV-650 spectrophotometer after the sample was diluted in acetone at a ratio of 1/50.*

4.3.7 Prevention of TPA-mediated decrease in GSH/GSSG ratio by PBP-3

Topical application of TPA resulted in significant decrease in the ratio of GSH/GSSG in epidermal cells compared to control (control 10.47 ± 0.07 vs TPA 6.06 ± 0.58). Ratios of GSH/GSSG in PBP-3- and PBP-5- treated epidermal cells (PBP-3 12.08 ± 0.68, PBP-5 13.31 ± 0.43) were similar to those in controls. Pre-treatment with PBP-3 prevented the TPA-mediated decrease in the GSH/GSSG ratio (PBP-3 + TPA 10.17 ± 0.37), whereas PBP-5 was less effective (PBP-5 + TPA 7.15 ± 0.60).

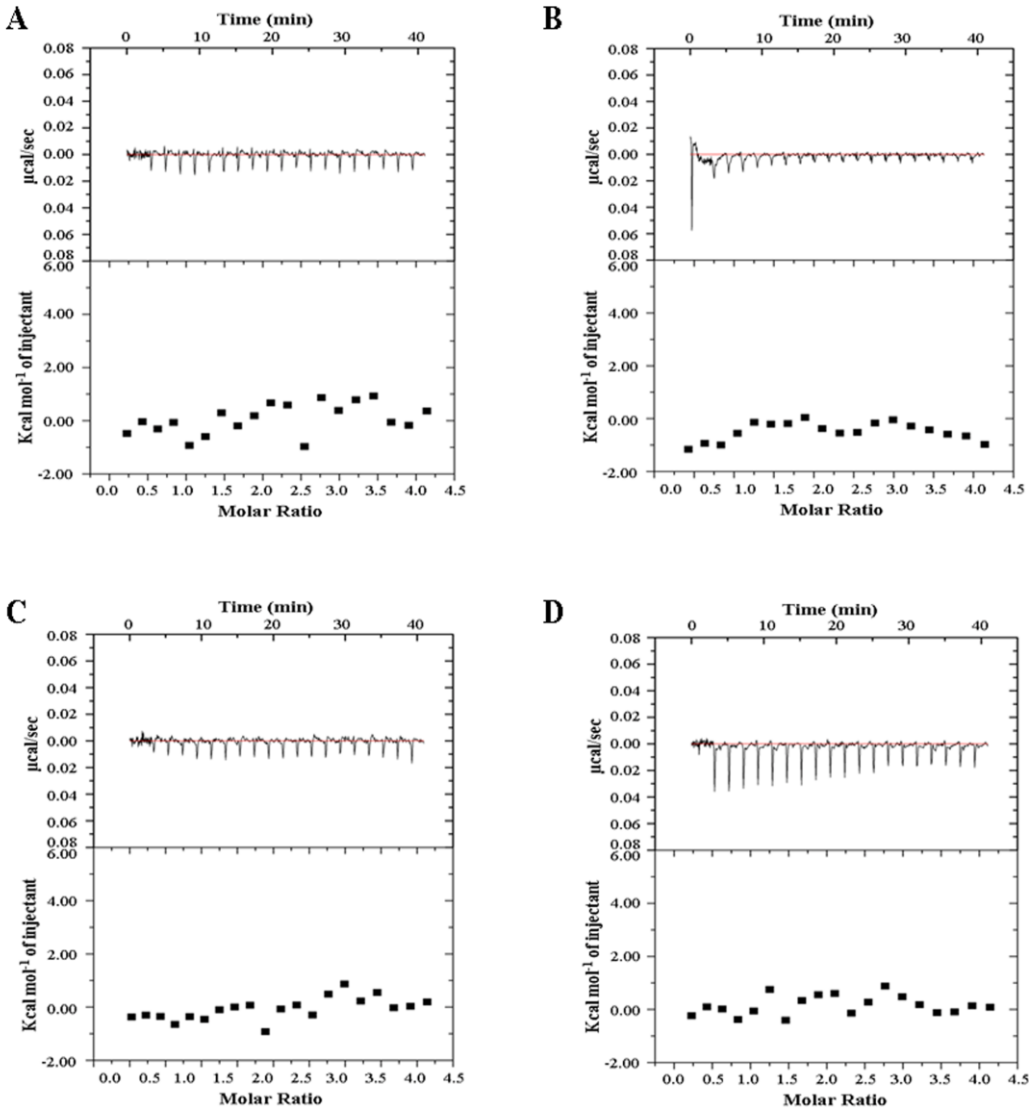

FIGURE 4.21: Titration microcalorimetry of TPA by PBP-3 or PBP-5. *Titration curve of TPA by PBP-3 at* **(A)** *37 °C.* **(B)** *20 °C.Titration curve of TPA by PBP-3 at* **(C)** *37 °C.* **(D)** *20 °C. Instrumental baseline was subtracted from the raw exothermic heat pulse data from each injection to obtain normalized integrated heat. Thermo- grams were evaluated using Origin (version7; OriginLab).*

4.4 DISCUSSION

Various modifiers of the tumor promotion process and their mechanisms of action have generally been studied employing TPA as a tumor promoter in a mouse skin model [157,158]. Both green tea and black tea have been shown to suppress TPA-mediated tumor-promoting effects in mouse skin [29,38]. However, the active component(s) that contributed to the observed anti-tumor-promoting effects in black tea have not been well characterized. In an earlier study the major black tea polyphenols, i.e., PBPs (about 10-20% of the dry weight of black tea powder) were shown to possess anti-promoting effects

in a two-stage mouse skin carcinogenesis model [60]. Amongst the polymeric polyphenols, PBPs 1-3 were observed to possess relatively stronger anti-promoting effects compared to PBPs 4 and 5 as demonstrated by a decrease in the TPA-induced epidermal cell proliferation. PBP-mediated decrease in cell proliferation correlated with the decrease in the activation of MAPKs (p-JNK, p-ERK, p-p38, p-AKT) and transcription factors (AP-1 and NF-κB) and resulted in altered latency, multiplicity and incidence of skin papillomas as compared to DMBA/TPA treated group [60]. Although a variety of intracellular signalling cascades are activated in response to TPA, studies have shown that the primary site of action of phorbol esters is located on cell membranes and that PKC acts as the possible receptor for the same. Because the mechanisms of anti-promoting actions of PBPs are not known, the major aim of this study was to further elucidate the anti-promoting activity of PBPs thus obtaining a deeper insight into the role of the PKC signaling cascade in mouse skin carcinogenesis.

Lee and Lin observed phytopolyphenols to inhibit TPA-induced activity/translocation of PKC in mouse fibroblast cells *in vitro* [158]. Chen et al have investigated the effects of black tea polyphenols such as theaflavin, the mixture of theaflavin-3-gallate and theaflavin-3'-gallate, theaflavin-3,3'-digallate, thearubigin (McDonnell et al.) and a major green tea polyphenol, EGCG on TPA-induced PKC activity/translocation in NIH3T3 cells [159]. Most of the tea polyphenols inhibited TPA-induced activity/translocation of PKC, although the extent of inhibition differed. Our results clearly demonstrate that pre-treatment with PBPs 1-3 significantly decreased the TPA-induced activity of PKC and its translocation from cytosol to cell membrane upon topical treatment of mouse skin *in vivo*. To our knowledge, this is the first report on investigations on the mechanisms of anti-promoting effects of PBPs *in vivo,* wherein PBPs 1-3, EGCG and curcumin (positive control) were demonstrated to decrease the TPA-induced translocation of PKC isozymes (α, β, γ, ε, η) and activity, although the extent of inhibition differed. Furthermore, the mechanisms of anti-promoting effects of PBPs were studied in the same model system in which PBPs have been shown to possess anti-promoting effects, employing relevant experimental conditions [60]. Similar and comprehensive *in vivo* studies on the effects of EGCG and TFs on the activity, protein levels, localization, and mechanism of translocation of PKC are not available, although inhibition of PKC translocation has been reported with other plant polyphenols such as curcumin and tannic acid, although with varying degree [134,139]. Moreover, PKC isoforms have been shown to regulate cell processes such as proliferation, differentiation,

survival, inflammation, cell death, epidermal tumor formation and progression. Available evidence also shows that the activation of some TPA-dependent PKCs, especially PKCα and ε, is crucial for tumorigenesis and tumor progression [160]. Therefore, studies on the effects of PBPs on TPA-induced PKCα and ε levels/activity may provide insight into the functional relevance of PBPs in chemoprevention. Mechanistic aspects of the chemopreventive actions of PBPs on TPA-induced levels of PKC isozymes as assayed by western blot analysis of mouse skin and HaCat cell (only PKCα) have been further complemented and confirmed by confocal microscopy data. These results suggest that PBPs 1-3 mediate inhibition of TPA-induced PKC translocation from cytosol to membrane, whereas PBP-5 was less effective.

Several lines of evidence indicate that phosphorylation of PKC at three specific positions is crucial for the translocation and activation of PKC [161]. Activation-loop phosphorylation at Thr497 at N-terminal is the primary event for further phosphorylation of the C-terminal region at the turn motif (Thr638) and hydrophobic motif (Ser657) [156]. A number of cellular upstream kinase(s) such as PDK1, AKT and PI3K have been postulated to phosphorylate PKC at the activation loop (Thr497). Several reports suggest a direct or indirect relationship between these upstream kinase(s) and their role in activation of PKC [162-165]. Our study shows that TPA-induced levels of phosphorylated PKCα at the activation loop (Thr497) and C-terminal motif (Thr638 and Ser657) are decreased by inhibitors of upstream kinases, which suggest their crucial role in TPA-induced PKCα phosphorylation, although the extent of inhibition by them differed. Maximum inhibition of PKCα phosphorylation at all three different positions occurs with a cocktail of upstream kinases inhibitors, suggesting that most of the members of the signalling cascade leading up to the phosphorylation of PKCα are blocked by kinase inhibitors, further strengthening our understanding of the roles of AKT, PDK and PI3K in phosphorylation of PKCα. Interestingly, PBP-3 was also found to decrease the TPA-induced PKCα phosphorylation at Thr497, Thr638 and Ser657. Further, PBP-3 decreases the TPA-induced phosphorylation of AKT1 at Ser473 and Thr308 and the PDK1 protein level in mouse skin, which are known to mediate phosphorylation of PKCα. Because interference due to PBP-3, PBP-5 and kinase inhibitors in measurements of chemiluminescence has been ruled out, the observed effects on the levels of enzyme proteins or phosphorylated proteins do not seem to be due to methodological issues. However, cross talk from other signalling cascades and effects of PBPs on other pathways need to be investigated to obtain a better understanding. Whereas similar modulatory

effects of EGCG or TFs on AKT1, PDK1 and PKC phosphorylation are not available, effects of EGCG or TFs on the modulation of PI3K have been reported [166,167]. TPA has been shown to induce PI3K activity in JB6 cells *in vitro* and to inhibit AP-1 activation and cell transformation by blocking PI3K activity [168,169]. Altogether, our results suggest that PBP-3 mimics the effects of kinase inhibitors and regulates the phosphorylation and further translocation of PKCα in epidermal layers of mouse skin by modulating TPA-induced PI3K/AKT/PDK1 pathway.

The observed effects of PBP-3 on PKC and AKT phosphorylation and on PDK1 protein levels were further correlated with TPA-induced alteration in response markers such as cox-2 (inflammation), cyclin D1 and PCNA (proliferation) and Bax as well as Bcl-2 (apoptosis markers), and the pattern of results is similar to those observed with EGCG or TFs or other polyphenols in *in vivo* or *in vitro* model systems [29,60,146,170-172]. Interestingly, PBP-mediated enhancement in TPA-altered Bax/Bcl-2 ratio suggests protection against carcinogenesis, due to the elimination of cells by apoptosis. Furthermore, the effects of PBP-3 pre-treatment on TPA-mediated NF-κB transactivation by inhibition of IKK and phosphorylation of IκB-α in mouse skin and HaCat cell are similar to those reported with EGCG, TFs, and other polyphenols *in vivo* and *in vitro* [172-177]. Despite differences in structure, molecular weight and others properties between monomeric, oligomeric and polymeric tea polyphenols, the commonality in effects/actions on PI3K/AKT/PDK and PKC signal transduction pathway, response markers and anti-promoting effects is interesting. This commonality in mode of action suggests some common factor i.e. antioxidant nature or property of these compounds. Interestingly, it may be the alteration in TPA-induced redox status by this antioxidant that is responsible for commonality in mode of actions. Because PBP-3 pre-treatment significantly prevented the TPA-mediated decrease in GSH/GSSG ratio in epithelial cells, PBP-3-mediated antioxidant mechanism seems to be responsible for the inhibition of the tumor-promoting ability of TPA, although a contribution of alternative/ additional pathways/mechanisms cannot be ruled out, as these have not been investigated. The observed lack of binding/interaction between PBP-3 and TPA *in vitro* suggests that the resultant PBP-3-mediated alterations in TPA-induced changes in mouse skin are not likely to be due to a decreased level of TPA reaching the epithelial cells in the PBP-3 + TPA combination because of a potential interaction compared to TPA, although the possibility of cells/extract-mediated binding/interaction cannot be ruled out.

The reported relatively stronger anti-promoting activities of PBP-3 compared to PBP-5 are probably due to differences in structure (in terms of gallic acid content PBP-3 147 mg/g and PBP-5 264 mg/g), solubility (PBP-3 is relatively more water soluble than PBP-5), bioavailability, and half-life/stability of parent/product and/or additional inhibition of phosphorylation of PKCα at specific sites. However, in the absence of information about the molecular structure and weight of PBP fractions, it is difficult to compare their relative efficacies within themselves and with other monomeric and oligomeric tea polyphenols at equimolar concentration. PBPs are thought to be relatively high molecular weight than EGCG/theaflavins [32] and may not be able to enter into the cell. Our observations of PBP-mediated biological activities after topical application suggest a modulation of membrane receptors for the observed effects. Similar biological activities of PBPs on other tissue may need to be further investigated after oral administration to simulate the route of exposure as experienced by tea drinkers.

The present findings suggest strong chemo-protective activities of PBP-3 compared to PBP-5, which may be due to differences in inhibition of TPA-induced PKC translocation/activity and specific phosphorylation. In the mouse skin model, the modulation of TPA-induced PI3K seems to be a critical regulator of AKT and/or PDK1, resulting in the regulation of activity and translocation of PKC leading to alterations in downstream targets related to cell proliferation, cell death and inflammation. Similar mechanistic studies in different model systems along with appropriate bioavailability information on PBP fractions and other black tea flavanols will enhance the understanding of the chemopreventive/chemotherapeutic effects of plant-derived polyphenols, which might further aid in elucidating cellular targets for meaningful evaluation of the chemopreventive potential of black tea in humans. To summarise, our study demonstrates that PBPs modulate TPA-induced molecular and biochemical alterations in mouse skin through a PKC-dependent mechanism via the PI3K/AKT/PDK1 pathway.

5.1 INTRODUCTION

Oral cancer is the tenth most prevalent cancer worldwide and the second most common cancer in Indian males [178]. Despite the improvement in medical technology and therapeutic approaches, the 5-year survival rate of this disease has not improved over the last 4–5 decades. Many natural and/or synthetic compounds are being evaluated for their preventive and/or therapeutic efficacy or their ability to modulate the efficacy or toxicity of established chemotherapeutic agent(s). The use of plant-derived antioxidants as chemopreventives and/or chemotherapeutics and/or modulators of chemotherapeutic/ toxic responses of other agents are likely to be acceptable in clinical trials because of their demonstrated biological activities through the modulation of a number of biochemical pathways in experimental systems and because of their low toxicity.

Turmeric, the powdered rhizome of *Curcuma longa;* has long been reported to have anti-inflammatory, anti-mutagenic, anti-oxidant, anti-carcinogenic, anti-viral, and anti-fungal effects in both cultured cells and animal models [145,179-181]. Turmeric and/or its active component curcumin have been shown to inhibit experimentally induced tumorigenesis in several animal models [110,122,128,182]. Anti-initiating and/or anti-promoting activities of turmeric/curcumin have been well documented in experimental model systems at different organ sites when administered prior to, during, or following exposure to a carcinogen or tumor promoter [97]. However, reports of its effects on carcinogen-induced tumor subsequent to their formation are very limited.

Currently, curcumin is under evaluation in clinical trials in many countries (http://ctri.nic.in; http://clinicaltrials.gov/; http://www.cancer.gov/clinicaltrials). The efficacy of curcumin has been established when it is administered before or after the carcinogen or tumor-promoter treatment. To simulate the order of its administration and to study the effects of turmeric after tumor development, the experiments in this study were conducted to investigate the effects of dietary turmeric post-treatment, on tumor growth and various molecular and biochemical markers (apoptosis and cell proliferation) in 7, 12- dimethylbenz(a)anthracene (DMBA)-induced hamster buccal pouch (HBP) tumors.

HBP is a well-established animal model for studying oral carcinogenesis [183,184] and efficacy of preventive and therapeutic agents. Our study demonstrates that post-treatment with turmeric significantly decreases DMBA-induced tumor growth (volume and multiplicity) due to modulation of mitogen-activated protein kinase (MAPK)

signalling and transcription factors, thereby affecting cell proliferation and apoptosis in HBP, although it appears to have very limited therapeutic effect.

5.2 METHODS

5.2.1 Animal treatment

Inbred male Syrian hamsters (Generation used 8^{th}-10^{th}, 6-8 weeks old; Animal house, ACTREC, India) received a standard pellet diet and plain drinking water *ad libitum.* Initially, the hamsters were topically treated with DMBA (0.5%) in corn oil or with corn oil (carcinogen untreated control, group C) using a Gilson pipette (80 µl ≈ 0.4 mg) in experiments 1-3. In experiment 4, a Camlin no. 4 paintbrush was used to apply DMBA on the right buccal pouch of hamster. All DMBA applications were made three times per week for 12 consecutive weeks to induce tumors (Fig. 5.1). After tumor development at 12 weeks, animals were either shifted to a powdered control diet (standard laboratory diet, groups 12DC2 and 12DC3) or an experimental diet of 1% turmeric in standard laboratory diet (groups 12DT2 and 12DT3) as described [185], for 2 weeks in experiment 1 and for 3 weeks in experiment 2 (Fig. 5.1) . In subsequent experiments, animals with DMBA-induced HBP tumors at 12 weeks without pre-defined tumor volumes (i.e., experiment 3 using a Gilson pipette application) and with a pre-defined range of tumor volumes (i.e., experiment 4 using Camlin no. 4 paintbrush application), as well as appropriate controls, were randomized into five groups. Of these, half of the animals continued on the powdered control diet (group 12DC4) and the other half were shifted to a powdered experimental diet (1% turmeric in standard laboratory diet, group 12DT4) for 4 weeks, respectively (Fig. 5.1). To rule out DMBA discontinuation as a cause of decrease in tumor burden, DMBA treatment was continued until the end of the experiment in another set of animals that were shifted to a powdered control diet (group 16DC4) and a powdered experimental diet (group 16DT4) (Fig. 5.1). The dosage of turmeric was equivalent to the level of curcumin (0.05%) showing biological activity in experimental systems [186]. Animals in all groups were observed for apparent signs of toxicity such as weight loss or mortality during the entire study period. Hamsters were euthanized (by CO_2 chamber) 16 weeks after the first dose of the carcinogen. Their buccal pouches were excised, and a portion of the tissue (tumor and non-tumor) was fixed in 10% buffered formalin for histopathological evaluation and immunohistochemical staining, while the rest of the tissue was snap frozen in liquid

nitrogen and stored at -80°C until preparation of different extracts. Hamsters were scored for multiplicity (average number of tumors per animal) and tumor burden [mean tumor volume × mean number of tumors; tumor volume was calculated employing the formula $4/3\pi r^3$, where r is the radius of tumor in mm and r = (d1/2 + d2/2)/2 where d1 and d2 are the minimum and maximum diameters of the tumors in mm], both at the time of randomization of animals after tumor development (12 weeks) and at the time of sacrificing the animals (16 weeks). Tumor burden was computed in two ways: (1) the difference between the tumor burden (mm^3) at 16 weeks and 12 weeks was calculated, and (b) the tumor burden (mm^3) at 16 weeks was divided by the tumor burden (mm^3) at 12 weeks to find the relative change in tumor burden.

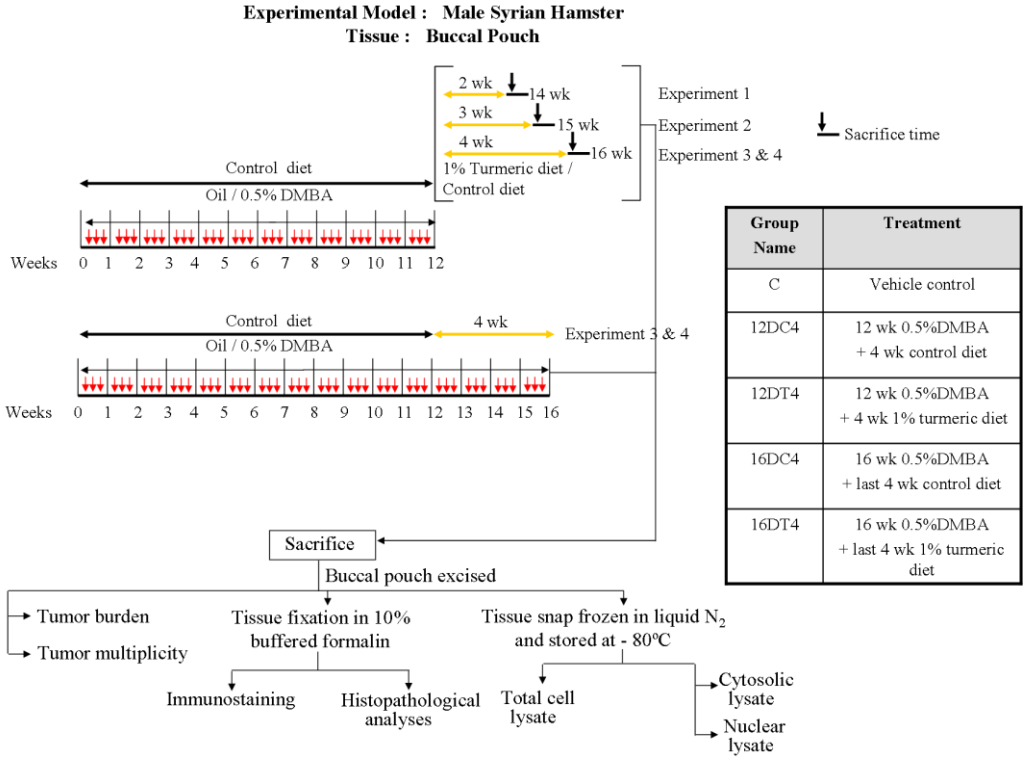

FIGURE 5.1: Experimental design for evaluating the effects of dietary turmeric post-treatment on DMBA-induced HBP tumors. *0.5% DMBA in corn oil/corn oil was topically applied with a Gilson pipette (80 µl ≈ 0.4 mg) in experiments 1-3 or with a Camlin no. 4 paintbrush in experiment 4 to the right buccal pouch of hamster three times per week for 12 weeks to induce tumor development. After tumor development (12 weeks), animals were either shifted to powdered control diet (standard laboratory diet, groups 12DC2 and 12DC3) or experimental diet (1% turmeric diet, groups 12DT2 and 12DT3) for 2 weeks in experiments 1 and 3 weeks in experiment 2. After tumor development, in experiments 3 and 4, one set of animals was shifted to control diet (group 12DC4) and experimental diet (group 12DT4, 1% turmeric diet) and another set of animals was shifted to control diet (group 16DC4) and experimental diet (group16DT4, 1% turmeric diet) along with continuation of DMBA to week 16. Animals were sacrificed after 14, 15 and 16 weeks after the first dose of carcinogen in experiments 1, 2 and 3, 4, respectively.*

Buccal pouches of animals were excised, and a portion of the tissue (tumor and non-tumor) was fixed in 10% buffered formalin, while the rest was snap frozen in liquid nitrogen and stored at −80 °C.

5.2.2 Protein immunoblotting

Total cell, cytosolic, and nuclear extracts were prepared from HBP as described in Materials and methods (Chapter 3; section 3.4.1 and 3.4.2) [138]. For preparation of different extracts, a part of the tumor-bearing buccal pouch was used. The expressions of various proteins were studied by SDS-PAGE followed by immunoblotting as described in Materials and methods (Chapter 3; section 3.6). All primary and secondary antibodies were first standardized for their dilution and then used accordingly. β-actin or Histone H1 was used as loading controls for all proteins depending upon the fraction. Densitometry of various analyte proteins and their respective loading controls from the same blot was performed using Image J 1.43 (NIH) software as described in Materials and methods (Chapter 3; section 3.6.5).

Protein	% gel	Amount of protein	Primary antibody dilution	Secondary antibody dilution
Caspase-3	12%	Total cell lysate, 50 μg	1:2000	1:5000
Caspase-9	10%	″	1:1000	1:4000
Cox-2	8%	″	1:1000	1:5000
Cyclin D1	10%	Total cell lysate, 100 μg	1:500	1:4000
Cytochrome c	12%	Total cell lysate, 50 μg	1:1000	1:6000
Bax	12%	″	1:1000	1:5000
Bcl-2	12%	″	1:1000	1:5000
IKK	12%	Cytosolic lysate, 50 μg	1:1000	1:4000
IκB-α	12%	″	1:1000	1:5000
pIκB-α	12%	″	1:1000	1:5000
c-jun	12%	Nuclear lysate, 50 μg	1:1000	1:5000
c-fos	12%	Nuclear lysate, 100 μg	1:1000	1:5000
NF-κB	10%	Cytosolic & nuclear lysate, 100 μg	1:1000	1:5000
ERK 1/2	10%	Total cell lysate, 50 μg	1:2000	1:6000
p38	12%	″	1:2000	1:6000
p-ERK	12%	″	1:1000	1:5000
p-p38	12%	″	1:1000	1:4000
p53	10%	″	1:1000	1:4000
p21	12%	Total cell lysate, 100 μg	1:500	1:3000
PCNA	10%	Total cell lysate, 50 μg	1:1000	1:4000
Survivin	12%	″	1:1000	1:4000
β-actin	Loading controls (same blots were stripped)		1:2000	1:6000
Histone H1			1:1000	1:4000

5.2.3 Immunohistochemical staining

For immunohistochemical (IHC) staining, tumor and non-tumor tissue were fixed in 10% buffered formalin. The expression of PCNA (dilution 1:50)/cox-2 (dilution 1:25)/Survivin (dilution 1:100)/p53 (dilution 1:25)/Bax (dilution 1:25) and Bcl-2 (dilution 1:25) were assayed in paraffin-embedded 5 μm tissue sections, as described in Materials and methods (Chapter 3; section 3.9). Detection was conducted using Vectastain ABC system kit (Vector Laboratories, Burlingame, CA, USA). Diaminobenzidine was employed as the chromogenic substrate, and slides were counterstained with Mayer's haematoxylin. Images were captured with a Zeiss microscope (Imager Z1) to which was attached an Axiocam MRc5 digital camera. For negative or isotype controls, the primary antibody was replaced with TBS or respective antibody serum (used at respective antibody concentration). In each batch slides with positive control(s) (p53, survivin and PCNA) were also processed simultaneously. For staining of nuclear protein, semi quantitative analysis was conducted using Image J 1.43 (NIH) software. PCNA labeling index/Survivin labeling index/p53 labeling index was calculated by counting the number of positively stained cells × 100/total number of cells in photomicrographs of tumor section of at least 10 different randomly selected fields, with at least five hamsters per group.

5.2.4 Terminal deoxynucleotidyl transferase biotin-dUTP nick end labeling (TUNEL) assay

Apoptosis was assayed in formalin-fixed, paraffin-embedded 5 μm tissue sections, according to the manufacturer's instructions (*In-situ* TUNEL assay kit, Promega, Madison, WI, USA), as described in Materials and methods (Chapter 3; section 3.10). The nuclei of the apoptized cells were stained brown in color. The apoptotic index was calculated by counting the number of positively stained cells × 100/total number of cells in photomicrographs of tumor sections of at least 10 different randomly selected fields, with at least five hamsters per group.

5.2.5 Prostaglandin E-2 (PGE-2) measurement

The inflammatory response in hamster buccal pouch tissues was measured as the levels of PGE-2 in buccal pouches of hamsters belonging to various groups by enzyme immuno assay (EIA) employing PGE-2 EIA kit from Cayman Chemical Company (Ann Arbor, MI) according to the manufacturer's protocol.

5.2.5.1 Sample (lysate) preparation and purification

The tissues preserved at -80 °C were thawed and weighed. 0.5 g tissue was homogenized in 1-2 ml of homogenization buffer (0.1 M sodium phosphate buffer, pH 7.4, containing 1 mM EDTA and 10 μM indomethacin). Acetone (2-4 times the sample volume) was added to the sample and after 5 min incubation at room temperature (RT), tubes were centrifuged at 1,500 x g for 10 min. Supernatant was collected and acetone was removed by vacuum centrifugation. The dried pellet was reconstituted with 1 M acetate buffer, pH 4.0 before purified using C-18 SPE cartridge. Prior to the addition of sample, C-18 cartridge was activated by rinsing with 5 ml methanol (HPLC grade) and then with 5 ml ultra-pure water (cartridge should not be allowed to dry). Sample was then loaded on the cartridge. The cartridge was rinsed with 5 ml ultra-pure water, followed by 5 ml of HPLC grade hexane (the cartridge was dried at this step). PGE-2 was then eluted with 5 ml ethyl acetate containing 1% methanol. The ethyl acetate was evaporated to dryness (trace quantities of organic solvent will affect the EIA). The dry pellet was dissolved in EIA buffer and then, used for EIA.

5.2.5.2 EIA assay

Each sample was assayed in duplicate. The various component are added in the wells in the plate format mentioned below:-

	1	2	3	4	5	6	7	8	9	10
A	Blk	S1	S1	1	1	9	9	17	17	17
B	Blk	S2	S2	2	2	10	10	18	18	18
C	NSB	S3	S3	3	3	11	11	19	19	19
D	NSB	S4	S4	4	4	12	12	20	20	20
E	B_o	S5	S5	5	5	13	13	21	21	21
F	B_o	S6	S6	6	6	14	14	22	22	22
G	B_o	S7	S7	7	7	15	15	23	23	23
H	TA	S8	S8	8	8	16	16	24	24	24

Well	EIA buffer	Standard / sample	Tracer	Antibody
Blk	-	-	-	-
TA	-	-	5 μl (at devl. step)	-
NSB	100 μl	-	50 μl	-
B_0	50 μl	-	50 μl	50 μl
Standard / sample	-	50 μl	50 μl	50 μl

100 μl of EIA buffer was added to non-specific binding (NSB) wells and 50 μl to maximum binding (B_o) wells. 50 μl of standard/sample was added to the designated wells. This was followed by the addition of 50 μl of PGE-2 AChE tracer to each well except the total activity (TA) and the blank (Blk) wells. 50 μl of PGE-2 monoclonal antibody was then added to each well except the TA, NSB, and the Blk wells. The plate

was then carefully covered with a plastic film and incubated for 18 h at 4 °C. The following day, wells were emptied and washed 5-7 times with the wash buffer. 200 µl of Ellman's reagent was added to each well for the development and 5 µl of tracer to the TA well. The plate was covered and incubated at 37 °C for 60-90 min. The plate was read at 405 nm at around the time when the absorbance of B_o well is in the range of 0.3-0.8 absorbance unit (A.U).

The average absorbance readings from the NSB wells were subtracted from the average absorbance readings of B_o wells to obtain the corrected maximum binding (corrected B_o). The % B/ B_o was then calculated for all standard/samples. The amount of PGE-2 in the samples was determined from the standard curve plotted for % B/B_o of standards (S1-S8) vs. PGE-2 concentration. Results were expressed as PGE-2 ng/ml homogenate

5.2.6 Statistical analysis

Densitometry and cell counting were conducted using Image J 1.43 (NIH) software. Statistical analysis was performed using SPSS 15.0 software (IBM, Inc., Chicago IL, USA). Data are presented as mean ± SE. Means of all data were compared using ANOVA with post-hoc Bonferroni's or Mann-Whitney test. $p \leq 0.05$ was considered statistically significant.

5.3 RESULTS

Based on the net bodyweight gain, survival and histopathological evaluation of tissues, no toxicity or mortality was observed in animals belonging to the various treatment groups during the experimental period.

5.3.1 Dietary turmeric post-treatment inhibits DMBA-induced tumor growth in hamsters

Application of 0.5% DMBA three times per week for 12 weeks led to 100% tumor incidence in buccal pouches of hamsters. All of the animals developed squamous cell carcinomas (SCCs) with dysplastic changes in their buccal pouches, and the average numbers of tumors per animal were 1.7, 4.7, 3.5 and 7 in experiment 1-4, respectively

(Table 5.1). The average tumor volume shifted (at 12 weeks) to different treatment groups ranged from 14-28 mm^3 in different experiments (Tables 5.2 and 5.3). A pipette was used as the mode of DMBA application in experiment 1-3, whereas in experiment 4 a Camlin no. 4 paintbrush was used. Dietary turmeric (1%) exposures were maintained for 2 weeks (experiment 1), 3 weeks (experiment 2) and 4 weeks (experiments 3 and 4), and sacrifice time were 14 weeks (experiment 1), 15 weeks (experiment 2), and 16 weeks (experiments 3 and 4). Except for the mode of DMBA application (i.e. pipette vs Camlin no. 4 paintbrush), others parameters were identical in experiment 3 and 4. Detailed outcome of the parameters in experiments 1-4 are shown in Table 5.1.

TABLE 5.1: Incidence, multiplicity and volumes of tumors in various treatment groups

	Experiment 1	**Experiment 2**	**Experiment 3**	**Experiment 4**
DMBA (0.5%) application	3x/wk for 12 wk	3x/wk for 12 wk	3x/wk for 12 or 16 wk	3x/wk for 12 or 16 wk
Mode of DMBA application	Pipette	Pipette	Pipette	Camlin No. 4 paintbrush
Dietary turmeric (1%) exposure	2 wk	3 wk	4 wk	4 wk
Sacrifice time	14 wk	15 wk	16 wk	16 wk
Number of animals	$n \geq 6$	$n \geq 11$	$n \geq 7$	$n \geq 10$
Tumor incidence (at 12wk)	100%	100%	100%	100%
Tumor multiplicity range (at sacrifice time)	0.87 - 1.7	3.1 - 4.7	2-1 - 3.5	4 - 7
Tumor volume range (mm^3) (at 12 wk)	2.6 - 87.5	2.6 - 89.9	0.5-121.2	4.1-49.7
Tumor volume range (mm^3) (at sacrifice time)	12. 5 – 181.2	29.7 - 970	9.2-1285	14.6 - 904.3
Tumor volume range (mm^3) (sacrifice time -12 wk)	16.5 - 173.6	24.5-965.6	26.1-1164.6	10.3 - 856.4
Tumor volume range (mm^3) (sacrifice time/ 12 wk)	2.5 – 45.7	1.8 - 54	1.3 – 216.6	2.1 – 84.2

TABLE 5.2: Tumor volumes in HBP in animals belonging to different treatment groups, experiment 3

		12 wk	16 wk	16 wk -12 wk	16 wk/12 wk
GROUP 12DC4 (n=7)	Total tumor volume (mm^3)	188	1772	1584	116
	mean ± S.E	26 ± 14.5	253 ± 91.1	226 ± 77	16.5 ± 4.4
	Tumor volume range	7.3 - 113.1	86.8 - 229.4	79.4 - 225	6.9 - 54.8
GROUP 12DT4 (n=7)	Total tumor volume (mm^3)	193	1181	987	61.3
	mean ± S.E	27 ± 8.7	168 ± 31.2	141 ± 31	8.7 ± 2
	Tumor volume range	9.9 - 71.6	92.6 – 300	46.2 - 283.2	1.96 - 17.9
GROUP 16DC4 (n=7)	Total tumor volume (mm^3)	199.7	1911	1711	266.7
	mean ± S.E	28 ± 16.1	273 ± 170	244 ± 154	38.1 ± 29.7
	Tumor volume range	0.5 - 121.2	9.2 - 1285	26.1 - 1164.6	3.8 - 216.6
GROUP 16DT4 (n=8)	Total tumor volume (mm^3)	200	954	754	234.6
	mean ± S.E	25 ± 11.9	119 ± 29	94 ± 26	29.3 ± 15.7
	Tumor volume range	0.5 - 96.9	32.7 - 294.5	27.9 – 245	1.3 - 126.1

After treatment with 1% dietary turmeric, tumor growth i.e. tumor burden and multiplicity was inhibited in animals shifted to turmeric diet (groups 12DT2 and12DT3) for 2 and 3 weeks, compared to the animals on the control diet (groups 12DC2 and 12DC3), respectively (experiments 1 and 2, Figs. 5.2A, and 5.2B, respectively). In these experiments, tumor multiplicity decreased by 47% (group 12DT2) and 44% (group 12DT3) compared to the respective controls (groups 12DC2 and 12DC3) (Fig. 5.2B). The observed inhibition in tumor growth may have been due to dietary turmeric exposure and/or discontinuation of carcinogen (DMBA) exposure. To rule out the role of DMBA discontinuation; in experiment 3, following tumor development (12 weeks), animals were randomized into four groups wherein the duration of treatment with dietary turmeric was increased to 4 weeks to reveal more pronounced effects. When the relative changes in the tumor burden (16weeks/12 weeks) were analyzed at the end of experiment, there was a significant decrease in the tumor burden in group 12DT4 receiving turmeric compared to the control group 12DC4, although there was no statistically significant decrease in tumor burden in group 16DT4, which received turmeric, compared to control group 16DC4, despite a 56% decrease in tumor burden (16 weeks-12 weeks) between group 16DT4 (treated) vs. group 16DC4 (control) (Table 5.2 and Fig. 5.2C). The lack of statistical significance in tumor burden appears to be due to large variations/uncommon distribution of tumor volumes in groups 16DC4 and 16DT4 (Fig. 5.2C) [26.1-1164.6 mm^3 (16 weeks-12 weeks) in group 16DC4, 27.9-245 mm^3 (16 week-12 week) in group 16DT4, or 0.5 –

121.2 mm^3 in group 16DC4, and 0.5 - 96.9 in group 16DT4 (Table 5.2)]. Dietary turmeric also significantly decreased the DMBA-induced tumor multiplicity by 40% in both groups 12DT4 and 16DT4 when compared to control groups 12DC4 and 16DC4, respectively (Fig. 5.2D). Variation in tumor burden or multiplicity in animals in experiments 1-3 may have been due to the administration of the DMBA through a pipette, which can be seen in tumor volume range at the time of randomization (i.e., 12 weeks) (Table 5.1).

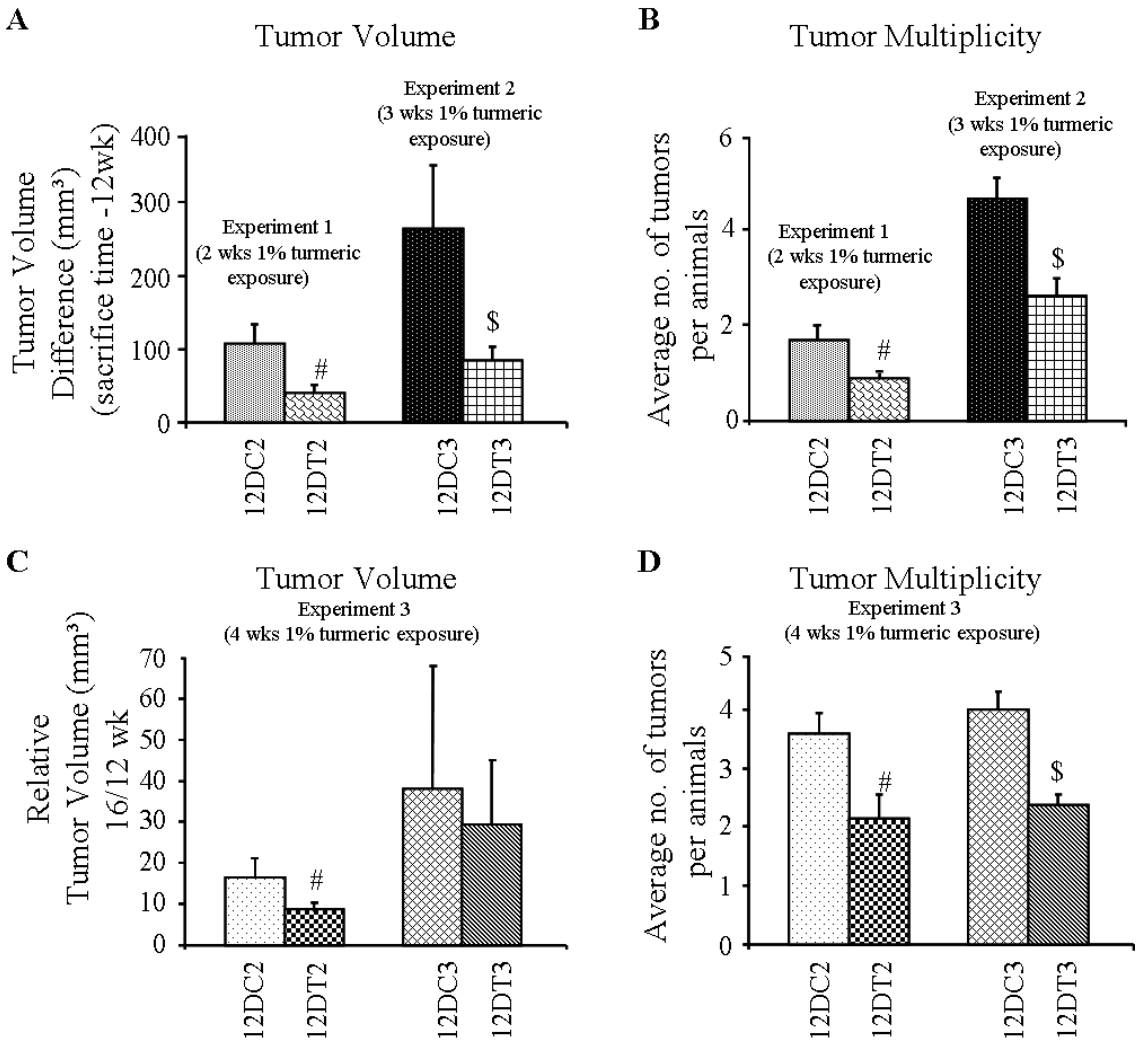

FIGURE 5.2: Effect of dietary turmeric (1%) post-treatment on DMBA-induced tumor volume and tumor multiplicity in HBP tumors.*Effect of dietary turmeric post-treatment on* **(A)** *Tumor volume in experiments 1 and 2.***(B)***Tumor multiplicity in experiments 1 and 2. Data represent mean ± SE of atleast 6 and 11 animals, respectively. Differences among groups were determined by one-way ANOVA followed by Bonferroni's test, $p \leq 0.05$.***(C)** *Tumor volume in experiment 3.* **(D)** *Tumor multiplicity in experiment 3. Data represent mean ± SE of atleast 7 animals. Differences among groups were determined by one-way ANOVA followed by Mann-Whitney, $p \leq 0.05$. '#' significant when compared with 12DC4; '$' significant when compared with 16DC4.*

The application of carcinogen with a Camlin no. 4 paintbrush was more effective than application with a pipette in inducing higher tumor multiplicity with an approximately similar range of tumor volume. This result could be possibly due to the more uniform exposure of non-toxic doses of carcinogen to a larger area of buccal pouches (Table 5.3). Tumors were induced by applying DMBA with a Camlin no. 4 paintbrush, and these animals, which had a narrow range of DMBA-induced HBP tumors (1-5 mm diameter), were randomized into four groups so the effect of dietary turmeric could be determined. Animals treated with corn oil alone did not develop tumors.

TABLE 5.3: Tumor volumes in HBP in animals belonging to different treatment groups, experiment 4

		12 wk	16 wk	16 wk -12 wk	16 wk/12 wk
GROUP 12DC4 (n=10)	Total tumor volume (mm^3)	205.2	3437.1	3231.8	322.8
	mean ± S.E	20.5 ± 5.6	343.7 ± 27.9	323.1 ± 25.6	32.2 ± 8.4
	Tumor volume range	4.1 - 49.7	203.5 - 504.6	198.3 - 455.5	7.1 - 84.2
GROUP 12DT4 (n=13)	Total tumor volume (mm^3)	278.8	1453.1	1168.2	66.4
	mean ± S.E	21.4 ± 3.6	111.7 ± 21	89.8 ± 21.3	5.1 ± 3.4
	Tumor volume range	4.1 - 49.7	14.6 - 234.3	10.3 - 218	2.1 – 7.4
GROUP 16DC4 (n=12)	Total tumor volume (mm^3)	169.1	4291.5	4122.4	405.1
	mean ± S.E	14.1 ± 6.6	357.5 ± 63.2	343.5 ± 60	38.7 ± 4.2
	Tumor volume range	4.1 - 47.6	143.1 - 904.3	138.9 - 856.4	13.6 – 56.9
GROUP 16DT4 (n=11)	Total tumor volume (mm^3)	221.8	2042.4	1820.6	117.34
	mean ± S.E	20.1 ± 4.1	185.6 ± 33.2	165.8 ± 29.5	9.8 ± 1.2
	Tumor volume range	4.1 - 37.6	54.4 - 396.3	50.2 - 362.8	6.6 - 18.6

Tumor burden calculated using the difference in the mean tumor volumes in animals at weeks 16 and 12 of DMBA treatment showed that the animals receiving 1% dietary turmeric without or with continuation of carcinogen treatments after week 12 showed a tumor burden that significantly decreased by 63% (from 3231 to 1168 mm^3) and 55% (from 4122 to 1820 mm^3), respectively (Fig. 5.3A left hand panel). Relative tumor burden calculated by dividing the mean tumor volumes at week 16 by mean tumor volumes at week 12 of DMBA treatment showed that the animals receiving 1% dietary turmeric without or with DMBA continuation after 12 weeks had relative tumor burden that significantly decreased by 79% and 71%, respectively (Fig. 5.3A right hand panel). Furthermore, 1% dietary turmeric treatment resulted in a significant decrease in the DMBA-induced tumor multiplicity in groups 12DT4 and 16DT4 (43% and 42%, respectively), when compared to respective controls (groups 12DC4 and 16DC4) (Fig.

5.3B). Details of tumor volume in experiments 3 and 4 are shown in Tables 5.2 and 5.3. Histopathological analyses of buccal mucosa also revealed that animals receiving only the control diet did not show any gross tumors or histological changes (Fig. 5.3C). Conversely, 12 and 16 weeks of DMBA treatment produced SCC with dysplastic changes and well-developed SCCs or *in situ* carcinomas in the buccal pouches of hamsters, respectively (Fig. 5.3C). Post-treatment with dietary turmeric inhibited the growth of SCCs in tumor-bearing animals receiving 1% turmeric diet irrespective of whether carcinogen treatment was stopped at week 12 or continued to week 16 (groups 12DT4 and 16DT4) (Fig. 5.3C).

5.3.2 Dietary turmeric post-treatment increases the DMBA-mediated apoptosis

Decrease in tumor burden and multiplicity in HBP tumors upon turmeric treatment suggest its role in apoptosis and/or cell proliferation. To investigate the effects of dietary turmeric on apoptosis, buccal pouch tumor extracts were prepared and analyzed for apoptosis markers. Compared to vehicle control (C), buccal pouches of tumor-bearing animals at weeks 12 and 16 of DMBA treatment (groups 12DC4 and 16DC4) showed a significant decrease in the levels of pro-apoptotic protein, Bax, and an increase in the levels of Bcl-2, an anti-apoptotic protein (Fig. 5.4A). Significant abrogation of DMBA-induced expression of anti-apoptotic protein Bcl-2 was observed in tumor-bearing animals receiving a 1% turmeric diet irrespective of whether carcinogen treatment was stopped at week 12 or continued to week 16 (groups 12DT4 and 16DT4). However, the increase in the expression of Bax, a pro-apoptotic marker, was observed, though a significant increase was attained only in group 16DT4 compared to 16DC4 (Fig. 5.4A). Dietary turmeric-mediated inhibition of DMBA-induced anti-apoptotic response was also reflected in an increased Bax/Bcl-2 ratio in quantitative western blot analysis (Fig. 5.4B). Immunohistochemical staining of Bax and Bcl-2 in HBP tumor tissue (Fig. 5.4C) showed that intensity and/or area of staining of these analyte(s) was modulated; these results were similar to the results observed in the western blotting assay.

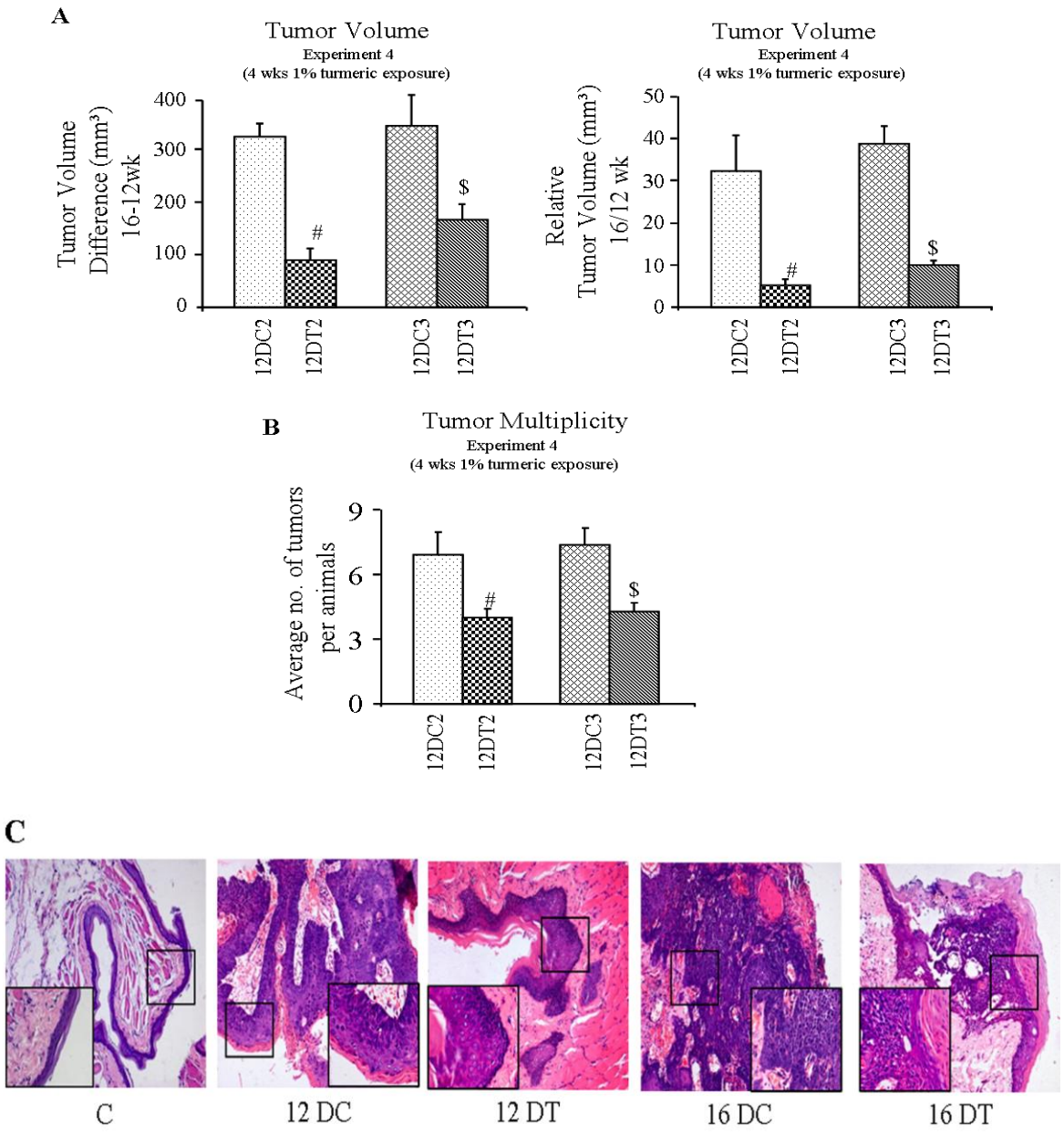

FIGURE 5.3: Effect of dietary turmeric (1%) post-treatment on DMBA-induced HBP tumors. *Effect of dietary turmeric post-treatment on* **(A)** *Tumor volume in experiment 4.***(B)** *Tumor multiplicity in experiment 4. Data represent mean ± SE of atleast 10 animals. Differences among groups were determined by one-way ANOVA followed by Bonferroni's test, $p \leq 0.05$. '#' significant when compared with 12DC4; '$' significant when compared with 16DC4.* **(C)** *Representative photomicrograph of haematoxylin and eosin (H & E, magnification X 100; insert shows 400 X magnification) stained buccal mucosa sections from hamsters belonging to the various treatment groups.*

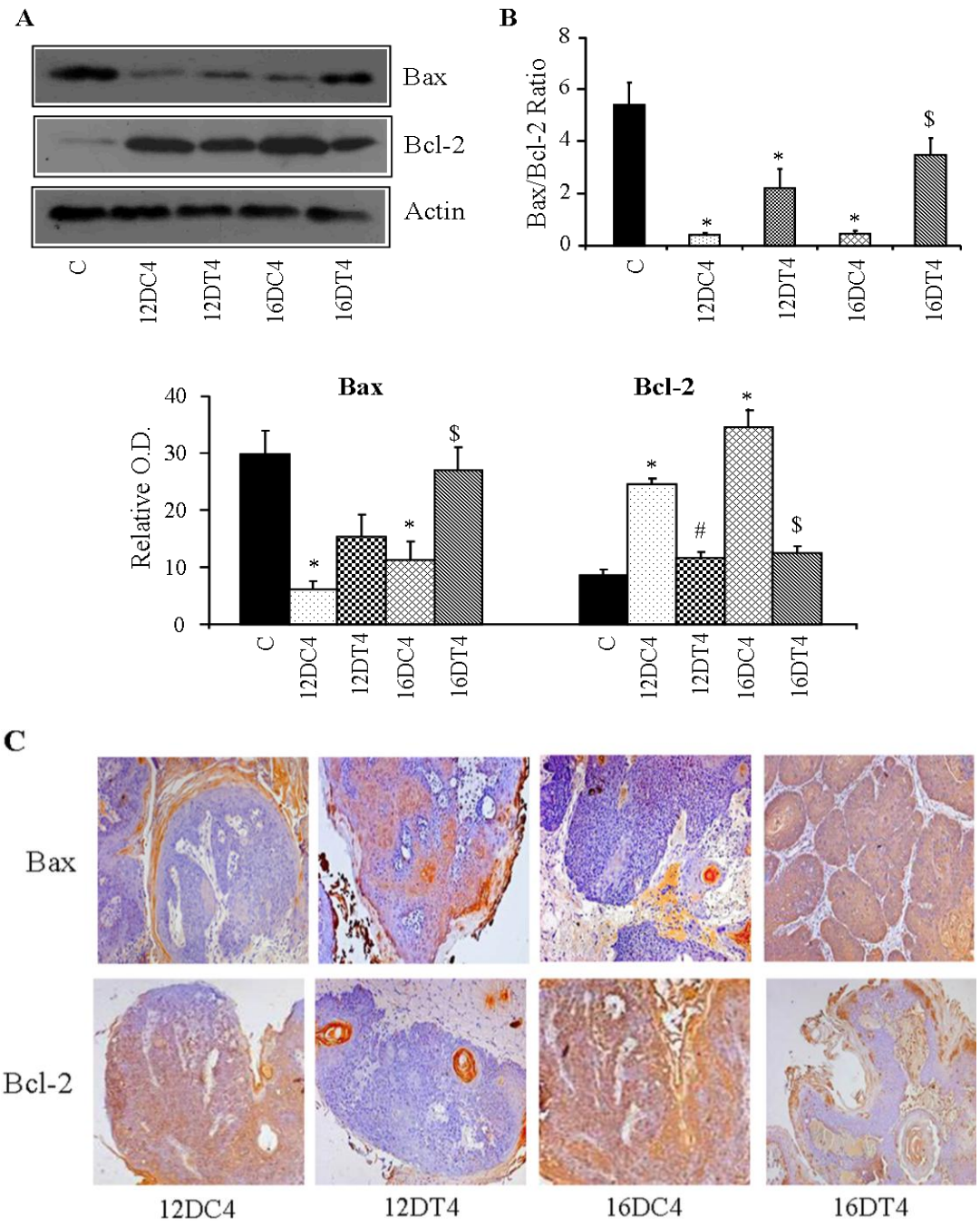

FIGURE 5.4: Effect of dietary turmeric (1%) post-treatment on DMBA-induced apoptosis-related markers in HBP tumor tissue.(A) *Representative blots and relative levels of Bax and Bcl-2 measured in total cell protein of HBP by western blotting using specific antibodies.* **(B)** *Extent of apoptosis in HBP was determined by calculating the ratio of normalized band intensity of Bax and Bcl-2.* **(C)***Representative photomicrographs showing immunohistochemical detection (magnification X 100; insert shows 400 X magnification) of Bax and Bcl-2 in formalin-fixed, paraffin-embedded HBP sections, with atleast five hamsters per group. Quantification of all the total cell protein was done by normalizing the band density to that of β-actin. Data represent mean ± SE of five observations. Differences among groups were determined by one-way ANOVA followed by Bonferroni's test, $p \leq 0.05$. '#' significant when compared with 12DC4; '$' significant when compared with 16DC4; '*' significant when compared with vehicle control.*

Semi-quantitative measurements of apoptotic index measured in HBP tumor tissue by IHC showed that 4 weeks of dietary turmeric treatment increased apoptosis by 1.7- and 1.4 fold in groups where carcinogen treatment was given up to weeks 12 and 16, respectively, as confirmed by TUNEL assay (Fig. 5.5A). These findings were further corroborated by alterations in other apoptosis-related markers. Compared with vehicle control (C), buccal pouches of tumor-bearing animals receiving DMBA treatment for 12 and 16 weeks (groups 12DC4 and 16DC4) showed a significant decrease in the levels of caspase-3, caspase-9, and cytochrome c (Fig. 5.5B) and increase in the levels of p53 and p21 (Fig. 5.6A). Dietary turmeric post-treatment significantly increased the expression of caspase-3, caspase-9 and cytochrome c in tumor-bearing animals (groups 12DT4 and 16DT4), whereas the levels of p53 and p21 decreased in groups 12DT4 and 16DT4 compared to respective controls (groups 12DC4 and 16DC4) (Fig. 5.6A). The p53 finding was further complemented by IHC staining; depicting a significant decrease in DMBA-mediated enhancement of p53 labeling index upon turmeric treatment in HBP tumor tissue (Fig. 5.6B).

Effects of dietary turmeric post-treatment were also evaluated on another apoptosis marker, survivin, which is known to be the smallest of the known inhibitors of apoptosis (IAP) family proteins. Survivin inhibits apoptosis by suppressing caspase-3 and caspase-7, thereby modulating the G2/M phase of the cell cycle through association with mitotic spindles. Results herein, showed that application of DMBA significantly increased the levels of survivin in tumor-bearing animals receiving DMBA for 12 and 16 weeks (groups 12DC4 and 16DC4, respectively) compared to controls (Fig. 5.7A). Dietary turmeric for 4 weeks significantly decreased the DMBA-induced expression of survivin, irrespective of whether carcinogen treatment was applied for 12 weeks (group 12DT4) or continued for 16 weeks (group 16DT4) (Fig. 5.7A). This finding was further strengthened by immunohistochemical staining; a significant decrease in DMBA-mediated enhancement of survivin labeling index upon turmeric treatment was observed for HBP tumor tissue (Fig. 5.7B).

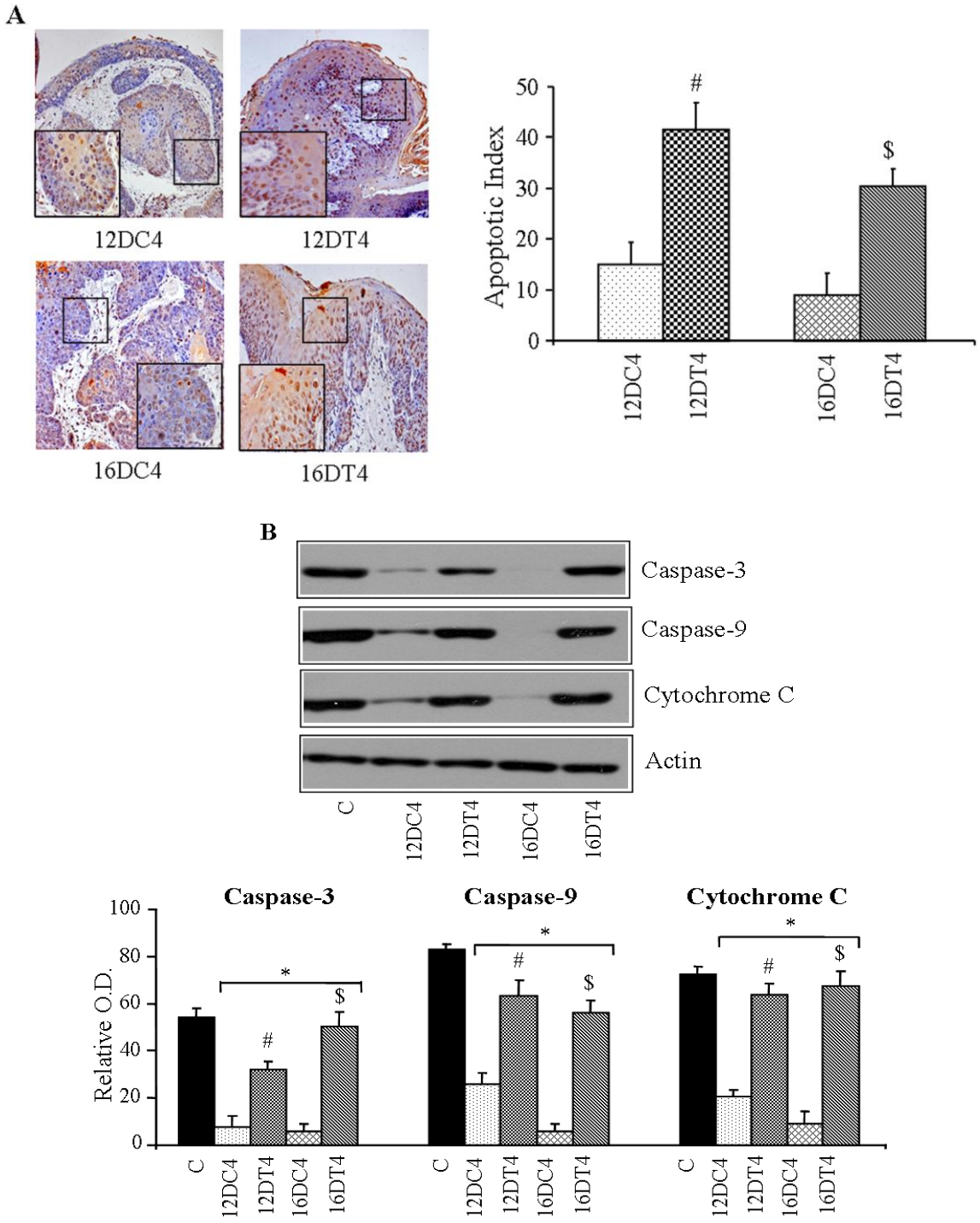

FIGURE 5.5: Effect of dietary turmeric (1%) post-treatment on DMBA-induced apoptosis related markers in HBP tumor tissue.(A)*Representative photomicrographs showing apoptotic cells (magnification X 100; insert shows 400 X magnification) via TUNEL assay in formalin-fixed, paraffin-embedded HBP sections, with atleast five hamsters per group.***(B)** *Representative blots and relative levels of caspase-3, caspase-9 and cytochrome c measured in total cell protein of HBP by western blotting using specific antibodies. Quantification of all the total cell protein was done by normalizing the band density to that of β-actin. Apoptotic index was calculated as number of positively stained cells x 100/ total number of cells. Semi quantitative analysis was done by Image J 1.43 (NIH) software by counting the brown stained nuclei in photomicrographs of tumor part*

of atleast 10 different randomly selected fields/section/animal. Data represent mean ± SE of five observations. Differences among groups were determined by one-way ANOVA followed by Bonferroni's test, p ≤ 0.05. '#' significant when compared with 12DC4; '$' significant when compared with 16DC4; '' significant when compared with vehicle control.*

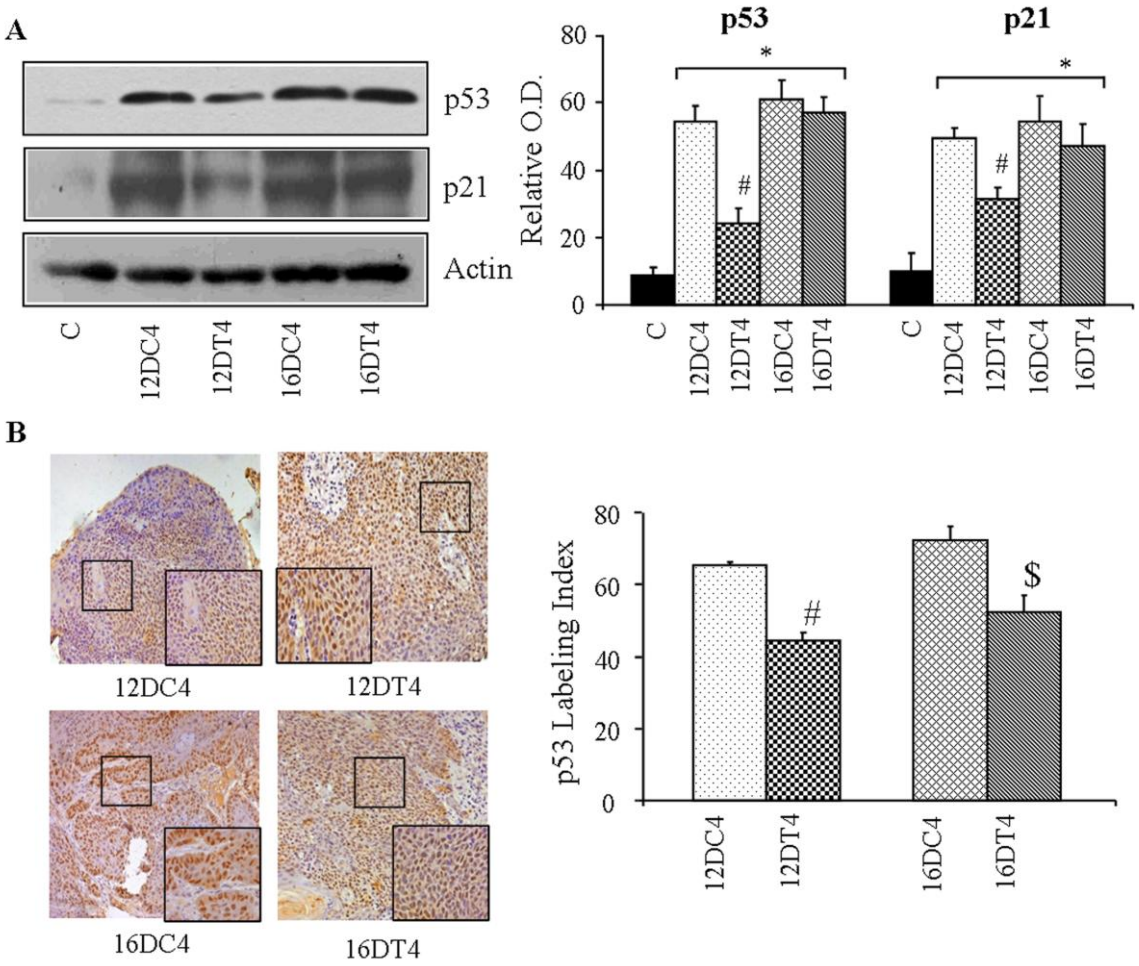

FIGURE 5.6: Effect of dietary turmeric (1%) post-treatment on DMBA-induced apoptosis related markers in HBP tumor tissue. (A) *Representative blots and relative levels of p53 and p21 measured in total cell protein of HBP by western blotting using specific antibodies.* **(B)***Representative photomicrographs showing immunohistochemical detection (magnification X 100; insert shows 400 X magnification) of p53 labeling index. p53 labeling index was calculated as number of positively stained cells x 100/ total number of cells. Semi quantitative analysis was done by Image J 1.43 (NIH) software by counting the brown-stained nuclei in photomicrographs of tumor part of atleast 10 different randomly selected fields/section/hamster, with atleast five hamsters per group. Data represent mean ± SE of five observations. Differences among groups were determined by one-way ANOVA followed by Bonferroni's test, p ≤ 0.05. '#' significant when compared with 12DC4; '$' significant when compared with 16DC4; '*' significant when compared with vehicle control.*

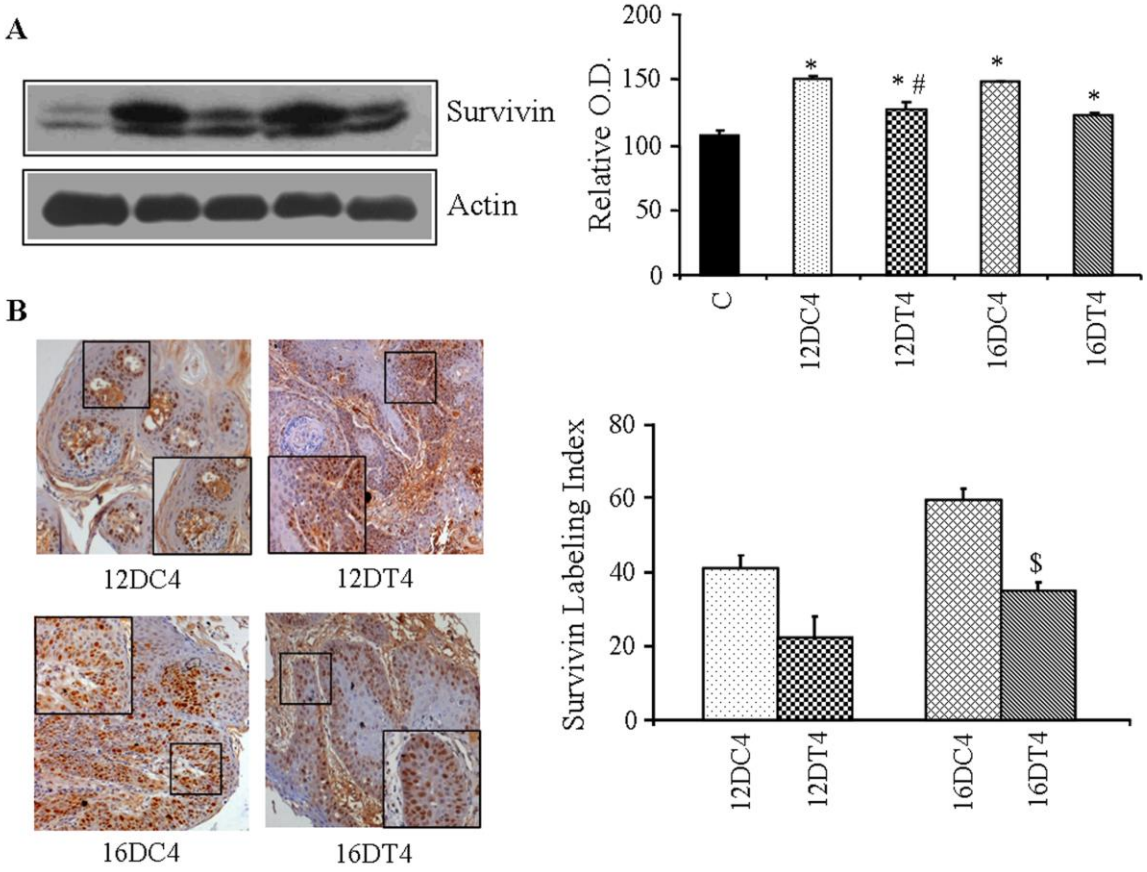

FIGURE 5.7: Effect of dietary turmeric (1%) post-treatment on DMBA-induced survivin in HBP tumor tissue. (A) *Representative blot and relative level of survivin measured in total cell protein of HBP by western blotting using specific antibody.***(B)** *Representative photomicrographs showing immunohistochemical detection (magnification X 100; insert shows 400 X magnification) of survivin labeling index. Survivin labeling index was calculated as number of positively stained cells x 100/ total number of cells. Semi quantitative analysis was done by Image J 1.43 (NIH) software by counting the brown-stained nuclei in photomicrographs of tumor part of atleast 10 different randomly selected fields/section/hamster, with atleast five hamsters per group. Data represent mean ± SE of five observations. Differences among groups were determined by one-way ANOVA followed by Bonferroni's test, $p \leq 0.05$. '#' significant when compared with 12DC4; '$' significant when compared with 16DC4; '*' significant when compared with vehicle control.*

5.3.3 Dietary turmeric post-treatment decreases DMBA-mediated cell proliferation

To examine the role of cell proliferation in turmeric-mediated decrease in tumor burden and multiplicity in HBP SCC tumors, cell proliferation markers were analyzed in HBP SCC tumor extracts. Buccal pouches of animals treated with DMBA (groups 12DC4 and 16DC4) showed a significant increase in the protein levels of proliferating cell nuclear antigen (PCNA) and cyclin D1 compared to the control (Fig. 5.8A). Dietary turmeric post-treatment led to a significant decrease in the DMBA-induced expression of PCNA irrespective of whether carcinogen treatment was applied for 12 weeks or

continued for 16 weeks (groups 12DT4 and 16DT4). In contrast, a decrease in the levels of cyclin D1 was observed only when carcinogen treatment was applied for 12 weeks (group 12DT4) and not in the group where carcinogen treatment was applied for 16 weeks (group 16DT4) (Fig. 5.8A). Similar alterations in the levels of PCNA were seen in HBP tumor tissue analyzed using IHC (Fig. 5.8B). Thus, dietary turmeric decreased DMBA-induced level of cell proliferation markers.

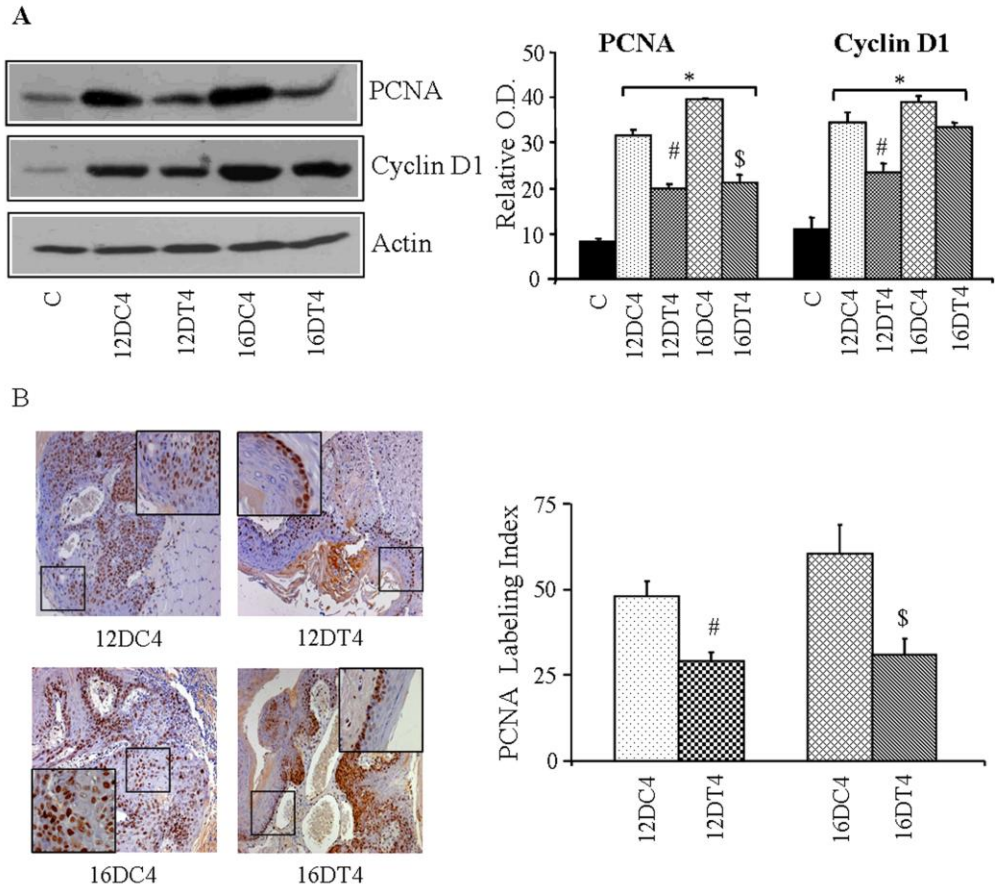

FIGURE 5.8: Effect of dietary turmeric (1%) post-treatment on DMBA-induced cell proliferation markers in HBP tumor tissue.(A)*Representative blot and relative levels of PCNA and cyclin D1 measured in total cell protein of HBP by western blotting using specific antibodies. Quantification was done by normalizing the band density to that of β-actin.* **(B)** *Representative photomicrographs showing immunohistochemical detection (magnification X 100; insert shows 400 X magnification) of PCNA protein in formalin-fixed, paraffin-embedded HBP sections. PCNA labeling index was calculated as number of positively stained cells x 100/ total number of cells. Semi quantitative analysis was done by Image J 1.43 (NIH) software by counting the brown-stained nuclei in photomicrographs of tumor part of atleast 10 different randomly selected fields/section/hamster, with at least five hamsters per group. Data represent mean ± SE of five observations. Differences among groups were determined by one-way ANOVA followed by Bonferroni's test, $p \leq 0.05$. '#' significant when compared with 12DC4; '$' significant when compared with 16DC4; '*' significant when compared with vehicle control.*

5.3.4 Dietary turmeric post-treatment decreases the DMBA-induced activation of nuclear transcription factors and MAPK

Having observed the effects of dietary turmeric post-treatment on DMBA-mediated apoptosis and cell proliferation markers in HBP, we next investigated its effects on transcription factors such as c-jun, c-fos, and NF-κB (upstream effectors of apoptosis and cell proliferation markers) [187,188]. Activation of c-jun, c-fos, and NF-κB was determined by assaying their levels in nuclear extracts. As shown in Fig. 5.9, the levels of c-jun, c-fos, and NF-κB were significantly increased in tumor-bearing animals receiving DMBA application for 12 and 16 weeks. Four weeks of dietary turmeric post-treatment significantly decreased the DMBA-induced expressions of c-jun, c-fos, and NF-κB, irrespective of whether carcinogen treatment was applied for 12 weeks or continued upto 16 weeks (groups 12DT4 and 16DT4, respectively) (Fig. 5.9).

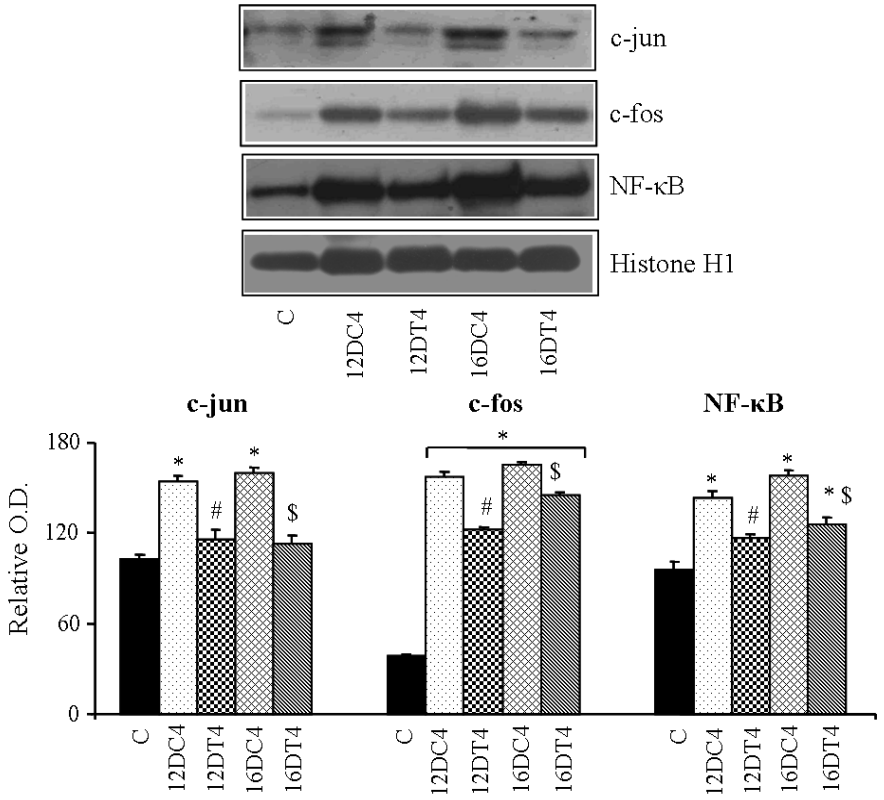

FIGURE 5.9: Effect of dietary turmeric (1%) post-treatment on DMBA-mediated alterations in transcription factors related proteins. *Representative blot and relative levels of c-jun, c-fos, and NF-κB measured in nuclear extracts of HBP by western blotting using specific antibodies. Quantification was done by normalizing the band density to that of Histone H1. Data represent mean ± SE of five observations. Differences among groups were determined by one-way ANOVA followed by Bonferroni's test, $p \leq 0.05$. '#' significant when compared with 12DC4; '$' significant when compared with 16DC4; '*' significant when compared with vehicle control.*

One of the plausible mechanisms underlying inhibition of NF-κB activation involves repression of phosphorylation and subsequent degradation of the inhibitory unit, IκB-α, which hampers subsequent nuclear translocation of the functionally active subunit NF-κB. To understand this mechanism, we further investigated the effects of dietary turmeric post-treatment on NF-κB inhibitory proteins. Cytosolic levels of NF-κB and IκB-α were significantly decreased in animals receiving DMBA for 12 and 16 weeks (groups 12DC4 and 16DC4, respectively) compared to controls (Fig. 5.10). However, post-treatment of dietary turmeric significantly increased the levels of IκB-α irrespective of whether carcinogen treatment was applied for 12 weeks or continued upto 16 weeks (groups 12DT4 and 16DT4), whereas a significant increase in the expressions of cytosolic NF-κB was observed only in group 16DT4 compared to group 16DC4 (Fig. 5.10). The cytosolic levels of IKK and pIκB-α were also significantly increased in tumor bearing animals receiving DMBA for 12 and 16 weeks (groups 12DC4 and 16DC4, respectively) compared to controls (Fig. 5.10). In contrast, dietary turmeric post-treatment significantly decreased the levels of IKK and pIκB-α, irrespective of whether carcinogen treatment was applied for 12 weeks or continued upto 16 weeks (groups 12DT4 and 16DT4) (Fig. 5.10). These results suggest that dietary turmeric inhibits DMBA-induced translocation of NF-κB to the nucleus through blockade of IκB-α phosphorylation and IKK.

To study the role of MAPKs known to regulate downstream proto-oncogenes (c-jun, c-fos) and NF-κB activation, effects of dietary turmeric post-treatment on DMBA-induced phosphorylation of ERK and p38 were investigated. Compared with controls, tumor-bearing animals receiving DMBA for 12 and 16 weeks (groups 12DC4 and 16DC4, respectively), showed a significant increase in the levels of p-ERK and p-p38 (groups 12DC4 and 16DC4) (Fig. 5.11). Four weeks of dietary turmeric post-treatment significantly decreased the levels of p-ERK in 12DT4 and 16DT4, while a decrease in the levels of p-p38 was observed only with 12 weeks of DMBA treatment (group 12DT4) and not in the group in which DMBA treatment was continued upto 16 weeks (Fig. 5.11). Western blot analysis showed that dietary turmeric suppressed DMBA-induced phosphorylation of ERK and p38 MAPKs, while levels of unphosphorylated MAPKs were unchanged in all of the treatment groups (Fig. 5.11).

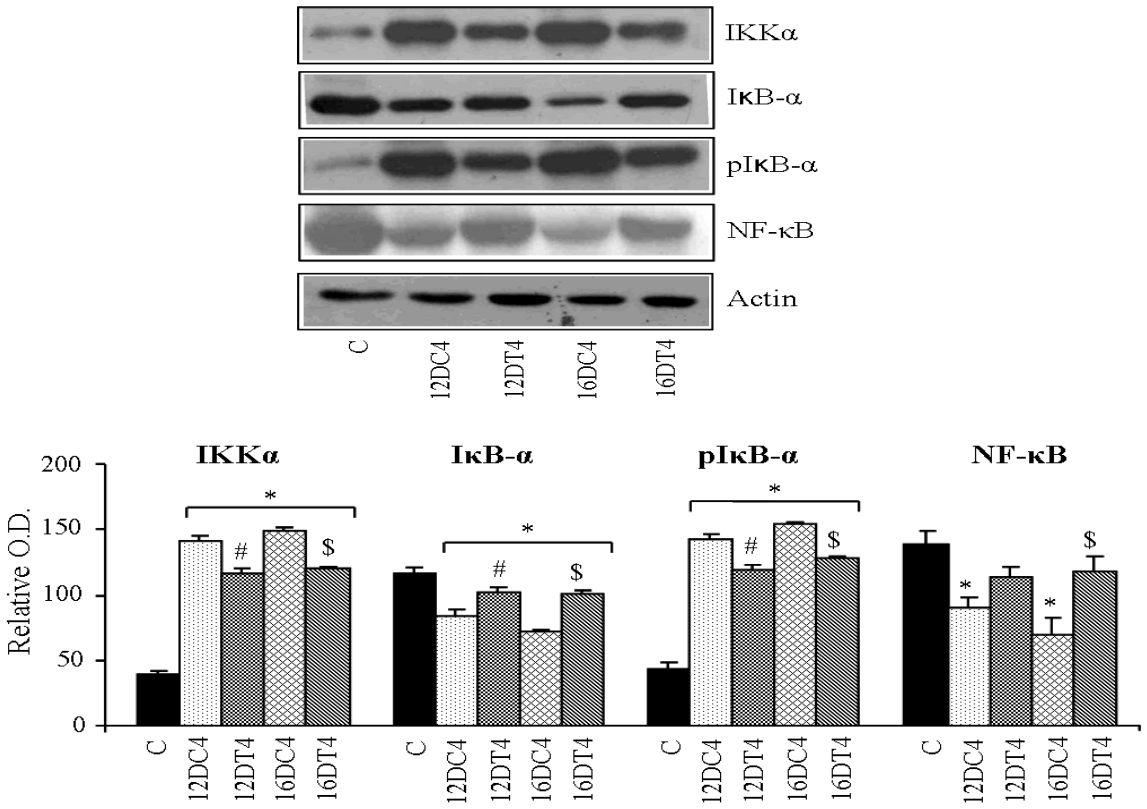

FIGURE 5.10: Effect of dietary turmeric (1%) post-treatment on DMBA-mediated alterations in cytosolic NF-κB family proteins. *Representative blots and relative levels of IKK, IκB-α, pIκB-α and NF-κB measured in cytosolic extracts of HBP by western blotting using specific antibodies. Quantification was done by normalizing the band density to that of β-actin. Data represent mean ± SE of five observations. Differences among groups were determined by one-way ANOVA followed by Bonferroni's test, $p \leq 0.05$. '#' significant when compared with 12DC4; '$' significant when compared with 16DC4; '*' significant when compared with vehicle control.*

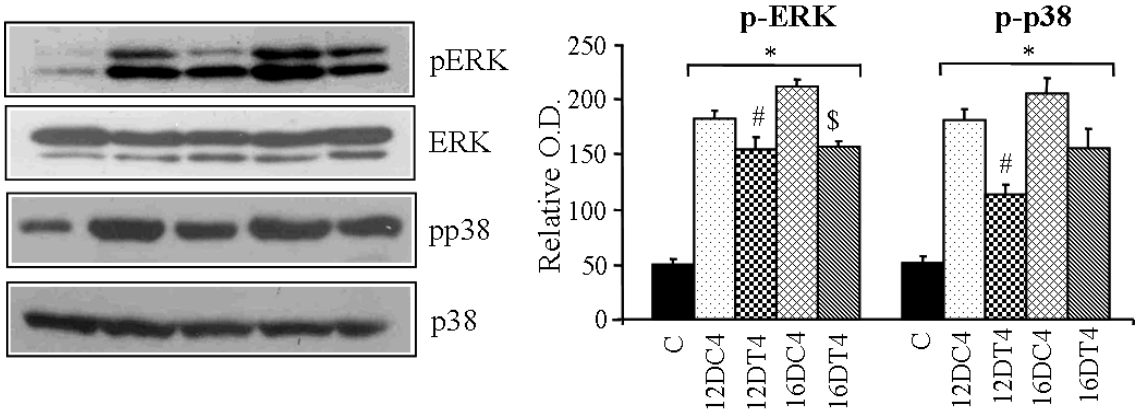

FIGURE 5.11: Effect of dietary turmeric (1%) post-treatment on DMBA-mediated alterations in MAPK proteins. *Representative blots and relative levels ofphospho-MAPKs (p-ERK and p-p38) measured in total cell protein of HBP by western blotting using specific antibodies. Protein levels of p-ERK and p-p38 were normalised to that of respective total kinase, levels of each of which remained unaltered under same*

experimental conditions. Data represent mean ± SE of five observations. Differences among groups were determined by one-way ANOVA followed by Bonferroni's test, $p \leq 0.05$. '#' significant when compared with 12DC4; '$' significant when compared with 16DC4; '' significant when compared with vehicle control..*

5.3.5 Dietary turmeric post-treatment decreases the DMBA-induced inflammation

NF-κB and/or MAPKs (at least in parts) are known to play a critical role in regulating the induction of cyclooxygenase-2 (cox-2), an enzyme associated with inflammation and tumorigenesis [187-190]. Having observed the inhibitory effect of turmeric on DMBA-induced transcription factors and NF-κB family proteins, we next examined the effect of dietary turmeric on inflammatory response. DMBA applications significantly increased the levels of cox-2 in animals receiving DMBA for 12 and 16 weeks (groups 12DC4 and 16DC4, respectively) compared to the controls. Level of cox-2 was barely detectable in the control (Fig. 5.12A). In contrast, dietary turmeric post-treatment significantly decreased the DMBA-induced expressions of cox-2 when carcinogen treatment was applied for 12 weeks (groups 12DT4), while its effect was not significant when DMBA treatment was applied upto 16 weeks. This finding was supported by immunohistochemical staining of cox-2 in HBP tumor tissue (Fig. 5.12B), wherein dietary turmeric decreased the high expression of cox-2 staining only in group 12DT4 compared with group 12DC4. These results were strengthened by data showing that dietary turmeric attenuated levels of PGE-2 when DMBA treatment was applied for 12 weeks (group 12DT4), suggesting a sustained decrease in DMBA-induced inflammation only when DMBA was applied for 12 weeks (Fig. 5.12C).

To summarize, dietary turmeric post-treatment had effects on apoptosis, cell proliferation, inflammation and NF-κB family-related proteins/markers in DMBA-induced HBP tumors.

5.4 DISCUSSION

Use of medicinal plants or their active principles in the prevention and/or treatment of chronic diseases are based on the experience of traditional systems of medicine from different ethnic societies; their use in modern medicine suffers from lack of scientific evidence. Only a few medicinal plants have attracted the interest of scientists, and one such plant is *Curcuma longa*. Curcumin (diferuloylmethane), a phenolic compound that has been identified as the major pigment in turmeric, possesses both anti-inflammatory and antioxidant properties. Chemopreventive efficacy of turmeric/curcumin

has been demonstrated when administered prior to, during, and subsequent to a carcinogen/tumor promoter. However, effects of its post-treatment (i.e. after tumor development) have not been previously reported.

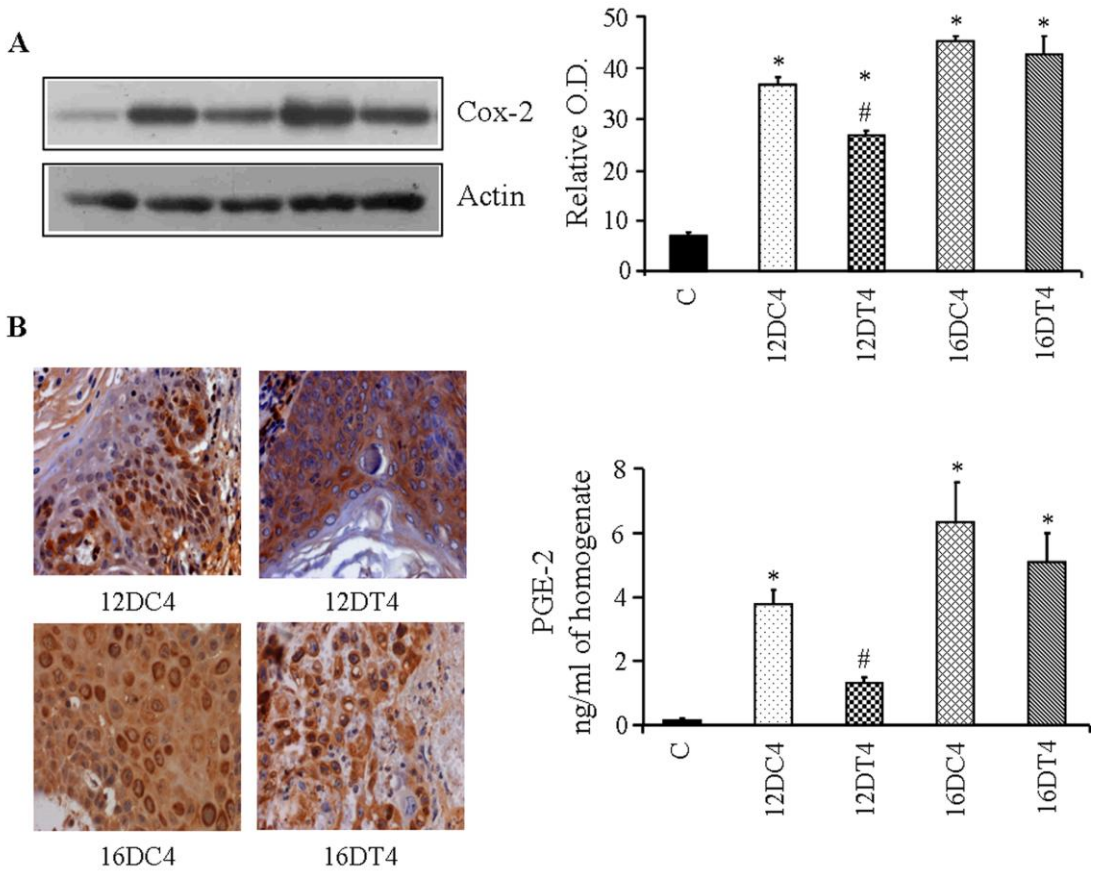

FIGURE 5.12: Effect of dietary turmeric (1%) post-treatment on DMBA-induced inflammatory response in HBP tumor tissue.(A) *Representative blot and relative level of cox-2 were measured in total cell protein of HBP by western blotting using specific antibody. Quantification was done by normalizing the band density to that of β-actin.* **(B)** *Representative photomicrographs showing immunohistochemical detection of cox-2 protein in formalin-fixed, paraffin-embedded HBP sections, with atleast five hamsters per group (magnification X 100; insert shows 400 X magnification).* **(C)***Inflammation in buccal pouch of hamsters measured as levels of PGE-2 by enzyme-immuno assay. Data represent mean ± SE of five observations. Differences among groups were determined by one-way ANOVA followed by Bonferroni's test, $p \leq 0.05$. '#' significant when compared with 12DC4; '$' significant when compared with 16DC4; '*' significant when compared with vehicle control.*

The present investigation was undertaken to evaluate the post-treatment effects of dietary turmeric on DMBA-induced oral tumors. Whole turmeric powder was preferred over the pure active principle compound curcumin and was delivered through diet to simulate the exposure as it occurs in humans. In practical application, holding

turmeric/curcumin diet in the mouth might be a convenient and economical method of sustained delivery of turmeric/curcumin to the oral cavity, as it increases the bioavailability as well as contact time of chemopreventive agents. In the current study, we were able to explore this concept due to the feeding habit of hamsters; the diet was mixed with turmeric (1%) and fed to animals after tumor development. This provides a good opportunity for studying effects of even the weakest of chemopreventive agents without compromising with the route of administration during clinical trials.

Exposure to turmeric for 2, 3 and 4 weeks resulted in decrease in tumor burden except in experiment no 3 in which no significant decrease was observed, despite a 56% decrease in total tumor volume. This result may have been due to larger variation in tumor volume at the time of randomization. Post-treatment with dietary turmeric for 2, 3, and 4 weeks also decreases the tumor multiplicity in HBP tumors. Higher tumor multiplicity was observed in experiment 4, where DMBA was applied using paint brush as compared to experiment 1-3 in which a pipette was used to topically treat the buccal pouches of hamsters. In case of pipette application, the carcinogen becomes concentrated in certain area or pockets, leading to restricted exposure and toxicity. In the paintbrush application, the uniform spread of carcinogen in larger area of buccal pouch results in relatively more initiated cells and less toxicity with similar range of tumor volume. In addition, the reduction in HBP tumor burden and multiplicity with dietary turmeric was mainly due to a reduction in the number of newly developed small tumors, with less effect on large tumors. Although the effects of turmeric or other polyphenols post-treatment have not been reported in immunocompetent mice bearing primary tumors, effects of a few polyphenols have been evaluated after tumor development in nude/immunocompromised mice bearing transplanted tumors. In these studies, deceases in tumor growth compared to respective controls have been reported at 2, 3, and 4 week of exposure [191-193]. Though the bioavailability of chemopreventive agents when administered orally is likely to be less in comparison to i.p. administration, observed decreases in tumor growth after dietary turmeric dosage appears to be similar. A similar decrease in tumor size was also observed after i.p. administration of resveratrol. Because there are no such reports on curcumin applied after tumor development, we also compared our results with reports in which chemopreventive agents were administered prior to, during, and after the carcinogen treatment, and the direction of changes was similar [52,97,133,182,194]. Li *et al.* (2002) showed that curcumin (10 mmol applied topically, 3 times/week for 18 weeks) and/or tea (6 mg tea solids/ml given through

drinking water, 3 times/week for 18 weeks) decreased the DMBA-induced HBP tumors (0.5%, 3 times/week for 6 weeks), when given alone or in combination after carcinogen treatment and continued until the end of the experiment [133]. The decrease in tumor burden and tumor multiplicity of HBP tumors in the present study suggests that dietary turmeric post-treatment inhibited the growth of tumors in oral mucosa. The observed decrease in tumor growth is likely due to the modulation of cellular pathways associated with cell proliferation and/or apoptosis and/or inflammation by dietary turmeric. Although exposure to 1% dietary turmeric for 2, 3, and 4 weeks resulted in a significant decrease in tumor growth, enhanced decrease in tumor growth related to exposure duration 2 vs. 3 and 4 weeks and at 3 vs. 4 weeks was not observed. This probably suggests that an extended exposure to dietary turmeric did not further enhance tumor growth inhibition or that the experimental conditions were such that smaller differences, if present, could not be discerned. The observed growth inhibition of tumor may have occurred due to enhanced apoptosis or decreased cell proliferation or both. Bax, a pro-apoptotic protein, and Bcl-2, an anti-apoptotic protein, are important markers for apoptosis. Over expression of Bcl-2, a key event in malignant transformation has been reported to be associated with down-regulation of Bax [195]. To our knowledge, literature on other polyphenols-related biochemical parameters after tumor development in primary tumors is not readily available. Increase in Bax and decrease in DMBA-induced Bcl-2 levels with turmeric treatment accounts for the observed higher Bax/Bcl-2 ratio and the apoptotic index. These result suggest protection against DMBA-induced HBP tumors by augmenting apoptosis, as reported in transplantable tumors and/or immuno compromised/nude mice, although with other polyphenols [191,196-198]. These results suggest that Bcl-2 inhibits apoptosis and enhances viability of cells by preventing mitochondrial release of cytochrome c eventually resulting in inhibition of caspase activity that executes the cell death program [199]. The cell death pathways eventually result in the proteolytic activation of caspase-3 and -9, effector caspases that cleave proteins essential for cell survival. The results of the present study also provide evidence for apoptosis induction by turmeric treatment as revealed by decreased levels of survivin, p21 and p53 as reported with other polyphenols in a mouse xenograft model [200]. In this study, decreased expression of Bcl-2 and survivin with turmeric was associated with enhanced expression of cytochrome c, caspase-9 and caspase-3 in DMBA-induced HBP tumors. These results are similar to those observed with different polyphenols in xenografts grown in nude mice, which facilitated the evasion of apoptosis in HBP

carcinomas [193,201,202]. The present study clearly demonstrates that apoptosis may be one of the mechanisms by which dietary turmeric inhibits tumor growth through a mitochondria-mediated, caspase-dependent apoptotic pathway.

The observed decrease in apoptosis and up-regulation of PCNA and cyclin D1 in DMBA-induced HBP tumors is in line with the earlier reports in which levels of PCNA-positive cells increased progressively through oral malignant epithelium and were more concentrated in the oral SCC [203,204].Significant decreases in PCNA were observed at both the time points, irrespective of continuation of carcinogen treatment, while cyclin D1 levels decreased at week 12 but not at week 16. This probably suggests differences in the mechanisms of alteration of cyclin D1 and PCNA [205]. However, the observed turmeric-mediated decrease in cell proliferation markers in tumor-bearing animals showed same direction of results as observed with gallic acid (0.3 or 1%) or resveratrol or grape seed polyphenols in xenografts grown in nude mice [197,201,206].

Inflammation is one of the early events occurring in HBP SCC. The observed decrease in DMBA-induced cox-2 protein with turmeric in HBP tumors is in agreement with reports of a nude mouse xenograft model in which EGCG, combinations of curcumin, EGCG and lovastatin as well as lycopene suppressed the expression of cox-2 and PGE-2 [200,207]. A decrease in turmeric-mediated defense against DMBA-induced inflammation (levels of cox-2 and PGE-2) was observed only up to week 12 and not at week 16, possibly due to continuation of carcinogen treatment. Turmeric is a cox-2 inhibitor; this can be inferred from our observations which are consistent with those of Li et al. (2005), in which cox-2 inhibitors were found to inhibit PGE-2 biosynthesis [208]. Curcumin has been shown to be an indirect inhibitor of cox-2 [209]. Control of cox-2 induction involves a complex array of regulatory factors including NF-κB and AP-1 transcription factors [189]. Effects of dietary turmeric post-treatment on DMBA-mediated NF-κB transactivation by inhibition of IKK and phosphorylation of IκB-α were similar to those observed after curcumin pre-treatment in mouse skin [188]. Furthermore, AP-1 transcription factor has been shown to be a critical regulator of cox-2 expression in many cell lines. The observed decrease in DMBA-induced proto-oncogene (c-jun and c-fos) levels in HBP tumors upon dietary turmeric is an agreement with our previous reports in which exposure to dietary turmeric was given prior to, along with, or subsequent to DMBA-treatment [182]. Our results are also in agreement with other studies in which curcumin has been shown to inhibit the transcriptional regulators of c-jun, c-fos and/or NF-κB *in-vitro* (cancer cell lines) and *in-vivo* (DEN-treated rat liver, TPA-treated mouse

skin) and in xenografts from human medulloblastoma cell lines [210]. Altogether, it is plausible that turmeric inhibits cox-2 expression by inactivating transcription factors such as NF-κB and AP-1 in HBP tumors.

One of the most extensively investigated intracellular signaling cascades involved in pro-inflammatory responses is the MAPK pathway. Our data supports the hypothesis that turmeric inhibits cox-2 expression in DMBA-induced HBP tumors, possibly by blocking downstream proto-oncogenes (c-jun, c-fos) and NF-κB activation, which is further regulated by MAPK signalling cascade [188]. Parameters related to cell proliferation, apoptosis, and inflammation, when evaluated by IHC, essentially showed same direction of results as observed when analyzed by quantitative western blot analyses.

Notably, although dietary turmeric post-treatment has been observed to modulate expression of several DMBA-induced molecular and biochemical markers in HBP tumors, their levels continued to be significantly different from controls. In this study, the observed effects on already developed tumors were due to turmeric and not due to withdrawal of carcinogen after tumor development. Moreover, throughout the evaluation, turmeric was found to affect the carcinogen/tumor-induced parameters without influencing their basal levels, suggesting that its effects on normal function or physiology are likely to be minimal. Therefore, toxicity and/or related problems may be avoided.

Because the absorption levels of curcumin in the body are very low; it may be necessary to consistently consume turmeric in the diet on a regular basis, especially during or after carcinogen exposure, for its protective effects to be observed. The strength of this study in showing the modulatory effect(s) of turmeric would have been enhanced if circulating levels of curcumin and/or its metabolites were measured in exposed animals. In the present study, an ideal evaluation should have included comparison with an established anti-cancer agent. However, that was not done or intended and curcumin is not expected to compete with established anti-cancer agent(s). Notably, the effects observed in HBP may not be observed in internal organs like liver, lung, kidney etc. after tumor development since the bioavailability of curcumin is low, whereas in this study, the feeding habit of hamsters (i.e. storing food in the cheek pouch) increases the direct contact time as well as bioavailability of turmeric. The study was however, carried out for only 4 weeks after tumor development because an increase of tumor size and aggressiveness would hinder the caloric/food intake, thereby reducing the availability of turmeric and/or inhibiting tumor growth.

Our studies indicate that turmeric possess chemotherapeutic effects to some extent. Considering limited effects on tumor burden and multiplicity, curcumin cannot replace established anti-cancer agents, but it may be helpful in reducing toxicity and enhancing efficacy of established chemotherapeutic agent(s) when administered in combination. In addition to chemopreventive effects, additional ability of curcumin to reducing toxicity following chemotherapy has also been reported. The use of such a combination however needs to be evaluated in an animal experimental system before it is used in humans.

In conclusion, the results of the present study provide evidence for apoptosis induction in HBP SCC tumor tissue by dietary turmeric post-treatment as revealed by increased Bax/Bcl-2 ratio and apoptotic index. Along with this, decreased cell proliferation has also been shown. Our finding also suggests that dietary turmeric inhibits DMBA-induced cell inflammation markers (cox-2 and PGE-2) by blocking the MAPK and NF-κB signalling cascade, which may provide molecular basis for suppression of tumor promotion (through apoptosis and cell proliferation) in DMBA-induced HBP tumors.

6.1 INTRODUCTION

Polycyclic aromatic hydrocarbons (PAHs) are ubiquitous environmental agents, many of which have been identified as toxic, mutagenic and/or potent human carcinogens [211,212]. PAHs occur widely in the environment as a result of incomplete combustion of fossil fuels and other organic matter, and human exposure to PAHs is therefore unavoidable [213]. Humans are exposed to complex mixtures of PAHs which have been implicated in inducing skin, lungs and breast cancer. Benzo(a)pyrene, a well- known ubiquitous carcinogen belonging to the PAHs group of compounds, is metabolically activated by phase I enzymes (or CYP1A class of cytochrome P450 (CYP450) enzymes) to form a highly mutagenic reactive electrophile, benzo(a)pyrenediol-epoxide (BPDE). Though phase II enzymes catalyze the detoxification of BPDE, some of the reactive electrophiles interact covalently with DNA to form adducts that mark the early initiation event. Unrepaired/misrepaired adducts lead to mutation in genes involved in proliferation, growth and apoptosis and finally to a disease condition such as cancer [214].

Plant-derived natural compounds are receiving increasing attention as chemopreventives because of their low toxicity and high tolerability. The efficacy of polyphenols has been established when administered before or after the carcinogen treatment and have been shown to modulate carcinogen-induced incidence/multiplicity/latency period of tumor development [9].Curcumin/turmeric has been shown to possess chemopreventive activity at both initiation and promotion stages of chemical-induced carcinogenesis [97,128,134,186,215]. Earlier studies have shown that dietary curcumin pre-treatment decreases the formation of B(a)P-derived DNA adducts in mouse tissues by inhibiting carcinogen-induced phase I enzymes and directly inducing phase II enzymes [134]. Effects of turmeric/curcumin after exposure to carcinogen on the repair or disappearance of adducts, if any, are not known. Hence, in the present study effect of curcumin post-treatment, if any, on the disappearance of BPDE-DNA adducts in tissues of mice have been evaluated. Herein, the study demonstrates that dietary curcumin treatment subsequent to B(a)P exposure enhanced the disappearance of BPDE-DNA adducts, judged by the decrease in the levels of BPDE-DNA adducts. This could probably be due to the curcumin-mediated enhancement of apoptosis of DNA adduct-containing cells and/or repair of DNA-adducts in mouse tissues.

6.2 METHODS

6.2.1 Animal treatment

Six to eight-week old inbred male Swiss albino mice (Generation used 11-18th, Animal house, ACTREC, India) received control/experimental diet and plain drinking water *ad libitum* during the experimental period. Two different sets of experiments (1 and 2) were conducted at different times. Initially, corn oil (0.1 ml, V group) or B(a)P (1 mg in 0.1 ml corn oil, BP group) was administered by gavage to all animals that were maintained on standard laboratory diet (Fig. 6.1). After 24 h of corn oil or B(a)P administration, mice were randomized into seven subgroups. One of the subgroups (from both the groups V and BP) was sacrificed at 24 h time point [subgroups $V_{(+24h)}$ and $BP_{(+24h)}$] whereas half of the 6 subgroups (from both the groups) were continued on the powdered control diet (standard laboratory diet) and the other half were shifted to powdered experimental diet (0.05% curcumin in standard laboratory diet) prepared as described [110]. In experiment 1, mice shifted to control/experimental diets were sacrificed after 24, 72 and 120 h [$BP_{(+48h)}$, $BP_{(+96h)}$, $BP_{(+144h)}$ (control diet)/ $BP_{(+48h)}$ + C 24h, $BP_{(+96h)}$ + C 72h, $BP_{(+144h)}$ + C 120h (experimental diet)]; whereas in experiment 2, they were sacrificed after 7, 14 and 28 days [$BP_{(+8d)}$, $BP_{(+15d)}$, $BP_{(+29d)}$ (control diet) / $BP_{(+8d)}$ + C 7d, $BP_{(+15d)}$ + C 14d, $BP_{(+29d)}$ + C 28d (experimental diet)]. Both the experiments 1 and 2 had independent $V_{(+24h)}$ and $BP_{(+24h)}$ groups. Animals in all subgroups were observed for any apparent signs of toxicity such as weight loss or mortality during the entire study period. Their liver and lungs were perfused and excised, and a part of liver/lungs tissue were fixed in 10% buffered formalin for histopathological evaluation and immunohistochemical staining, while the rest of the tissues were snap frozen in liquid nitrogen and stored at -80 °C until preparation of extract. The experimental conditions i.e. dose, route of B(a)P administration, sacrifice time, dose and route of curcumin exposure employed in the present study were chosen on the basis of our earlier studies demonstrating the effect of curcumin on the formation of BPDE-DNA adducts in mouse liver and lungs[186,216].

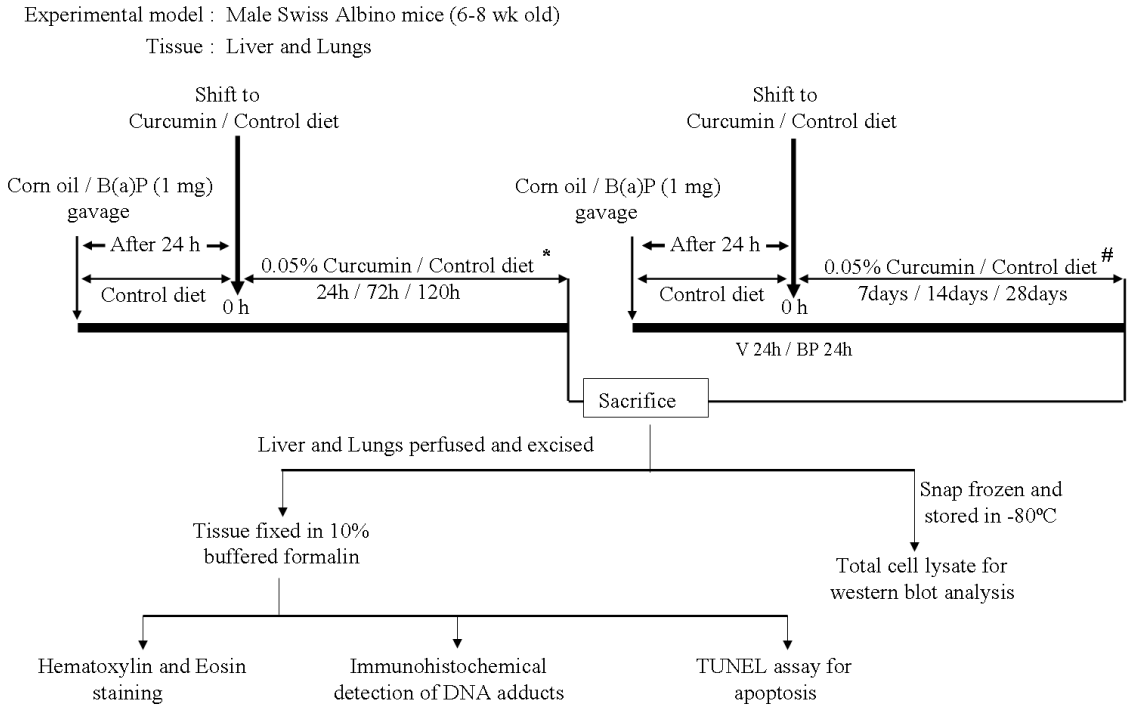

* Corn oil (V, vehicle treated group) - Control diet treated subgroups [$V_{(+24h)}$, $V_{(+48h)}$, $V_{(+96h)}$, $V_{(+144h)}$], Curcumin diet treated subgroups ($V_{(+48h)}$ + C 24h, $V_{(+96h)}$ + C 72h, $V_{(+144h)}$ + C 120h)
B(a)P treated group (BP group) - Control diet subgroups [$BP_{(+24h)}$, $BP_{(+48h)}$, $BP_{(+96h)}$, $BP_{(+144h)}$], Curcumin diet treated subgroups ($BP_{(+48h)}$ + C 24h, $BP_{(+96h)}$ + C 72h, $BP_{(+144h)}$ + C 120h)

# Corn oil (V, vehicle treated group) - Control diet treated subgroups ($V_{(+24h)}$, $V_{(+8d)}$, $V_{(+15d)}$, and $V_{(+29d)}$], Curcumin diet treated subgroups ($V_{(+8d)}$ + C 7d, $V_{(+15d)}$ + C 14d, and $V_{(+29d)}$+ C 28d)
B(a)P treated group (BP group) - Control diet treated subgroups [$BP_{(+24h)}$, $BP_{(+8d)}$, $BP_{(+15d)}$, $BP_{(+29d)}$], Curcumin diet treated subgroups ($BP_{(+8d)}$ + C7d, $BP_{(+15d)}$ + C14d, $BP_{(+29d)}$ + C28d)

FIGURE 6.1: Experimental design for studying the effect of curcumin post-treatment on disappearance of BPDE-DNA adducts in mouse tissues.

6.2.2 Protein immunoblotting

Total cell extracts from mouse liver and lungs were prepared by a previously described cell fractionation procedure [138] presented in Materials and methods (Chapter 3; section 3.4.1 and 3.4.2). The expressions of various proteins in different lysates were studied by SDS-PAGE followed by immunoblotting as described in Materials and methods (Chapter 3; section 3.6). All primary and secondary antibodies were first standardized for their dilutions and then used accordingly. β-actin was used as loading control. Densitometry of various analyte proteins and their respective loading controls from the same blot was performed using Image J 1.43 (NIH) software as described in Materials and methods (Chapter 3; section 3.6.5).

Protein	% gel	Amount of protein	Primary antibody dilution	Secondary antibody dilution
Bax	12%	Total cell lysate, 50 µg	1:1000	1:5000
Bcl-2	12%	″	1:1000	1:5000
Caspase-3	12%	″	1:2000	1:5000
PCNA	10%	″	1:1000	1:4000
Cyclin D1	10%	″	1:500	1:4000
β-actin	Loading controls (same blots were stripped)		1:2000	1:6000

6.2.3 Measurement of BPDE-DNA adducts

The interaction of BPDE with DNA was studied by immunohistochemical staining using monoclonal antibody recognizing BPDE-DNA adducts as described [217]. The formalin-fixed, paraffin embedded 5 µm tissue sections (on poly L-lysine coated slides) were deparaffinised using two successive changes of xylene for 15 min each and then immersing the slides in xylene + alcohol (in equal ratio) for 10 min. Rehydration of tissue sections was performed by sequential incubations for 5 min each in absolute ethanol, 95% and 70% ethanol. Sections were washed successively with tap water, ditilled water (D/W) and 1X phosphate buffer saline (PBS) (9.1 mM Na_2HPO_4, 1.4 mM KH_2PO_4, 2.6 mM KCl, and 135 mM NaCl, pH 7.4) for 5 min each. Sections were incubated for 1 h at 37 °C in a humidified chamber with RNase (100 µg/ml) in Tris buffer (8.1 mM Tris base, 1 mM EDTA, 0.4 M NaCl, pH 7.5). Sections were thenwashed with 1X PBS, treated with proteinase K in Tris buffer (10 µg/ml) at room temperature (RT) for 7 min and washed with 1X PBS. To denature the DNA, slides were incubated with 4 N HCl for 7 min at RT and then neutralized with 50 mM Tris base for 5 min at RT. After washing the slides with 1X PBS, non-specific binding was blocked by incubating sections with 3% normal horse serum (prepared in PBS) at 37 °C for 1 h in a humidified chamber. Sections were then incubated with anti BPDE-DNA monoclonal antibody clone 5D11 (1:30 dilution) overnight at 4 °C. For each reaction, a negative control was included by replacing the addition of primary antibody with PBS buffer on one of the sections on the same slide. Next day, after washing twice with PBS for 5 min each, slides were incubated with biotinylated anti-mouse secondary antibody for 30 min at 37 °C for 1 h in a humidified chamber. Following washing of the sections twice with 1X PBS (5 min each), endogenous peroxidase was blocked by treating the slides with 3% H_2O_2 in methanol for 30 min at RT in dark. To remove excess of methanol, sections were washed thrice with 1X PBS for 5 min each and then, incubated with Avidin-Biotin Complex (ABC) reagent

(from Vectastain Elite kit) for 30 min at 37 °C in a humidified chamber. The slides were rinsed with 1% Triton-X 100 (prepared in PBS), thrice for 30 sec. After washing with PBS, sections were stained with diaminobenzidine (DAB) solution (8 mg DAB in 10 ml D/W + 10 µl H_2O_2), till visible brown coloration appear on the sections. The slides were washed immediately with water, counterstained with haematoxylin and washed with tap water. Slides were dehydrated, cleared in serial ethanols and xylenes and cover slips mounted with D.P.X. Images were captured with Zeiss Microscope (Imager Z1) to which an Axiocam MRc5 digital camera was attached.Quantitative analysis of the images (magnification X 400) was performed by modified digital image analysis protocols as described previously [218].

6.2.4 Digital image analysis

IHC photomicrographs were used for developing semi-automated analysis protocol. As a first step, we used a color de-convolution plug-in to un-mix the pure DAB, and hematoxylin stained areas leaving a complimentary image. The pixel intensities of separated DAB or hematoxylin images range from 0 to 255. Value 0 represents the darkest shade of the color whereas 255 represent the lightest shade of the color in the image. In-order to select the DAB-stained (brown) nuclei, the threshold feature of the Image J 1.43 (NIH) software was used. Further to assign an automated percentage of pure DAB staining patterns in the nucleus, a macro was developed and plugged in the Image J 1.43 (NIH) software to obtain an automated counting of the pixel wise percentage contribution of high positive, medium positive and low positive pixels/intensity in an image i.e. the number of pixels of a specific intensity value vs. their respective intensity zone (Fig. 6.2). For measurement of BPDE-DNA adducts, similar area of tissue sections (mm^2) and number of cells (~800 cells/section/animal), in terms of total adduct intensity (%) as well as nuclei containing % of high, medium and low intensity due to BPDE-DNA adducts was analyzed within different treatment groups. However, apoptosis were measured in terms of total apoptotic nuclei intensity as well as % of apoptotic positive and negative cells, in similar area of tissue sections (mm^2) and number of cells (~800 cells/ section/ animal) in different treatment groups. In this method, pixel intensities were categorized into 4 zone(s) ranges from 0–60 for a score value of high positive (3+), 61–120 for medium positive (2+), 121–170 for low positive (1+). Pixels values beyond 170 were empirically analyzed and were found to be negative (0, blue stained nuclei) cells.

After determining these numbers, we applied them to a simple algebraic formula as shown below to determine the percent contribution of high positive/ medium positive/ low positive intensity. Further, the actual number of high positive, medium positive, and low positive cells were analyzed by using the formula:

$$\text{Percentage of high positive/medium positive/low positive intensity} = \frac{\text{Percentage of high positive/medium positive/low positive DAB color intensity pixels} \times \text{Score of the zone}}{\text{Total number of pixels in the image}}$$

In order to determine the total percentage intensity (of adducts containing nuclei and/or apoptotic nuclei), the following formula was used.

$$\text{Total percentage of intensity (Adduct containing cells/Apoptotic nuclei)} = \text{Percentage of (high positive intensity + medium positive intensity + low positive intensity)}$$

Quantitative analysis was performed in photomicrographs of 10 randomly selected fields per section per mouse with atleast three mice per group. More than 800 cells were counted per section per mouse.

6.2.5 Terminal deoxynucleotidyl transferase biotin-dUTP nick end labeling (TUNEL) assay

Apoptosis was assayed in formalin-fixed, paraffin-embedded 5 μm tissue sections, according to the manufacturer's instructions (*In-situ* TUNEL assay kit, Promega, Madison, WI, USA), as described in Materials and methods (Chapter 3; section 3.10). The nuclei of the apoptized cells were stained brown in color. Levels of apoptosis/apoptotic index was computed in two ways: (1) quantitative comparison of the images (magnification X 400) in terms of % intensity was done by modified digital image analysis protocols as described above (section 6.2.4, Fig. 6.2), and (2) by counting the number of positively stained cells × 100/ total number of cells in the photomicrographs of tissue sections (without taking into account the color intensity) in the same image by using cell counter plug-in of Image J 1.43 (NIH) software, of at least 10 different randomly selected fields/section/mouse with atleast three mice per group. More than 800 cells were counted per section per mouse.

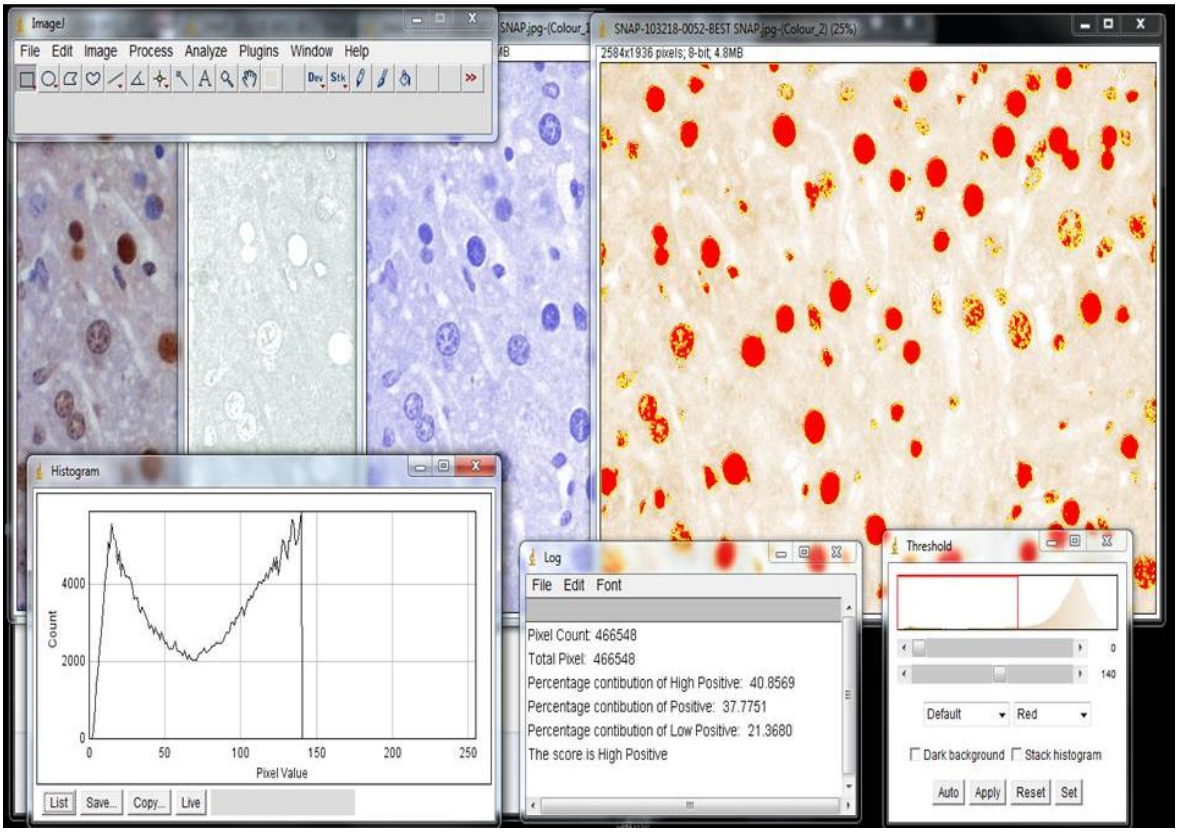

FIGURE 6.2: Representation of digital image analysis algorithm to calculate the levels of BPDE-DNA adducts and apoptotic nuclei in photomicrographs of mouse tissue sections.

6.2.6 Statistical analysis

Densitometry and quantitative analysis of images were performed using Image J 1.43 (NIH) software. Statistical analysis was performed using SPSS 15.0 software (IBM, Inc., Chicago, IL, USA) and STATA 12 software (StataCorp, Texas, USA). Data are presented as mean $\pm$ SE. Means of (western blot analysis) data were compared using ANOVA with post-hoc testing. Statistical comparisons of levels of BPDE-DNA adducts and TUNEL positivity among the groups were made using Poisson regression, which is specific for data representing counts or number of events and can handle cases where few or no events occur. $p \leq 0.05$ was considered statistically significant.

6.3 RESULTS

Based on the net body weight gain and histopathological evaluation of tissues, no toxicity or mortality was observed in animals belonging to the various treatment groups during the experimental period (Figs. 6.3 and 6.4).

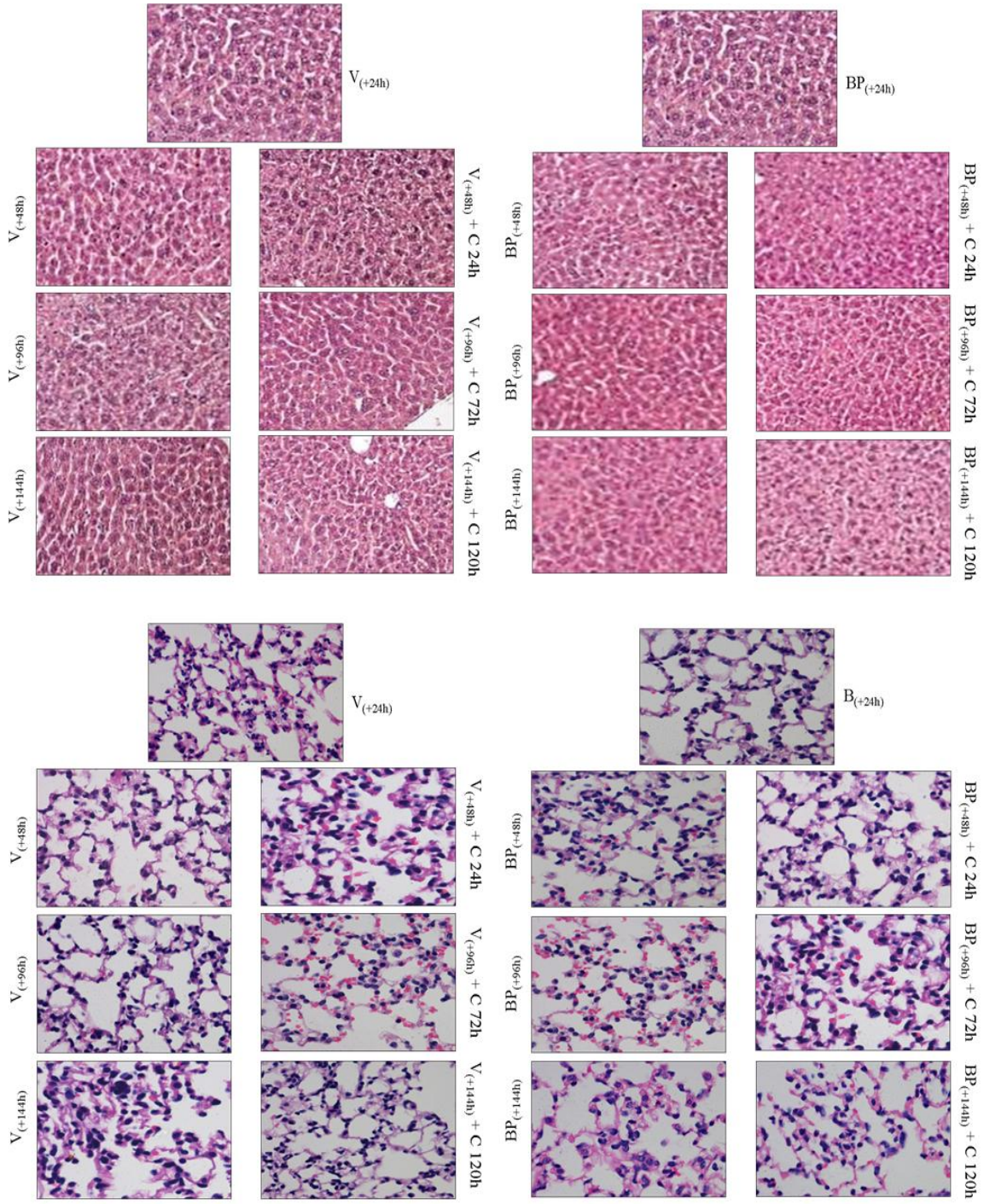

FIGURE 6.3:Effect of curcumin post-treatment on B(a)P-induced alterations in tissue of mice (Experiment 1). *Representative photomicrographs of haematoxylin and eosin (H & E) stained liver and lungs sections (magnification X 400) from mice belonging to the various treatment groups in experiment 1.*

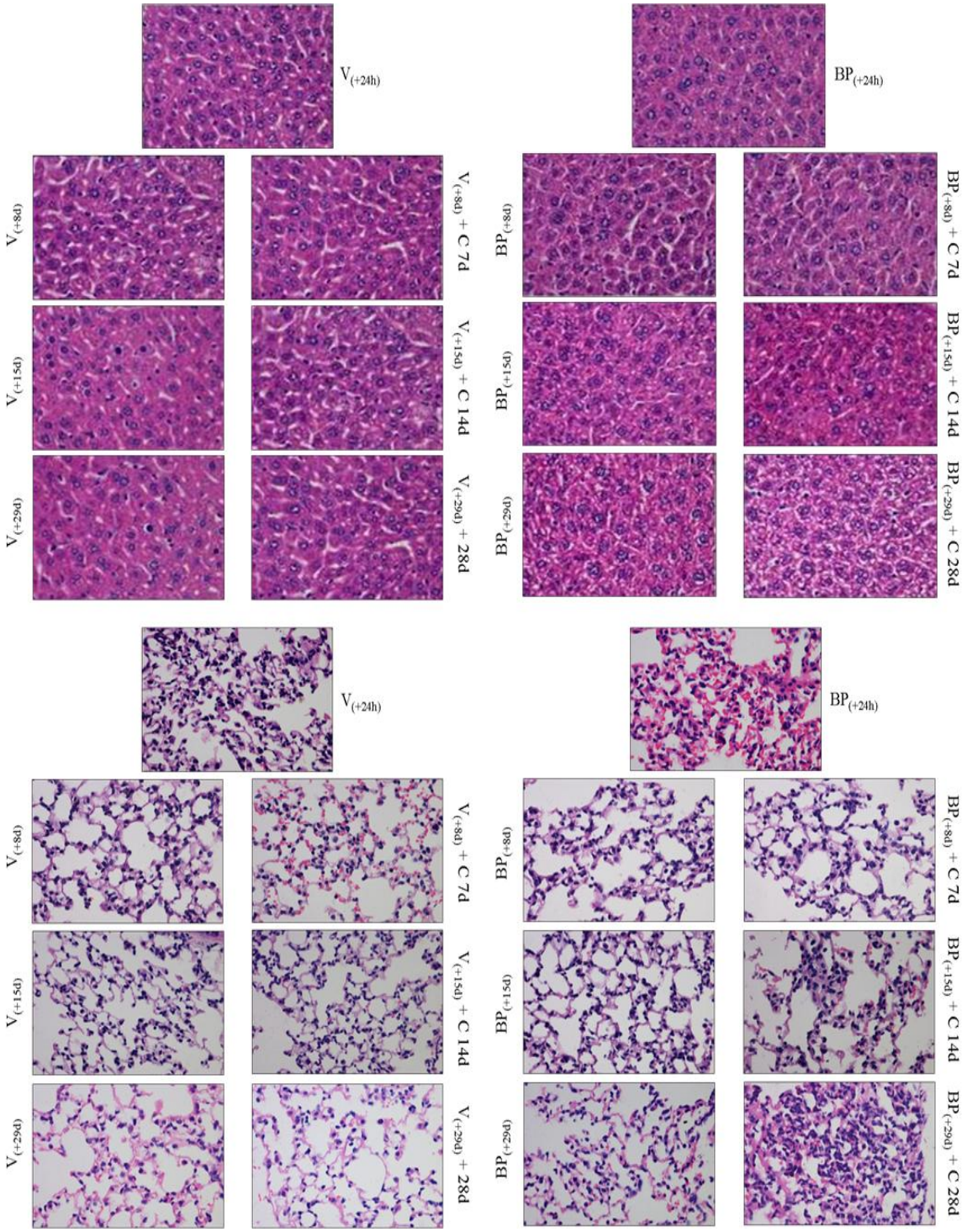

FIGURE 6.4:Effect of curcumin post-treatment on B(a)P-induced alterations in tissue of mice (Experiment 2). *Representative photomicrographs of haematoxylin and eosin (H & E) stained liver and lungs sections (magnification X 400) from mice belonging to the various treatment groups in experiment 2.*

6.3.1 Effect of dietary curcumin post-treatment on disappearance of BPDE-DNA adducts in mouse tissues

6.3.1.1 Measurement of BPDE-DNA adducts at 24, 72 and 120 h

In animals receiving vehicle [subgroups $V_{(+24h)}$, $V_{(+48h)}$, $V_{(+96h)}$, $V_{(+144h)}$] or vehicle + curcumin (subgroups $V_{(+48h)}$ + C 24h, $V_{(+96h)}$ + C 72h, $V_{(+144h)}$ + C 120h) treated groups, BPDE-DNA adducts were not detected in liver and lungs of mice, while detectable levels of BPDE-DNA adduct(s) were observed by immunohistochemical staining following 24 h of B(a)P administration in these tissues (subgroup $BP_{(+24h)}$, maintained on standard laboratory diet) (Figs. 6.5 and 6.6) as reported [186,216], suggesting specificity of reagent (antibody) and demonstrating major difference in the levels of BPDE-DNA adducts between exposed and non-exposed animals/tissues. Levels of BPDE-DNA adducts were measured in similar area of tissue sections (mm^2) and number of cells (~800 cells/section/animal), in terms of total adduct intensity as well as nuclei containing % of high, medium and low intensity due to BPDE-DNA adducts. It was observed that with passage of time, mice on control diet for 24, 72 and 120 h [subgroups $BP_{(+48h)}$, $BP_{(+96h)}$, $BP_{(+144h)}$] showed a time-related significant decrease in total adduct(s) intensity (levels) in liver and lungs of mice when compared to the levels in subgroup $BP_{(+24h)}$ and subgroup of preceding or following time point (Figs. 6.5, 6.6, 6.9A and 6.9B). Interestingly, mice that were shifted to 0.05% curcumin diet and sacrificed at 24, 72 and 120 h (subgroups $BP_{(+48h)}$ + C 24h, $BP_{(+96h)}$ + C 72h, $BP_{(+144h)}$ + C 120h), showed significantly higher decrease in levels of adducts (intensity) in liver and lungs of mice, when compared to $BP_{(+24h)}$ as well as respective time-matched controls [subgroups $BP_{(+48h)}$, $BP_{(+96h)}$, $BP_{(+144h)}$] (Figs. 6.5, 6.6, 6.9A and 6.9B). This decrease was also evident when comparison of % intensity of nuclei containing high, medium and low levels of adducts was made, between curcumin treated and respective time-matched controls. In liver, the observed decrease in total adduct intensity in B(a)P-treated [subgroups $BP_{(+48h)}$, $BP_{(+96h)}$, $BP_{(+144h)}$] as well as B(a)P + curcumin (subgroups $BP_{(+48h)}$ + C 24h, $BP_{(+96h)}$ + C 72h, $BP_{(+144h)}$ + C 120h) appears to be contributed mainly by reduction in % intensity of nuclei containing high and medium levels of adducts while in lungs, it was due to decrease in nuclei containing high levels of adducts both in B(a)P [subgroups $BP_{(+48h)}$, $BP_{(+96h)}$, $BP_{(+144h)}$] as well as B(a)P + curcumin treated groups (subgroups $BP_{(+48h)}$ + C 24h, $BP_{(+96h)}$ + C 72h, $BP_{(+144h)}$ + C 120h) (Figs. 6.5 and 6.6). It is to note that % intensity of nuclei containing low levels of adducts remained similar in all the subgroups i.e. animals

given B(a)P [subgroups $BP_{(+24h)}$, $BP_{(+48h)}$, $BP_{(+96h)}$, $BP_{(+144h)}$] and B(a)P + curcumin (subgroups $BP_{(+48h)}$ + C 24h, $BP_{(+96h)}$ + C 72h, $BP_{(+144h)}$ + C 120h) (Figs. 6.5 and 6.6). Together, results suggest that dietary curcumin led to enhanced decrease in nuclei containing high and medium levels of adducts in liver, whereas in lungs curcumin-mediated enhanced decrease was mainly observed in nuclei containing high levels of adduct(s).

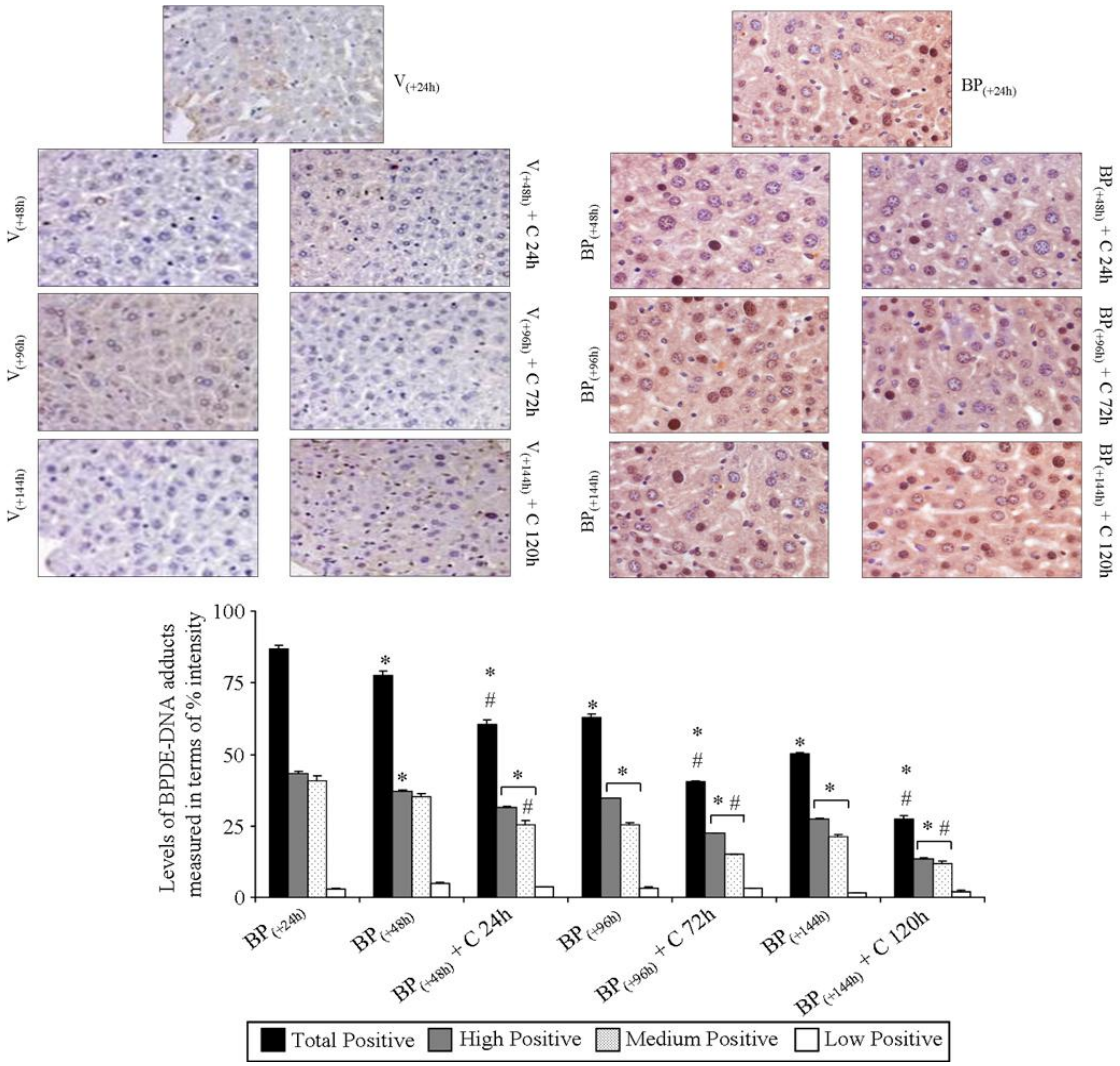

FIGURE 6.5: Effect of curcumin post-treatment on levels of BPDE-DNA adducts in mouse liver (Experiment 1). *Representative photomicrographs showing immunohistochemical detection of BPDE-DNA adduct(s) levels (magnification X 400)in formalin-fixed, paraffin-embedded tissue sections of mouse liver, using a monoclonal antibody specifically recognizing BPDE-DNA adducts. Quantitative analysis was done by digital image analysis as described under Materials and methods (section 6.2.4) in photomicrographs of 10 randomly selected fields/ section/ mouse, with atleast three mice per group. Data represent mean ± SE of three observations. Differences among groups were determined by Poisson regression analysis ($p \leq 0.05$) using STATA 12 software. '*' significant when compared with $BP_{(+24h)}$ subgroup; '#' significant when compared with respective time matched controls.*

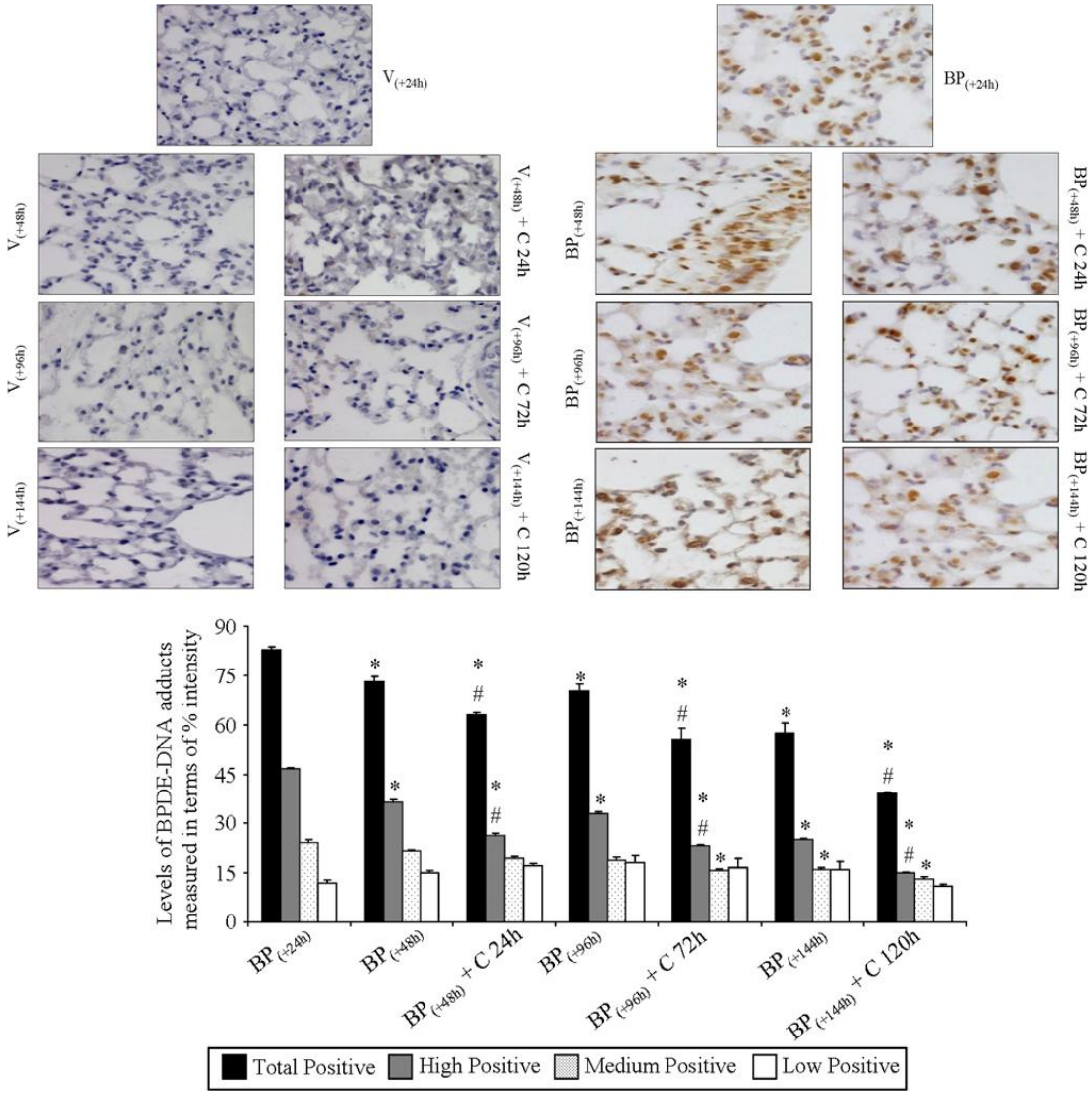

FIGURE 6.6: Effect of curcumin post-treatment on levels of BPDE-DNA adducts in mouse lungs (Experiment 1). *Representative photomicrographs showing immunohistochemical detection of BPDE-DNA adduct(s) levels (magnification X 400)in formalin-fixed, paraffin-embedded tissue sections of mouse lungs, using a monoclonal antibody specifically recognizing BPDE-DNA adducts. Quantitative analysis was done by digital image analysis as described under Materials and methods (section 6.2.4) in photomicrographs of 10 randomly selected fields/section/ mouse, with atleast three mice per group. Data represent mean ± SE of three observations. Differences among groups were determined by Poisson regression analysis ($p \leq 0.05$) using STATA 12 software. '∗' significant when compared with $BP_{(+24h)}$ subgroup; '#' significant when compared with respective time matched controls.*

6.3.1.2 Measurement of BPDE-DNA adducts at 7, 14 and 28 days

As observed in experiment 1, levels of BPDE-DNA adducts were not detected in vehicle [subgroups $V_{(+24h)}$, $V_{(+8d)}$, $V_{(+15d)}$, $V_{(+29d)}$] or vehicle + curcumin (subgroups $V_{(+8d)}$ + C 7d, $V_{(+15d)}$ + C 14d, $V_{(+29d)}$ + C 28d) treated groups in liver and lungs of mice, while detectable levels of BPDE-DNA adducts were observed (stained nuclei) following 24 h of single dose of B(a)P in liver and lungs of mice (Figs. 6.7 and 6.8). Significant differences were not observed in subgroups $V_{(+24h)}$ and$BP_{(+24h)}$ in two different sets of experiments conducted at different times. As observed in experiment 1, mice on control diet for 7, 14 and 28 days [subgroups $BP_{(+8d)}$, $BP_{(+15d)}$, $BP_{(+29d)}$] showed a time-related significant decrease in total adduct levels as seen by adduct intensity in liver and lungs of mice when compared to subgroup $BP_{(+24h)}$ as well as subgroup of preceding or following time point. Interestingly, mice that were shifted to 0.05% curcumin diet and sacrificed at 7, 14 and 28 days (subgroups $BP_{(+8d)}$ + C7d, $BP_{(+15d)}$ + C14d, $BP_{(+29d)}$ + C28d), showed significantly higher decrease in total levels of adduct intensity in liver and lungs of mice, when compared to $BP_{(+24h)}$ and respective time-matched controls [subgroups $BP_{(+8d)}$, $BP_{(+15d)}$, $BP_{(+29d)}$] (Figs. 6.7, 6.8, 6.9C and 6.9D). This decrease was also evident when comparison of % intensity of nuclei containing high, medium and low levels of adducts was made, between curcumin treated and time-matched controls. In liver, the observed decrease in total adduct intensity appears to be contributed mainly by reduction in % intensity of nuclei containing high and low levels of adducts, whereas in lungs, it was mainly due to decrease in intensity of nuclei containing high levels of adducts in mice shifted to 0.05% curcumin diet and sacrificed at 7, 14 and 28 days (subgroups $BP_{(+8d)}$ + C7d, $BP_{(+15d)}$ + C14d, $BP_{(+29d)}$ + C28d), when compared to $BP_{(+24h)}$ and respective time-matched controls [subgroups $BP_{(+8d)}$, $BP_{(+15d)}$, $BP_{(+29d)}$] (Figs. 6.7 and 6.8). Results suggest that dietary curcumin further enhanced the decrease in total adduct intensity in liver and lungs of mice, although the extent of decrease varied.

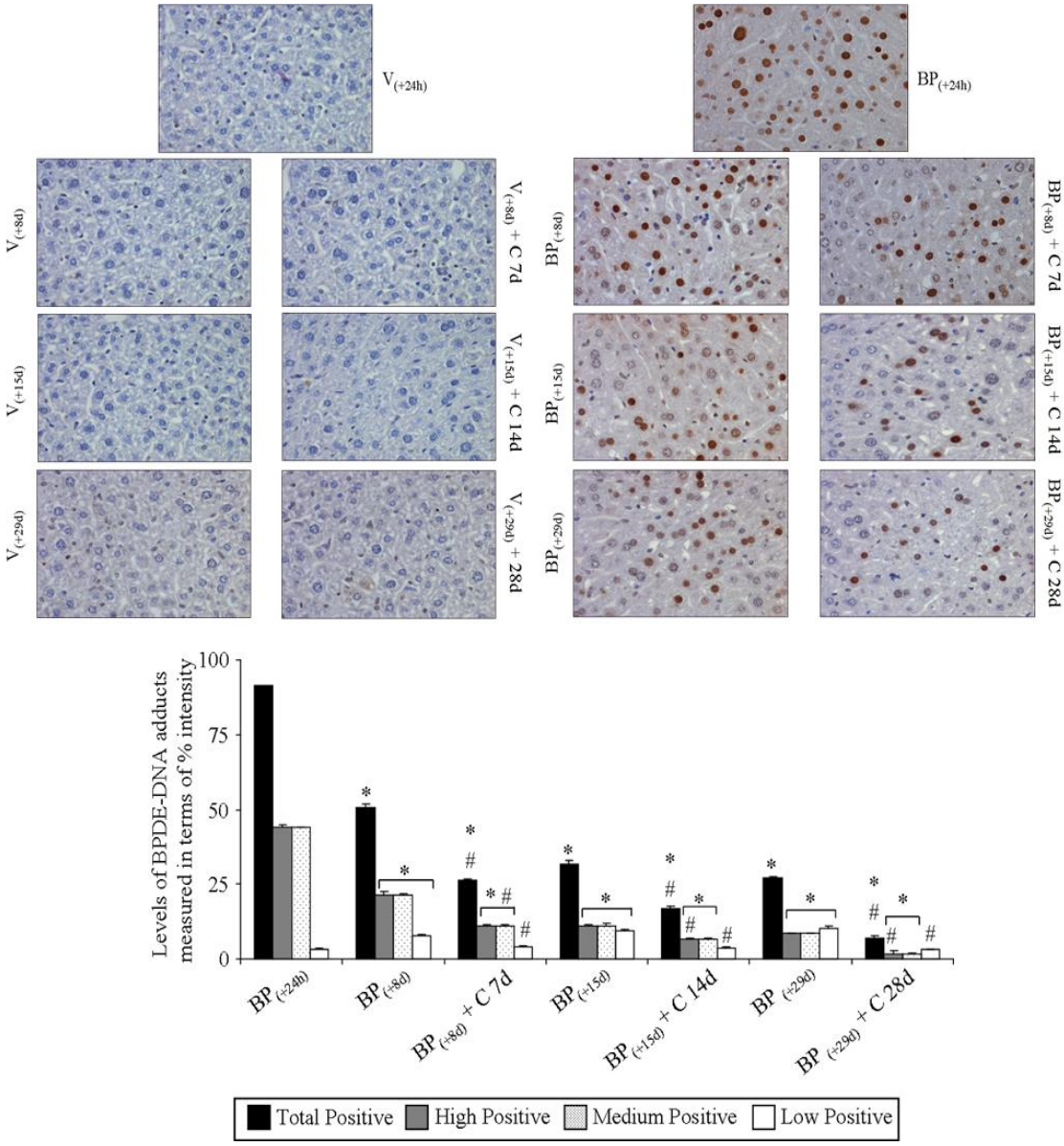

FIGURE 6.7: Effect of curcumin post-treatment on levels of BPDE-DNA adducts in mouse liver (Experiment 2). *Representative photomicrographs showing immunohistochemical detection of BPDE-DNA adduct(s) levels (magnification X 400)in formalin-fixed, paraffin-embedded tissue sections of mouse liver, using a monoclonal antibody specifically recognizing BPDE-DNA adducts. Quantitative analysis was done by digital image analysis as described under Materials and methods (section 6.2.4) in photomicrographs of 10 randomly selected fields/section/ mouse, with atleast three mice per group. Data represent mean ± SE of three observations. Differences among groups were determined by Poisson regression analysis ($p \leq 0.05$) using STATA 12 software. '∗' significant when compared with $BP_{(+24h)}$ subgroup; '#' significant when compared with respective time matched controls.*

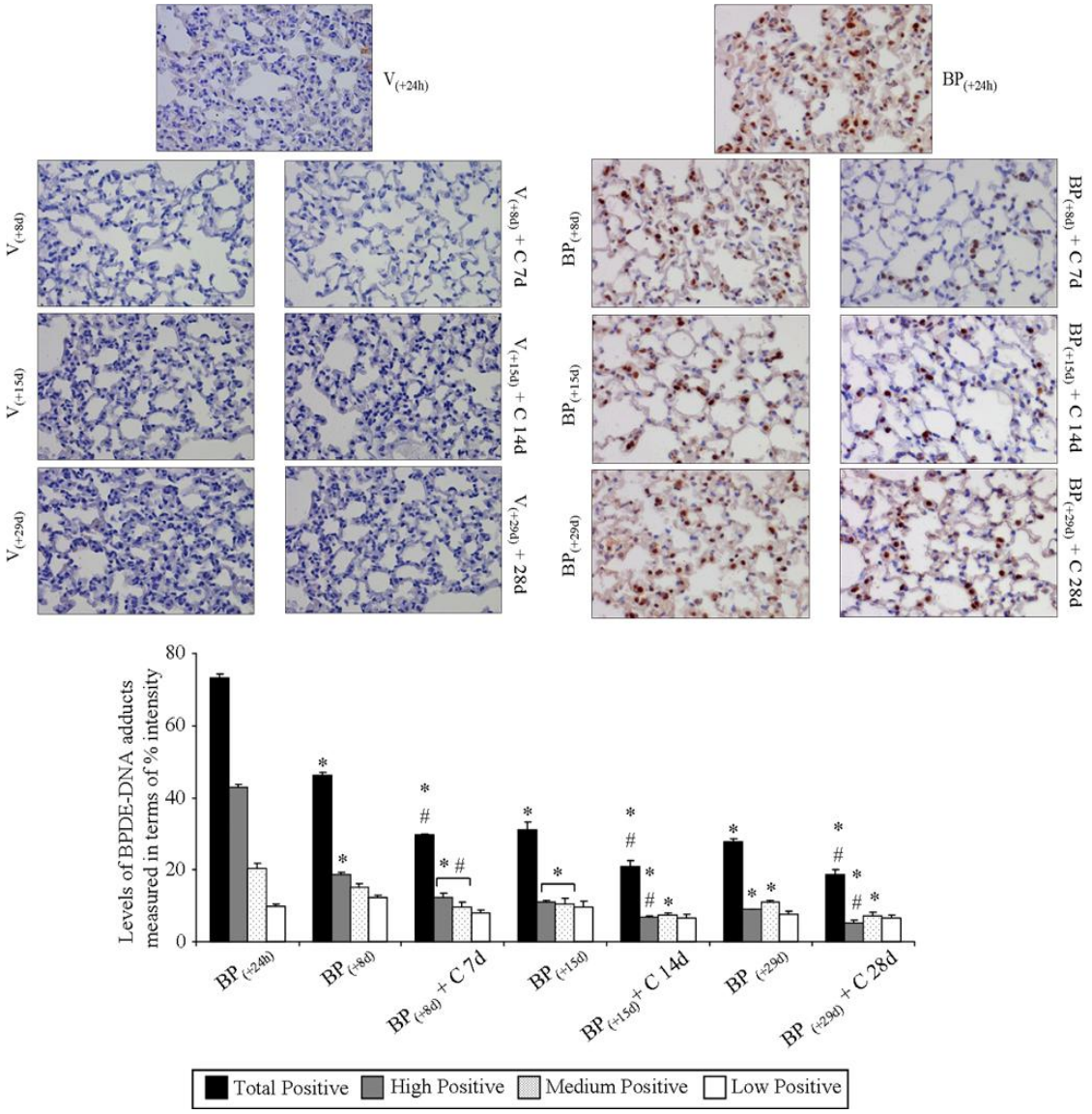

FIGURE 6.8: Effect of curcumin post-treatment on levels of BPDE-DNA adducts in mouse lungs (Experiment 2). *Representative photomicrographs showing immunohistochemical detection of BPDE-DNA adduct(s) levels (magnification X 400)in formalin-fixed, paraffin-embedded tissue sections of mouse lungs, using a monoclonal antibody specifically recognizing BPDE-DNA adducts. Quantitative analysis was done by digital image analysis as described under Materials and methods (section 6.2.4) in photomicrographs of 10 randomly selected fields/section/ mouse, with atleast three mice per group. Data represent mean ± SE of three observations. Differences among groups were determined by Poisson regression analysis ($p \leq 0.05$) using STATA 12 software. '∗' significant when compared with $BP_{(+24h)}$ subgroup; '#' significant when compared with respective time matched controls.*

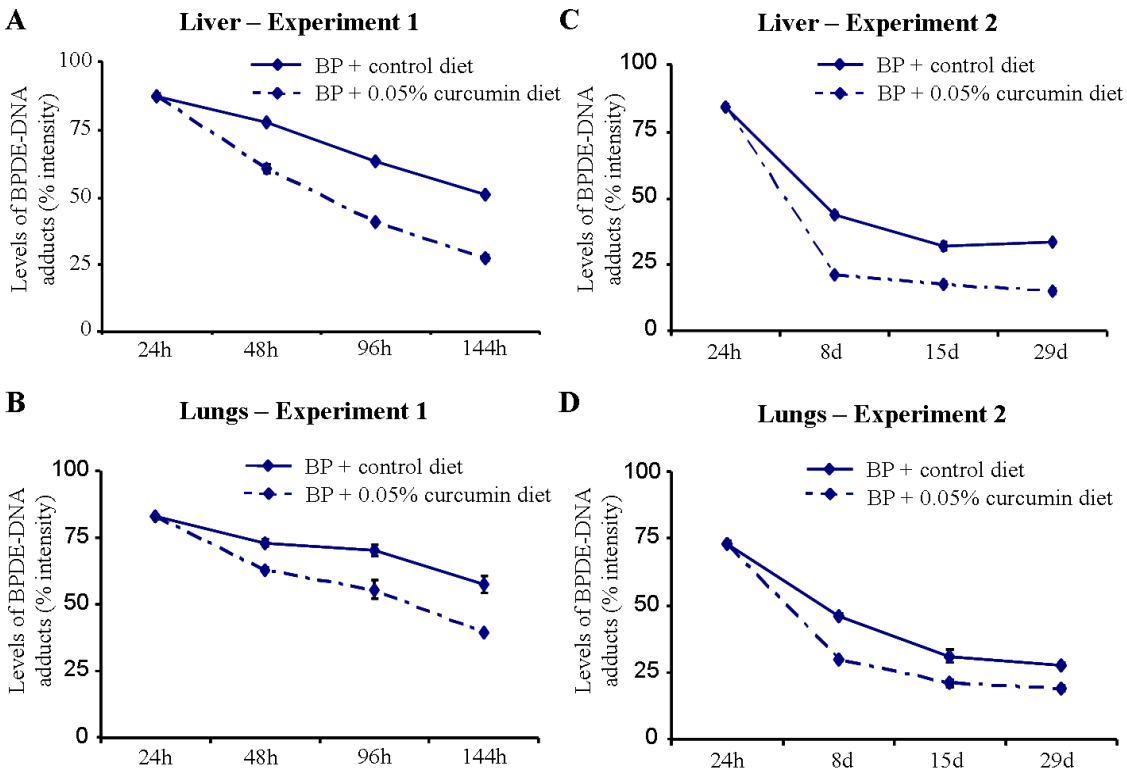

FIGURE 6.9: Levels of BPDE-DNA adducts in mouse liver and lungs (Experiments 1 and 2).

6.3.2 Effect of dietary curcumin post-treatment on levels of apoptosis in mouse tissues

6.3.2.1 Measurement of apoptotic index at 24, 72 and 120 h by TUNEL assay

The observed decrease in levels of BPDE-DNA adducts in liver and lungs may be attributed to increased loss of adducts containing cells and/or enhanced DNA repair and/or dilution of adducted DNA by newly synthesized non-adducted DNA. To investigate the effect of dietary curcumin post-treatment on B(a)P-induced cell turnover in mouse liver and lungs, TUNEL assay was employed. Turnover of cells by apoptosis in liver and lungs were measured in similar area of tissue sections (mm^2) and number of cells (~800 cells/section/animal). Apoptotic index was measured in terms of total apoptotic nuclei intensity as well as % of apoptotic positive and negative cells. Notably, 5-10% and 20-35% of total apoptotic nuclei were detected in liver and lungs tissues of vehicle [subgroups $V_{(+24h)}$, $V_{(+48h)}$, $V_{(+96h)}$, $V_{(+144h)}$] or vehicle + curcumin (subgroups $V_{(+48h)}$ + C 24h, $V_{(+96h)}$ + C 72h, $V_{(+144h)}$ + C 120h) treated groups, respectively (Figs. 6.10 and 6.11). Compared to vehicle treated group (V group), significant increase in % of

positive cells/ % intensity of total apoptotic nuclei was observed following 24 h of single dose of B(a)P [subgroup $BP_{(+24h)}$] in mouse liver, whereas in lungs, it was similar to vehicle treated group (Figs. 6.10 and 6.11). It was observed that as compared to subgroup $BP_{(+24h)}$, mice on control diet for 24, 72 and 120 h [subgroups $BP_{(+48h)}$, $BP_{(+96h)}$, $BP_{(+144h)}$] showed increase in apoptotic cells as judged by % of TUNEL positive apoptotic cells (apoptotic index) and/or % intensity of total apoptotic nuclei in liver and lungs of mice. Interestingly, mice those were shifted to 0.05% curcumin diet and sacrificed at 72 and 120 h (subgroups $BP_{(+96h)}$ + C 72h, $BP_{(+144h)}$ + C 120h) showed further increase in B(a)P-mediated apoptosis as seen by increase in numbers of apoptotic cells as well as % intensity of total apoptotic nuclei, when compared to $BP_{(+24h)}$ as well as respective time-matched controls [subgroups $BP_{(+96h)}$ and $BP_{(+144h)}$] (Figs. 6.10, 6.10, 6.14A and 6.14B). These observations thus suggest that dietary curcumin further enhances the B(a)P-induced apoptosis which would indirectly confer protection by increasing the removal of adduct containing cells.

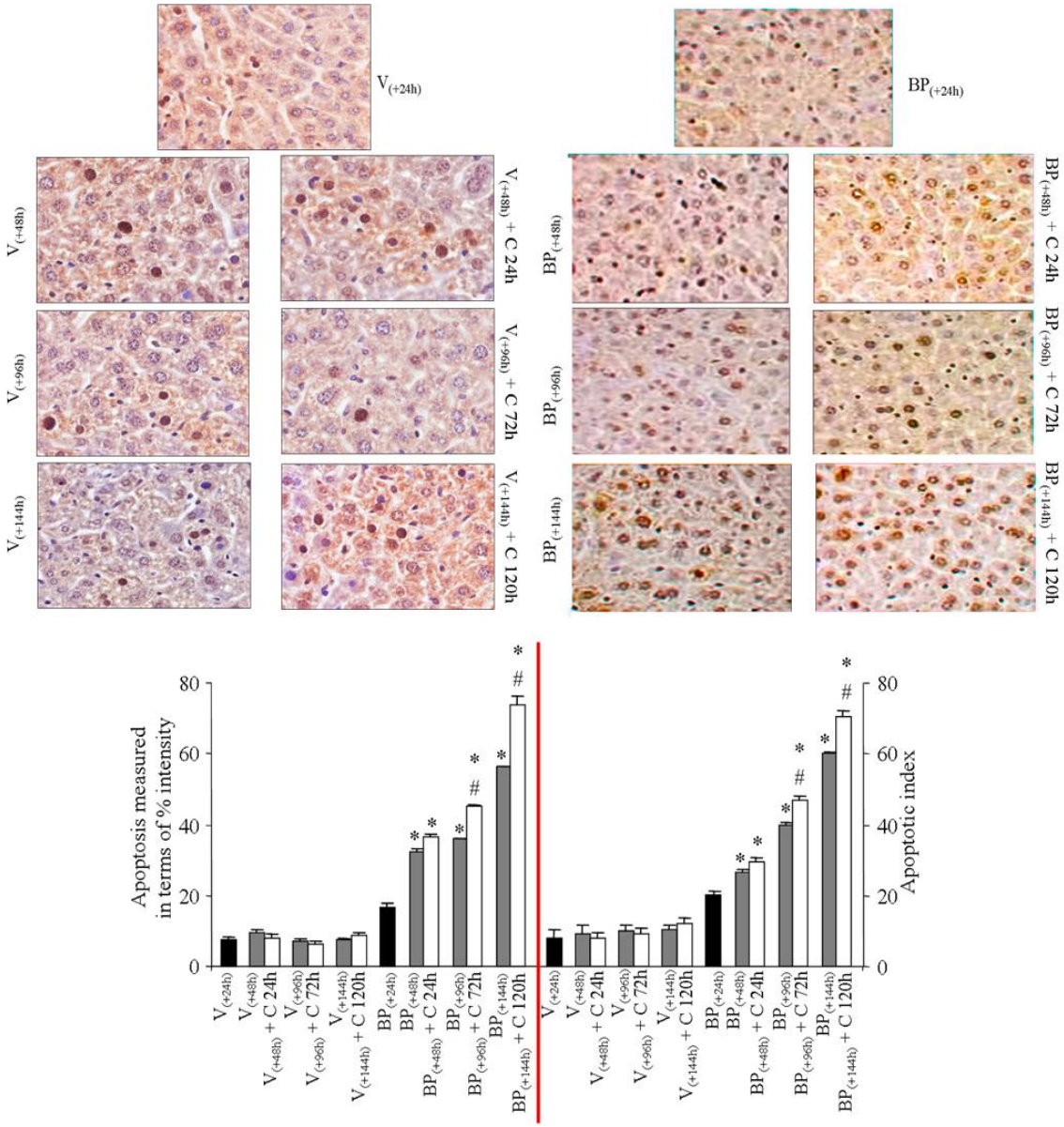

FIGURE 6.10: Effect of curcumin post-treatment on apoptosis in B(a)P-treated mouse liver (Experiment 1). *Representative photomicrographs showing immunohistochemical detection of levels of cell turnover or extent of apoptosis (magnification X 400), analyzed by TUNEL assay in formalin-fixed, paraffin-embedded tissue sections of mouse liver. Quantitative analysis was done by digital image analysis as described under Materials and methods (section 6.2.4) in photomicrographs of 10 randomly selected fields/section/mouse, with atleast three mice per group. Data represent mean ± SE of three observations. Differences among groups were determined by Poisson regression analysis ($p \leq 0.05$) using STATA 12 software. '∗' significant when compared with $BP_{(+24h)}$ subgroup; '#' significant when compared with respective time matched controls.*

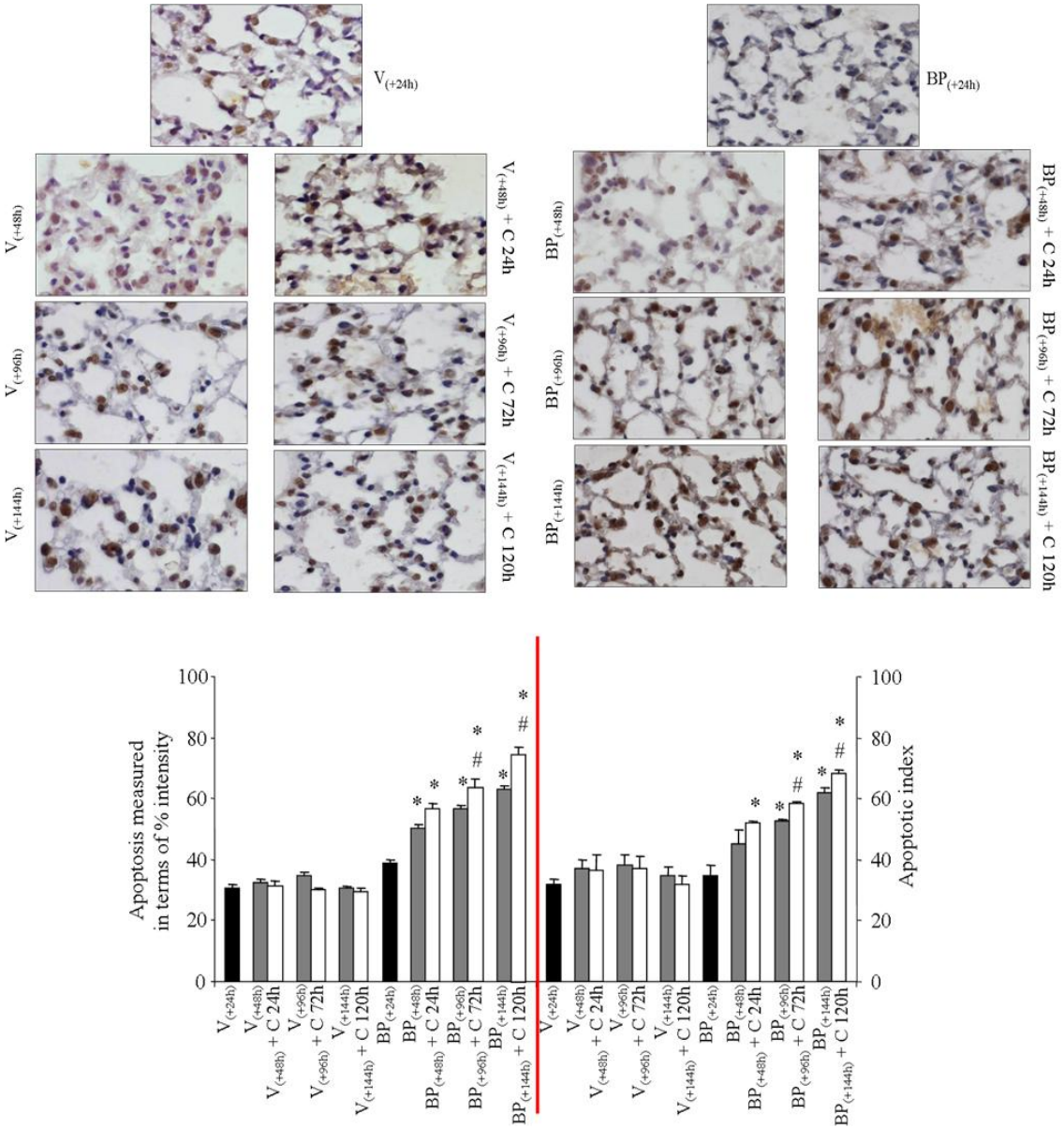

FIGURE 6.11: Effect of curcumin post-treatment on apoptosis in B(a)P-treated mouse lungs (Experiment 1). *Representative photomicrographs showing immunohistochemical detection of levels of cell turnover or extent of apoptosis (magnification X 400), analyzed by TUNEL assay in formalin-fixed, paraffin-embedded tissue sections of mouse lungs. Quantitative analysis was done by digital image analysis as described under Materials and methods (section 6.2.4) in photomicrographs of 10 randomly selected fields/section/mouse, with atleast three mice per group. Data represent mean ± SE of three observations. Differences among groups were determined by Poisson regression analysis ($p \leq 0.05$) using STATA 12 software. '∗' significant when compared with $BP_{(+24h)}$ subgroup; '#' significant when compared with respective time matched controls.*

6.3.2.2 Measurement of apoptotic index at 7, 14 and 28 dayby TUNEL assay

As observed in experiment 1, 5-10% and 20-35% of total apoptotic cells (apoptotic index) were detected in liver and lungs tissues of vehicle [subgroups $V_{(+24h)}$, $V_{(+8d)}$, $V_{(+15d)}$, $V_{(+29d)}$] or vehicle + curcumin (subgroups $V_{(+8d)}$ + C 7d, $V_{(+15d)}$ + C 14d, $V_{(+29d)}$ + C 28d) treated group, respectively (Figs. 6.12 and 6.13). It was observed that compared to subgroup $BP_{(+24h)}$, mice on control diet for 7 day (subgroups $BP_{(+8d)}$ showed increase in apoptosis as judged by increase in % of positive cells (apoptotic index) and/or % intensity of total apoptotic nuclei in liver and lungs of mice whereas decrease in apoptosis was observed in mice on control diet for 14 and 28 day in liver [$BP_{(+15d)}$, $BP_{(+29d)}$] (Figs. 6.12, 6.13, 6.14C and 6.14D). Interestingly, mice that were shifted to 0.05% curcumin diet and sacrificed at 7, 14 and 28 days did not show any difference in the level of apoptosis in liver and lungs of mice, when compared to $BP_{(+24h)}$ and respective time-matched controls [subgroups $BP_{(+8d)}$, $BP_{(+15d)}$, $BP_{(+29d)}$]; except in liver at 8 days, where mice showed decrease in % of positive apoptotic cells (apoptotic index) and/or % intensity of total apoptotic nuclei (Figs. 6.12, 6.13, 6.14C and 6.14D). Observed decrease in DNA adducts without enhancement in the levels of apoptosis in liver and lungs suggests role of DNA repair and/or dilution of BPDE-DNA adducts in tissue cells.

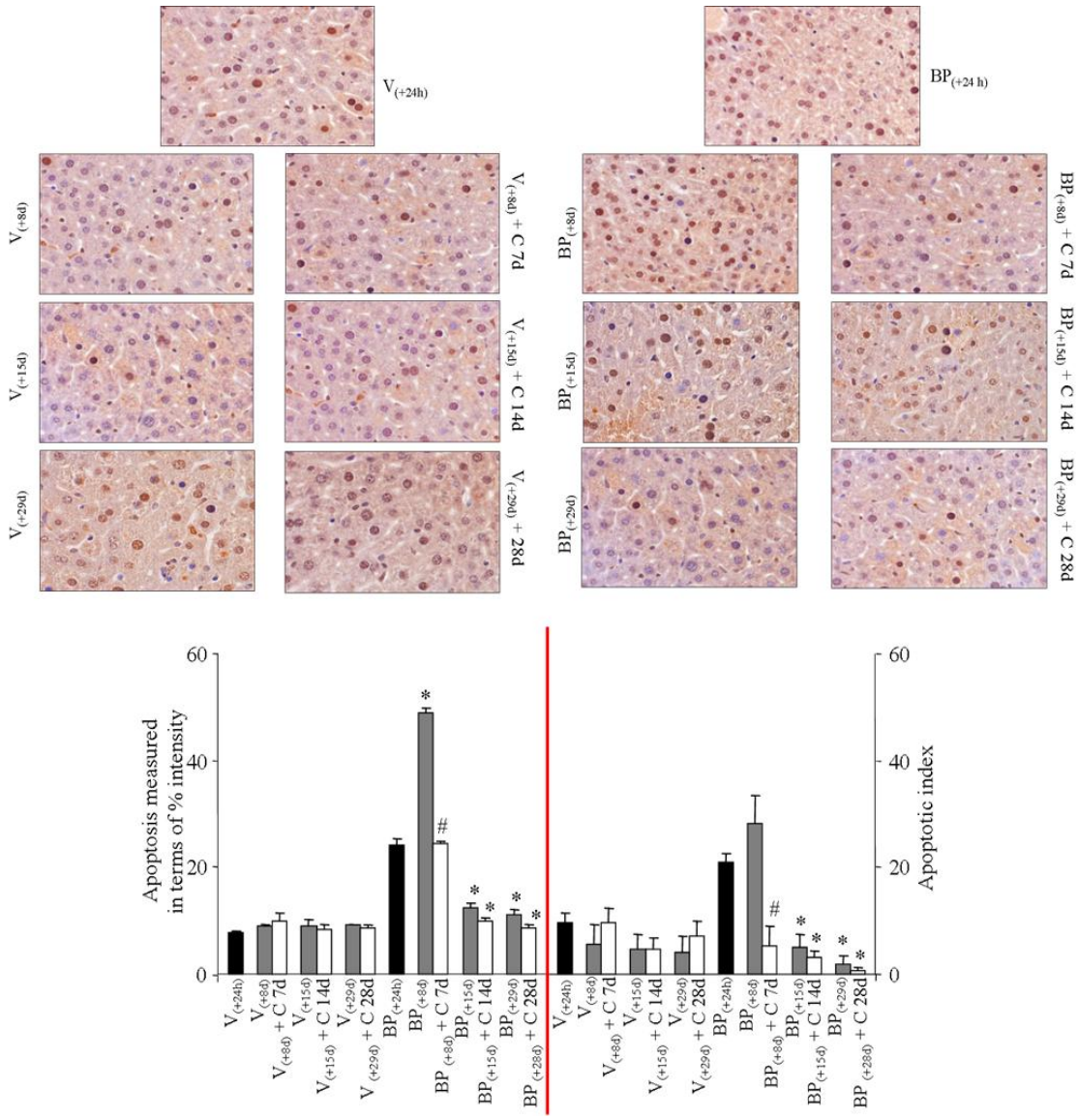

FIGURE 6.12: Effect of curcumin post-treatment on apoptosis in B(a)P-treated mouse liver (Experiment 2).*Representative photomicrographs showing immunohistochemical detection of levels of cell turnover or extent of apoptosis (magnification X 400), analyzed by TUNEL assay in formalin-fixed, paraffin-embedded tissue sections of mouse liver. Quantitative analysis was done by digital image analysis as described under Materials and methods (section 6.2.4) in photomicrographs of 10 randomly selected fields/section/mouse, with atleast three mice per group. Data represent mean ± SE of three observations. Differences among groups were determined by Poisson regression analysis ($p \leq 0.05$) using STATA 12 software. '∗' significant when compared with $BP_{(+24h)}$ subgroup; '#' significant when compared with respective time matched controls.*

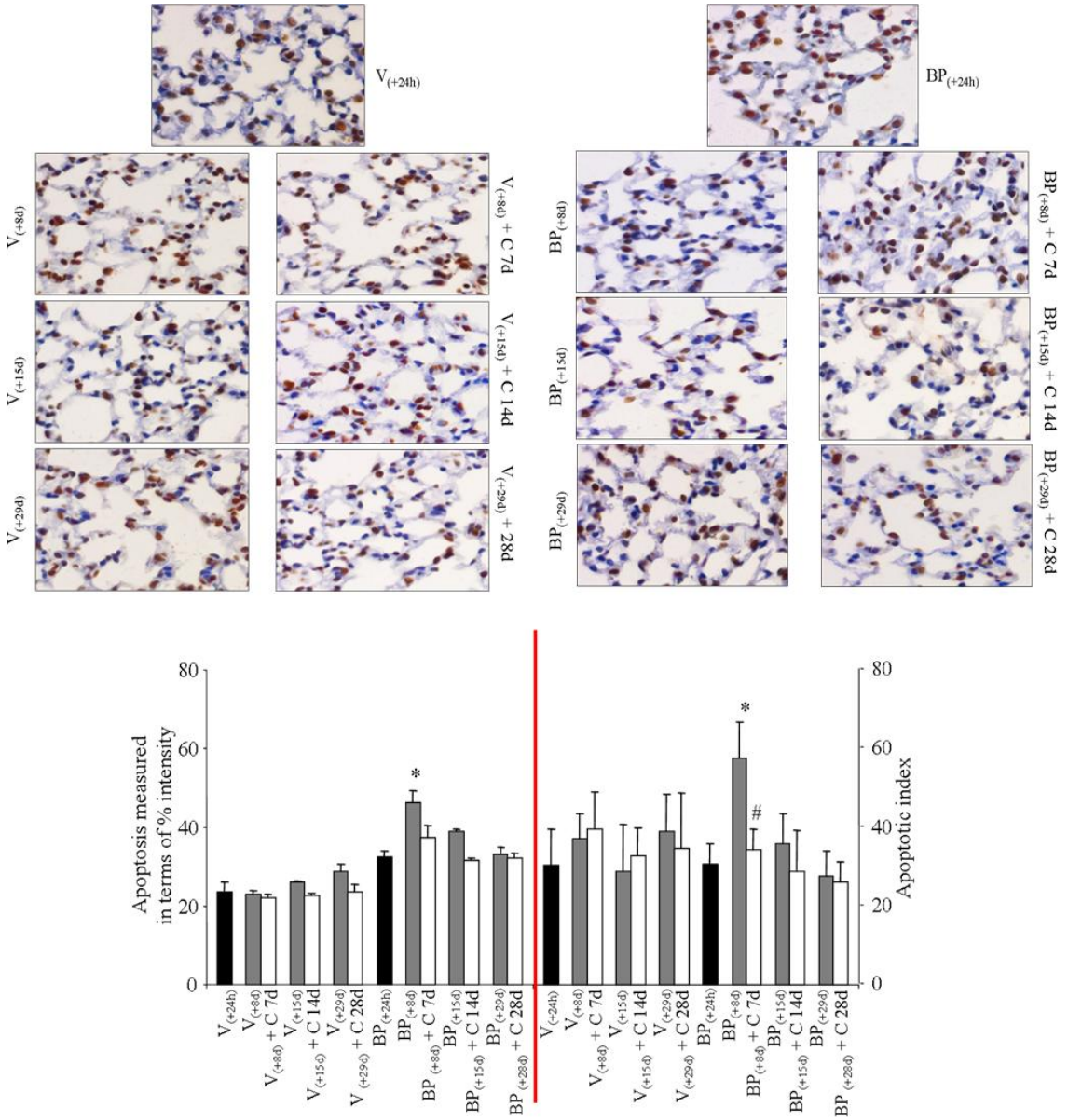

FIGURE 6.13: Effect of curcumin post-treatment on apoptosis in B(a)P-treated mouse lungs (Experiment 2). *Representative photomicrographs showing immunohistochemical detection of levels of cell turnover or extent of apoptosis (magnification X 400), analyzed by TUNEL assay in formalin-fixed, paraffin-embedded tissue sections of mouse lungs. Quantitative analysis was done by digital image analysis as described under Materials and methods (section 6.2.4) in photomicrographs of 10 randomly selected fields/section/mouse, with atleast three mice per group. Data represent mean ± SE of three observations. Differences among groups were determined by Poisson regression analysis ($p \leq 0.05$) using STATA 12 software. '∗' significant when compared with $BP_{(+24h)}$ subgroup; '#' significant when compared with respective time matched controls.*

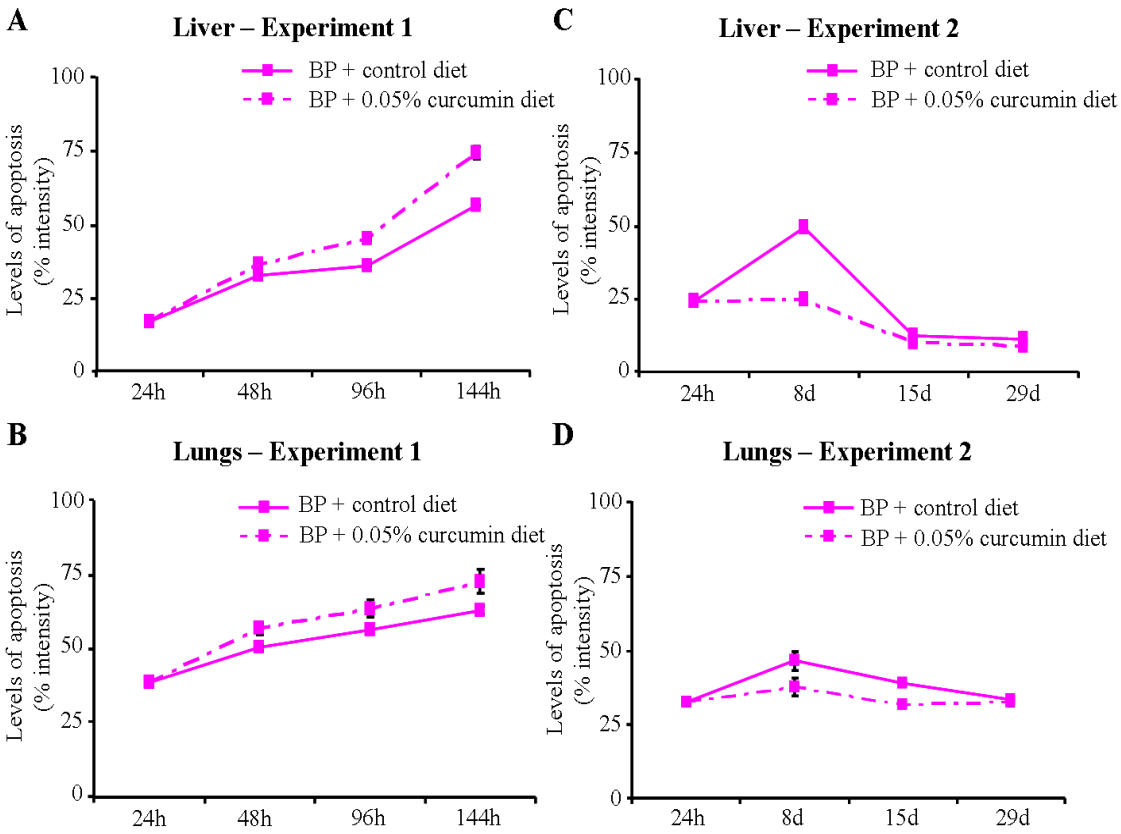

FIGURE 6.14: Levels of apoptosis in mouse liver and lungs (Experiments 1 and 2).

6.3.2.3 Measurement of apoptosis-related markers at 24, 72 and 120 h

Further, to confirm post-treatment effects of dietary curcumin in enhancement of apoptosis measured by TUNEL positivity; protein levels of apoptosis related markers were analyzed in liver and lungs of mice by immunoblotting. It is to be noted that levels of apoptosis markers (Bax, Bcl-2 and caspase-3) remained similar in vehicle [subgroups $V_{(+24h)}$, $V_{(+48h)}$, $V_{(+96h)}$, $V_{(+144h)}$] or vehicle + curcumin (subgroups $V_{(+48h)}$ + C 24h, $V_{(+96h)}$ + C 72h, $V_{(+144h)}$ + C 120h)treated groups in liver and lungs of mice (Figs. 6.15A and 6.16A). No change in levels of apoptosis markers (Bax, Bcl-2 and caspase-3) was observed following 24 h of single dose of B(a)P [subgroups $BP_{(+24h)}$] in mouse liver and lungs, when compared to vehicle treated group (V group). On comparison with subgroup $BP_{(+24h)}$, mice on control diet for 24, 72 and 120 h [subgroups $BP_{(+48h)}$, $BP_{(+96h)}$, $BP_{(+144h)}$] showed significant increase in protein level of Bax in liver (72 and 120 h) and lungs (120 h). Mice shifted to 0.05% curcumin diet (subgroups $BP_{(+48h)}$ + C 24h, $BP_{(+96h)}$ + C 72h, $BP_{(+144h)}$ + C 120h) showed significant increase in level of Bax protein in liver (72 and 120h) and lungs (24 and 120h), when compared with respective levels in $BP_{(+24h)}$ and respective time matched controls (Figs. 6.15A and 6.16A). Concurrent to this, level of

Bcl-2 protein was unaltered in mice on control diet [subgroups $BP_{(+48h)}$, $BP_{(+96h)}$, $BP_{(+144h)}$] compared to BP 24h. Importantly, mice that were shifted to 0.05% curcumin diet (subgroups $BP_{(+48h)}$ + C 24h, $BP_{(+96h)}$ + C 72h, $BP_{(+144h)}$ + C 120h) showed decrease in levels of Bcl-2 in liver (72 and 120 h) and lungs (120h), when compared with $BP_{(+24h)}$ and respective time matched controls (Figs. 6.15A and 6.16A). These observations, together, account for the progressive increment seen in the Bax/Bcl-2 ratio upon dietary curcumin post-treatment, thereby indicating that post-treatment with curcumin further enhances the apoptosis in B(a)P-treated mice (Figs. 6.15B and 6.16B). In addition, significant increase was also observed in the protein expression of caspase-3, the death executioner, at 72 and 120 h in liver and at 120 h in lungs of mice shifted to curcumin diet when compared with respective time matched controls (Figs. 6.15A and 6.16A). This correlates well with the enhancement observed in apoptotic index as well as in Bax/Bcl-2 ratio upon curcumin treatment. Overall, these results suggest that curcumin-mediated enhanced apoptosis in B(a)P-treated mice could be one of the plausible reason contributing towards the decrease in BPDE-DNA adducts in liver and lungs of mice.

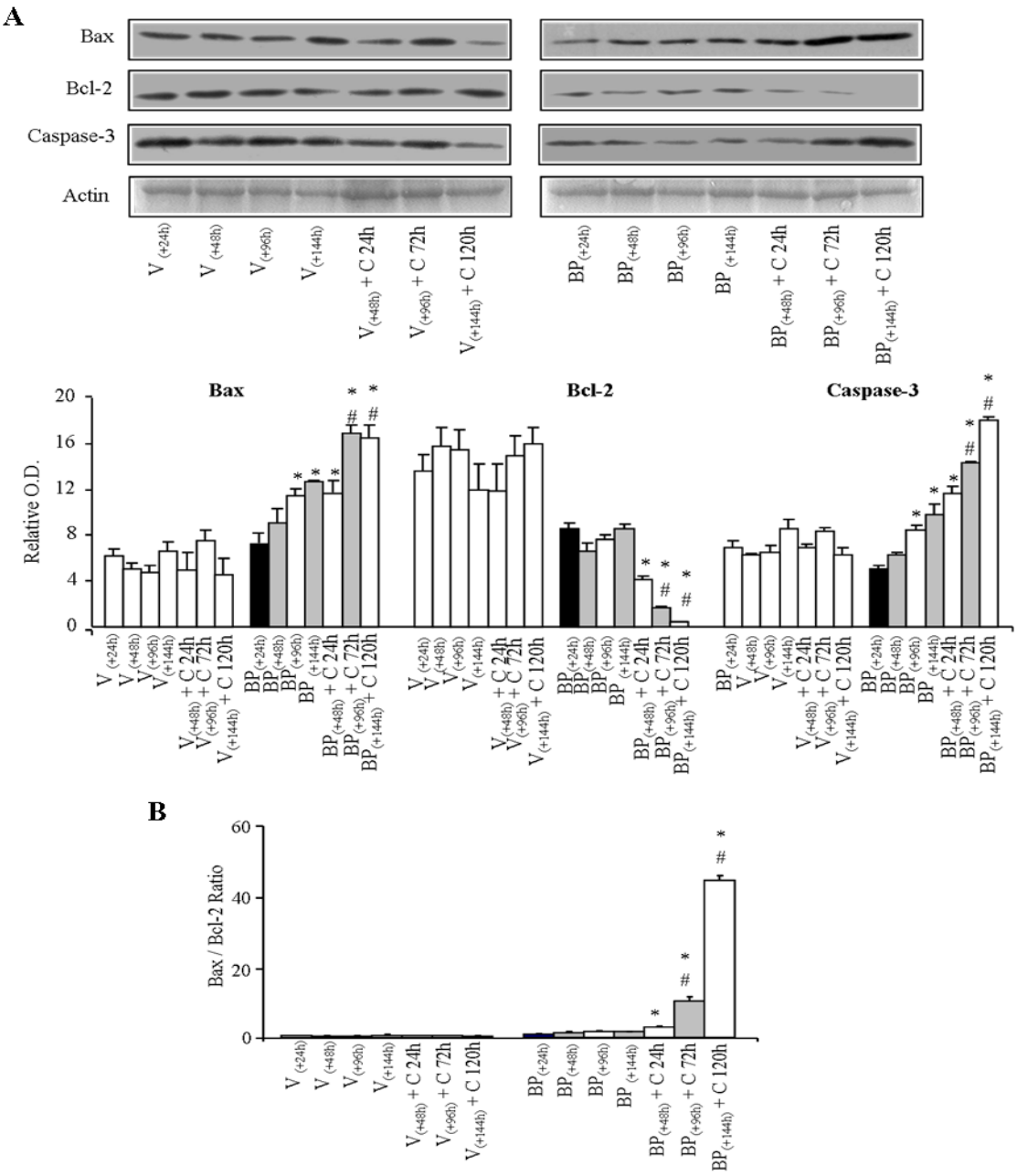

FIGURE 6.15: Effect of curcumin post-treatment on apoptosis-related biochemical markers in B(a)P-treated mouse liver (Experiment 1). *Representative blots and relative levels of Bax, Bcl-2 and caspase-3 protein measured in total cell lysates prepared from mouse liver and analyzed by immunoblotting using specific antibodies. β-actin was used as the loading control. (B) Extent of apoptosis was determined by calculating the ratio of normalized band intensity of Bax and Bcl-2 in liver of mouse. Data represent mean ± SE of three observations. Differences among groups were determined by one-way ANOVA followed by Bonferroni's test, $p \leq 0.05$. '∗' significant when compared with $BP_{(+24h)}$ subgroup; '#' significant when compared with respective time matched controls.*

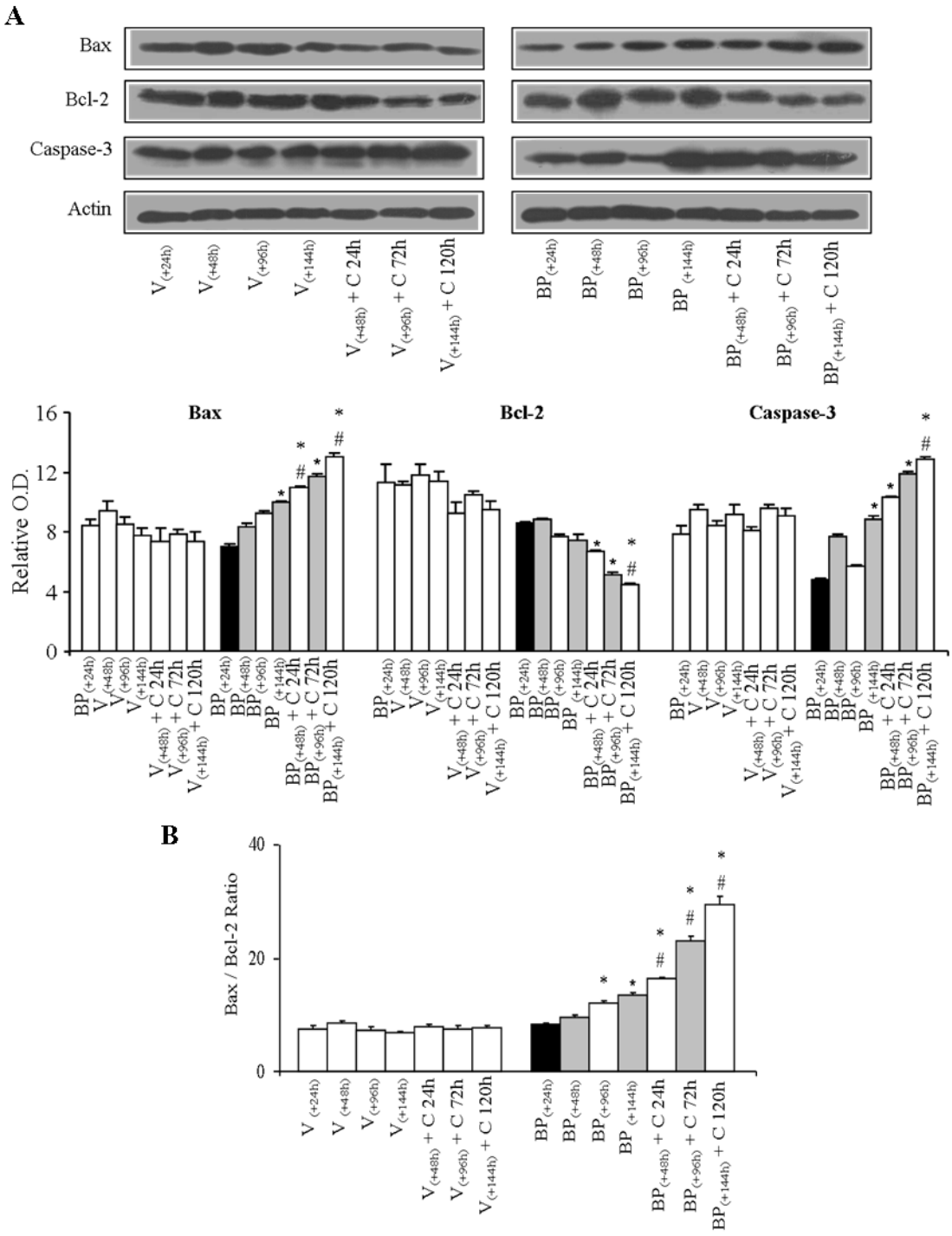

FIGURE 6.16: Effect of curcumin post-treatment on apoptosis-related biochemical markers in B(a)P-treated mouse lungs (Experiment 1). *Representative blots and relative levels of Bax, Bcl-2 and caspase-3 protein measured in total cell lysates prepared from mouse lungs and analyzed by immunoblotting using specific antibodies. β-actin was used as the loading control. (B) Apoptosis was determined by calculating the ratio of normalized band intensity of Bax and Bcl-2 in lungs of mouse. Data represent mean ± SE of three observations. Differences among groups were determined by one-way ANOVA followed by Bonferroni's test, $p \leq 0.05$. '∗' significant when compared with $BP_{(+24h)}$ subgroup; '#' significant when compared with respective time matched controls.*

6.3.2.4 Measurement of apoptosis-related markers at 7, 14 and 28 days

Further, to confirm post-treatment effects of dietary curcumin on apoptosis measured by TUNEL positivity; protein levels of apoptosis related markers were analyzed in liver and lungs of mice by immunoblotting. As observed in experiment 1, levels of apoptosis markers (Bax, Bcl-2 and caspase-3) remained similar in vehicle [subgroups $V_{(+24h)}$, $V_{(+8d)}$, $V_{(+15d)}$, $V_{(+29d)}$] or vehicle + curcumin (subgroups $V_{(+8d)}$ + C 7d, $V_{(+15d)}$ + C 14d, $V_{(+29d)}$ + C 28d) treated groups in liver and lungs of mice (Figs. 6.17 and 6.18). No change in levels of apoptosis markers (Bax, Bcl-2 and caspase-3) was observed in liver and lungs of mice on control diet for 8, 15 & 29 days [subgroups $BP_{(+8d)}$, $BP_{(+15d)}$, $BP_{(+29d)}$] when compared with that at $BP_{(+24h)}$. Mice shifted to 0.05% curcumin diet (subgroups $BP_{(+8d)}$ + C7d, $BP_{(+15d)}$ + C14d, $BP_{(+29d)}$ + C28d) showed significant increase in level of Bax protein in liver (14d and 28d) and lungs (28d), when compared with respective time matched controls (Figs. 6.17 and 6.18). Levels of Bcl-2 were similar in liver of mice shifted to 0.05% curcumin diet (subgroups $BP_{(+8d)}$ + C7d, $BP_{(+15d)}$ + C14d, $BP_{(+29d)}$ + C28d) when compared to $BP_{(+24h)}$ as well as respective time matched controls, whereas decrease was observed in lungs (14d and 28d) of mice shifted to curcumin diet when compared to $BP_{(+24h)}$ as well as respective time matched controls (Figs. 6.17A and 6.18A). In addition, significant increase was noticed in the protein expression of caspase-3, the death executioner, at 14 and 28 days in liver and at 28 days in lungs of mice shifted to curcumin diet when compared to $BP_{(+24h)}$ as well as respective time matched controls. Observed decrease in DNA adducts without enhancement in levels of apoptosis in liver and lungs suggest role of DNA repair and/or dilution of BPDE-DNA adducts in tissue cells.

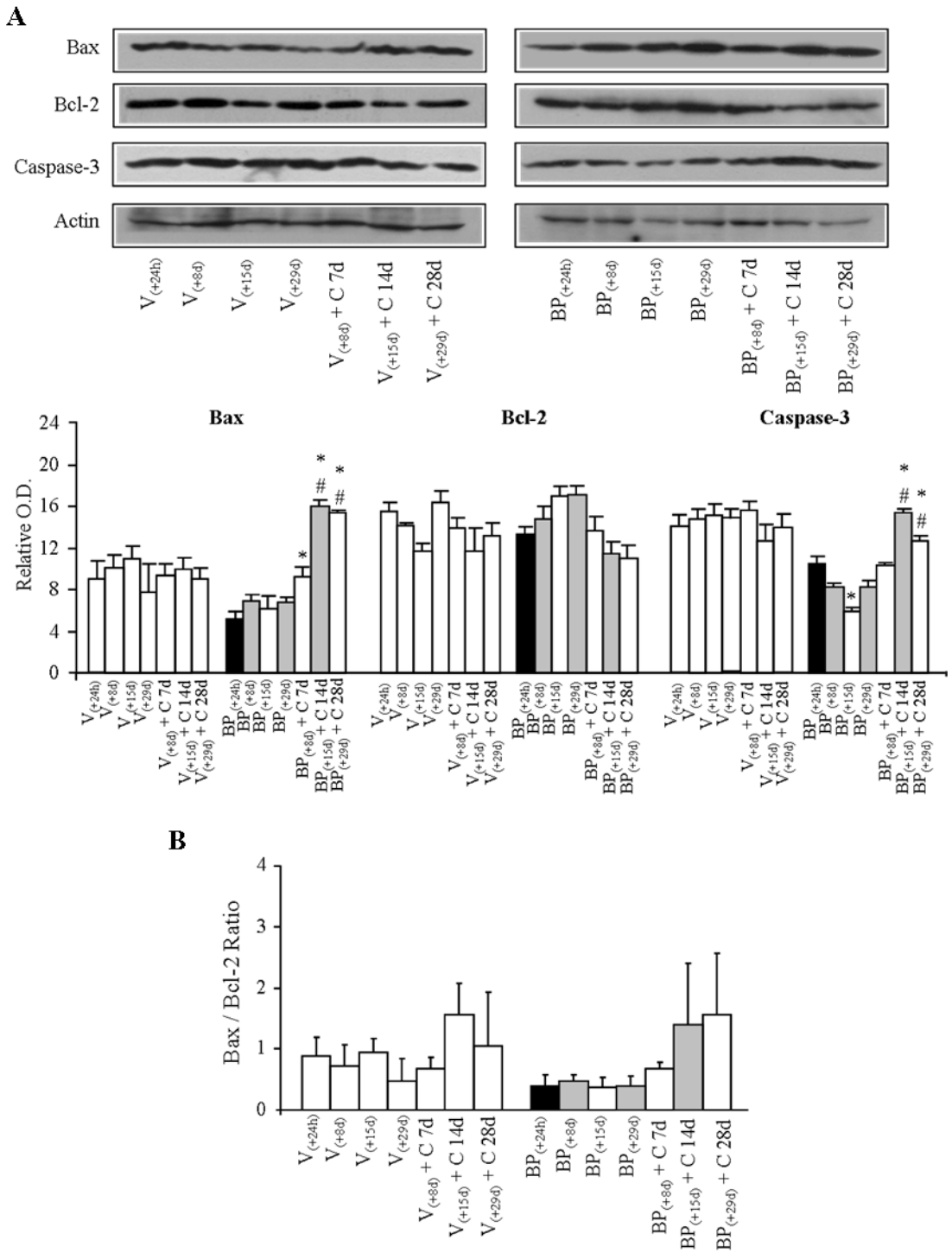

FIGURE 6.17: Effect of curcumin post-treatment on apoptosis-related biochemical markers in B(a)P-treated mouse liver (Experiment 2). **(A)** *Representative blots and relative levels of Bax, Bcl-2, caspase-3 protein measured in total cell lysates prepared from mouse liver and analyzed by immunoblotting using specific antibodies. β-actin was used as the loading control.* **(B)** *Extent of apoptosis was determined by calculating the ratio of normalized band intensity of Bax and Bcl-2 in liver of mouse. Data represent mean ± SE of three observations. Differences among groups were determined by one-way ANOVA followed by Bonferroni's test, $p \leq 0.05$. '∗' significant when compared with $BP_{(+24h)}$ subgroup; '#' significant when compared with respective time matched controls.*

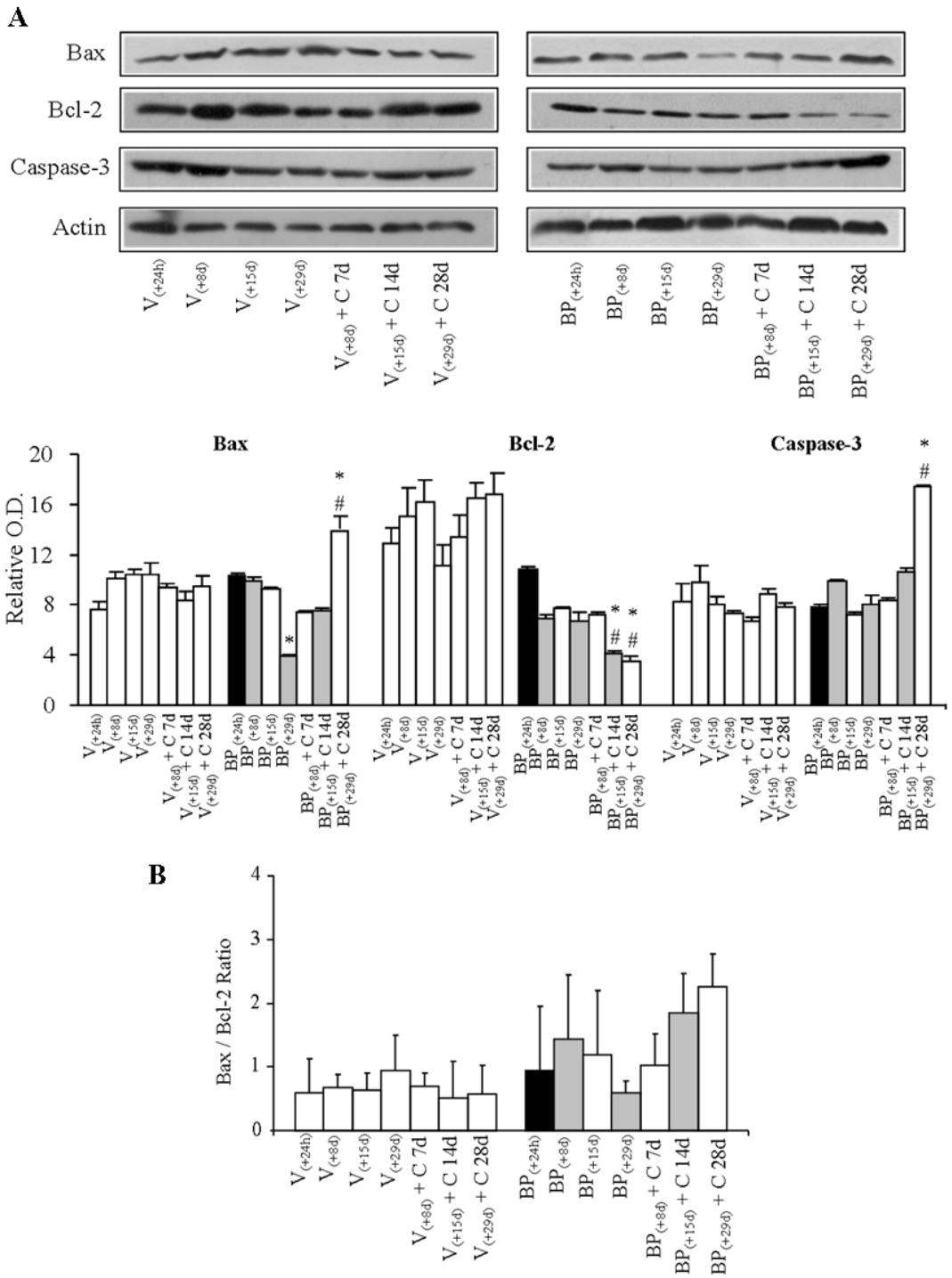

FIGURE 6.18: Effect of curcumin post-treatment on apoptosis-related biochemical markers in B(a)P-treated mouse lungs (Experiment 2). (**A)** *Representative blots and relative levels of Bax, Bcl-2, caspase-3 protein measured in total cell lysates prepared from mouse lungs and analyzed by immunoblotting using specific antibodies. β-actin was used as the loading control.***(B)** *Extent of apoptosis was determined by calculating the ratio of normalized band intensity of Bax and Bcl-2 in lungs of mouse. Data represent mean ± SE of three observations. Differences among groups were determined by one-way ANOVA followed by Bonferroni's test, $p \leq 0.05$. '∗' significant when compared with $BP_{(+24h)}$ subgroup; '#' significant when compared with respective time matched controls.*

6.3.3 Effect of dietary curcumin post-treatment on levels of cell proliferation markers in mouse tissues

6.3.3.1 Measurement of cell proliferation markers at 24, 72 and 120 h

In addition to the role of apoptosis in disappearance of BPDE-DNA adducts, contribution of dilution of adduct containing DNA by newly synthesized non-adducted DNA, protein levels of cell proliferation markers such as PCNA in mouse liver and lungs were analyzed and compared by immunoblotting analysis. Levels of PCNA remained similar in vehicle [subgroups $V_{(+24h)}$, $V_{(+48h)}$, $V_{(+96h)}$, $V_{(+144h)}$] or vehicle + curcumin (subgroups $V_{(+48h)}$ + C 24h, $V_{(+96h)}$ + C 72h, $V_{(+144h)}$ + C 120h)treated groups in liver and lungs of mice (Figs. 6.19A, 6.19B, 6.20A and 6.20B). Similarly, no change in levels of PCNA was observed following 24 h of single dose of B(a)P (subgroups $BP_{(+24h)}$) in mouse liver and lungs, when compared to vehicle treated group (V group) (Figs. 6.19A, 6.19B, 6.20A and 6.20B). Furthermore, mice on control diet [subgroups $BP_{(+48h)}$, $BP_{(+96h)}$, $BP_{(+144h)}$] showed increase in the levels of PCNA in liver and lungs when compared to subgroup $BP_{(+24h)}$, except in liver at 48 h. Interestingly, mice that were shifted to 0.05% curcumin diet (subgroups $BP_{(+48h)}$ + C 24h, $BP_{(+96h)}$ + C 72h, $BP_{(+144h)}$ + C 120h) showed significant decrease in levels of PCNA in liver (72 and 120 h) and lungs (120 h), when compared with respective time matched controls (Figs. 6.19A ,6.19B, 6.20A and 6.20B). As observed in case of PCNA, similar trend was observed in cyclin D1, wherein significant curcumin-mediated decrease in level of cyclin D1 was observed in lungs of mice, when compared to respective time matched controls (Fig. 6.19B).

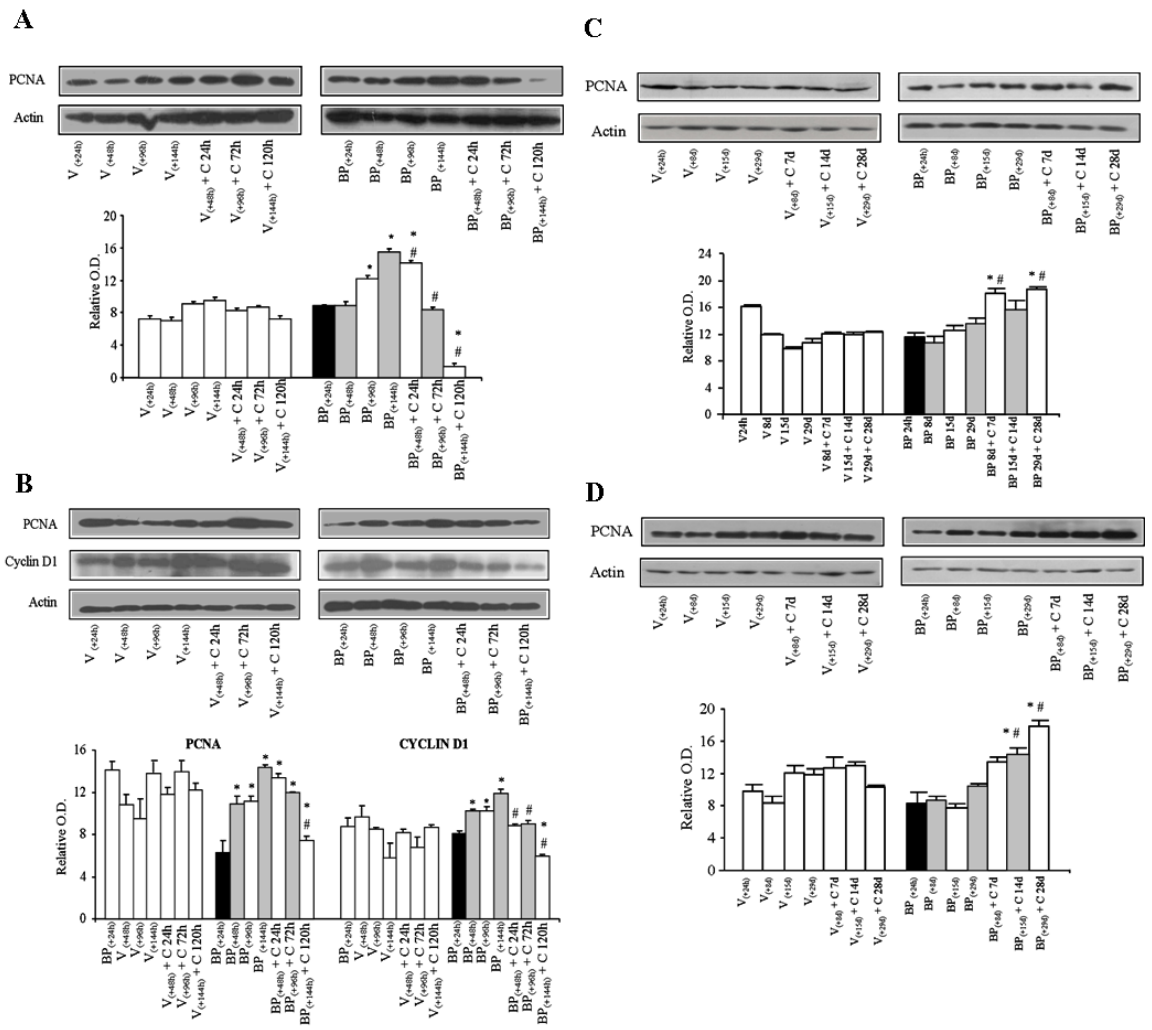

FIGURE 6.19: Effect of curcumin post-treatment on cell proliferation markers in B(a)P-treated mouse tissues (Experiments 1 and 2). *Representative blots and relative levels of* **(A)** *PCNA (liver),* **(B)** *PCNA and cyclin D1 (lungs),* **(C)** *PCNA (liver),* **(D)** *PCNA (lungs); proteins measured in total cell lysates prepared from mouse tissues and analyzed by immunoblotting using specific antibodies. β-actin was used as the loading control. Data represent mean ± SE of three observations. Differences among groups were determined by one-way ANOVA followed by Bonferroni's test, $p \leq 0.05$. '*' significant when compared with $BP_{(+24h)}$ subgroup; '#' significant when compared with respective time matched controls.*

6.3.3.2 Measurement of cell proliferation markers at 7, 14 and 28 days

Similar comparative evaluations of cell proliferation markers were undertaken in liver and lungs of mice at 7, 14 and 28 days. As analyzed in experiment 1, proliferation was assessed by comparing levels of PCNA. As observed in experiment 1, levels of PCNA remained similar in vehicle [subgroups $V_{(+24h)}$, $V_{(+8d)}$, $V_{(+15d)}$, $V_{(+29d)}$] or vehicle + curcumin (subgroups $V_{(+8d)}$ + C 7d, $V_{(+15d)}$ + C 14d, $V_{(+29d)}$ + C 28d) treated groups in liver and lungs of mice (Figs. 6.19C, 6.19D, 6.20C and 6.20D). No change in levels of PCNA was observed in liver and lungs of mice on control diet for 8, 15 & 29 days

[subgroups $BP_{(+8d)}$, $BP_{(+15d)}$, $BP_{(+29d)}$] when compared with that at $BP_{(+24h)}$. Interestingly, mice that were shifted to 0.05% curcumin diet (subgroups $BP_{(+8d)}$ + C 7d, $BP_{(+15d)}$ + C 14d, $BP_{(+29d)}$ + C 28d) showed increase in levels of PCNA in liver (7 and 28 d) and lungs (14 and 28 d), when compared to that in $BP_{(+24h)}$ as well as respective time matched controls (Figs. 6.19C, 6.19D, 6.20C and 6.20D).

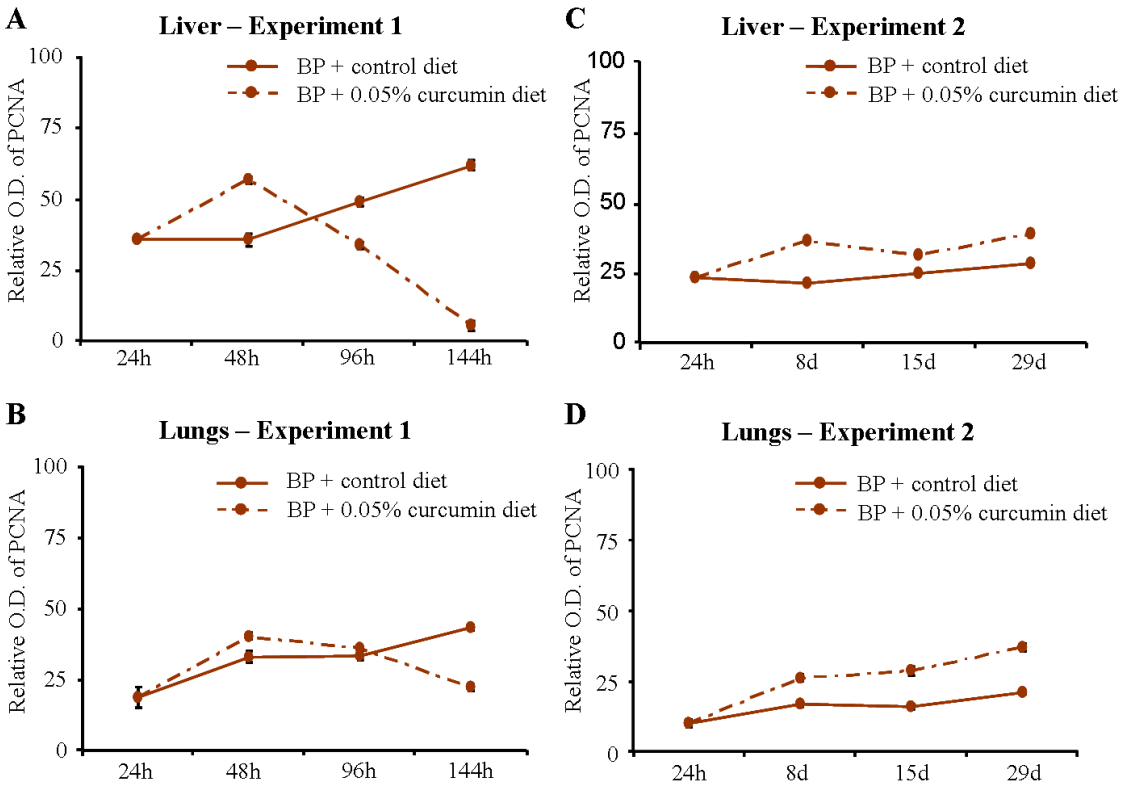

FIGURE 6.20: Levels of PCNA in mouse liver and lungs.

6.4 DISCUSSION

Humans are exposed to complex mixtures of polycyclic aromatic hydrocarbons (PAHs), which have been implicated in inducing skin, lungs and breast cancer. PAH-induced carcinogenesis involves a number of steps including; (i) the enzymatic activation of the PAH into metabolites; (ii) the covalent binding of the PAH metabolites to DNA; and (iii) the induction of mutations that serve to initiate the transformation process as a results of PAH-DNA adducts. Levels of DNA adducts measured at any point in time, reflect tissue-specific rates of adducts formation and removal, which in turn, depends upon carcinogen activation/detoxification, DNA repair, adduct instability, tissue turnover etc. The concept that cancer can be prevented or that certain diet derived substances can postpone its onset is receiving increasing attention [6,219]. Turmeric/curcumin pre-

treatment has been demonstrated to decrease the formation of BPDE-DNA adducts in tissues of mice/rats as a result of decrease in B(a)P-induced phase I enzymes and/or induction of phase II enzymes [134,216]. In several studies post-treatment of curcumin has been shown to decrease multiplicity of carcinogen-induced tumor formation in experimental models such as B(a)P-induced forestomach tumors, NDEA-induced hepatocarcinogenesis, DMBA-induced mammary tumorigenesis, AOM-induced colon tumors etc.[110,112,128].Observed decrease in tumor multiplicity due to exposure to turmeric/curcumin after exposure to carcinogen is likely to be due to decrease in cell proliferation and/or loss of initiated/DNA adduct containing cells. To understand the effect of post-treatment of curcumin on disappearance of BPDE-DNA adducts, levels of BPDE-DNA adducts were measured at various time intervals in liver and lungs of mice after allowing the formation of equal/similar levels of adducts and then exposing the animals to dietary curcumin. Levels of BPDE-DNA adducts were measured in tissue sections by immunohistochemical staining wherein adduct specific antibody was employed and levels were quantitated by measuring the adduct-intensity by image analyses [218]. Although the method employed for quantitation of BPDE-DNA adducts does not provide absolute levels of DNA adducts per unit weight of DNA or defined number of normal nucleotides, it is capable of allowing unbiased relative comparison of adduct levels per equal area and/or similar number of cells. Non-destructive measurement method provides localization of adducts within cells in reasonable time and cost and multiple samples can be processed in a batch employing defined conditions.

Absence of BPDE-DNA adducts in tissue sections from liver and lungs of mice receiving vehicle or dietary curcumin and significant as well as measurable levels of BPDE-DNA adducts were observed in these tissues following 24 h of B(a)P administration as reported in mouse skin, liver and lungs [186,220,221]. The time-dependent [$BP_{(+48h)}$, $BP_{(+96h)}$, $BP_{(+144h)}$/ $BP_{(+8d)}$, $BP_{(+15d)}$, $BP_{(+29d)}$] decrease in the levels of BPDE-DNA adducts in liver and lungs compared to that in $BP_{(+24h)}$ following the single dose of carcinogen exposure was similar to those observed by others investigators in mouse/rat skin during 24 h–28 days[220,222]. The time-related decrease in the levels of DNA adducts was relatively higher in liver than lungs when compared to respective levels in $BP_{(+24h)}$. Our results clearly demonstrate that dietary curcumin (0.05%) post-treatment (subgroups $BP_{(+48h)}$ + C 24h, $BP_{(+96h)}$ + C 72h, $BP_{(+144h)}$ + C 120h and $BP_{(+8d)}$ + C 7d, $BP_{(+15d)}$ + C 14d, $BP_{(+29d)}$ + C 28din experiments 1 and 2, respectively) further enhanced the decrease in the levels of BPDE-DNA adducts both in liver and lungs at 48-

144 h (experiment 1) and 8-28 days (experiment 2) when compared to their levels in $BP_{(+24h)}$ as well as respective time-matched controls [subgroups $BP_{(+48h)}$, $BP_{(+96h)}$, $BP_{(+144h)}$ and $BP_{(+8d)}$, $BP_{(+15d)}$, $BP_{(+29d)}$ in experiments 1 and 2, respectively).Our observation of high levels of BPDE-DNA adducts 24 h after the carcinogen treatment and sharp decreases within 1 wk (~8 days) is also in agreement with observation reported in mouse/rat skin [222]. The probable reasons for the observed time-related decrease in the levels of BPDE-DNA adducts in liver and lungs could be due to loss or turnover of DNA adducts containing cells and/or repair of carcinogen-DNA adducts and/or dilution of adducted DNA with newly synthesized non-adducted DNA. The observed curcumin-mediated enhancement in disappearance of BPDE-DNA adducts is likely to be due to modulation of one or more of above mentioned processes. Analyses conducted to identify the reasons for curcumin-mediated enhanced disappearance of BPDE-DNA adducts showed that basal levels of apoptosis/turnover in control liver (5-10%) and lungs (20-35 %) were significantly enhanced by single dose of B(a)P only in liver (17-24%) but not in lungs (32-38%). Subsequently, time-related increase in % apoptosis was observed in both the tissues (subgroups $BP_{(+48h)}$, $BP_{(+96h)}$, $BP_{(+144h)}$; 32-56 %) and these rates or levels were further enhanced in B(a)P-treated animals exposed to dietary curcumin (subgroups $BP_{(+48h)}$ + C 24h, $BP_{(+96h)}$ + C 72h, $BP_{(+144h)}$ + C 120h; 37-73 %) when compared with the levels in $BP_{(+24h)}$ and respective time-matched controls [subgroups $BP_{(+96h)}$ and $BP_{(+144h)}$]. Apoptosis measured employing semi-quantitative and quantitative assays and parameters showed good agreement in direction and extent of change that appears to be one of the major contributors in disappearance of BPDE-DNA adducts in tissues studied. Quantitative analysis and comparison of immunohistochemical assays measuring BPDE-DNA adducts and apoptosis in tissue sections has the advantage that comparison is being made with preceding or subsequent paraffin-embedded section from the same portion of the tissue and that is likely to be relevant and meaningful. Curcumin-mediated enhancement of apoptosis in B(a)P-treated (normal liver and lungs tissue cells) cells has some similarity with its effects in terms of enhancement of apoptosis observed in transformed or immortalized cells in culture [68,223,224]. To our knowledge, this is an initial *in vivo* report demonstrating that dietary curcumin augmented the expression of caspase-3 and increased the Bax/Bcl-2 ratio and apoptotic index in normal cells in response to B(a)P-induced DNA damage and probably this in turn, accounts for the enhanced disappearance of adduct containing nuclei, although the degree of responses varied.

The other potential contributor in observed relative decrease in BPDE-DNA adducts is cell proliferation and its role was assessed by comparing the levels of PCNA by western blot analysis. It was seen from experiment 1 that levels of PCNA were enhanced post B(a)P-treatment especially at later time points [subgroups $BP_{(+96h)}$ and $BP_{(+144h)}$] and B(a)P-mediated increases were significantly decreased by dietary curcumin when compared to time matched B(a)P-treated controls (subgroups $BP_{(+96h)}$ + C 72h, $BP_{(+144h)}$ + C 120h in liver and $BP_{(+144h)}$ + C 120h in lungs). In experiment 2, levels of PCNA were not altered significantly at 8-28 days post B(a)P [$BP_{(+8d)}$, $BP_{(+15d)}$, $BP_{(+29d)}$] both in liver and lungs while curcumin treatment resulted in significant increase in levels of PCNA (subgroups $BP_{(+8d)}$ + C 7d, $BP_{(+29d)}$ + C 28d in liver, and $BP_{(+15d)}$ + C 14d, $BP_{(+29d)}$ + C 28d in lungs). It may be noted that exposure to dietary curcumin alone does not alter the levels of PCNA in liver and lungs of mice.

After considering and comparing the slope of time related and curcumin-mediated changes in BPDE-DNA adducts, levels of cells undergoing apoptosis and cell proliferation, it is seen that observed decrease in BPDE-DNA adducts in experiment 1 is mainly contributed by curcumin-mediated enhanced apoptosis while in experiment 2 dilution of BPDE-DNA adducts by newly synthesized non-adducted DNA due to cell proliferation appears to be the reason (Figs. 6.9, 6.14 and 6.20). In both these experiments apoptosis (experiment 1) and cell proliferation (experiment 2) alone may not be sufficient to result in the extent of decrease and indirectly suggests the role of DNA repair. Since DNA-repair related activity of enzyme and/or protein levels have not been measured, it remains a suggestive evidence and need experimental evidence to overcome this shortcoming in the present study. Our results also fail to demonstrate curcumin-mediated alterations in BPDE-DNA repair rate.

In spite of this shortcoming, our study provides first experimental evidence of quantitative analysis of dietary curcumin-mediated enhanced disappearance of BPDE-DNA adducts in liver and lungs of B(a)P-treated mice *in vivo*. Furthermore, our results indicate that curcumin post-treatment augments B(a)P-induced apoptosis and that eventually resulted in increased loss of adducts containing cells in mice sacrificed at 24-120 h, suggesting role of apoptosis and/or DNA repair in removal of adduct containing cells. Curcumin-mediated enhanced loss in BPDE-DNA adduct containing cells probably results in reduction in numbers of initiated cells in respective tissues and this along with curcumin-mediated inhibition of cell proliferation in these tissue leads to decrease in tumor multiplicity/tumor area/volume.

7.1 INTRODUCTION

Lung cancer is the most prevalent cancer worldwide in men and most common cause of cancer-related death worldwide [178]. Numerous epidemiological studies have shown that smoking is the major cause of ~90% of lung cancer cases [225-227], and smokers have a 20-fold greater risk of developing lung cancer when compared with persons who have never smoked.

Despite the improvement in medical technology and therapeutic approaches, the 5-year survival rate of this disease has not improved over the last 4-5 decades. Best approaches to curb lung cancer mortality are prevention of smoking initiation and improved methods for smoking cessation. However, the prevalence of tobacco smoking has not changed much during the last three decades [228]. Moreover, former smokers are also at high risk for lung cancer. Therefore, there is an urgent need to develop alternate strategies to reduce lung cancer mortality. Two promising approaches are development of effective chemopreventive agents for both current and former smokers and identification of biomarkers that may help in the early detection of lung cancer.

Out of the 60 carcinogens, nitrosamine 4-(methylnitrosamino)-1-(3- pyridyl)-1-butanone (NNK) and benzo(a)pyrene [B(a)P] are the most important representative carcinogens found in tobacco and tobacco smoke[229]. The tobacco-specific NNK and B(a)P, a prototypical polycyclic aromatic hydrocarbon (PAH), are two of the most potent tobacco smoke carcinogens in rodent models and are strongly implicated in the etiology of lung cancer in smokers [226,230]. B(a)P is metabolized into anti-7,8-dihydroxy-9,10-epoxy-7,8,9,10-tetrahydro benzo(a) pyrene (BPDE), as a major ultimate carcinogen of B(a)P.

Plant-derived natural compounds are receiving increasing attention as chemopreventives for both current and former smokers because of low toxicity and high tolerability. Experimental chemoprevention studies and epidemiological investigations have shown polyphenols to be protective against lung cancer development [64,231-233] and still the search of additional chemopreventive agents is on-going worldwide.

Turmeric and/or its active component curcumin have been shown to inhibit experimentally induced tumorigenesis in several animal models [97,110,122,128,182]. Turmeric/curcumin pre-treatment has been shown to decrease the B(a)P-induced CYP1A1/1A2 activity [215] and the iso-enzymes involved in the metabolism of PAH [B(a)P]. In the present study, we have examined the chemopreventive effects of curcumin if any, on B(a)P-induced experimental lung tumorigenicity in A/J mice. Further, we have

attempted to investigate the possible mechanisms of chemo-protective action of curcumin in A/J mouse lung tumor model.

Our study demonstrates inhibitory effects of dietary curcumin on B(a)P-induced lung tumor burden wherein modulation of cell proliferation and apoptosis markers were noted in this model system.

7.2 METHODS

7.2.1 Animal treatment

Female A/J mice (generation used - 37/38), 6-8 weeks of age, were obtained from The Jackson Laboratory (Bar Harbor, ME, USA) for breeding in Animal house of ACTREC. Inbred female A/J mice (6-8 weeks old, Animal house, ACTREC, India) were randomized into four different groups (group I = Vehicle control (Corn, oil, 0.1 ml); group II = Curcumin control (Cur, 0.05% curcumin in standard laboratory diet); group III = B(a)P (BP, 3 µmol, twice a week for eight weeks); group IV = Curcumin + B(a)P (Cur + BP). The experimental design is shown in figure 7.1. Initially, mice were fed with control diet (powdered standard laboratory diet, groups I and III) or experimental diet (0.05% curcumin in powdered standard laboratory diet, groups II and IV) prepared as described [110] for 2 weeks. Mice of groups 3 and 4 received B(a)P (3 µmol) by gavage, twice a week for 8 weeks and sacrificed after 28 weeks from the last dose of carcinogen. Mice in groups I and II received corn oil as vehicle. The dose and route of curcumin (0.05%) and carcinogen employed in the study was chosen on the basis of results from our previous studies and has been shown to reduce multiplicity, volume and/or incidence of carcinogen-induced tumors at various sites in experimental animals [110,122,128]. Animals in all groups were observed for apparent signs of toxicity such as weight loss (by recording body weights of animals at regular interval i.e. once a week) or mortality during the entire study period. Animals of all groups were sacrificed after 36^{th} week from the first dose of oil/carcinogen and lungs were perfused and excised. Mice were scored for incidence and multiplicity (average number of visible tumors per animal). The whole left lung lobe of all animals belonging to different treatment groups were fixed in 10% buffered formalin for subsequent histopathological analyses. Visible tumors on the remaining lobes of carcinogen-treated mice were microdissected and stored along with its lobes, together with the right lung lobes from respective groups, at -80 °C for immunoblotting studies.

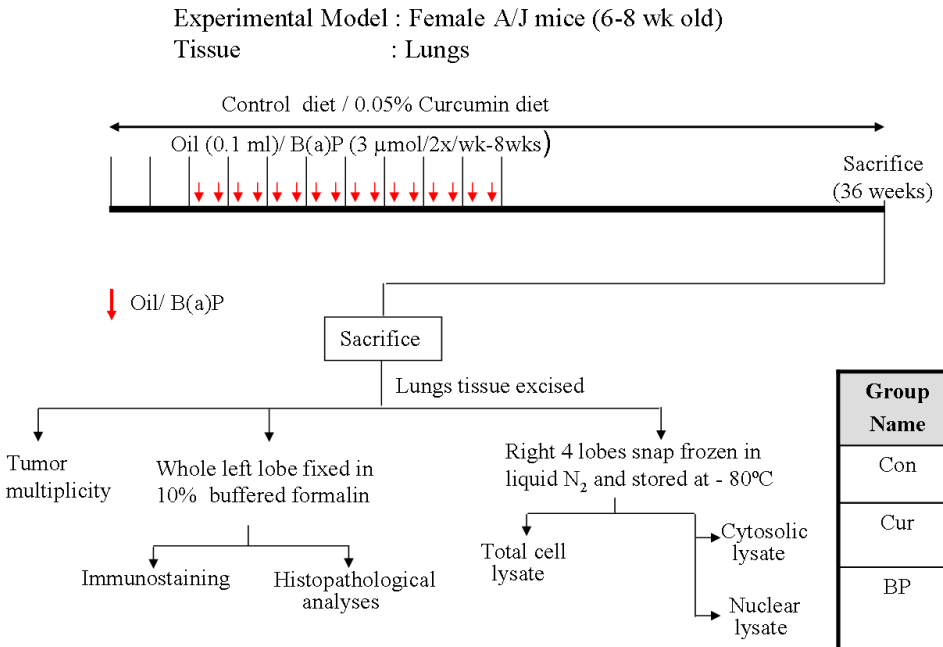

Group Name	Treatment
Con	Vehicle control
Cur	Curcumin (0.05%)
BP	B(a)P (3 µmol/2x/wk-8wks)
Cur + BP	Curcumin (0.05%) + B(a)P

FIGURE 7.1: Experimental design for studying the effect of curcumin treatment on B(a)P-induced lung tumors in A/J mouse model.

7.2.2 Histopathological analysis

Formalin-fixed, paraffin-embedded, four 5 µm thick step tissue sections (each 200 µm apart) were cut and stained with hematoxylin and eosin. The numbers and area of proliferative lesions were counted in each step section and expressed as an average and total area per mouse.

Proliferative lesions in the lungs were classified as hyperplasia, adenoma or adenocarcinoma based on recommendations published by the Mouse Models of Human Cancers Consortium [234]. The category 'adenoma with cellular pleomorphism' (also known as adenoma with dysplasia and adenoma with progression) was added based on previously published literature: an adenoma in which ≥10 cells are pleomorphic, characterized by large cell and/or nuclear size; increased cytoplasmic-to-nuclear ratio; prominent nucleoli; nuclear crowding and increased numbers of mitotic figures with no evidence of parenchymal invasion by pleomorphic cells [233,235-237].Images of representative proliferative lesions have been presented in figure 7.3.

Mice were scored for multiplicity (average number of visible tumors per animal) and tumor area. To determine the area of proliferative lesions, tile scan images of the lesions were taken using an LSM 510 Meta Carl Zeiss confocal system with argon 488-

nm or helium/neon 543-nm lasers. The images were obtained using an Axio Observer Z.1 microscope at a magnification of 10 X and saved as tiff files. Subsequently, the tumor size was determined with the Image J 1.43 (NIH) precalibrated to convert pixels into square microns according to magnification used for acquiring the image. In Image J 1.43 (NIH), the proliferative lesions was outlined with a free hand drawing tool, the area was converted into a single object and the size of this object measured in square microns (μm^2). These data were imported into an Excel file. Further, mean ± SE of numbers and area of different proliferative lesions in the lungs (per mouse) was calculated and are presented in table 7.2 and 7.3.

7.2.3 Protein immunoblotting

Total cell extracts were prepared by a previously described cell fractionation procedure presented in Materials and methods (Chapter 3; section 3.4.1) [138]. For preparations of total cell extract, normal lungs [groups I (Con) and II (Cur)] or microdissected lung tumors [groups III (BP) and IV (Cur + BP)] were used. The expressions of various proteins were studied by SDS-PAGE followed by immunoblotting as described in Materials and methods (Chapter 3; section 3.6). β-actin was used as loading control. Densitometry of various analyte proteins and their respective loading controls from the same blot was performed using Image J 1.43 (NIH) software as described in Materials and methods (Chapter 3; section 3.6.5).

Protein	% gel	Amount of protein	Primary antibody dilution	Secondary antibody dilution
Bax	12%	Total cell lysate, 50 μg	1:1000	1:5000
Bcl-2	12%	″	1:1000	1:5000
Cox-2	8%	″	1:1000	1:5000
Caspase-3	12%	″	1:2000	1:5000
PCNA	10%	″	1:1000	1:4000
Cyclin D1	10%	″	1:500	1:4000
β-actin	Loading controls (same blots were stripped)		1:2000	1:6000

7.2.4 Immunohistochemical staining and analysis

For immunohistochemical (IHC) staining, the whole left lung lobe of controls and carcinogen-treated mice were fixed in 10% buffered formalin. The expression of cyclin D1 (dilution 1:50)/ PCNA (dilution 1:25)/ Ki-67 (dilution 1:100)/ Bax (dilution 1:25)/ Bcl-2 (dilution 1:25)/ AKT (pS473) (dilution 1:50)/ AKT (pT308) (dilution 1:50) were

assayed in paraffin-embedded 5 μm tissue sections, as described in Materials and methods (Chapter 3; section 3.9). Detection was conducted using Vectastain ABC system kit (Vector Laboratories, Burlingame, CA, USA). Diaminobenzidine was employed as the chromogenic substrate, and slides were counterstained with Mayer's haematoxylin. Images were captured with a Zeiss microscope (Imager Z1) to which an Axiocam MRc5 digital camera was attached. For negative or isotype controls, the primary antibody was replaced with PBS/ TBS or respective antibody serum (used at respective antibody concentration). Quantitative analysis of the images (magnification X 400) was done by modified digital image analysis protocols as described previously (Chapter 6; section 6.2.4) [218]. For nuclear protein staining, analysis was performed by counting the total percentage intensity and percentage intensity of high positive, medium positive, and low positive cells; depending upon the color intensities of brown stained nuclei in photomicrographs of atleast 10 randomly selected fields/left lobe section/mouse with atleast four mice per group. More than 1,000 tumor cells were counted per lung tissue section of mice.

However, for cytoplasm protein staining, images of left lobe of lung tissues were used, and the percent area of high positive (3+), medium positive (2+), low positive (1+) that stained brown and negative (0) were calculated as described previously (Chapter 6; section 6.2.4) [218] through Image J 1.43 (NIH) software. Unlike measurements in nuclei, intensity of color in cytoplasm was measured without employing any threshold value. In this method, ranges of pixel intensities were categorized from 0–60 for a score value of high positive (3+), 61–120 for medium positive (2+), 121–170 for low positive (1+) and 171-255 for negative (0). Quantitative analysis was performed by counting pixel wise percentage contribution of total intensity and percentage intensity of high positive, medium positive, and low positive regions in photomicrographs of 10 randomly selected fields/left lobe sections/mouse with atleast four mice per group.

7.2.5 Terminal deoxynucleotidyl transferase biotin-dUTP nick end labeling (TUNEL) assay

Apoptosis was assayed in formalin-fixed, paraffin-embedded 5 μm tissue sections, according to the manufacturer's instructions (*In-situ* TUNEL assay kit, Promega, Madison, WI, USA), as described in Materials and methods (Chapter 3; section 3.12). The nuclei of the apoptotic cells were stained brown in color. Quantitative analysis of the images (magnification X 400) was done by modified digital image analysis protocols as

described previously (Chapter 6; section 6.2.4) [218]. For nuclear protein staining, analysis was performed by counting the total intensity and percentage intensity of high positive, medium positive, low positive cells; depending upon the color intensities of brown stained nuclei in photomicrographs of atleast 10 randomly selected fields/left lobe sections/mouse with atleast three mice per group. More than 1,000 tumor cells were counted per section of mouse lungs.

7.2.6 Statistical analysis

Densitometry and quantitative analysis of images were performed using Image J 1.43 (NIH) software. Statistical analysis was performed using SPSS 15.0 software (IBM, Inc., Chicago, IL, USA) and STATA 12 software (StataCorp, Texas, USA). Data are presented as mean $\pm$ SE. Statistical comparisons among the groups were done using Poisson regression, which is specific for data representing counts or number of events and can handle cases where few or no events occur. Means of western blot analysis data were compared using one-way ANOVA followed by Bonferroni's test. $p \leq 0.05$ was considered statistically significant.

7.3 RESULTS

Observation of the mice once a week for net body weight gain, survival and signs of toxicity, such as changes in fur color or texture, motor and behavioral abnormalities and palpable masses, did not reveal toxicity or mortality in animals belonging to the various treatment groups during the experimental period.

7.3.1 Effect of dietary curcumin on B(a)P-induced pulmonary tumors

Control and experimental animals were sacrificed 36 weeks post first dose of carcinogen/vehicle, and incidence and multiplicity of visible lung tumors and numbers and area of microscopic lesions were compared between control and various treatment groups. A/J mice receiving vehicle oil and maintained on control or 0.05% curcumin diet for 36 weeks did not develop any visible or microscopic tumors through out the experimental period (Table 7.1, Fig. 7.2). However, administration of B(a)P (3 µmol/2x/wk-8wks) through gavage induced visible lung tumors (22.9 ± 1.6) in 100% of A/J mice maintained on control diet and sacrificed at 36 weeks from the first dose of carcinogen (Table 7.1). It was observed that animals maintained on dietary curcumin, 2 wks prior to first dose of carcinogen, during 8 wks of carcinogen and 28 wks post-

carcinogen treatment showed decrease in B(a)P-induced tumor multiplicity (10.7 ± 0.95; by 53%), although tumor incidence was 100% (Table 7.1).

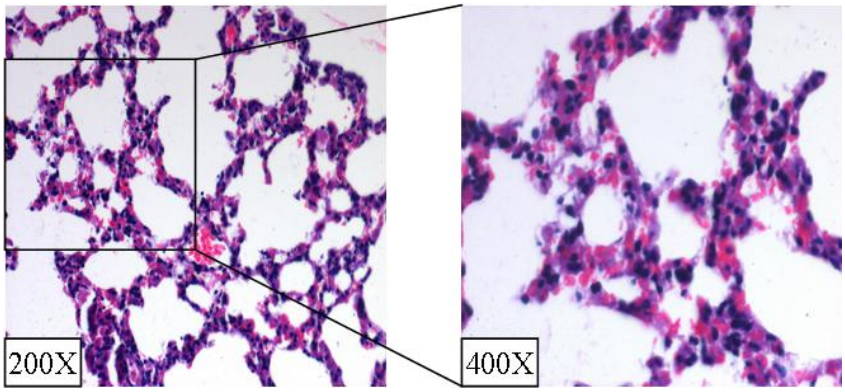

FIGURE 7.2: Haematoxylin & Eosin (H & E) **stained images of representative cross-sections of normal lungs tissues from animals belonging to vehicle control group.**

Microscopic lesions observed in lung tissues of mice were classified as hyperplastic foci, adenoma, adenoma with cellular pleomorphism and adenocarcinoma based on established criteria [234]. Images of representative lung tissue sections showing the various microscopic lesions have been presented in figures 7.3 and 7.4.

TABLE 7.1: Effect of dietary curcumin on B(a)P-induced lung tumors incidence and multiplicity in A/J mice

S. No.	Group	No. of mice	Body weight (g) (mean ± SE)		Tumors	
			Initial	At Termination	Tumor Incidence (%)	Tumors per mouse (mean ± SE)
1	Control (oil)	10	17.13 ± 0.4	23.88 ± 0.42	_	_
2	Curcumin	10	17.12 ± 0.4	23.33 ± 0.64	_	_
3	B(a)P	10	17.97 ± 0.26	22.4 ± 0.38	100 %	22.9 ± 1.6
4	Curcumin + B(a)P	10	17.56 ± 0.22	23.59 ± 0.35	100 %	10.7* ± 0.95

* significant when compared with B(a)P

TABLE 7.2: Relative differences (%) in incidence, multiplicity and area of lung tumors/microscopic lesions in B(a)P and curcumin + B(a)P treated A/J mice

	Hyperplastic foci		Adenoma		Adenoma with cellular pleomorphism		Adenocarcinoma	
	B(a)P	Cur + B(a)P	B(a)P	Cur + B(a)P	B(a)P	Cur + B(a)P	B(a)P	Cur + B(a)P
% of animals bearing tumor/ lesions	100 %	100 %	100 %	100 %	77 % (7/9 animals)	62 % (5/8 animals)	66 % (6/9 animals)	37 % (3/8 animals)
% multi-- plicity (av. no. of lesions/ mouse)	100 %	127 %	100 %	57 %	100 %	11 %	100 %	47 %
% total area/ mouse	100 %	49 %	100 %	74%	100 %	29 %	100 %	34%

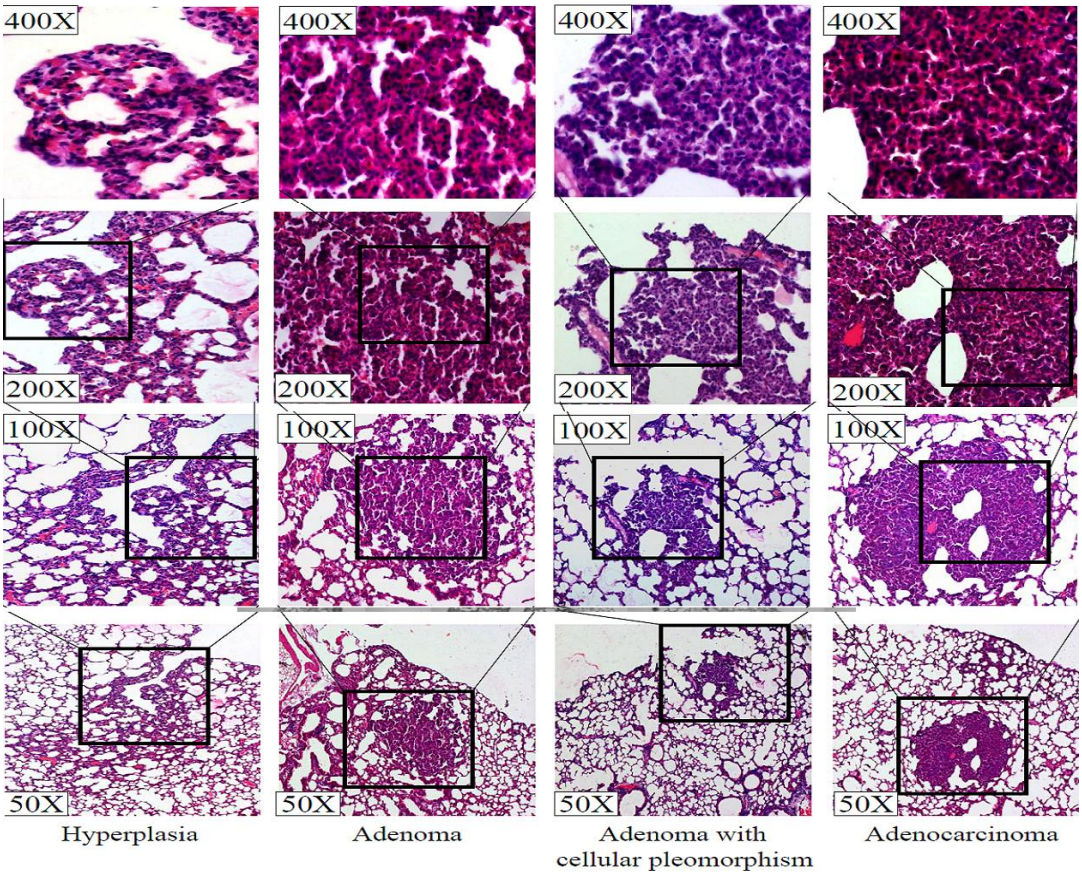

FIGURE 7.3: Different microscopic proliferative lesions in B(a)P-induced lung tumors of A/J mouse (Based on recommendations published by the Mouse Models of Human Cancer Consortium)[234].

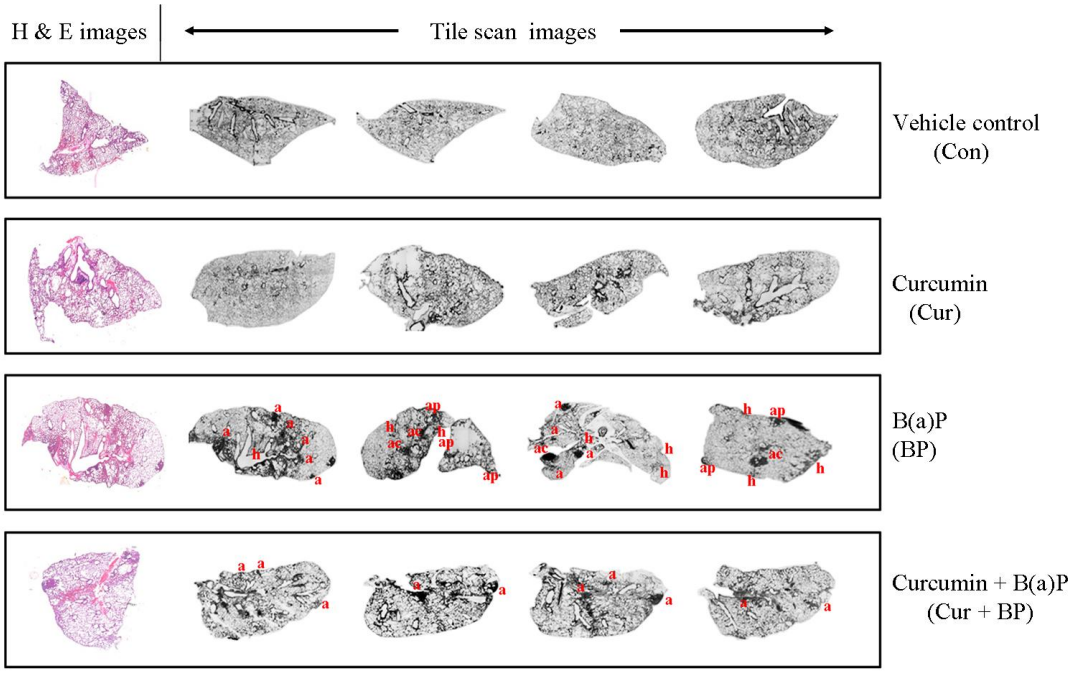

FIGURE 7.4: Haematoxylin & Eosin (H & E) and tile scan images of representative cross-sections of left lung lobe from animals belonging to different treatment groups. *The alphabet h, a, ap, and ac represent hyperplasia, adenoma, adenoma with cellular pleomorphism and adenocarcinoma.*

No pulmonary microscopic proliferative lesions and tumors were detected in any of the lungs/sections of vehicle or curcumin controls (Table 7.3, Figs. 7.2 and 7.4). Incidences of pulmonary hyperplastic foci, adenoma, adenoma with cellular pleomorphism and adenocarcinoma were 100, 100, 77, 66%, respectively in B(a)P-treated (group III) whereas incidence of hyperplastic foci, adenoma, adenoma with cellular pleomorphism and adenocarcinoma were 100, 100, 62, 37%, respectively in Curcumin + B(a)P (group IV), and the differences observed were not statistically significant (Table 7.2). As shown in Table 7.3, multiplicities of hyperplastic foci, adenoma, adenoma with cellular pleomorphism and adenocarcinoma in mice treated with carcinogen only (group III) were 7.67 ± 1.17, 16.22 ± 0.52, 6.11 ± 3.47 and 1.89 ± 0.68, respectively. Dietary curcumin however, significantly decreased the multiplicities of adenoma (9.25 ± 1.85, $P \leq 0.0001$) and adenoma with cellular pleomorphism (0.63 ± 0.26, $P \leq 0.0001$) although the multiplicities of hyperplastic foci (9.75 ± 1.94, $P \leq 0.146$) and adenocarcinoma (0.88 ± 0.48, $P \leq 0.087$) were not significantly different when compared to group III [B(a)P treated group] (Table 7.3).

After observing curcumin-mediated decrease in number of microscopic pulmonary lesions, we further checked the effect of curcumin on area of microscopic

pulmonary lesions per mouse as well. To answer this question, the total area of each microscopic lesion was measured using the Image J 1.43 (NIH) software.

TABLE 7.3: Effect of dietary curcumin on B(a)P-induced microscopic pulmonary lesions numbers in A/J mice

S. No.	Group	No. of mice	Hyperplastic foci per mouse	Adenoma per mouse	Adenoma with cellular pleomorphism per mouse	Adeno-carcinoma per mouse
1	Control (oil)	9	–	–	–	–
2	Curcumin	9	–	–	–	–
3	B(a)P	9	7.67 ± 1.17	16.22 ± 0.52	6.11 ± 3.47	1.89 ± 0.68
4	Curcumin + B(a)P	8	9.75 ± 1.94	9.25* ± 1.85	0.63* ± 0.26	0.88 ± 0.48

* significant when compared with B(a)P

There were no microscopic lesions in control and vehicle treated animals. In mice treated with B(a)P, total area of microscopic lesions per mouse for hyperplasia, adenoma, adenoma with cellular pleomorphism and adenocarcinoma were found to be 0.8 ± 0.01, 1.07 ± 0.005, 1.09 ± 0.029 and 0.23 ± 0.049. Dietary curcumin however, significantly decreased the area of above lesions by 51, 25, 70 and 65%, respectively (Table 7.4).

TABLE 7.4: Effect of dietary curcumin on area of B(a)P-induced microscopic pulmonary lesions in A/J mice

S. No.	Group	No. of mice	Hyperplastic foci area per mouse (mm^2)	Adenoma area per mouse (mm^2)	Adenoma with cellular pleomorphism area per mouse (mm^2)	Adeno-carcinoma area per mouse (mm^2)
1	Control (oil)	9	–	–	–	–
2	Curcumin	9	–	–	–	–
3	B(a)P	9	0.8 ± 0.01	1.07 ± 0.005	1.09 ± 0.029	0.23 ± 0.049
4	Curcumin + B(a)P	8	0.39* ± 0.03	0.80* ± 0.07	0.32* ± 0.09	0.08* ± 0.02

* significant when compared with B(a)P

7.3.2 Effect of curcumin treatment on B(a)P-mediated apoptosis in lung tumor tissue of mouse

Decrease in visible tumor multiplicity and area of microscopic lesions in lung tumors upon curcumin treatment suggests its role in apoptosis and/or cell proliferation. To investigate this, lung tumor extracts were used for western blot analysis and left lung lobes (equal size and similar cell numbers) were used for comparative immunohistochemical analysis of apoptosis related markers such as Bax, Bcl-2 and caspase-3. In western blot analysis, levels of Bax and Bcl-2 protein in curcumin treated group were comparable with those of vehicle control. As compared to vehicle and curcumin control (normal lungs), levels of pro-apoptotic protein, Bax was significantly decreased, whereas levels of Bcl-2, an anti-apoptotic protein was increased significantly in the lung tumor extracts of B(a)P-treated mice (Fig. 7.5A). Importantly, dietary curcumin treatment significantly abrogated the B(a)P-induced expression of Bcl-2, and increased the expression of Bax in lung tumor extracts. Dietary curcumin-mediated inhibition of B(a)P-induced anti-apoptotic response was also reflected in increased Bax/Bcl-2 ratio (Fig. 7.5B). Furthermore, in immunohistochemical analysis of entire left lobe, total % intensity of Bax and Bcl-2 proteins in curcumin control (group III) was similar to vehicle control (group I). Compared to vehicle/curcumin control, total % intensity of Bax protein was significantly decreased whereas total % intensity of Bcl-2 protein was significantly increased in the left lobe derived tissues sections (bearing tumor) in B(a)P-treated mice. Dietary curcumin significantly increased the B(a)P-altered total intensity of Bax protein, whereas it decreased the B(a)P-induced total intensity of Bcl-2 in lung tumor tissues. This decrease was also evident when % intensity of high, medium and low levels of cytoplasm staining was compared among lung tissues sections from animals belonging to different treatment groups. Results suggest that modulations of Bax and Bcl-2 in B(a)P-treated mice upon curcumin treatment was mainly contributed by alteration in % intensity of high positive stained region (Fig. 7.5B). Furthermore, quantitative measurements of apoptotic index in terms of total apoptotic nuclei intensity as well as % of positive apoptotic cells in left lobe of mice showed that dietary curcumin treatment increased apoptosis in lung tumor tissues of B(a)P-treated mice, as observed by the TUNEL assay (Fig. 7.7).

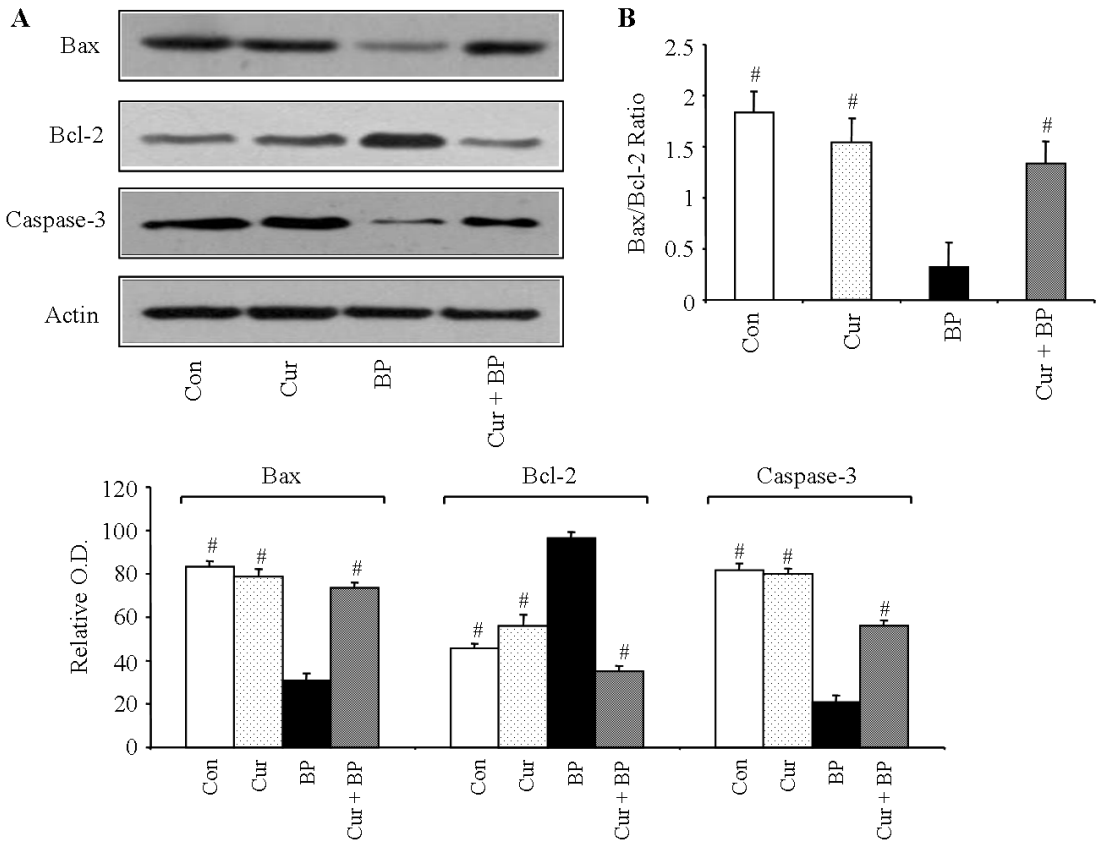

FIGURE 7.5: Effect of curcumin treatment on apoptosis-related markers in B(a)P-treated mouse lungs/lung tumors.(A) *Representative blots and relative levels of Bax, Bcl-2 and caspase-3 protein measured in total cell lysates prepared from mouse lung tissue (control and curcumin treated) and lung tumors [B(a)P and curcumin + B(a)P treated) and analyzed by immunoblotting using specific antibodies. β-actin was used as the loading control.* **(B)** *Extent of apoptosis was determined by calculating the ratio of normalized band intensity of Bax and Bcl-2 in respective tissues. Data represent mean ± SE of three observations. Differences among groups were determined by one-way ANOVA followed by Bonferroni's test, $p \leq 0.05$. '∗' significant when compared with control; '#' significant when compared with B(a)P.*

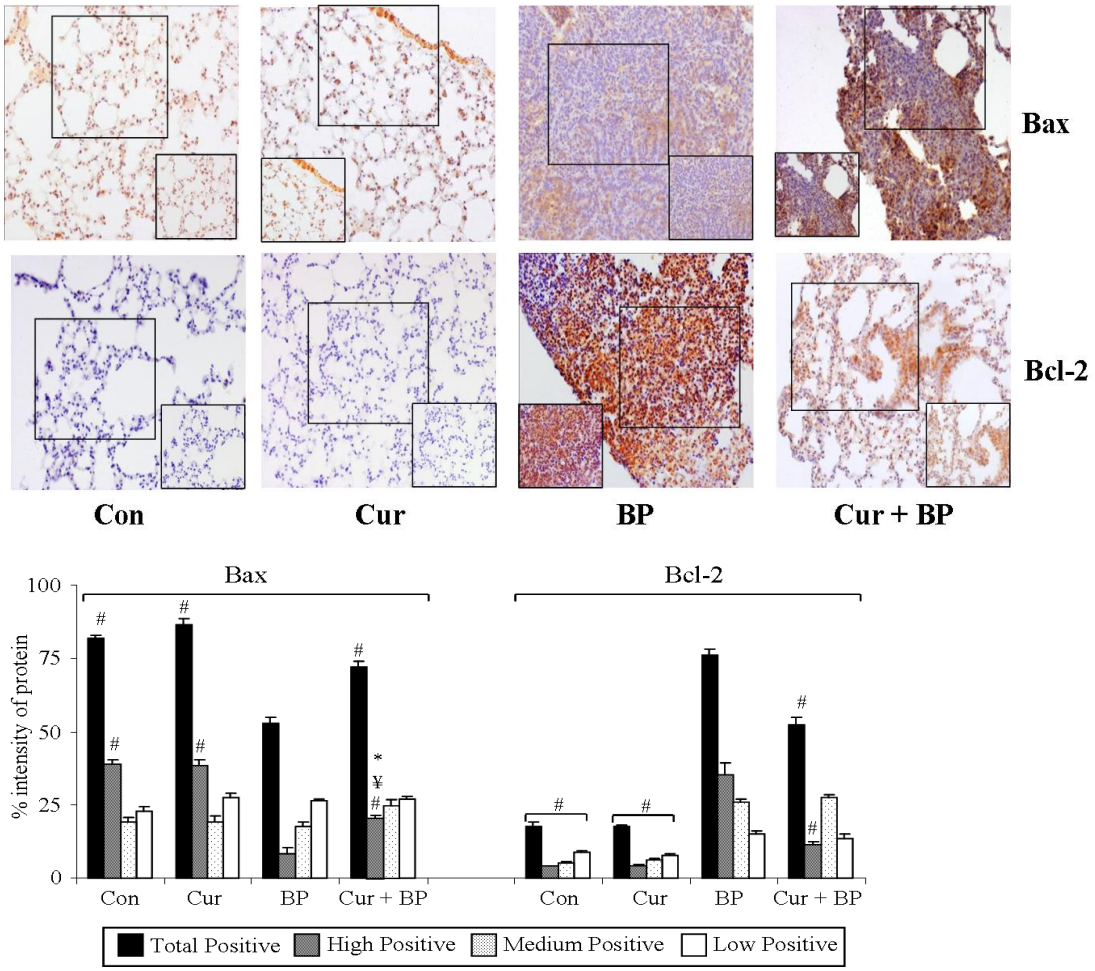

FIGURE 7.6: Effect of curcumin treatment on apoptosis-related markers in B(a)P-treated mouse lungs measured by immunohistochemical staining. *Representative photomicrographs showing immunohistochemical detection of % intensity of Bax and Bcl-2 (magnification X 200; insert shows 400 X magnification) in formalin-fixed, paraffin-embedded tissue sections of mouse lungs, using specific antibodies. Quantitative analysis was done by digital image analysis as described under Materials and methods (section 7.2.4) in photomicrographs of 10 randomly selected fields/section/mouse, with atleast three mice per group. Data represent mean ± SE of three observations. Differences among groups were determined by Poisson regression analysis ($p \leq 0.05$) using STATA 12 software. '*' significant when compared with control; '#' significant when compared with B(a)P; '¥' significant when compared with curcumin.*

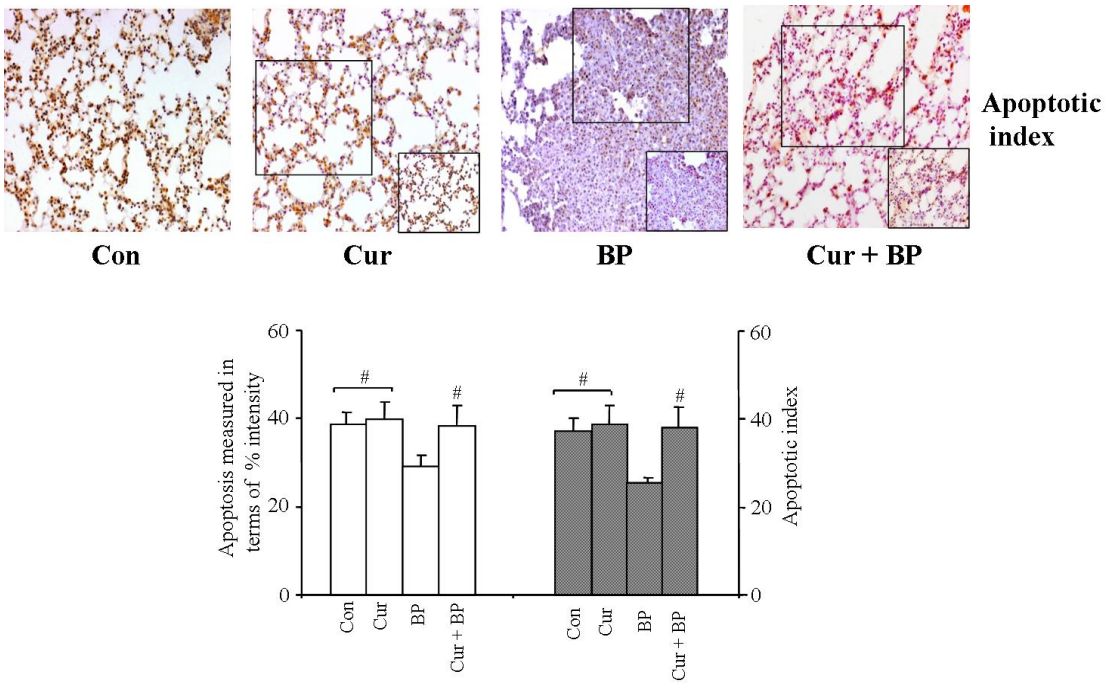

FIGURE 7.7: Effect of curcumin treatment on apoptotic index in B(a)P-treated mouse lungs measured by TUNEL assay. *Representative photomicrographs showing immunohistochemical detection of levels of cell turnover or extent of apoptosis (magnification X 200; insert shows 400 X magnification) in formalin-fixed, paraffin-embedded tissue sections of mouse lungs, using specific antibody. Quantitative analysis was done by digital image analysis as described under Materials and methods (section 6.2.4) in photomicrographs of 10 randomly selected fields/section/mouse, with atleast three mice per group. Data represent mean ± SE of three observations. Differences among groups were determined by Poisson regression analysis ($p \leq 0.05$) using STATA 12 software. '#' significant when compared with B(a)P.*

7.3.3 Effect of curcumin treatment on B(a)P-induced cell proliferation and survival-related proteins in lungs/lung tumor tissue of mouse

To examine the role of cell proliferation if any, in dietary curcumin-mediated decrease in tumor area and multiplicity in lung tumors, extracts from lung tumor were compared by western blot analysis and left lung lobe (equal size and similar cell numbers) was used for comparative immunohistochemical analysis of cell proliferation markers such as cyclin D1, PCNA and Ki-67. Level of cyclin D1 and PCNA protein in curcumin treated group was comparable with those of vehicle control, when measured by western blot analysis. As compared to vehicle and curcumin control (normal lungs), levels of cyclin D1 and PCNA protein was significantly increased in lung tumor tissues of B(a)P-treated mice (Fig. 7.8). However, dietary curcumin treatment significantly decreased the B(a)P-induced

expression of cyclin D1 and PCNA in lung tumor extracts (Fig. 7.8). To complement the results from western blot analysis, immunohistochemical staining of cyclin D1, PCNA and Ki-67 were carried out in left lobe derived tissues sections of mice. Compared to vehicle/curcumin control, total % intensity of cyclin D1, PCNA and Ki-67 proteins were significantly increased in the left lobe derived tissues sections (bearing tumor) in B(a)P-treated mice (Fig. 7.9). However, similar to western blot results, dietary curcumin significantly decreased the B(a)P-induced total intensity of cyclin D1, PCNA and Ki-67 proteins, respectively in tissue sections of mouse lungs. This decrease was also evident when comparison of % intensity of nuclei containing high, medium and low levels of protein(s) expression was made. The observed decrease in total % intensity of proteins appears to be contributed mainly by reduction in % intensity of nuclei containing high levels of cyclin D1, PCNA and Ki-67 protein expression (Fig. 7.9).

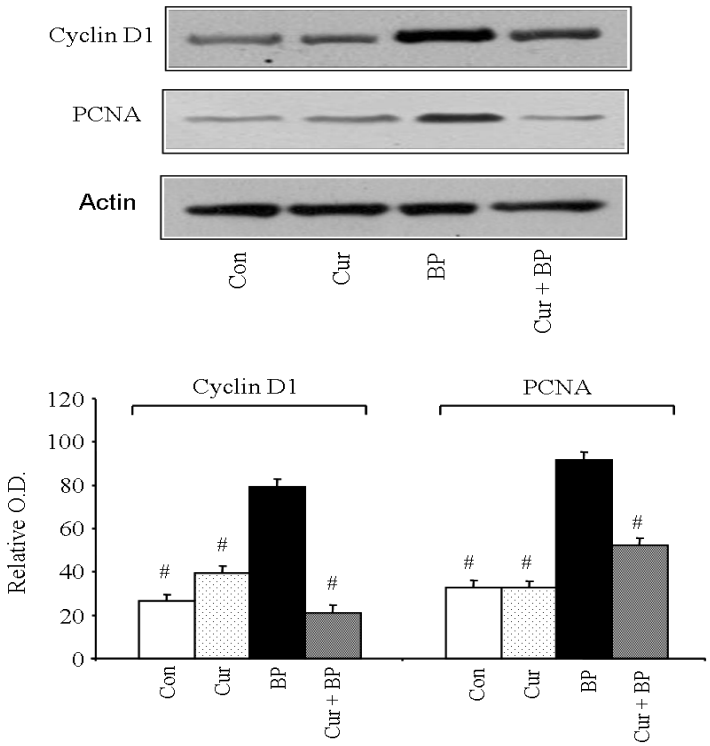

FIGURE 7.8: Effect of curcumin treatment on cell proliferation markers in B(a)P-treated mouse lungs/lung tumors.*Representative blots and relative levels of PCNA and cyclin D1 protein measured in total cell lysates prepared from mouse lungs/lung tumors and analyzed by immunoblotting using specific antibodies. β-actin was used as the loading control. Data represent mean ± SE of three observations. Differences among groups were determined by one-way ANOVA followed by Bonferroni's test, $p \leq 0.05$. '#' significant when compared with B(a)P.*

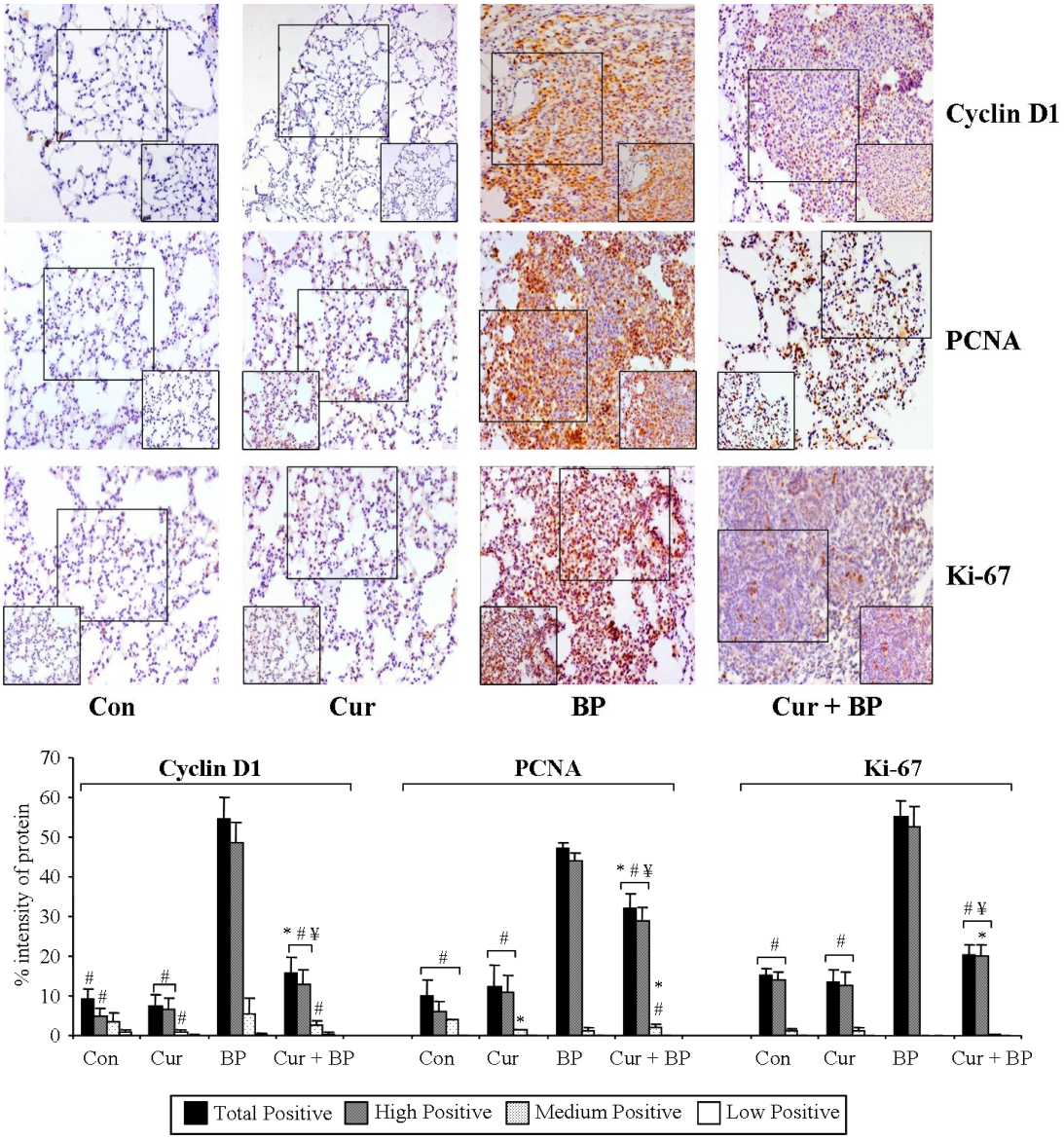

FIGURE 7.9: Effect of curcumin treatment on cell proliferation markers in B(a)P-treated mouse lungs measured by immunohistochemical staining. *Representative photomicrographs showing immunohistochemical detection of % intensity of cyclin D1, PCNA and Ki-67 (magnification X 200; insert shows 400 X magnification) in formalin-fixed, paraffin-embedded tissue sections of mouse lungs, using specific antibodies. Quantitative analysis was done by digital image analysis as described under Materials and methods (section 6.2.4) in photomicrographs of 10 randomly selected fields/ section/ mouse, with atleast four mice per group. Data represent mean ± SE of four observations. Differences among groups were determined by Poisson regression analysis ($p \leq 0.05$) using STATA 12 software. '*' significant when compared with control; '#' significant when compared with B(a)P; '¥' significant when compared with curcumin.*

Further, effect of dietary curcumin on phosphorylation of AKT was investigated. Compared to vehicle/curcumin control, total % intensity of phospho-AKT (S473 and T308) proteins were significantly increased in the lung tissues section bearing tumor in B(a)P-treated mice. Interestingly, dietary curcumin significantly decreased the B(a)P-

induced total intensity of phospho-AKT (S473 and pT308) proteins in left lobe of mouse. This decrease was also evident when comparison of % intensity of nuclei containing high, medium and low levels of protein(s) expression was made. The observed decrease in total % intensity of proteins appear to be attributed mainly by reduction in % intensity of high stained region in levels of phospho-AKT (S473 and pT308) protein expression (Fig. 7.10).

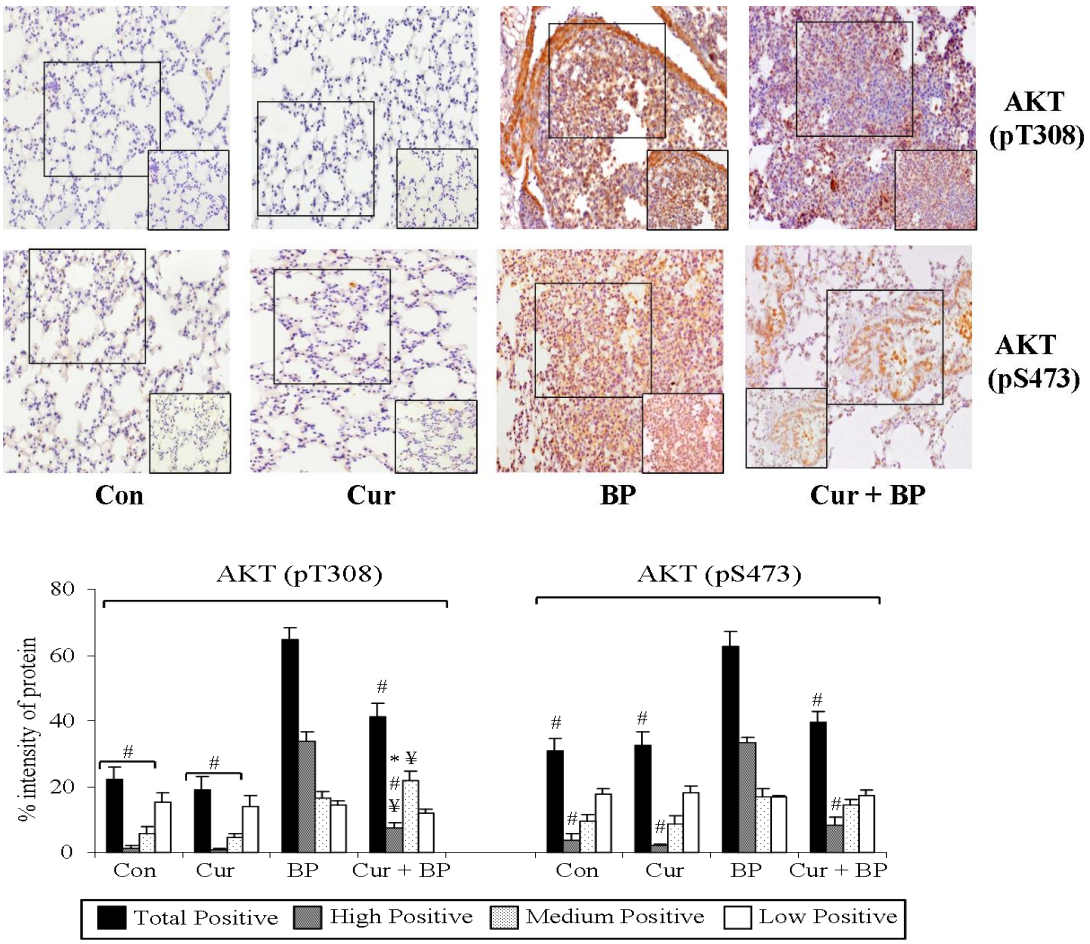

FIGURE 7.10: Effect of curcumin treatment on AKT phosphorylation in B(a)P-treated mouse lungs measured by immunohistochemical staining. *Representative photomicrographs showing immunohistochemical detection of % intensity of AKT (pT308) and AKT (pS473) (magnification X 200; insert shows 400 X magnification) in formalin-fixed, paraffin-embedded tissue sections of mouse lungs, using specific antibodies. Quantitative analysis was done by digital image analysis as described under Materials and methods (section 7.2.4) in photomicrographs of 10 randomly selected fields/section mouse, with atleast three mice per group. Data represent mean ± SE of three observations. Differences among groups were determined by Poisson regression analysis ($p \leq 0.05$) using STATA 12 software. '*' significant when compared with control; '#' significant when compared with B(a)P; '¥' significant when compared with curcumin.*

7.3.4 Effect of curcumin treatment on B(a)P-induced inflammation marker in lung tumor tissue of mouse

Having observed the effects of dietary curcumin treatment on B(a)P-mediated apoptosis and cell proliferation markers in lung tumors, we next examined the effect of dietary curcumin on B(a)P-induced inflammatory response marker in lung tumor extracts by western blot analysis. Level of cox-2 protein in curcumin treated group was comparable with those of vehicle control, when measured by western blot analysis. As compared to vehicle and curcumin control (normal lungs), levels of cox-2 protein was significantly increased in lung tumor tissues of B(a)P-treated mice (Fig. 7.11). However, dietary curcumin treatment significantly decreased the B(a)P-induced expression of cox-2 in lung tumor tissues (Fig. 7.11).

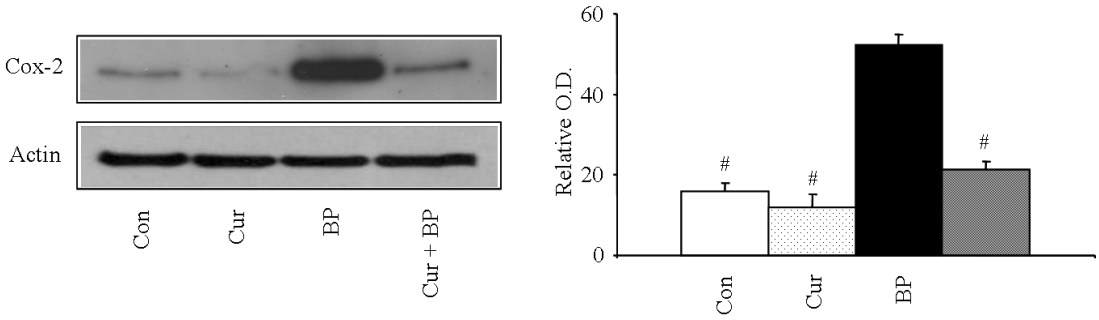

FIGURE 7.11: Effect of curcumin treatment on cell inflammation marker in B(a)P-treated mouse lungs/lung tumors.*Representative blots and relative levels of cox-2 protein were measured in total cell lysates prepared from mouse lungs/lung tumors and analyzed by immunoblotting using specific antibody. β-actin was used as the loading control. Data represent mean ± SE of three observations. Differences among groups were determined by one-way ANOVA followed by Bonferroni's test, $p \leq 0.05$. '#' significant when compared with B(a)P.*

7.4 DISCUSSION

The present investigation was undertaken to examine the chemopreventive efficacy/tumor inhibitory effects of curcumin against B(a)P-induced experimental lung carcinogenesis in A/J mice, measured in terms of incidence and multiplicity of visible lung tumors. Further, effects of dietary curcumin was also observed on numbers and area of microscopic lesions classified as hyperplasia, adenoma, adenoma with cellular pleomorphism and adenocarcinoma based on recommendations published by the Mouse Models of Human Cancers Consortium[234]. Our results showed absence of spontaneous

visible tumors in animals of control and/or curcumin group as compared to the reports where incidence of spontaneous lung tumors have been observed in A/J mice [237-239]. This is probably because of diet rich in plant-derived proteins inhibiting spontaneous tumor formation in A/J mice, under the experimental conditions employed in our study. In the present study, B(a)P-induced lung tumor incidence, multiplicity, histological types were similar to those observed by others for this model, although optimal time for induction of tumors was longer in our study (36 weeks) as compared to reported studies (26 weeks)[131]. This further suggests the role of diet in delaying the onset of B(a)P-induced lung tumor formation in A/J mice. Dietary constituents such as indoles, isothiocyanates etc. when added to NIH-07 diet resulted in significant inhibition of tumor multiplicity[240-242]. However, the role of diet in the present study is speculative and/or suggestive evidence and remains to be proved. Diet employed in other studies wherein spontaneous lung tumors have been reported was synthetic AIN-76 containing (g/kg): vitamin free casein, 200; dl-methionine, 3; cornstarch, 470; dyetrose corn starch, 50; dextrose, 130; cellulose, 50; corn oil, 50; salt mix, 35; vitamin mix, 10; choline bitartrate, 2; while diet employed in our study contained (g/kg): cracked wheat, 410; roasted bengal gram powder, 500; casein powder, 50; refined oil, 10 (v/w); skimmed milk powder, 10; yeast powder, 5 and common salt, 5; and known to induce phase II enzymes[186].

B(a)P-treatment resulted in development of hyperplasia and adenoma in 100% of animals (9/9 animals) while incidence of adenoma with cellular pleomorphism and adenocarcinoma were observed to be 77% (7/9 animals) and 66% (6/9 animals), respectively. The observed differences are not significant and therefore, more numbers of animals need to be included to see the effects of dietary curcumin on adenocarcinoma. Dietary curcumin decrease the multiplicity of lung adenoma without inhibiting the tumor incidence, while multiplicity of hyperplastic foci and adenocarcinoma was not altered. However, it may be noted that curcumin significantly decrease the areas of microscopic hyperplastic foci, adenomas, adenomas with cellular pleomorphism and adenocarcinoma. Turmeric/curcumin has been shown to modulate incidence and/or multiplicity and/or latency period of chemical-induced carcinogenesis at various organ sites in several experimental models [97]. Observed differential effects of curcumin in terms of incidence vs multiplicity, and adenoma vs adenocarcinoma and hyperplastic foci are similar to those observed with others polyphenols and/or chemopreventive agents [233,237]. Curcumin has been shown to inhibit CYP1A1/ CYP1A2 and CYP 2B1 *in vitro*, which are involved in metabolism of tobacco derived carcinogens i.e. B(a)P and NNK [215]. Curcumin has

also been reported to inhibit B(a)P-induced activity and levels of CYP1A1/1A2 in mouse tissues [186] and to induce phase II enzymes/isozymes [186]. Earlier studies from our laboratory have shown that curcumin treatment decreased the formation of carcinogen-DNA adducts in mouse tissue [243]. In a recent study, we have observed curcumin-mediated enhancement in disappearance of BPDE DNA-adducts in mouse tissues (Chapter 6). Altogether, observed curcumin-mediated alteration results in decrease in levels of carcinogen-derived DNA adducts or DNA damage, ultimately leading to decrease of tumor multiplicity. In addition, the lung tumor inhibitory effects of curcumin treatment could also be due to inhibition of cell proliferation and/or induction of apoptosis as reported for curcumin [99,Chapter 5] as well as other chemopreventive agents [232,238, 244].

Bax, a pro-apoptotic protein, and Bcl-2, an anti-apoptotic protein, are important mediators/ markers for apoptosis. Overexpression of Bcl-2, a key event in malignant transformation has been reported to be associated with down-regulation of Bax. Observed increase in curcumin-mediated Bax/Bcl-2 ratio and enhanced apoptotic index and activation of caspase-3 results in elimination of carcinogen damaged cells thereby leading to protection against B(a)P-induced tumorigenesis[186]. Similar reports on modulatory effects on Bax/Bcl-2 ratio and apoptotic index and activation of caspases have also been observed with curcumin as well as other polyphenols in several *in vitro* and *in vivo* systems [245,246]. These results are in agreement with our recent report wherein dietary turmeric (1%) post-treatment has been shown to enhance DMBA-mediated apoptosis and inhibits cell proliferation resulting in decreased tumor burden in hamsters buccal pouch [99,Chapter 5]. This suggests the common mode of actions of polyphenol(s) when administered after exposure to carcinogen. Turmeric/curcumin has been shown to inhibit carcinogen/ tumor promoter-mediated cell proliferation both *in vitro* and *in vivo*[97].

The observed decrease in apoptosis and upregulation of PCNA, cyclin D1 and Ki-67 in B(a)P-induced lung tumors is in line with earlier reports [238]. Significant curcumin-mediated decreases observed in our study on the expression of PCNA and cyclin D1 in B(a)P-induced lung tumors are in line with earlier reports on polyphenols i.e. indole-3-carbinol [238]. Curcumin decreased B(a)P-induced activation of AKT, a key protein involved in cell survival resulting in decreased cell survival of damaged cells. The observed inhibition of phosphorylation of AKT could also lead to induction of apoptosis.

The A/J mouse model has been extensively used for studying the effects of chemopreventive agents on lung tumor formation [247,248]. Others groups have

previously shown the chemopreventive effects of polyphenols when given before, during, or after the carcinogen treatment [231,249]. Our observations of curcumin-mediated decrease in B(a)P-induced lung tumors in A/J mouse differ from those reported by Hecht et al., (1999) [131]. It may be noted that experiment by Hecht et al. (1999) was conducted in 1999 and experimental conditions employed by them were different from our experimental conditions on several counts as given below which may have contributed to differences in the outcome of results.

S. No.	**Parameters**	**Present study**	**Hecht et al., (1999) study [131]**
1	Carcinogen used	B(a)P	B(a)P + NNK
2	Curcumin dose	0.05% in diet	0.2% in diet
3	Curcumin exposure	2 weeks prior, during carcinogen exposure and subsequent till 36 weeks	1 week after the exposure to carcinogen for 26 weeks
4	Total exposure time to curcumin	38 weeks	26 weeks
5	End point measurements	Visible + microscopic lesions i.e. hyperplastic foci, adenomas, adenomas with cellular pleomorphism and adenocarcinoma	Visible surface tumors, no evaluation of microscopic lesions and histogical types
		Curcumin has been shown to be relatively better inhibitor of B(a)P metabolizing CYP1A1/1A2 compared to NNK metabolizing CYP2B1	

Considering differences in this observation, curcumin-mediated effects need to be replicated in the same laboratory and confirmed by independent observations in other laboratories. Overall, evidence available so far suggests turmeric/curcumin to be better chemopreventive agent than its chemotherapeutic activity. Based on the effect of curcumin on apoptosis and/or cell proliferation, it may be having some of the effects/properties shown by anti-cancer agent(s) although it is not likely to match chemotherapeutic activity of established anti-cancer agents. Considering the effects of curcumin on carcinogen-modulated cell proliferation and/or apoptosis, it will be worthwhile to study the effects of curcumin on enhancement of chemotherapeutic efficacy of some established anti-cancer agents or reduce their toxicity.

In conclusion, the results of the present study show that dietary curcumin administered prior, during and subsequent to the carcinogen treatment inhibits B(a)P-induced lung-tumors. The observed inhibition appears to be due to curcumin-mediated

inhibition of cell proliferation and enhancement of apoptosis of DNA damage containing cells.

8.1 SUMMARY OF THE WORK

Cancer continues to be one of the major cause of deaths in developed countries and accounts for over 12% of deaths globally [250]. Majority of human cancers are caused, mediated, or modified by environmental factors. Although dose and duration of exposure to exogenous/endogenous carcinogen(s) is one of the determining factors, that alone is not sufficient to explain the exposure-related outcome, as majority of cancers result from complex interactions between environmental exposure(s) and genetic/acquired susceptibility or protective host factors. Causal relationships have been established for some cancers, for example, tobacco intake has been established as the cause for oral cancer, while for many other cancers the quest for a cause still continues. Elimination of proven carcinogens from the environment, i.e. primary prevention of cancer, and current treatment approaches have met with limited success. Based on the experience with some infectious diseases and the recent progress in cardiology, prevention of diseases appears to be one of the attractive, cost effective and achievable approaches However, the compounds that have shown chemopreventive efficacy in pre-clinical studies have met with limited success in clinical trials. Hence, much of the research is now focused on understanding the mechanistic aspects of their chemopreventive actions, rather than only tumor, as the end-point and/or it is implemented in clinical trials [22].It should also be remembered that carcinogenesis occurs over time, potentially with different mechanisms assuming primary importance during different stages of cancer development. Hence, interventions need to be tailored to the processes that occur at individual target organs over time. Also, there is need to develop models of clinical trials that can efficiently identify promising agents for cancer prevention in different target organs. This requires the identification of biomarkers that reflect clinical benefit, and, eventually the validation of these markers if they are to be used as surrogates.

8.1.1 Chapter 4: Polymeric black tea polyphenols modulate the localization and activity of 12-*O*-tetradecanoylphorbol-13-acetate-mediated kinase(s) in mouse skin: mechanisms of their anti-tumor-promoting action

Polymeric black tea polyphenols (PBPs) have been shown to possess anti-tumor-promoting effects in two-stage skin carcinogenesis. However, their mechanisms of action are not fully elucidated. In the present study, mechanisms of PBPs-mediated anti-promoting

effects were investigated in mouse model employing tumor promoter, 12-*O*-tetradecanoylphorbol-13-acetate (TPA). Compared to controls, single topical application of TPA to mouse skin increased the translocation of protein kinase C (PKC) from cytosol to membrane. Pre-treatment with PBPs 1-3 decreased TPA-induced translocation of PKC isozymes (α, β, η, γ, ε) from cytosol to membrane, whereas PBPs 4 and 5 were less effective. The levels of PKC δ and ζ in cytosol/membrane were similar in all the treatment groups. Complementary confocal microscopic evaluation showed a decrease in TPA-induced PKCα fluorescence in PBP-3 pre-treated membranes, whereas pre-treatment with PBP-5 did not show similar decrease. Based on the experiments with specific enzyme inhibitors and phosphospecific antibodies, both PBP-3 and PBP-5 were observed to decrease TPA-induced level and/or activity of phosphatidylinositol 3-kinase (PI3K) and AKT1 (pS473). An additional ability of PBP-3 to inhibit site-specific phosphorylation of PKCα at all the three positions responsible for its activation [PKCα (pT497), PKC PAN (βII pS660), PKC α/βII (pT638/641)] and AKT1 at Thr308 position, along with decrease in TPA-induced PDK1 protein level, correlated with the inhibition of translocation of PKC, which may impart relatively stronger chemo-protective activity to PBP-3 than to PBP-5. Altogether, PBP-mediated decrease in TPA-induced PKC phosphorylation correlated well with decreased TPA-induced NF-κB phosphorylation and downstream target proteins associated with proliferation, apoptosis and inflammation in mouse skin. Results suggest that anti-promoting effects of PBPs are due to modulation of TPA-induced PI3K-mediated signal transduction.

8.1.2 Chapter 5: Dietary turmeric post-treatment decreases DMBA-induced hamster buccal pouch tumor growth by altering cell proliferation and apoptosis-related markers

In the present study, post-treatment effects of dietary turmeric on markers related to apoptosis, cell proliferation, and inflammation in 7,12-dimethylbenz(a)anthracene (DMBA)-induced hamster buccal pouch (HBP) tumors were investigated. Tumors were induced by applying 0.5% DMBA topically to the HBP three times per week for 12 weeks. After tumor development, half of the animals continued on the control diet and the other half were shifted to a 1% turmeric diet for 4 weeks. To rule out DMBA discontinuation as a cause of inhibition in tumor growth, DMBA treatment was continued during dietary exposure of turmeric in another set of animals until the end of the experiment. The turmeric diet inhibited tumor

growth in animals with or without DMBA carcinogen treatment compared to the animals on the control diet. When compared to hamsters bearing tumors that remained on the control diet, the buccal pouches of hamsters bearing tumors receiving turmeric showed the following results: (1) decreased cell proliferation (diminished PCNA, cyclin D1, and Bcl-2) and PCNA labeling index, (2) enhanced apoptosis (increased Bax, caspase-3, caspase-9, and cytochrome c, and decreased survivin) and apoptotic index, (3) decreased inflammation (decreased cox-2), and (4) decreased MAPK activation (p-ERK and p-p38). These data indicate that tumor growth decreased due to the modulation of cellular pathways associated with cell proliferation and apoptosis.

8.1.3 Chapter 6: Dietary curcumin post-treatment enhances the disappearance of B(a)P-derived DNA adducts in mouse liver and lungs

In the present study, post-treatment effects of dietary curcumin on the levels of B(a)P-induced DNA adducts in mouse tissues were investigated. Mice were administered oil (Vehicle, V group) or B(a)P (1 mg gavage, BP group) and were randomized after 24 h into 7 subgroups. Animal belonging to one of the subgroups from both the groups were sacrificed at 24 h (i.e. V 24h or BP 24h, experiments 1 and 2) while half of the remaining 6 subgroups were either continued on control diet or shifted to 0.05% curcumin diet and sacrificed after 24, 72 and 120 h (experiment 1), and 7, 14, 28 days (experiment 2). Immunohistochemical staining employing specific antibody was used to measure the area and intensity of stained nuclear adducts in tissue sections and analyzed by image J analysis. Quantitative comparisons suggested time dependent decrease in the levels of BPDE-DNA adducts in B(a)P-treated animals and the observed decrease was further enhanced by curcumin exposure when compared to the levels in time-matched controls in experiments 1 and 2. To assess the contribution of apoptosis and/or dilution of adducted DNA by cell proliferation, if any in observed curcumin-mediated enhanced decrease of BPDE-DNA adducts; comparative evaluation of apoptosis (by TUNEL assay and related parameters) and cell proliferation (PCNA by western blot) was undertaken. Results suggested enhancement of B(a)P-induced apoptosis in liver and lungs by curcumin during 24-120 h while there was no such enhancement observed at 8-28 days. Overall results suggest curcumin-mediated enhancement

in apoptosis and DNA repair (experiment 1) and BPDE-DNA adducts dilution and/ or DNA repair (experiment 2) of BPDE-DNA adducts.

8.1.4 Chapter 7: Dietary curcumin inhibits B(a)P-induced lung tumors by modulating apoptosis and cell proliferation-related markers in A/J mice

In the present study, chemopreventive efficacy of curcumin against lung tumorigenesis induced by benzo(a)pyrene [B(a)P] in A/J mice was evaluated. B(a)P (3 µmol) was administered twice a week for eight weeks by gavage, whereas dietary curcumin (0.05%) was given 2 weeks prior, during carcinogen treatments and continued up to 36 weeks from the first dose of carcinogen. Curcumin treatment decreased the B(a)P-induced visible lung tumors, and microscopic adenoma and adenoma with cellular pleomorphism in B(a)P-treated mice. In addition, comparison and analysis of area of microscopic lesions showed that dietary curcumin decreased the B(a)P-induced lesions such as hyperplastic foci, adenoma, adenoma with cellular pleomorphism and adenocarcinoma in mice. Further, evaluation of lung tumors and/or left lobe for cell proliferation and apoptosis markers by western blot and immunohistochemistry respectively showed curcumin-mediated decrease in cell proliferation and enhancement of apoptosis appears to contribute to the observed inhibitory effects. These results clearly show the efficacy of curcumin in the prevention of B(a)P-induced lung tumorigenesis in A/J mice.

8.2 CONCLUSIONS

The mechanisms implicated in the inhibition of tumorigenesis by curcumin/PBPs are summarized (Fig. 8.1) and involve modulation of signalling kinases or xenobiotic-induced activation/translocation of kinases or modulation of tumor-induced responses ultimately leading to effects on genes and cell signalling pathways at multiple levels.

In case of curcumin, considering the reported biological effects of both turmeric and curcumin *in vivo* and the potential for the development of modern medicine, further investigations in well-designed experimental and human intervention studies are needed. On-going studies are likely to help in determining the usefulness of curcumin in prevention and therapy of specific diseases including cancer.

However, in case black tea, considering limited progress, further studies on (i) the characterization of major BTPs, (ii) comparative evaluations of their chemopreventive efficacy, bioavailability and pharmacokinetics and (iii) the mechanisms of chemopreventive actions of BTE and BTE-derived monomeric, oligomeric and polymeric polyphenols are needed before undertaking evaluation of their health effects in human. Information on above referred aspects of major BTPs could provide sound background for examining the effects of black tea on human health.

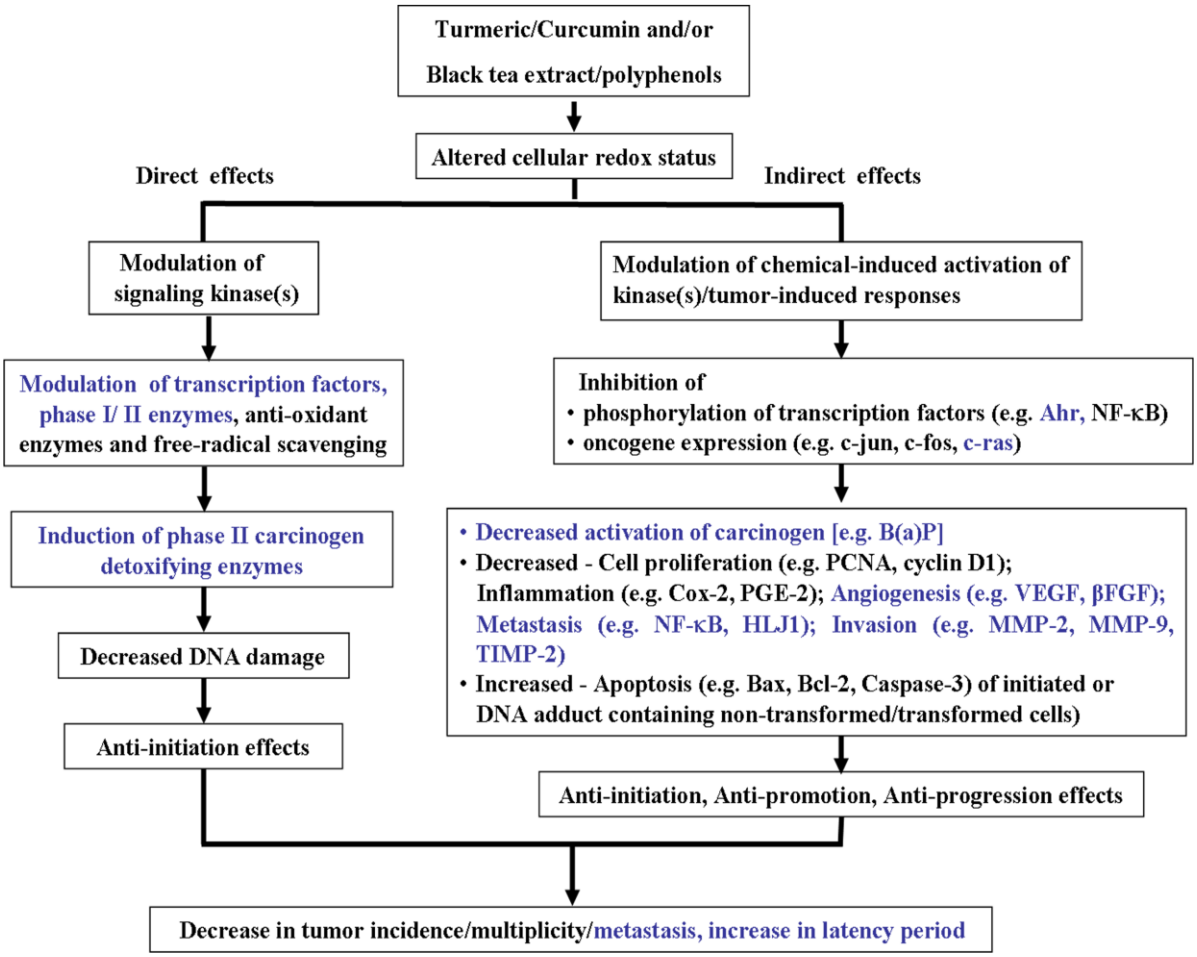

FIGURE 8.1: Summary of *in vivo* chemopreventive effects of turmeric/curcumin and/or black tea extract/polyphenols and underlying mechanisms (Adapted from Kumar et al., 2010, MRMC, 10, 492-505) [29].

8.3 CONTRIBUTION OF THE PRESENT STUDY TO THE EXISTING LITERATURE:-

Though numerous reports on chemopreventive effects of turmeric/curcumin and/or black tea derived polymeric polyphenols exist in literature, the present study contributes significantly in understanding the mechanism of their chemopreventive actions *in vivo* and several of these observations are first/initial reports.

- Pre-treatment with PBPs 1-3 decreased TPA-induced translocation of PKC isozymes (α, β, η, γ, ε) from cytosol to membrane, whereas PBPs 4 and 5 were less effective.
- PBP-3 pre-treatment decreased the TPA-induced phosphorylation of PKCα (pT497), PKCα/βII (pT638/641), and PKCα (pS657 + Y658), and PKC PAN (βII pS660), responsible for its activation/translocation.
- Pre-treatment with PBP-3 decreased the TPA-induced levels/activity of upstream kinase(s) [AKT (pT308 and pS473), PDK (pS241) and PI3K], responsible for PKC activation/phophorylations.
- Pre-treatment with PBP-3 decreased the TPA-induced NF-κB phosphorylation and downstream target proteins associated with proliferation (PCNA, cyclin D1), apoptosis (Bax and Bcl-2) and inflammation (cox-2) in mouse skin.
- PBP-3 pre-treatment decreased the TPA-induced NF-κB family proteins and NF-κB phosphorylation in HaCat cells.
- The study showed strong chemo-protective activities of PBP-3 compared to PBP-5, which may be due to differences in inhibition of TPA-induced PKC translocation/activity and specific phosphorylation.
- Dietary turmeric post-treatment inhibited the tumor growth i.e. tumor burden and tumor multiplicity in hamsters.
- Dietary turmeric post-treatment modulated the markers associated with cell proliferation (diminished PCNA, cyclin D1, and Bcl-2), apoptosis (increased Bax, caspase-3, caspase-9, and cytochrome c, and decreased survivin) and inflammation (decreased cox-2) in tumors of hamster buccal pouch.
- Dietary turmeric post-treatment increased the disappearance of BPDE DNA adducts in mouse liver and lungs, analyzed at 24 h, 72 h, 120 h, 1 wk, 2 wk and 4 wk.
- Dietary turmeric post-treatment augmented the apoptosis in mouse tissue at 48, 96 and 144 h, leading to enhanced removal of BPDE-DNA adduct containing cells.

- Dietary turmeric post-treatment did not alter the levels of apoptosis in mouse tissue at 1, 2 and 4 wk.
- Curcumin treatment inhibited the multiplicity and tumor size in B(a)P-induced lung tumor model.
- Curcumin treatment modulated the markers associated with cell proliferation (diminished PCNA, cyclin D1, and Ki-67), apoptosis (increased Bax, caspase-3) and inflammation (decreased cox-2) in A/J mouse lung tumors.
- To our knowledge, this is the first report where mechanisms of anti-promoting effects of PBPs *in vivo*, wherein PBPs 1-3, EGCG and curcumin (positive control) were demonstrated to decrease the TPA-induced translocation of PKC isozymes (α, β, γ, ε, η) and activity, although the extent of inhibition differed.

8.4 SHORTCOMINGS OF THE STUDY AND FUTURE PERSPECTIVE

- Chemo preventive and/or chemothereputic activities and mechanism(s) of observed biological activities of polyphenols have not been complemented by demonstrating the bioavailability of parent/products in plasma/tissue.
- Structure/Molecular weights of PBPs are not known.
- Poor bioavailability of polyphenols due to poor absorption and rapid metabolism.
- Effect observed after topical administration need to be established after oral administration as these compounds are consumed orally.
- Biochemical markers in tumor tissue extract may have been affected by variable potential contamination of non-tumor tissue.
- Effects of EGCG and TFs on the activity, protein levels, localization, and mechanism of translocation of PKC need to be investigated and compared with PBPs at the equimolar concentration *in vivo*/in the same experiment.
- Cross talk from other signalling cascades and effects of PBPs on other pathways need to be investigated to obtain a better understanding of the mechanisms of translocation/ activation of PKC.
- PBP-3 pre-treatment significantly prevented the TPA-mediated decrease in GSH/GSSG ratio in epithelial cells. PBP-3-mediated antioxidant mechanism seems to be responsible for the inhibition of the tumor-promoting ability of TPA, although a contribution of alternative/additional pathways/mechanisms cannot be ruled out, and requires future investigation.

- The observed lack of binding/interaction between PBP-3 and TPA *in vitro* suggests that the resultant PBP-3-mediated alterations in TPA-induced changes in mouse skin are not likely to be due to a decreased level of TPA reaching the epithelial cells in the PBP-3 + TPA combination because of a potential interaction compared to TPA, although the possibility of cells/extract-mediated binding/interaction needs to be checked.
- Our observations of PBP-mediated biological activities after topical application suggest a modulation of membrane receptors for the observed effects. Similar biological activities of PBPs on other tissue may need to be further investigated after oral administration to simulate the route of exposure as experienced by tea drinkers.
- In the mouse skin model, the modulation of TPA-induced PI3K seems to be a critical regulator of AKT and/or PDK1, resulting in the regulation of activity and translocation of PKC leading to alterations in downstream targets related to cell proliferation, cell death and inflammation. Similar mechanistic studies in different model systems along with appropriate bioavailability information on PBP fractions and other black tea flavanols need to be looked at as it will enhance the understanding of the chemopreventive/chemotherapeutic effects of plant-derived polyphenols, which might further aid in elucidating cellular targets for meaningful evaluation of the chemopreventive potential of black tea in humans.
- Effects of turmeric/curcumin or other polyphenols on post-treatment needs to be examined in immunocompetent mice bearing primary tumors.
- Exposure related effects of 1% dietary turmeric at different time points needs to be evaluated in DMBA-induced buccal pouch of hamster.
- The strength of this study in showing the modulatory effect(s) of turmeric would have been enhanced if circulating levels of curcumin and/or its metabolites were measured in exposed animals.
- Combination of curcumin and chemotherapeutics agents needs to be evaluated in an animal experimental system before it is used in humans.
- Although the present study documented that post-treatment with curcumin resulted in disappearance of BPDE-DNA adduct as a result of enhanced apoptosis in experiment 1, role of curcumin in enhanced DNA repair could not be ruled out and remains to be established.

- Crude extract and pure compounds need to be analyzed in same assay to identify the biologically active constituent and understand the influence of other members of the extract on the biological activity of active constituents.
- Effect of curcumin treatment on B(a)P-induced activation of nuclear transcription factors and MAPK need to be evaluated in A/J mouse lung tumor model.
- Analysis of effects of curcumin on the metabolic activation of B(a)P by phase I/II enzymes in A/J mouse lung tumor model need to be undertaken.
- After observing the effects of curcumin treatment on B(a)P-induced tumor incidence and size, further evaluation of curcumin at sequential time points need to be checked.

Taken together the results of the present study show strong chemo-protective activities of PBP-3 compared to PBP-5, which may be due to differences in inhibition of TPA-induced PKC translocation/activity and specific phosphorylation. Further, observed PBP-mediated inhibition in TPA-induced PKC phosphorylation correlated well with decreased TPA-induced NF-κB phosphorylation and downstream target proteins associated with proliferation, apoptosis and inflammation in mouse skin. It also emphasized that anti-promoting effects of PBPs are due to modulation of TPA-induced PI3K/AKT/PDK-mediated signal transduction. In addition to this, studies with curcumin post-treatment documents the disappearance of BPDE-DNA adducts as a result of enhanced apoptosis/repair/proliferation. Furthermore, the work is extended in showing that curcumin treatment exerts protective effects in A/J mice lung tumor model. Besides, this study also presents a comprehensive picture of effects of dietary turmeric post-treatment on various biomarkers in DMBA-induced HBP tumors. Some of these biomarkers are likely to be helpful in monitoring clinical trials and evaluating drug effect measurements. That is, curcumin/turmeric/black tea-derived PBPs modulate multiple cellular signaling pathways and interact with numerous molecular targets. Both turmeric (economical, well-accepted, naturally occurring non-nutrient dietary compound), and PBPs (second most consumed drink after water) can be used as an effective chemopreventive agent. It is important to mention here that a great deal of work needs to be done before cancer chemoprevention may find its way into mainstream medicine as standard care for the general population. An enhanced interdisciplinary and collaborative effort among academic institutions, industry, scientists, and other health care professionals is needed to drive the field of cancer chemoprevention forward and help to secure a cancer-free future.

BIBLIOGRAPHY

[1] Hanahan, D.; Weinberg, R. A. Hallmarks of cancer: the next generation. *Cell* **144:**646-674; 2011.

[2] Weinstein, I. B. Cancer prevention: recent progress and future opportunities. *Cancer Res.* **51:**5080s-5085s; 1991.

[3] Wattenberg, L. W. Chemoprevention of cancer. *Prev Med* **25:**44-45; 1996.

[4] Gescher, A. J.; Sharma, R. A.; Steward, W. P. Cancer chemoprevention by dietary constituents: a tale of failure and promise. *Lancet Oncol.* **2:**371-379; 2001.

[5] Moon, Y. J.; Wang, X.; Morris, M. E. Dietary flavonoids: effects on xenobiotic and carcinogen metabolism. *Toxicol.* In Vitro**20:**187-210; 2006.

[6] Surh, Y. J. Cancer chemoprevention with dietary phytochemicals. *Nat. Rev. Cancer* **3:**768-780; 2003.

[7] Pan, M. H.; Chiou, Y. S.; Wang, Y. J.; Ho, C. T.; Lin, J. K. Multistage carcinogenesis process as molecular targets in cancer chemoprevention by epicatechin-3-gallate. *Food & function* **2:**101-110; 2011.

[8] Chen, C.; Kong, A. N. Dietary chemopreventive compounds and ARE/EpRE signaling. *Free Radic. Biol. Med.* **36:**1505-1516; 2004.

[9] Maru, G. B.; Kumar, G.; Ghantasala, S.; Tajpara, P. Polyphenol(s)-mediated *in vivo* cellular responses during carcinogenesis. In: Watson, R. R.; Preedy, V. R.; Zibadi, S., eds. *Polyphenols in Health and Diseases*: Elsevier; 2013 (in press).

[10] Maru, G. B.; Ramchandani, A.; Sarkar, S. National state of the art report on *in vivo* and *in vitro* models of carcinogenesis. *Indian Association for Cancer Research (IACR)* Mumbai; 1998: 1-62.

[11] Crowell, J. A. The chemopreventive agent development research program in the Division of Cancer Prevention of the US National Cancer Institute: an overview. *Eur. J. Cancer* **41:**1889-1910; 2005.

[12] Steele, V. E.; Sharma, S.; Mehta, R.; Elmore, E.; Redpath, L.; Rudd, C.; Bagheri, D.; Sigman, C. C.; Kelloff, G. J. Use of *in vitro* assays to predict the efficacy of chemopreventive agents in whole animals. *J. Cell Biochem. Suppl.* **26:**29-53; 1996.

[13] Gerhauser, C.; Klimo, K.; Heiss, E.; Neumann, I.; Gamal-Eldeen, A.; Knauft, J.; Liu, G. Y.; Sitthimonchai, S.; Frank, N. Mechanism-based *in vitro* screening of potential cancer chemopreventive agents. *Mutation research* **523-524:**163-172; 2003.

[14] Rao, C. V.; Cooma, I.; Rodriguez, J. G.; Simi, B.; El-Bayoumy, K.; Reddy, B. S. Chemoprevention of familial adenomatous polyposis development in the APC(min) mouse model by 1,4-phenylene bis(methylene)selenocyanate. *Carcinogenesis* **21:**617-621; 2000.

[15] Saleem, M.; Kweon, M. H.; Yun, J. M.; Adhami, V. M.; Khan, N.; Syed, D. N.; Mukhtar, H. A novel dietary triterpene Lupeol induces fas-mediated apoptotic death of androgen-sensitive prostate cancer cells and inhibits tumor growth in a xenograft model. *Cancer Res.* **65:**11203-11213; 2005.

[16] Khavari, P. A. Modelling cancer in human skin tissue. *Nat. Rev. Cancer* **6:**270-280; 2006.

[17] Stoner, G.; Casto, B.; Ralston, S.; Roebuck, B.; Pereira, C.; Bailey, G. Development of a multi-organ rat model for evaluating chemopreventive agents: efficacy of indole-3-carbinol. *Carcinogenesis* **23:**265-272; 2002.

[18] Doi, K.; Wanibuchi, H.; Salim, E. I.; Shen, J.; Wei, M.; Mitsuhashi, M.; Kudoh, S.; Hirata, K.; Fukushima, S. Revised rat multi-organ carcinogenesis bioassay for whole-body detection of chemopreventive agents: modifying potential of S-methylcysteine. *Cancer Lett.* **206:**15-26; 2004.

[19] Anisimov, V. N.; Ukraintseva, S. V.; Yashin, A. I. Cancer in rodents: does it tell us about cancer in humans? *Nat. Rev. Cancer* **5:**807-819; 2005.

[20] Tsao, A. S.; Kim, E. S.; Hong, W. K. Chemoprevention of cancer. *CA Cancer J. Clin.* **54:**150-180; 2004.

[21] Patel, R.; Garg, R.; Erande, S.; Maru, G. B. Chemopreventive herbal anti-oxidants: current status and future perspectives. *J. Clin. Biochem. Nutr.* **40:**82-91; 2007.

[22] Seifried, H. E.; McDonald, S. S.; Anderson, D. E.; Greenwald, P.; Milner, J. A. The antioxidant conundrum in cancer. *Cancer Res.* **63:**4295-4298; 2003.

[23] Greenwald, P. Cancer chemoprevention. *Br. Med. J.* **324:**714-718; 2002.

[24] Sporn, M. B. Carcinogenesis and cancer: different perspectives on the same disease. *Cancer Res.* **51:**6215-6218; 1991.

[25] Lippman, S. M.; Hong, W. K. Cancer prevention science and practice. *Cancer Res.* **62:**5119-5125; 2002.

[26] Katiyar, S.; Mukhtar, H. Tea in chemoprevention of cancer. *International journal of oncology* **8:**221-238; 1996.

[27] Wu, C. D.; Wei, G. X. Tea as a functional food for oral health. *Nutrition* **18:**443-444; 2002.

[28] Mukhtar, H.; Ahmad, N. Green tea in chemoprevention of cancer. *Toxicological sciences : an official journal of the Society of Toxicology* **52:**111-117; 1999.

[29] Kumar, G.; Pillare, S. P.; Maru, G. B. Black tea polyphenols-mediated in vivo cellular responses during carcinogenesis. *Mini reviews in medicinal chemistry* **10:**492-505; 2010.

[30] Yang, G. Y.; Liao, J.; Li, C.; Chung, J.; Yurkow, E. J.; Ho, C. T.; Yang, C. S. Effect of black and green tea polyphenols on c-jun phosphorylation and H(2)O(2) production in transformed and non-transformed human bronchial cell lines: possible mechanisms of cell growth inhibition and apoptosis induction. *Carcinogenesis* **21:**2035-2039; 2000.

[31] Balentine, D. Manufacture and chemistry of tea. In: Huang, M.; Ho, C. T.; Lee, C., eds. *Phenolic Compounds in Food and their Effects on Health*. Washington, DC,: ACS; 1992: 103–117.

[32] Haslam, E. Thoughts on thearubigins. *Phytochemistry* **64:**61-73; 2003.

[33] Krishnan, R.; Maru, G. B. Isolation and analyses of polymeric polyphenol fractions from black tea. *Food Chemistry* **94:**331-340; 2006.

[34] Brown A. G.; Eyton W. B.; Holmes A.; D., O. W. Identification of the thearubigins as polymeric proanthocyanidins. *Nature* **221:**742-744; 1969.

[35] Ju, J.; Lu, G.; Lambert, J. D.; Yang, C. S. Inhibition of carcinogenesis by tea constituents. *Seminars in cancer biology* **17:**395-402; 2007.

[36] Chen, C.; Kong, A. N. Dietary cancer-chemopreventive compounds: from signaling and gene expression to pharmacological effects. *Trends in pharmacological sciences* **26:**318-326; 2005.

[37] Yang, C. S.; Chung, J. Y.; Yang, G.; Chhabra, S. K.; Lee, M. J. Tea and tea polyphenols in cancer prevention. *J Nutr* **130:**472S-478S; 2000.

[38] Park, A. M.; Dong, Z. Signal transduction pathways: targets for green and black tea polyphenols. *Journal of biochemistry and molecular biology* **36:**66-77; 2003.

[39] Del Rio, D.; Stewart, A. J.; Mullen, W.; Burns, J.; Lean, M. E.; Brighenti, F.; Crozier, A. HPLC-MSn analysis of phenolic compounds and purine alkaloids in green and black tea. *Journal of agricultural and food chemistry* **52:**2807-2815; 2004.

[40] Zhao, J.; Jin, X.; Yaping, E.; Zheng, Z. S.; Zhang, Y. J.; Athar, M.; DeLeo, V. A.; Mukhtar, H.; Bickers, D. R.; Wang, Z. Y. Photoprotective effect of black tea extracts against UVB-induced phototoxicity in skin. *Photochemistry and photobiology* **70:**637-644; 1999.

[41] Record, I. R.; Dreosti, I. E. Protection by black tea and green tea against UVB and UVA + B induced skin cancer in hairless mice. *Mutation research* **422:**191-199; 1998.

[42] Weisburger, J. H.; Rivenson, A.; Garr, K.; Aliaga, C. Tea, or tea and milk, inhibit mammary gland and colon carcinogenesis in rats. *Cancer letters* **114:**323-327; 1997.

[43] Murugan, R. S.; Uchida, K.; Hara, Y.; Nagini, S. Black tea polyphenols modulate xenobiotic-metabolizing enzymes, oxidative stress and adduct formation in a rat hepatocarcinogenesis model. *Free radical research* **42:**873-884; 2008.

[44] Shukla, Y.; Taneja, P. Anticarcinogenic effect of black tea on pulmonary tumors in Swiss albino mice. *Cancer letters* **176:**137-141; 2002.

[45] Landau, J. M.; Wang, Z. Y.; Yang, G. Y.; Ding, W.; Yang, C. S. Inhibition of spontaneous formation of lung tumors and rhabdomyosarcomas in A/J mice by black and green tea. *Carcinogenesis* **19:**501-507; 1998.

[46] Yang, G.; Wang, Z. Y.; Kim, S.; Liao, J.; Seril, D. N.; Chen, X.; Smith, T. J.; Yang, C. S. Characterization of early pulmonary hyperproliferation and tumor progression and their inhibition by black tea in a 4-(methylnitrosamino)-1-(3-pyridyl)-1-butanone-induced lung tumorigenesis model with A/J mice. *Cancer research* **57:**1889-1894; 1997.

[47] Lu, Y. P.; Lou, Y. R.; Xie, J. G.; Yen, P.; Huang, M. T.; Conney, A. H. Inhibitory effect of black tea on the growth of established skin tumors in mice: effects on tumor size, apoptosis, mitosis and bromodeoxyuridine incorporation into DNA. *Carcinogenesis* **18:**2163-2169; 1997.

[48] Javed, S.; Mehrotra, N. K.; Shukla, Y. Chemopreventive effects of black tea polyphenols in mouse skin model of carcinogenesis. *Biomedical and environmental sciences : BES* **11:**307-313; 1998.

[49] Huang, M. T.; Xie, J. G.; Wang, Z. Y.; Ho, C. T.; Lou, Y. R.; Wang, C. X.; Hard, G. C.; Conney, A. H. Effects of tea, decaffeinated tea, and caffeine on UVB light-induced complete carcinogenesis in SKH-1 mice: demonstration of caffeine as a biologically important constituent of tea. *Cancer research* **57:**2623-2629; 1997.

[50] Letchoumy, P. V.; Mohan, K. V.; Prathiba, D.; Hara, Y.; Nagini, S. Comparative evaluation of antiproliferative, antiangiogenic and apoptosis inducing potential of black tea polyphenols in the hamster buccal pouch carcinogenesis model. *Journal of carcinogenesis* **6:**19; 2007.

[51] Chandra Mohan, K. V.; Hara, Y.; Abraham, S. K.; Nagini, S. Comparative evaluation of the chemopreventive efficacy of green and black tea polyphenols in the hamster buccal pouch carcinogenesis model. *Clinical biochemistry* **38:**879-886; 2005.

[52] Chandra Mohan, K. V.; Devaraj, H.; Prathiba, D.; Hara, Y.; Nagini, S. Antiproliferative and apoptosis inducing effect of lactoferrin and black tea polyphenol combination on hamster buccal pouch carcinogenesis. *Biochimica et biophysica acta* **1760:**1536-1544; 2006.

[53] Mohan, K. V.; Letchoumy, P. V.; Hara, Y.; Nagini, S. Combination chemoprevention of hamster buccal pouch carcinogenesis by bovine milk lactoferrin and black tea polyphenols. *Cancer investigation* **26:**193-201; 2008.

[54] Lu, Y. P.; Lou, Y. R.; Lin, Y.; Shih, W. J.; Huang, M. T.; Yang, C. S.; Conney, A. H. Inhibitory effects of orally administered green tea, black tea, and caffeine on skin carcinogenesis in mice previously treated with ultraviolet B light (high-risk mice): relationship to decreased tissue fat. *Cancer research* **61:**5002-5009; 2001.

[55] Caderni, G.; De Filippo, C.; Luceri, C.; Salvadori, M.; Giannini, A.; Biggeri, A.; Remy, S.; Cheynier, V.; Dolara, P. Effects of black tea, green tea and wine extracts on intestinal carcinogenesis induced by azoxymethane in F344 rats. *Carcinogenesis* **21:**1965-1969; 2000.

[56] Wang, Z. Y.; Hong, J. Y.; Huang, M. T.; Reuhl, K. R.; Conney, A. H.; Yang, C. S. Inhibition of N-nitrosodiethylamine- and 4-(methylnitrosamino)-1-(3-pyridyl)-1-butanone-induced tumorigenesis in A/J mice by green tea and black tea. *Cancer research* **52:**1943-1947; 1992.

[57] Cao, J.; Xu, Y.; Chen, J.; Klaunig, J. E. Chemopreventive effects of green and black tea on pulmonary and hepatic carcinogenesis. *Fundamental and applied toxicology : official journal of the Society of Toxicology* **29:**244-250; 1996.

[58] Wang, Z. Y.; Huang, M. T.; Lou, Y. R.; Xie, J. G.; Reuhl, K. R.; Newmark, H. L.; Ho, C. T.; Yang, C. S.; Conney, A. H. Inhibitory effects of black tea, green tea, decaffeinated black tea, and decaffeinated green tea on ultraviolet B light-induced skin carcinogenesis in 7,12-dimethylbenz[a]anthracene-initiated SKH-1 mice. *Cancer research* **54:**3428-3435; 1994.

[59] Wang, Z. Y.; Wang, L. D.; Lee, M. J.; Ho, C. T.; Huang, M. T.; Conney, A. H.; Yang, C. S. Inhibition of N-nitrosomethylbenzylamine-induced esophageal tumorigenesis in rats by green and black tea. *Carcinogenesis* **16:**2143-2148; 1995.

[60] Patel, R.; Krishnan, R.; Ramchandani, A.; Maru, G. Polymeric black tea polyphenols inhibit mouse skin chemical carcinogenesis by decreasing cell proliferation. *Cell Prolif* **41:**532-553; 2008.

[61] Patel, R.; Ingle, A.; Maru, G. B. Polymeric black tea polyphenols inhibit 1,2-dimethylhydrazine induced colorectal carcinogenesis by inhibiting cell proliferation via Wnt/beta-catenin pathway. *Toxicology and applied pharmacology* **227:**136-146; 2008.

[62] Manna, S.; Mukherjee, S.; Roy, A.; Das, S.; Panda, C. K. Tea polyphenols can restrict benzo[a]pyrene-induced lung carcinogenesis by altered expression of p53-associated genes and H-ras, c-myc and cyclin D1. *The Journal of nutritional biochemistry* **20:**337-349; 2009.

[63] Morse, M. A.; Kresty, L. A.; Steele, V. E.; Kelloff, G. J.; Boone, C. W.; Balentine, D. A.; Harbowy, M. E.; Stoner, G. D. Effects of theaflavins on N-nitrosomethylbenzylamine-induced esophageal tumorigenesis. *Nutrition and cancer* **29:**7-12; 1997.

[64] Yang, G. Y.; Liu, Z.; Seril, D. N.; Liao, J.; Ding, W.; Kim, S.; Bondoc, F.; Yang, C. S. Black tea constituents, theaflavins, inhibit 4-(methylnitrosamino)-1-(3-pyridyl)-1-butanone (NNK)-induced lung tumorigenesis in A/J mice. *Carcinogenesis* **18:**2361-2365; 1997.

[65] Ammon, H. P.; Wahl, M. A. Pharmacology of Curcuma longa. *Planta Med.* **57:**1-7; 1991.

[66] Chattopadhyay, I.; Biswas, K.; Bandyopadhyay, U.; Banerjee, R. K. Turmeric and curcumin: Biological actions and medicinal applications. *Curr. Sci.* **87:**44-53; 2004.

[67] Govindrajan, V. S. Turmeric chemistry, technology and quality. *CRC Crit. Rev. Food Sci. Nutr.* **12:**199-301; 1979.

[68] Aggarwal, B. B.; Kumar, A.; Bharti, A. C. Anticancer potential of curcumin: preclinical and clinical studies. *Anticancer Res.* **23:**363-398; 2003.

[69] Joe, B.; Vijaykumar, M.; Lokesh, B. R. Biological properties of curcumin-cellular and molecular mechanisms of action. *Crit. Rev. Food Sci. Nutr.* **44:**97-111; 2004.

[70] Sharma, O. P. Antioxidant activity of curcumin and related compounds. *Biochem. Pharmacol.* **25:**1811-1812; 1976.

[71] Goel, A.; Kunnumakkara, A. B.; Aggarwal, B. B. Curcumin as "Curecumin": from kitchen to clinic. *Biochem. Pharmacol.* **75:**787-809; 2008.

[72] Commandeur, J. N.; Vermeulen, N. P. Cytotoxicity and cytoprotective activities of natural compounds. The case of curcumin. *Xenobiotica* **26:**667-680; 1996.

[73] Wang, Y. J.; Pan, M. H.; Cheng, A. L.; Lin, L. I.; Ho, Y. S.; Hsieh, C. Y.; Lin, J. K. Stability of curcumin in buffer solutions and characterization of its degradation products. *J. Pharm. Biomed. Anal.* **15:**1867-1876; 1997.

[74] Holder, G. M.; Plummer, J. L.; Ryan, A. J. The metabolism and excretion of curcumin (1,7-bis-(4-hydroxy-3-methoxyphenyl)-1,6-heptadiene-3,5-dione) in the rat. *Xenobiotica* **8:**761-768; 1978.

[75] Anand, P.; Kunnumakkara, A. B.; Newman, R. A.; Aggarwal, B. B. Bioavailability of curcumin: problems and promises. *Mol. Pharm.* **4:**807-818; 2007.

[76] Pan, M. H.; Huang, T. M.; Lin, J. K. Biotransformation of curcumin through reduction and glucuronidation in mice. *Drug Metab. Dispos.* **27:**486-494; 1999.

[77] Shoba, G.; Joy, D.; Joseph, T.; Majeed, M.; Rajendran, R.; Srinivas, P. S. Influence of piperine on the pharmacokinetics of curcumin in animals and human volunteers. *Planta Med.* **64:**353-356; 1998.

[78] Bradlow, H. L.; Telang, N. T.; Sepkovic, D. W.; Osborne, M. P. Phytochemicals as modulators of cancer risk. *Adv. Exp. Med. Biol.* **472:**207-221; 1999.

[79] Conney, A. H.; Lou, Y. R.; Xie, J. G.; Osawa, T.; Newmark, H. L.; Liu, Y.; Chang, R. L.; Huang, M. T. Some perspectives on dietary inhibition of carcinogenesis: studies with curcumin and tea. *Proc. Soc. Exp. Biol. Med.* **216:**234-245; 1997.

[80] Khafif, A.; Schantz, S. P.; Chou, T. C.; Edelstein, D.; Sacks, P. G. Quantitation of chemopreventive synergism between (-)-epigallocatechin-3-gallate and curcumin in normal, premalignant and malignant human oral epithelial cells. *Carcinogenesis* **19:**419-424; 1998.

[81] Navis, I.; Sriganth, P.; Premalatha, B. Dietary curcumin with cisplatin administration modulates tumour marker indices in experimental fibrosarcoma. *Pharmacol. Res.* **39:**175-179; 1999.

[82] Zsila, F.; Bikadi, Z.; Simonyi, M. Circular dichroism spectroscopic studies reveal pH dependent binding of curcumin in the minor groove of natural and synthetic nucleic acids. *Org. Biomol. Chem.* **2:**2902-2910; 2004.

[83] Awasthi, S.; Pandya, U.; Singhal, S. S.; Lin, J. T.; Thiviyanathan, V.; Seifert, W. E., Jr.; Awasthi, Y. C.; Ansari, G. A. Curcumin-glutathione interactions and the role of human glutathione S-transferase P1-1. *Chem. Biol. Interact.* **128:**19-38; 2000.

[84] Reddy, S.; Aggarwal, B. B. Curcumin is a non-competitive and selective inhibitor of phosphorylase kinase. *FEBS Lett.* **341:**19-22; 1994.

[85] Logan-Smith, M. J.; Lockyer, P. J.; East, J. M.; Lee, A. G. Curcumin, a molecule that inhibits the Ca2+-ATPase of sarcoplasmic reticulum but increases the rate of accumulation of Ca2+. *J. Biol. Chem.* **276:**46905-46911; 2001.

[86] Jung, Y.; Xu, W.; Kim, H.; Ha, N.; Neckers, L. Curcumin-induced degradation of ErbB2: A role for the E3 ubiquitin ligase CHIP and the Michael reaction acceptor activity of curcumin. *Biochim. Biophys. Acta* **1773:**383-390; 2007.

[87] Gupta, K. K.; Bharne, S. S.; Rathinasamy, K.; Naik, N. R.; Panda, D. Dietary antioxidant curcumin inhibits microtubule assembly through tubulin binding. *Febs. J.* **273:**5320-5332; 2006.

[88] Yang, F.; Lim, G. P.; Begum, A. N.; Ubeda, O. J.; Simmons, M. R.; Ambegaokar, S. S.; Chen, P. P.; Kayed, R.; Glabe, C. G.; Frautschy, S. A.; Cole, G. M. Curcumin inhibits formation of amyloid beta oligomers and fibrils, binds plaques, and reduces amyloid in vivo. *J. Biol. Chem.* **280:**5892-5901; 2005.

[89] Shim, J. S.; Kim, J. H.; Cho, H. Y.; Yum, Y. N.; Kim, S. H.; Park, H. J.; Shim, B. S.; Choi, S. H.; Kwon, H. J. Irreversible inhibition of CD13/aminopeptidase N by the antiangiogenic agent curcumin. *Chem. Biol.* **10:**695-704; 2003.

[90] Deshpande, S. S.; Maru, G. B. Effects of curcumin on the formation of benzo[a]pyrene derived DNA adducts *in vitro*. *Cancer Lett.* **96:**71-80; 1995.

[91] Strimpakos, A. S.; Sharma, R. A. Curcumin: preventive and therapeutic properties in laboratory studies and clinical trials. *Antioxid Redox Signal* **10:**511-545; 2008.

[92] Kawajiri, K.; Fujii-Kuriyama, Y. Cytochrome P450 gene regulation and physiological functions mediated by the aryl hydrocarbon receptor. *Arch Biochem Biophys* **464:**207-212; 2007.

[93] Patel, R.; Maru, G. Polymeric black tea polyphenols induce phase II enzymes via Nrf2 in mouse liver and lungs. *Free Radic Biol Med* **44:**1897-1911; 2008.

[94] Patel, R.; Garg, R.; Erande, S.; Maru, G. B. Chemopreventive herbal anti-oxidants: current status and future perspectives. *Journal of clinical biochemistry and nutrition* **40:**82-91; 2007.

[95] Castagna, M.; Takai, Y.; Kaibuchi, K.; Sano, K.; Kikkawa, U.; Nishizuka, Y. Direct activation of calcium-activated, phospholipid-dependent protein kinase by tumor-promoting phorbol esters. *J. Biol. Chem.* **257:**7847-7851; 1982.

[96] Garg, R.; Ramchandani, A.; Maru, G. B. Curcumin decreases 12-o-tetradecanoylphorbol-13-acetate-induced protein kinase C translocation to modulate downstream targets in mouse skin. *Carcinogenesis* **29:**1249-1257; 2008c.

[97] Maru, G. B.; Ramchandani, A. G.; Kumar, G.; Garg, R. Curcumin-mediated cellular responses in chemical carcinogenesis. In: Watson, R. R.; Preedy, V. R., eds. *Bioactive Foods and Extracts*. CRC press; 2010: 181–203.

[98] Kumar, G.; Dange, P.; Kailaje, V.; Vaidya, M. M.; Ramchandani, A. G.; Maru, G. B. Polymeric black tea polyphenols modulate the localization and activity of 12-O-tetradecanoylphorbol-13-acetate-mediated kinases in mouse skin: mechanisms of their anti-tumor-promoting action. *Free Radic Biol Med* **53:**1358-1370; 2012.

[99] Kumar, G.; Tajpara, P.; Maru, G. Dietary Turmeric Post-Treatment Decreases DMBA-Induced Hamster Buccal Pouch Tumor Growth by Altering Cell Proliferation and Apoptosis-Related Markers. *J Environ Pathol Toxicol Oncol* **31:**295-312; 2012.

[100] Pahl, H. L. Activators and target genes of Rel/NF-kappaB transcription factors. *Oncogene* **18:**6853-6866; 1999.

[101] Huang, M. T.; Smart, R. C.; Wong, C. Q.; Conney, A. H. Inhibitory effect of curcumin, chlorogenic acid, caffeic acid, and ferulic acid on tumor promotion in

mouse skin by 12-O-tetradecanoylphorbol-13-acetate. *Cancer research* **48:**5941-5946; 1988.

[102] Huang, M. T.; Ma, W.; Lu, Y. P.; Chang, R. L.; Fisher, C.; Manchand, P. S.; Newmark, H. L.; Conney, A. H. Effects of curcumin, demethoxycurcumin, bisdemethoxycurcumin and tetrahydrocurcumin on 12-O-tetradecanoylphorbol-13-acetate-induced tumor promotion. *Carcinogenesis* **16:**2493-2497; 1995.

[103] Huang, M. T.; Newmark, H. L.; Frenkel, K. Inhibitory effects of curcumin on tumorigenesis in mice. *Journal of cellular biochemistry* **27:**26-34; 1997.

[104] Huang, M. T.; Wang, Z. Y.; Georgiadis, C. A.; Laskin, J. D.; Conney, A. H. Inhibitory effects of curcumin on tumor initiation by benzo[a]pyrene and 7,12-dimethylbenz[a]anthracene. *Carcinogenesis* **13:**2183-2186; 1992.

[105] Azuine, M. A.; Bhide, S. V. Chemopreventive effect of turmeric against stomach and skin tumors induced by chemical carcinogens in Swiss mice. *Nutrition and cancer* **17:**77-83; 1992.

[106] Limtrakul, P.; Lipigorngoson, S.; Namwong, O.; Apisariyakul, A.; Dunn, F. W. Inhibitory effect of dietary curcumin on skin carcinogenesis in mice. *Cancer letters* **116:**197-203; 1997.

[107] Singh, S. V.; Hu, X.; Srivastava, S. K.; Singh, M.; Xia, H.; Orchard, J. L.; Zaren, H. A. Mechanism of inhibition of benzo[a]pyrene-induced forestomach cancer in mice by dietary curcumin. *Carcinogenesis* **19:**1357-1360; 1998.

[108] Azuine, M. A.; Kayal, J. J.; Bhide, S. V. Protective role of aqueous turmeric extract against mutagenicity of direct-acting carcinogens as well as benzo [alpha] pyrene-induced genotoxicity and carcinogenicity. *J Cancer Res Clin Oncol* **118:**447-452; 1992.

[109] Huang, M. T.; Lou, Y. R.; Ma, W.; Newmark, H. L.; Reuhl, K. R.; Conney, A. H. Inhibitory effects of dietary curcumin on forestomach, duodenal, and colon carcinogenesis in mice. *Cancer research* **54:**5841-5847; 1994.

[110] Deshpande, S. S.; Ingle, A. D.; Maru, G. B. Inhibitory effects of curcumin-free aqueous turmeric extract on benzo[a]pyrene-induced forestomach papillomas in mice. *Cancer letters* **118:**79-85; 1997.

[111] Ikezaki, S.; Nishikawa, A.; Furukawa, F.; Kudo, K.; Nakamura, H.; Tamura, K.; Mori, H. Chemopreventive effects of curcumin on glandular stomach carcinogenesis induced by N-methyl-N'-nitro-N-nitrosoguanidine and sodium chloride in rats. *Anticancer research* **21:**3407-3411; 2001.

[112] Rao, C. V.; Rivenson, A.; Simi, B.; Reddy, B. S. Chemoprevention of colon carcinogenesis by dietary curcumin, a naturally occurring plant phenolic compound. *Cancer research* **55:**259-266; 1995.

[113] Samaha, H. S.; Kelloff, G. J.; Steele, V.; Rao, C. V.; Reddy, B. S. Modulation of apoptosis by sulindac, curcumin, phenylethyl-3-methylcaffeate, and 6-phenylhexyl isothiocyanate: apoptotic index as a biomarker in colon cancer chemoprevention and promotion. *Cancer research* **57:**1301-1305; 1997.

[114] Kawamori, T.; Lubet, R.; Steele, V. E.; Kelloff, G. J.; Kaskey, R. B.; Rao, C. V.; Reddy, B. S. Chemopreventive effect of curcumin, a naturally occurring anti-inflammatory agent, during the promotion/progression stages of colon cancer. *Cancer research* **59:**597-601; 1999.

[115] Pereira, M. A.; Grubbs, C. J.; Barnes, L. H.; Li, H.; Olson, G. R.; Eto, I.; Juliana, M.; Whitaker, L. M.; Kelloff, G. J.; Steele, V. E.; Lubet, R. A. Effects of the phytochemicals, curcumin and quercetin, upon azoxymethane-induced colon cancer and 7,12-dimethylbenz[a]anthracene-induced mammary cancer in rats. *Carcinogenesis* **17:**1305-1311; 1996.

[116] Kim, J. M.; Araki, S.; Kim, D. J.; Park, C. B.; Takasuka, N.; Baba-Toriyama, H.; Ota, T.; Nir, Z.; Khachik, F.; Shimidzu, N.; Tanaka, Y.; Osawa, T.; Uraji, T.; Murakoshi, M.; Nishino, H.; Tsuda, H. Chemopreventive effects of carotenoids and curcumins on mouse colon carcinogenesis after 1,2-dimethylhydrazine initiation. *Carcinogenesis* **19:**81-85; 1998.

[117] Devasena, T.; Rajasekaran, K. N.; Menon, V. P. Bis-1,7-(2-hydroxyphenyl)-hepta-1,6-diene-3,5-dione (a curcumin analog) ameliorates DMH-induced hepatic oxidative stress during colon carcinogenesis. *Pharmacol Res* **46:**39-45; 2002.

[118] Perkins, S.; Verschoyle, R. D.; Hill, K.; Parveen, I.; Threadgill, M. D.; Sharma, R. A.; Williams, M. L.; Steward, W. P.; Gescher, A. J. Chemopreventive efficacy and pharmacokinetics of curcumin in the min/+ mouse, a model of familial adenomatous polyposis. *Cancer Epidemiol Biomarkers Prev* **11:**535-540; 2002.

[119] Mahmoud, N. N.; Carothers, A. M.; Grunberger, D.; Bilinski, R. T.; Churchill, M. R.; Martucci, C.; Newmark, H. L.; Bertagnolli, M. M. Plant phenolics decrease intestinal tumors in an animal model of familial adenomatous polyposis. *Carcinogenesis* **21:**921-927; 2000.

[120] Huang, M. T.; Lou, Y. R.; Xie, J. G.; Ma, W.; Lu, Y. P.; Yen, P.; Zhu, B. T.; Newmark, H.; Ho, C. T. Effect of dietary curcumin and dibenzoylmethane on formation of 7,12-dimethylbenz[a]anthracene-induced mammary tumors and lymphomas/leukemias in Sencar mice. *Carcinogenesis* **19:**1697-1700; 1998.

[121] Lin, C. C.; Lu, Y. P.; Lou, Y. R.; Ho, C. T.; Newmark, H. H.; MacDonald, C.; Singletary, K. W.; Huang, M. T. Inhibition by dietary dibenzoylmethane of mammary gland proliferation, formation of DMBA-DNA adducts in mammary glands, and mammary tumorigenesis in Sencar mice. *Cancer letters* **168:**125-132; 2001.

[122] Deshpande, S. S.; Ingle, A. D.; Maru, G. B. Chemopreventive efficacy of curcumin-free aqueous turmeric extract in 7,12-dimethylbenz[a]anthracene-induced rat mammary tumorigenesis. *Cancer letters* **123:**35-40; 1998.

[123] Singletary, K.; MacDonald, C.; Iovinelli, M.; Fisher, C.; Wallig, M. Effect of the beta-diketones diferuloylmethane (curcumin) and dibenzoylmethane on rat mammary DNA adducts and tumors induced by 7,12-dimethylbenz[a]anthracene. *Carcinogenesis* **19:**1039-1043; 1998.

[124] Inano, H.; Onoda, M.; Inafuku, N.; Kubota, M.; Kamada, Y.; Osawa, T.; Kobayashi, H.; Wakabayashi, K. Chemoprevention by curcumin during the promotion stage of tumorigenesis of mammary gland in rats irradiated with gamma-rays. *Carcinogenesis* **20:**1011-1018; 1999.

[125] Inano, H.; Onoda, M.; Inafuku, N.; Kubota, M.; Kamada, Y.; Osawa, T.; Kobayashi, H.; Wakabayashi, K. Potent preventive action of curcumin on radiation-induced initiation of mammary tumorigenesis in rats. *Carcinogenesis* **21:**1835-1841; 2000.

[126] Chuang, S. E.; Cheng, A. L.; Lin, J. K.; Kuo, M. L. Inhibition by curcumin of diethylnitrosamine-induced hepatic hyperplasia, inflammation, cellular gene products and cell-cycle-related proteins in rats. *Food Chem Toxicol* **38:**991-995; 2000a.

[127] Chuang, S. E.; Kuo, M. L.; Hsu, C. H.; Chen, C. R.; Lin, J. K.; Lai, G. M.; Hsieh, C. Y.; Cheng, A. L. Curcumin-containing diet inhibits diethylnitrosamine-induced murine hepatocarcinogenesis. *Carcinogenesis* **21:**331-335; 2000b.

[128] Thapliyal, R.; Naresh, K. N.; Rao, K. V.; Maru, G. B. Inhibition of nitrosodiethylamine-induced hepatocarcinogenesis by dietary turmeric in rats. *Toxicology letters* **139:**45-54; 2003.

[129] Sreepriya, M.; Bali, G. Chemopreventive effects of embelin and curcumin against N-nitrosodiethylamine/phenobarbital-induced hepatocarcinogenesis in Wistar rats. *Fitoterapia* **76:**549-555; 2005.

[130] Frank, N.; Knauft, J.; Amelung, F.; Nair, J.; Wesch, H.; Bartsch, H. No prevention of liver and kidney tumors in Long-Evans Cinnamon rats by dietary curcumin, but inhibition at other sites and of metastases. *Mutation research* **523-524:**127-135; 2003.

[131] Hecht, S. S.; Kenney, P. M.; Wang, M.; Trushin, N.; Agarwal, S.; Rao, A. V.; Upadhyaya, P. Evaluation of butylated hydroxyanisole, myo-inositol, curcumin, esculetin, resveratrol and lycopene as inhibitors of benzo[a]pyrene plus 4-(methylnitrosamino)-1-(3-pyridyl)-1-butanone-induced lung tumorigenesis in A/J mice. *Cancer letters* **137:**123-130; 1999.

[132] Dance-Barnes, S. T.; Kock, N. D.; Moore, J. E.; Lin, E. Y.; Mosley, L. J.; D'Agostino, R. B., Jr.; McCoy, T. P.; Townsend, A. J.; Miller, M. S. Lung tumor promotion by curcumin. *Carcinogenesis* **30:**1016-1023; 2009.

[133] Li, N.; Chen, X.; Liao, J.; Yang, G.; Wang, S.; Josephson, Y.; Han, C.; Chen, J.; Huang, M. T.; Yang, C. S. Inhibition of 7,12-dimethylbenz[a]anthracene (DMBA)-induced oral carcinogenesis in hamsters by tea and curcumin. *Carcinogenesis* **23:**1307-1313; 2002.

[134] Garg, R.; Ramchandani, A. G.; Maru, G. B. Curcumin decreases 12-O-tetradecanoylphorbol-13-acetate-induced protein kinase C translocation to modulate downstream targets in mouse skin. *Carcinogenesis* **29:**1249-1257; 2008.

[135] Manoharan, S.; Balakrishnan, S.; Menon, V. P.; Alias, L. M.; Reena, A. R. Chemopreventive efficacy of curcumin and piperine during 7,12-dimethylbenz[a]anthracene-induced hamster buccal pouch carcinogenesis. *Singapore Med J* **50:**139-146; 2009.

[136] Ushida, J.; Sugie, S.; Kawabata, K.; Pham, Q. V.; Tanaka, T.; Fujii, K.; Takeuchi, H.; Ito, Y.; Mori, H. Chemopreventive effect of curcumin on N-nitrosomethylbenzylamine-induced esophageal carcinogenesis in rats. *Jpn J Cancer Res* **91:**893-898; 2000.

[137] Imaida, K.; Tamano, S.; Kato, K.; Ikeda, Y.; Asamoto, M.; Takahashi, S.; Nir, Z.; Murakoshi, M.; Nishino, H.; Shirai, T. Lack of chemopreventive effects of lycopene and curcumin on experimental rat prostate carcinogenesis. *Carcinogenesis* **22:**467-472; 2001.

[138] Afaq, F.; Saleem, M.; Aziz, M. H.; Mukhtar, H. Inhibition of 12-O-tetradecanoylphorbol-13-acetate-induced tumor promotion markers in CD-1 mouse skin by oleandrin. *Toxicology and applied pharmacology* **195:**361-369; 2004.

[139] Szaefer, H.; Kaczmarek, J.; Rybczynska, M.; Baer-Dubowska, W. The effect of plant phenols on the expression and activity of phorbol ester-induced PKC in mouse epidermis. *Toxicology* **230:**1-10; 2007.

[140] Lowry, O. H.; Rosebrough, N. J.; Farr, A. L.; Randall, R. J. Protein measurement with the Folin phenol reagent. *J. Biol. Chem.* **193:**265-275; 1951.

[141] Laemmli, U. K. Cleavage of structural proteins during the assembly of the head of bacteriophage T4. *Nature* **227:**680-685; 1970.

[142] Long, W. P.; Chen, X.; Perdew, G. H. Protein kinase C modulates aryl hydrocarbon receptor nuclear translocator protein-mediated transactivation potential in a dimer context. *The Journal of biological chemistry* **274:**12391-12400; 1999.

[143] Hissin, P. J.; Hilf, R. A fluorometric method for determination of oxidized and reduced glutathione in tissues. *Analytical biochemistry* **74:**214-226; 1976.
[144] Burton, K. A study of the conditions and mechanism of the diphenylamine reaction for the colorimetric estimation of deoxyribonucleic acid. *Biochem J.* **62:**315-323; 1956.
[145] Surh, Y. Molecular mechanisms of chemopreventive effects of selected dietary and medicinal phenolic substances. *Mutation research* **428:**305-327; 1999.
[146] Chung, F. L.; Schwartz, J.; Herzog, C. R.; Yang, Y. M. Tea and cancer prevention: studies in animals and humans. *J Nutr* **133:**3268S-3274S; 2003.
[147] Moyers, S. B.; Kumar, N. B. Green tea polyphenols and cancer chemoprevention: multiple mechanisms and endpoints for phase II trials. *Nutr Rev* **62:**204-211; 2004.
[148] Sang, S.; Tian, S.; Stark, R. E.; Yang, C. S.; Ho, C. T. New dibenzotropolone derivatives characterized from black tea using LC/MS/MS. *Bioorganic & medicinal chemistry* **12:**3009-3017; 2004.
[149] Krishnan, R.; Maru, G. B. Inhibitory effect(s) of polymeric black tea polyphenol fractions on the formation of [(3)H]-B(a)P-derived DNA adducts. *Journal of agricultural and food chemistry* **52:**4261-4269; 2004.
[150] Krishnan, R.; Maru, G. B. Inhibitory effect(s) of polymeric black tea polyphenols on the formation of B(a)P-derived DNA adducts in mouse skin. *J Environ Pathol Toxicol Oncol* **24:**79-90; 2005.
[151] Newton, A. C. Regulation of the ABC kinases by phosphorylation: protein kinase C as a paradigm. *Biochem J* **370:**361-371; 2003.
[152] Keranen, L. M.; Dutil, E. M.; Newton, A. C. Protein kinase C is regulated in vivo by three functionally distinct phosphorylations. *Curr Biol* **5:**1394-1403; 1995.
[153] Newton, A. C. Protein kinase C: structural and spatial regulation by phosphorylation, cofactors, and macromolecular interactions. *Chem Rev* **101:**2353-2364; 2001.
[154] Alessi, D. R.; James, S. R.; Downes, C. P.; Holmes, A. B.; Gaffney, P. R.; Reese, C. B.; Cohen, P. Characterization of a 3-phosphoinositide-dependent protein kinase which phosphorylates and activates protein kinase Balpha. *Curr Biol* **7:**261-269; 1997.
[155] Dutil, E. M.; Toker, A.; Newton, A. C. Regulation of conventional protein kinase C isozymes by phosphoinositide-dependent kinase 1 (PDK-1). *Curr Biol* **8:**1366-1375; 1998.
[156] Cazaubon, S.; Bornancin, F.; Parker, P. J. Threonine-497 is a critical site for permissive activation of protein kinase C alpha. *Biochem J* **301** 443-448; 1994.
[157] Slaga, T. J. Overview of tumor promotion in animals. *Environ Health Perspect* **50:**3-14; 1983.
[158] Lee, S. F.; Lin, J. K. Inhibitory effects of phytopolyphenols on TPA-induced transformation, PKC activation, and c-jun expression in mouse fibroblast cells. *Nutrition and cancer* **28:**177-183; 1997.
[159] Chen, Y. C.; Liang, Y. C.; Lin-Shiau, S. Y.; Ho, C. T.; Lin, J. K. Inhibition of TPA-induced protein kinase C and transcription activator protein-1 binding activities by theaflavin-3,3'-digallate from black tea in NIH3T3 cells. *Journal of agricultural and food chemistry* **47:**1416-1421; 1999.
[160] Breitkreutz, D.; Braiman-Wiksman, L.; Daum, N.; Denning, M. F.; Tennenbaum, T. Protein kinase C family: on the crossroads of cell signaling in skin and tumor epithelium. *J Cancer Res Clin Oncol* **133:**793-808; 2007.

[161] Parekh, D. B.; Ziegler, W.; Parker, P. J. Multiple pathways control protein kinase C phosphorylation. *Embo J* **19:**496-503; 2000.
[162] Burgering, B. M.; Coffer, P. J. Protein kinase B (c-Akt) in phosphatidylinositol-3-OH kinase signal transduction. *Nature* **376:**599-602; 1995.
[163] Li, W.; Zhang, J.; Flechner, L.; Hyun, T.; Yam, A.; Franke, T. F.; Pierce, J. H. Protein kinase C-alpha overexpression stimulates Akt activity and suppresses apoptosis induced by interleukin 3 withdrawal. *Oncogene* **18:**6564-6572; 1999.
[164] Kroner, C.; Eybrechts, K.; Akkerman, J. W. Dual regulation of platelet protein kinase B. *The Journal of biological chemistry* **275:**27790-27798; 2000.
[165] Zeng, X.; Xu, H.; Glazer, R. I. Transformation of mammary epithelial cells by 3-phosphoinositide-dependent protein kinase-1 (PDK1) is associated with the induction of protein kinase Calpha. *Cancer research* **62:**3538-3543; 2002.
[166] Nomura, M.; Kaji, A.; He, Z.; Ma, W. Y.; Miyamoto, K.; Yang, C. S.; Dong, Z. Inhibitory mechanisms of tea polyphenols on the ultraviolet B-activated phosphatidylinositol 3-kinase-dependent pathway. *The Journal of biological chemistry* **276:**46624-46631; 2001.
[167] Pianetti, S.; Guo, S.; Kavanagh, K. T.; Sonenshein, G. E. Green tea polyphenol epigallocatechin-3 gallate inhibits Her-2/neu signaling, proliferation, and transformed phenotype of breast cancer cells. *Cancer research* **62:**652-655; 2002.
[168] Huang, C.; Schmid, P. C.; Ma, W. Y.; Schmid, H. H.; Dong, Z. Phosphatidylinositol-3 kinase is necessary for 12-O-tetradecanoylphorbol-13-acetate-induced cell transformation and activated protein 1 activation. *The Journal of biological chemistry* **272:**4187-4194; 1997.
[169] Dong, Z.; Huang, C.; Ma, W. Y. PI-3 kinase in signal transduction, cell transformation, and as a target for chemoprevention of cancer. *Anticancer research* **19:**3743-3747; 1999.
[170] Kundu, J. K.; Na, H. K.; Chun, K. S.; Kim, Y. K.; Lee, S. J.; Lee, S. S.; Lee, O. S.; Sim, Y. C.; Surh, Y. J. Inhibition of phorbol ester-induced COX-2 expression by epigallocatechin gallate in mouse skin and cultured human mammary epithelial cells. *J Nutr* **133:**3805S-3810S; 2003.
[171] Leone, M.; Zhai, D.; Sareth, S.; Kitada, S.; Reed, J. C.; Pellecchia, M. Cancer prevention by tea polyphenols is linked to their direct inhibition of antiapoptotic Bcl-2-family proteins. *Cancer research* **63:**8118-8121; 2003.
[172] Kim, S. O.; Kundu, J. K.; Shin, Y. K.; Park, J. H.; Cho, M. H.; Kim, T. Y.; Surh, Y. J. [6]-Gingerol inhibits COX-2 expression by blocking the activation of p38 MAP kinase and NF-kappaB in phorbol ester-stimulated mouse skin. *Oncogene* **24:**2558-2567; 2005.
[173] Plummer, S. M.; Holloway, K. A.; Manson, M. M.; Munks, R. J.; Kaptein, A.; Farrow, S.; Howells, L. Inhibition of cyclo-oxygenase 2 expression in colon cells by the chemopreventive agent curcumin involves inhibition of NF-kappaB activation via the NIK/IKK signalling complex. *Oncogene* **18:**6013-6020; 1999.
[174] Yang, C. S.; Landau, J. M.; Huang, M. T.; Newmark, H. L. Inhibition of carcinogenesis by dietary polyphenolic compounds. *Annu Rev Nutr* **21:**381-406; 2001.
[175] Kundu, J. K.; Surh, Y. J. Epigallocatechin gallate inhibits phorbol ester-induced activation of NF-kappa B and CREB in mouse skin: role of p38 MAPK. *Annals of the New York Academy of Sciences* **1095:**504-512; 2007.
[176] Nomura, M.; Ma, W.; Chen, N.; Bode, A. M.; Dong, Z. Inhibition of 12-O-tetradecanoylphorbol-13-acetate-induced NF-kappaB activation by tea

polyphenols, (-)-epigallocatechin gallate and theaflavins. *Carcinogenesis* **21:**1885-1890; 2000.

[177] Pan, M. H.; Lin-Shiau, S. Y.; Ho, C. T.; Lin, J. H.; Lin, J. K. Suppression of lipopolysaccharide-induced nuclear factor-kappaB activity by theaflavin-3,3'-digallate from black tea and other polyphenols through down-regulation of IkappaB kinase activity in macrophages. *Biochemical pharmacology* **59:**357-367; 2000.

[178] Bray, F.; Jemal, A.; Grey, N.; Ferlay, J.; Forman, D. Global cancer transitions according to the Human Development Index (2008-2030): a population-based study. *Lancet Oncol* **13:**790-801; 2012.

[179] Ruby, A. J.; Kuttan, G.; Babu, K. D.; Rajasekharan, K. N.; Kuttan, R. Anti-tumour and antioxidant activity of natural curcuminoids. *Cancer letters* **94:**79-83; 1995.

[180] Miquel, J.; Bernd, A.; Sempere, J. M.; Diaz-Alperi, J.; Ramirez, A. The curcuma antioxidants: pharmacological effects and prospects for future clinical use. A review. *Archives of gerontology and geriatrics* **34:**37-46; 2002.

[181] Rao, T. S.; Basu, N.; Siddiqui, H. H. Anti-inflammatory activity of curcumin analogues. *The Indian journal of medical research* **75:**574-578; 1982.

[182] Garg, R.; Ingle, A.; Maru, G. Dietary turmeric modulates DMBA-induced p21ras, MAP kinases and AP-1/NF-kappaB pathway to alter cellular responses during hamster buccal pouch carcinogenesis. *Toxicology and applied pharmacology* **232:**428-439; 2008b.

[183] Salley, J. J. Experimental carcinogenesis in the cheek pouch of the Syrian hamster. *Journal of dental research* **33:**253-262; 1954.

[184] Santis, H.; Shklar, G.; Chauncey, H. H. Histochemistry of Experimentally Induced Leukoplakia and Carcinoma of the Hamster Buccal Pouch. *Oral surgery, oral medicine, and oral pathology* **17:**207-218; 1964.

[185] Thapliyal, R.; Deshpande, S. S.; Maru, G. B. Effects of turmeric on the activities of benzo(a)pyrene-induced cytochrome P-450 isozymes. *J Environ Pathol Toxicol Oncol* **20:**59-63; 2001.

[186] Garg, R.; Gupta, S.; Maru, G. B. Dietary curcumin modulates transcriptional regulators of phase I and phase II enzymes in benzo[a]pyrene-treated mice: mechanism of its anti-initiating action. *Carcinogenesis* **29:**1022-1032; 2008a.

[187] Chun, K. S.; Kim, S. H.; Song, Y. S.; Surh, Y. J. Celecoxib inhibits phorbol ester-induced expression of COX-2 and activation of AP-1 and p38 MAP kinase in mouse skin. *Carcinogenesis* **25:**713-722; 2004.

[188] Chun, K. S.; Keum, Y. S.; Han, S. S.; Song, Y. S.; Kim, S. H.; Surh, Y. J. Curcumin inhibits phorbol ester-induced expression of cyclooxygenase-2 in mouse skin through suppression of extracellular signal-regulated kinase activity and NF-kappaB activation. *Carcinogenesis* **24:**1515-1524; 2003.

[189] Kojima, M.; Morisaki, T.; Izuhara, K.; Uchiyama, A.; Matsunari, Y.; Katano, M.; Tanaka, M. Lipopolysaccharide increases cyclo-oxygenase-2 expression in a colon carcinoma cell line through nuclear factor-kappa B activation. *Oncogene* **19:**1225-1231; 2000.

[190] Schulze-Osthoff, K.; Ferrari, D.; Riehemann, K.; Wesselborg, S. Regulation of NF-kappa B activation by MAP kinase cascades. *Immunobiology* **198:**35-49; 1997.

[191] Garvin, S.; Ollinger, K.; Dabrosin, C. Resveratrol induces apoptosis and inhibits angiogenesis in human breast cancer xenografts in vivo. *Cancer letters* **231:**113-122; 2006.

[192] Wu, S. L.; Sun, Z. J.; Yu, L.; Meng, K. W.; Qin, X. L.; Pan, C. E. Effect of resveratrol and in combination with 5-FU on murine liver cancer. *World journal of gastroenterology : WJG* **10:**3048-3052; 2004.

[193] Yang, X. R.; Wang, Y. Y.; La, K. K.; Peng, L.; Song, X. H.; Shi, X. G.; Zhu, X. F.; Leung, P. C.; Ko, C. H.; Ye, C. X. Inhibitory effects of cocoa tea (Camellia ptilophylla) in human hepatocellular carcinoma HepG2 *in vitro* and *in vivo* through apoptosis. *The Journal of nutritional biochemistry*; 2011.

[194] Bhuvaneswari, V.; Rao, K. S.; Nagini, S. Altered expression of anti and proapoptotic proteins during chemoprevention of hamster buccal pouch carcinogenesis by tomato and garlic combination. *Clinica chimica acta; international journal of clinical chemistry* **350:**65-72; 2004.

[195] Marone, M.; Scambia, G.; Mozzetti, S.; Ferrandina, G.; Iacovella, S.; De Pasqua, A.; Benedetti-Panici, P.; Mancuso, S. bcl-2, bax, bcl-XL, and bcl-XS expression in normal and neoplastic ovarian tissues. *Clin Cancer Res* **4:**517-524; 1998.

[196] Choi, S.; Oh, J. Y.; Kim, S. J. Ginsenoside Rh2 induces Bcl-2 family proteins-mediated apoptosis in vitro and in xenografts in vivo models. *Journal of cellular biochemistry* **112:**330-340; 2011.

[197] Kaur, M.; Velmurugan, B.; Rajamanickam, S.; Agarwal, R.; Agarwal, C. Gallic acid, an active constituent of grape seed extract, exhibits anti-proliferative, pro-apoptotic and anti-tumorigenic effects against prostate carcinoma xenograft growth in nude mice. *Pharmaceutical research* **26:**2133-2140; 2009.

[198] Zhou, H. B.; Chen, J. J.; Wang, W. X.; Cai, J. T.; Du, Q. Anticancer activity of resveratrol on implanted human primary gastric carcinoma cells in nude mice. *World journal of gastroenterology : WJG* **11:**280-284; 2005.

[199] Kirkin, V.; Joos, S.; Zornig, M. The role of Bcl-2 family members in tumorigenesis. *Biochimica et biophysica acta* **1644:**229-249; 2004.

[200] Tang, F. Y.; Pai, M. H.; Wang, X. D. Consumption of lycopene inhibits the growth and progression of colon cancer in a mouse xenograft model. *Journal of agricultural and food chemistry* **59:**9011-9021; 2011.

[201] Akhtar, S.; Meeran, S. M.; Katiyar, N.; Katiyar, S. K. Grape seed proanthocyanidins inhibit the growth of human non-small cell lung cancer xenografts by targeting insulin-like growth factor binding protein-3, tumor cell proliferation, and angiogenic factors. *Clin Cancer Res* **15:**821-831; 2009.

[202] Li, Z.; Xu, X.; Huang, Y.; Ding, L.; Wang, Z.; Yu, G.; Xu, D.; Li, W.; Tong, D. Swainsonine activates mitochondria-mediated apoptotic pathway in human lung cancer A549 cells and retards the growth of lung cancer xenografts. *International journal of biological sciences* **8:**394-405; 2012.

[203] Kohno, Y.; Patel, V.; Kim, Y.; Tsuji, T.; Chin, B. R.; Sun, M.; Bruce Donoff, R.; Kent, R.; Wong, D.; Todd, R. Apoptosis, proliferation and p12(doc-1) profiles in normal, dysplastic and malignant squamous epithelium of the Syrian hamster cheek pouch model. *Oral oncology* **38:**274-280; 2002.

[204] Schwartz, J. L.; Gu, X.; Kittles, R. A.; Baptiste, A.; Shklar, G. Experimental oral carcinoma of the tongue and buccal mucosa: possible biologic markers linked to cancers at two anatomic sites. *Oral oncology* **36:**225-235; 2000.

[205] Maga, G.; Hubscher, U. Proliferating cell nuclear antigen (PCNA): a dancer with many partners. *Journal of cell science* **116:**3051-3060; 2003.

[206] Yu, L.; Sun, Z. J.; Wu, S. L.; Pan, C. E. Effect of resveratrol on cell cycle proteins in murine transplantable liver cancer. *World journal of gastroenterology : WJG* **9:**2341-2343; 2003.

[207] Ye, F.; Zhang, G. H.; Guan, B. X.; Xu, X. C. Suppression of esophageal cancer cell growth using curcumin, (-)-epigallocatechin-3-gallate and lovastatin. *World journal of gastroenterology : WJG* **18:**126-135; 2012.
[208] Li, N.; Sood, S.; Wang, S.; Fang, M.; Wang, P.; Sun, Z.; Yang, C. S.; Chen, X. Overexpression of 5-lipoxygenase and cyclooxygenase 2 in hamster and human oral cancer and chemopreventive effects of zileuton and celecoxib. *Clin Cancer Res* **11:**2089-2096; 2005.
[209] Rao, C. V. Regulation of COX and LOX by curcumin. *Advances in experimental medicine and biology* **595:**213-226; 2007.
[210] Spiller, S. E.; Logsdon, N. J.; Deckard, L. A.; Sontheimer, H. Inhibition of nuclear factor kappa-B signaling reduces growth in medulloblastoma in vivo. *BMC cancer* **11:**136; 2011.
[211] Goldman, R.; Enewold, L.; Pellizzari, E.; Beach, J. B.; Bowman, E. D.; Krishnan, S. S.; Shields, P. G. Smoking increases carcinogenic polycyclic aromatic hydrocarbons in human lung tissue. *Cancer research* **61:**6367-6371; 2001.
[212] Mastrangelo, G.; Fadda, E.; Marzia, V. Polycyclic aromatic hydrocarbons and cancer in man. *Environ Health Perspect* **104:**1166-1170; 1996.
[213] Phillips, D. H. Polycyclic aromatic hydrocarbons in the diet. *Mutation research* **443:**139-147; 1999.
[214] Boysen, G.; Hecht, S. S. Analysis of DNA and protein adducts of benzo[a]pyrene in human tissues using structure-specific methods. *Mutation research* **543:**17-30; 2003.
[215] Thapliyal, R.; Maru, G. B. Inhibition of cytochrome P450 isozymes by curcumins in vitro and in vivo. *Food Chem Toxicol* **39:**541-547; 2001.
[216] Thapliyal, R.; Deshpande, S. S.; Maru, G. B. Mechanism(s) of turmeric-mediated protective effects against benzo(a)pyrene-derived DNA adducts. *Cancer letters* **175:**79-88; 2002.
[217] Zhang, Y. J.; Weksler, B. B.; Wang, L.; Schwartz, J.; Santella, R. M. Immunohistochemical detection of polycyclic aromatic hydrocarbon-DNA damage in human blood vessels of smokers and non-smokers. *Atherosclerosis* **140:**325-331; 1998.
[218] Chatterjee, S.; Malhotra, R.; Varghese, F.; Bukhari, A. B.; Patil, A.; Budrukkar, A.; Parmar, V.; Gupta, S.; De, A. Quantitative Immunohistochemical Analysis Reveals Association between Sodium Iodide Symporter and Estrogen Receptor Expression in Breast Cancer. *PloS one* **8:**e54055; 2013.
[219] Choudhuri, T.; Pal, S.; Agwarwal, M. L.; Das, T.; Sa, G. Curcumin induces apoptosis in human breast cancer cells through p53-dependent Bax induction. *FEBS letters* **512:**334-340; 2002.
[220] Alexandrov, K.; Rojas, M.; Bourgeois, Y.; Chouroulinkov, I. The persistence of benzo[a]pyrene diol-epoxide deoxyguanosine adduct in mouse skin and its disappearance in rat skin. *Carcinogenesis* **4:**1655-1657; 1983.
[221] Ashurst, S. W.; Cohen, G. M.; Nesnow, S.; DiGiovanni, J.; Slaga, T. J. Formation of benzo(a)pyrene/DNA adducts and their relationship to tumor initiation in mouse epidermis. *Cancer research* **43:**1024-1029; 1983.
[222] Bjelogrlic, N. M.; Makinen, M.; Stenback, F.; Vahakangas, K. Benzo[a]pyrene-7,8-diol-9,10-epoxide-DNA adducts and increased p53 protein in mouse skin. *Carcinogenesis* **15:**771-774; 1994.
[223] Jiang, M. C.; Yang-Yen, H. F.; Yen, J. J.; Lin, J. K. Curcumin induces apoptosis in immortalized NIH 3T3 and malignant cancer cell lines. *Nutrition and cancer* **26:**111-120; 1996.

[224] Shankar, S.; Srivastava, R. K. Involvement of Bcl-2 family members, phosphatidylinositol 3'-kinase/AKT and mitochondrial p53 in curcumin (diferulolylmethane)-induced apoptosis in prostate cancer. *International journal of oncology* **30:**905-918; 2007.

[225] Hoffmann, D.; Hoffmann, I.; El-Bayoumy, K. The less harmful cigarette: a controversial issue. a tribute to Ernst L. Wynder. *Chem Res Toxicol* **14:**767-790; 2001.

[226] IARC. Tobacco smoke and involuntary smoking. *IARC monographs on the evaluation of carcinogenic risks to humans / World Health Organization, International Agency for Research on Cancer* **83:**1-1438; 2004.

[227] IARC. Tobacco smoking. *IARC***:**199; 1986.

[228] IARC Cruciferous Vegetables, Isothiocyanates and Indoles. *IARC Handbooks on Cancer Prevention*. Lyon; 2004: 171-176.

[229] Hecht, S. S. Tobacco carcinogens, their biomarkers and tobacco-induced cancer. *Nat Rev Cancer* **3:**733-744; 2003.

[230] Hecht, S. S. Tobacco smoke carcinogens and lung cancer. *Journal of the National Cancer Institute* **91:**1194-1210; 1999.

[231] Yang, Y. M.; Conaway, C. C.; Chiao, J. W.; Wang, C. X.; Amin, S.; Whysner, J.; Dai, W.; Reinhardt, J.; Chung, F. L. Inhibition of benzo(a)pyrene-induced lung tumorigenesis in A/J mice by dietary N-acetylcysteine conjugates of benzyl and phenethyl isothiocyanates during the postinitiation phase is associated with activation of mitogen-activated protein kinases and p53 activity and induction of apoptosis. *Cancer research* **62:**2-7; 2002.

[232] Kassie, F.; Matise, I.; Negia, M.; Lahti, D.; Pan, Y.; Scherber, R.; Upadhyaya, P.; Hecht, S. S. Combinations of N-Acetyl-S-(N-2-Phenethylthiocarbamoyl)-L-Cysteine and myo-inositol inhibit tobacco carcinogen-induced lung adenocarcinoma in mice. *Cancer Prev Res (Phila)* **1:**285-297; 2008.

[233] Dagne, A.; Melkamu, T.; Schutten, M. M.; Qian, X.; Upadhyaya, P.; Luo, X.; Kassie, F. Enhanced inhibition of lung adenocarcinoma by combinatorial treatment with indole-3-carbinol and silibinin in A/J mice. *Carcinogenesis* **32:**561-567; 2011.

[234] Nikitin, A. Y.; Alcaraz, A.; Anver, M. R.; Bronson, R. T.; Cardiff, R. D.; Dixon, D.; Fraire, A. E.; Gabrielson, E. W.; Gunning, W. T.; Haines, D. C.; Kaufman, M. H.; Linnoila, R. I.; Maronpot, R. R.; Rabson, A. S.; Reddick, R. L.; Rehm, S.; Rozengurt, N.; Schuller, H. M.; Shmidt, E. N.; Travis, W. D.; Ward, J. M.; Jacks, T. Classification of proliferative pulmonary lesions of the mouse: recommendations of the mouse models of human cancers consortium. *Cancer research* **64:**2307-2316; 2004.

[235] Conaway, C. C.; Wang, C. X.; Pittman, B.; Yang, Y. M.; Schwartz, J. E.; Tian, D.; McIntee, E. J.; Hecht, S. S.; Chung, F. L. Phenethyl isothiocyanate and sulforaphane and their N-acetylcysteine conjugates inhibit malignant progression of lung adenomas induced by tobacco carcinogens in A/J mice. *Cancer research* **65:**8548-8557; 2005.

[236] Estensen, R. D.; Jordan, M. M.; Wiedmann, T. S.; Galbraith, A. R.; Steele, V. E.; Wattenberg, L. W. Effect of chemopreventive agents on separate stages of progression of benzo[alpha]pyrene induced lung tumors in A/J mice. *Carcinogenesis* **25:**197-201; 2004.

[237] Kassie, F.; Kalscheuer, S.; Matise, I.; Ma, L.; Melkamu, T.; Upadhyaya, P.; Hecht, S. S. Inhibition of vinyl carbamate-induced pulmonary adenocarcinoma by

indole-3-carbinol and myo-inositol in A/J mice. *Carcinogenesis* **31:**239-245; 2010.

[238] Kassie, F.; Matise, I.; Negia, M.; Upadhyaya, P.; Hecht, S. S. Dose-dependent inhibition of tobacco smoke carcinogen-induced lung tumorigenesis in A/J mice by indole-3-carbinol. *Cancer Prev Res (Phila)* **1:**568-576; 2008.

[239] Hecht, S. S.; Kenney, P. M.; Wang, M.; Upadhyaya, P. Dose-response study of myo-inositol as an inhibitor of lung tumorigenesis induced in A/J mice by benzo. *Cancer letters* **167:**1-6; 2001.

[240] Morse, M. A.; Amin, S. G.; Hecht, S. S.; Chung, F. L. Effects of aromatic isothiocyanates on tumorigenicity, O6-methylguanine formation, and metabolism of the tobacco-specific nitrosamine 4-(methylnitrosamino)-1-(3-pyridyl)-1-butanone in A/J mouse lung. *Cancer research* **49:**2894-2897; 1989.

[241] Morse, M. A.; Wang, C. X.; Stoner, G. D.; Mandal, S.; Conran, P. B.; Amin, S. G.; Hecht, S. S.; Chung, F. L. Inhibition of 4-(methylnitrosamino)-1-(3-pyridyl)-1-butanone-induced DNA adduct formation and tumorigenicity in the lung of F344 rats by dietary phenethyl isothiocyanate. *Cancer research* **49:**549-553; 1989.

[242] Wattenberg, L. W. Effects of dietary constituents on the metabolism of chemical carcinogens. *Cancer research* **35:**3326-3331; 1975.

[243] Garg, R.; Maru, G. B. Dietary curcumin enhances benzo(a)pyrene-induced apoptosis resulting in decrease in BPDE-DNA adducts in mice. *J Environ Pathol Toxicol Oncol* **28**; 2009.

[244] Kassie, F.; Anderson, L. B.; Scherber, R.; Yu, N.; Lahti, D.; Upadhyaya, P.; Hecht, S. S. Indole-3-carbinol inhibits 4-(methylnitrosamino)-1-(3-pyridyl)-1-butanone plus benzo(a)pyrene-induced lung tumorigenesis in A/J mice and modulates carcinogen-induced alterations in protein levels. *Cancer research* **67:**6502-6511; 2007.

[245] Hecht, S. S.; Upadhyaya, P.; Wang, M.; Bliss, R. L.; McIntee, E. J.; Kenney, P. M. Inhibition of lung tumorigenesis in A/J mice by N-acetyl-S-(N-2-phenethylthiocarbamoyl)-L-cysteine and myo-inositol, individually and in combination. *Carcinogenesis* **23:**1455-1461; 2002.

[246] Han, W.; Gills, J. J.; Memmott, R. M.; Lam, S.; Dennis, P. A. The chemopreventive agent myoinositol inhibits Akt and extracellular signal-regulated kinase in bronchial lesions from heavy smokers. *Cancer Prev Res (Phila)* **2:**370-376; 2009.

[247] Hecht, S. S. Chemoprevention by isothiocyanates. *Journal of cellular biochemistry* **22:**195-209; 1995.

[248] Chung, E. L. Chemoprevention of lung cancer by isothiocyanates and their conjugates in A/J mouse. *Exp Lung Res* **27:**319-330; 2001.

[249] Lin, J. M.; Amin, S.; Trushin, N.; Hecht, S. S. Effects of isothiocyanates on tumorigenesis by benzo[a]pyrene in murine tumor models. *Cancer letters* **74:**151-159; 1993.

[250] Zinov'eva, V. N.; Spasov, A. A. [Mechanisms of plant polyphenols anti-cancer effects. I. Blockade of carcinogenesis initiation]. *Biomeditsinskaia khimiia* **58:**160-175; 2012.